Molecular architecture influences on material properties of pharmaceutical compounds

Miren Ramirez

Doctor of Philosophy

Aston University

September 2010

THESIS SUMMARY

Aston University

Molecular architecture influences on material properties of pharmaceutical compounds

Miren Ramirez

Doctor of Philosophy

September 2010

Salt formation has extensively been studied as a strategy to improve drug solubility but it has not been explored as a strategy to improve mechanical properties. A better understanding of which factors of the solid state can have an influence in the mechanical properties of pharmaceutical powders can help to optimise and reduce cost of tablet manufacturing.

The aim of this study was to form different series of amine salts of flurbiprofen, gemfibrozil and diclofenac and to establish predictive relationships between architectural characteristics and physicochemical and mechanical properties of the salts.

For this purpose, three different carboxylic acid drugs were selected: flurbiprofen, gemfibrozil and diclofenac, similar in size but varying in flexibility and shape and three different series of counterions were also chosen: one with increasing bulk and no hydroxyl groups to limit the hydrogen bonding potential; a second one with increasing number of hydroxyl groups and finally a third series, related to the latter in number of hydroxyl groups but with different molecular shape and flexibility.

Physico-chemical characterization was performed (DSC, TGA, solubility, intrinsic dissolution rate, particle size, true density) and mechanical properties measured using a compaction replicator.

Strained molecular conformations produce weaker compacts as they have higher energy than preferred conformations that usually lie close to energy minimums and oppose plastic deformation.

It was observed that slip planes, which correspond to regions of weakest interaction between the planes, were associated with improved plasticity and stronger compacts. Apart from hydrogen bonds, profuse van der Waals forces can result in ineffective slip planes.

Salts displaying two-dimensional densely hydrogen bonded layers produced stronger compacts than salts showing one-dimensional networks of non-bonded columns, probably by reducing the attachment energy between layers. When hydrogen bonds are created intramolecularly, it is possible that the mechanical properties are compromised as they do not contribute so much to create two-dimensional densely bonded layers and they can force molecules into strained conformations.

Some types of hydrogen bonding network may be associated with improved mechanical properties, such as type II, or $R_4^3(10)$ using graph-set notation, versus type III, or $R_8^4(12)$, columns.

This work clearly demonstrates the potential of investigating crystal structure-mechanical property relationship in pharmaceutical materials.

ACKNOWLEDGMENTS

This thesis arose in part out of years of research before I arrived at Aston University. I would like to thank Dr Sarah David for her preliminary work on mechanical properties of pharmaceutical powders.

I would like to record my gratitude to Dr Barbara Conway for her supervision, advice, availability and guidance from the very early stage of this research as well as for the trust she put on me to decide the direction of the research.

I gratefully acknowledge Professor Carl Schwalbe for his crucial contribution to the crystallography section and for his inspiring passion for science.

Many thanks to Peter Timmins. I greatly benefited from his advice and he kindly made available to me all the resources available at Bristol Myers-Squibb. Thank you for such a wonderful team. Vivian Gray, Mike Tobyn, John Gamble and Wayne Sinclair offered me much of their time.

To Jiteen Kansara for his help with lab equipment and for creating such a nice working atmosphere.

This work would not have been possible without EPSRC UK National Crystallography Service at their two centres in Southampton and the synchrotron-based facility at the Diamond Light Source.

My parents deserve special mention for their continuous encouragement and so does my husband, because he also believes that sometimes you need to go far just to come back.

LIST OF CONTENTS

LIST OF TABLES

LIST OF FIGURES

1 Introduction

1.1 The drug discovery pipeline

Traditionally most drugs have been discovered either by identifying the active ingredient from traditional remedies or by chance. A newer approach has been used to understand how disease and infection are controlled at the molecular and physiological level and to target specific entities based on this knowledge. New technologies and Data Management/Informatics systems based on mathematical modelling techniques are now employed to speed up this process.

New Chemical Entities (NCEs) often begin in the laboratory with chemists, scientists and pharmacologists who identify cellular and genetic factors that play a role in specific diseases. They search for chemical and biological substances that target these biological markers and are likely to have drug-like effects. Out of every 10,000 new compounds identified during the discovery process, only five are considered safe for testing in human volunteers after preclinical evaluations, and only 1 will obtain the authorization marketing (PhRMA 2006) (see Fig 1.1).

Fig 1.1 Drug development pipeline (adapted from Pharmaceutical Research and Manufacturers of America profile)

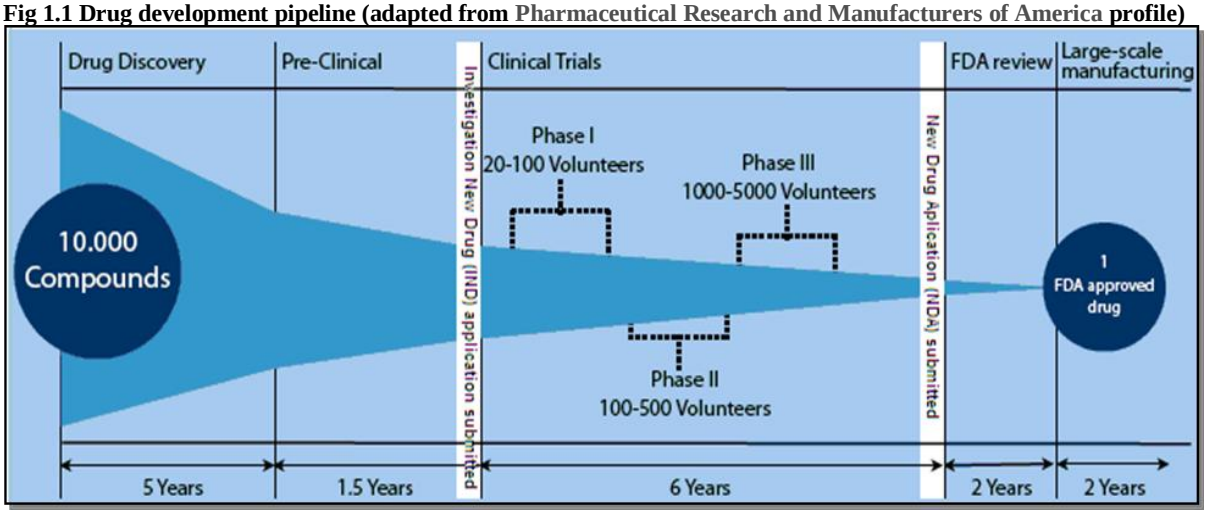

Drug development is a costly and intensive process. Of all compounds investigated for use in humans only a small fraction is eventually approved, and only after heavy investment in pre-clinical development, clinical trials, and safety monitoring to determine the safety and efficacy of a compound. The cost for a new chemical entity is estimated to be as high as 1.7 billion USD (Mullin 2003). Half of this amount is opportunity costs; others are costs for the development of all

unsuccessful drugs. Increasing failure rates in clinical trials are thought to be driving increased drug development costs.

Only after rigorous study and testing, which can take as long as 12 years, will governmental authorities grant permission for the company to market and sell the drug. In special circumstances, such as the search for effective drugs to treat AIDS, the Food and Drug Administration (FDA) has encouraged an abbreviated process for drug testing and approval called fast-tracking. Depending on a number of considerations, a company may apply for and be granted a patent for the drug or the process of producing the drug for about 20 years. Similarly, the Medicines and Healthcare products Regulatory Agency (MHRA) is prepared to consider fast tracking applications when there are compelling reasons for believing that the product would provide a major breakthrough in the treatment of patients for certain conditions or in the event of a shortage of supply of essential products.

Scientists use a variety of techniques to identify and isolate a target and learn more about its functions and how these influence disease. Compounds are then identified that have various interactions with drug targets helpful in treatment of a specific disease. Researchers analyze and compare each drug target to others based on their association with a specific disease and their ability to regulate biological and chemical compounds in the body. Tests are conducted to confirm that interactions with the drug target are associated with a desired change in the behaviour of diseased cells. Research scientists can then confirm that a lead compound or substance is one that is believed to have potential to treat disease. Laboratory scientists can compare known substances with new compounds to determine their likelihood of success. Leads are sometimes developed as collections, or libraries, of individual molecules that possess properties needed in a new drug. Lead optimization compares the properties of various lead compounds and provides information to help pharmaceutical and biotechnology companies select the compound or compounds with the greatest potential to be developed into safe and effective medicines. Formulation scientists and material scientists proceed to the physicochemical and mechanical characterisation of the compound. Often during this same stage of development, lead prioritization studies are conducted *in vivo* and *in vitro* to compare various lead compounds and how they are metabolized and affect the body.

1.1.1 Clinical testing

Clinical testing usually comprises Phase I, Phase II and Phase III clinical studies (see Fig 1.1). In each successive phase, increasing numbers of patients are tested. There are a large number of firms worldwide that support clinical trials and perform clinical trials services for pharmaceutical companies.

- *Phase I studies:* are designed to verify safety and tolerability of the candidate drug in humans and typically take six to nine months. These are the first studies conducted in humans. A small number of subjects, usually from 20 to 100 healthy volunteers, take the investigational drug for short periods of time. Testing includes observation and careful documentation of the pharmacodynamics and the pharmacokinetics of the drug
- *Phase II studies:* are designed to determine effectiveness and further study the safety of the candidate drug in humans. Depending upon the type of investigational drug and the condition it treats, this phase of development generally takes from six months up to three years. Testing is conducted with up to several hundred patients suffering from the condition the investigational drug is designed to treat. This testing determines safety and effectiveness of the drug in treating the condition and establishes the minimum and maximum doses. Most Phase II studies are placebo controlled and double-blinded, meaning that neither patients nor researchers evaluating the compound know who is receiving the investigational drug or placebo.
- *Phase III studies* provide expanded testing of effectiveness and safety of an investigational drug, usually in randomized, and blinded clinical trials. Depending upon the type of drug candidate and the condition it treats, this phase usually requires one to four years of testing. In Phase III, safety and efficacy testing is conducted with several hundred to thousands of volunteer patients suffering from the condition the investigational drug treats.

The low number of new drugs reaching the market in recent years is a concern for public health and for the drug development enterprise. A high failure rate of clinical development programmes has been identified as a major cause for the pharmaceutical productivity gap, but regulatory approval rates may also have a role (Eichler et al. 2010).

Of the NCEs that enter the human testing phase 78% are never marketed (DiMasi et al. 2003). Between 1 January and 31 December 2009, 48 NCEs had a regulatory outcome from the European Medicines Agency (EMA); 29 (60%) were recommended by Committee for Medicinal Products for

Human Use (CHMP) for marketing authorization, and 19 (40%) received a negative CHMP opinion or were withdrawn before an opinion was delivered. Of the 29 approved NCE applications, 21 (72%) requested scientific advice from the CHMP during the course of drug development, compared with 11 (58%) of the 19 applications with a negative outcome. The proportion of small and medium-sized enterprises among the applicants for marketing authorization application that had negative outcomes (6/19; 32%) was higher than the proportion among the applicants for which the marketing authorization applications were approved (4/29; 14%) (EMA 2010). Given that for the 40% of products with a negative regulatory outcome, failure came at the end of a full development programme and after patients in clinical trials had been exposed to potential risks, these data raise concerns from both a public health and an opportunity-cost perspective. It is crucial to understand if the negative outcome is the result of a failed drug or of a failed drug development plan. Retrospective analysis of assessment reports for negative marketing authorization applications support the possibility that, in many instances, the regulators' conclusions were not of a clearly negative benefit–risk profile (a failed drug) but of inadequate demonstration of efficacy and/or safety (a failed development strategy or immature application) (Eichler et al. 2010).

1.2 Oral dosage forms

Oral drug delivery is the most desirable and preferred method of administering therapeutic agents for their systemic effects. In addition, oral delivery is generally considered as the first route investigated in the discovery and development of new drug entities and pharmaceutical formulations, mainly because of patient acceptance, convenience in administration, and cost-effective manufacturing process. For many drug substances, conventional, immediate-release formulations provide clinically effective therapy while maintaining the required balance of pharmacokinetic and pharmacodynamic profiles with an acceptable level of safety to the patient. In 2000, the use of solid oral dosage such as tablets accounted for approximately 60 % of the total frequency of all pharmaceutical dosage forms. In addition to this 90 % of all drugs were supplied in tablet form even if they are presented in other medicinal forms (Pickering et al. 2000). However, the potential for oral dosage form development is sometimes limited for therapeutic agents that are poorly absorbed in the gastrointestinal (GI) tract and unstable to various enzymes, in particular, to proteolytic enzymes, such as peptide and protein drugs. The overall process of oral delivery is frequently impaired by several physiological and pharmaceutical challenges that are associated with the inherent physicochemical nature of the drugs, such as poor solubility, and/or the variability in GI conditions, such as pH, presence of food, transit times, expression of *P*-Glycoprotein (*P*-Gp) and CYP3A, as well as enzymatic activity in the

alimentary canal. Other disadvantages of the oral route include: late onset of action, not suitable for non-cooperant patients, uncertainty of absorption and potential for irritancy to gastric mucosa.

1.3 Drug solubility

Due to the recent introduction of combinatorial chemistry and high throughput screening in identifying new chemical entities, the solubility of the new molecules has decreased sharply (Lipinski 2000). While solubilities less than 20 µg/ml were practically non-existent until the 1980s, the situation has changed so much that in the present, drug candidates with intrinsic solubilities of 1 µg/ml are common. According to recent experience, approximately one-third of new compounds synthesized in medicinal chemistry laboratories have an aqueous solubility of less than 10 µg/ml, another third have a solubility from 10 to 100 µg/ml and the solubility of the remaining third is >100 µg/ml (Serajuddin 2007). It is important, therefore, to know the physicochemical properties of the drug. Amongst the drug-related properties there are: size, shape, solubility in the absorption site and relative lipophilicity of the ionised and unionised forms. Properties of the epithelial cell membrane influence drug absorption, depending on the location and the function of the membrane. Structural features include pores and tight junctions. Epithelial cells of the lining of the intestinal tract are joined by tight junctions that limit diffusion of substances between cells. The presence of electrical charge across the cell membrane influences the movement of ions in and out of the cell. Some parts of the GI tract are more permeable than others. Other membrane-related properties are vascularity and effective absorbing surface. In the small intestine the absorbing surface is maximised as a consequence of the submucosal folds and the microvilli making it the main site of absorption for most drugs.

Fig 1.2 Necessary processes for oral drug action. Adapted from Banakar (1991)

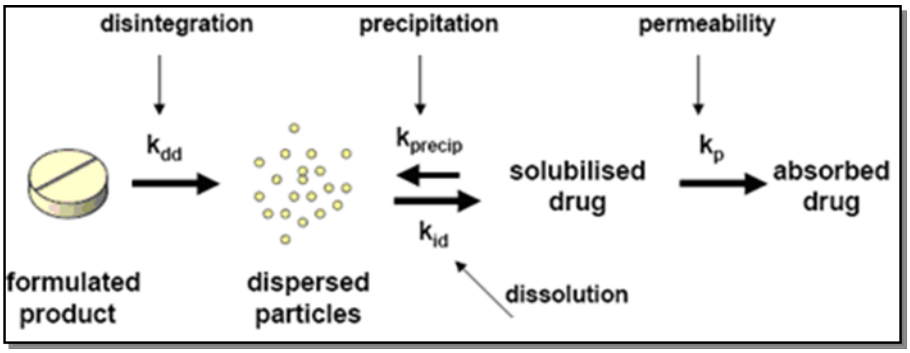

The dynamic nature of the GI environment requires that drug release and uptake be completed within a designed time frame. It is well recognised that drug solubility plays a pivotal role in dissolution and absorption (Bakatselou et al. 1991; Charman et al. 1997; Dressman and Reppas 2000). In the last

decade there has been an increased focus on solubility as the major factor limiting the absorption of lipophilic compounds generated in high throughput drug discovery programmes (Lipinski 2000). The availability of *in vivo* solubility data during early drug development can provide valuable insight for drug selection, formulation, and predicting oral drug absorption, but obtaining such information is very challenging due to problems associated with using human GI fluids. Such problems include limited resources, institutional review board concerns, and inherent molecular and biological variations, thus making routine *in vivo* assays impractical during the lead identification stage. For these reasons, considerable research effort has focused on developing *in vitro* GI fluids that mimic *in vivo* conditions (Staggers et al. 1990; Bakatselou et al. 1991; Charman et al. 1997; Dressman et al. 1998; Dressman and Reppas 2000). Developing such mimics is complex because drug dissolution in GI fluid is both dynamic and highly individualized.

GI fluid composition and interactions with formulation components vary considerably from site to site within the GI tract, and following food intake. Several different fluid mimics have been investigated, many of them containing bile acid mixed micelles to mimic both fed and fasted states (Staggers et al. 1990; Bakatselou et al. 1991). A method allowing quick evaluation of a number of different media could provide greater insight into solubility and its role in drug absorption, thereby providing a solubility map across a number of possible mimics.

1.3.1 Biopharmaceutics Classification (BCS)

When solubility and dissolution rate of the relevant polymorphic forms are sufficiently high and controlled, concerns with respect to bioavailability and stability are minimal. The BCS criteria of high solubility and rapid dissolution should be considered in regulatory decisions (Amidon et al. 1995; Yu et al. 2002).

Amidon et al. (1995) proposed a biopharmaceutical classification system that classifies drugs in four classes according to their solubility and permeability across the GI mucosa. The system was adopted by the FDA and it aims to improve the efficiency of drug development and recommend a class of immediate-release (IR) solid oral dosage forms for which bioequivalence may be assessed based on *in vitro* dissolution tests. The four classes are (see Fig 1.3):

- *Class I*: High Permeability, High Solubility: e.g. paracetamol, metronidazole, diazepam
- *Class II* : High Permeability, Low Solubility: amiodarone, lansoprazole, diclofenac
- *Class III*: Low Permeability, High Solubility: amoxicillin, frusemide, ciprofloxacin

- *Class IV*: Low Permeability, Low Solubility: methotrexate, amphotericin B, colistin

Fig 1.3 Biopharmaceutics classification criteria

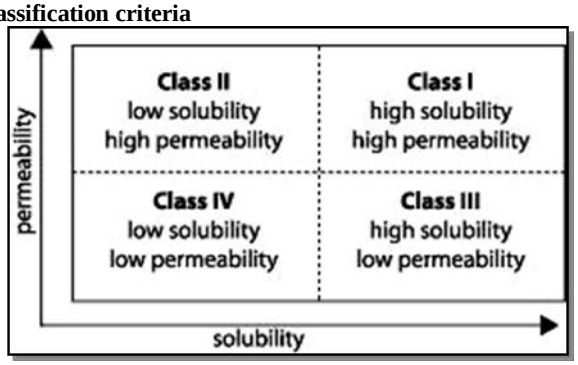

A drug substance is considered highly soluble when the highest dose strength is soluble in < 250 ml water over a pH range of 1 to 7.5 (FDA guidance states pH = 7.5, EU guidance states pH = 6.8). A drug substance is considered highly permeable when the extent of absorption in humans is determined to be > 90% of an administered dose, based on mass-balance or in comparison to an intravenous reference dose. A drug product is considered to be rapidly dissolving when > 85% of the labelled amount of drug substance dissolves within 30 minutes using USP apparatus I or II in a volume of < 900 ml buffer solutions.

The regulatory acceptance of *in vitro* testing as a reliable surrogate for an *in vivo* bioequivalent study is commonly referred to as a "biowaiver". Currently FDA, BCS (2000) guidance allows biowaivers for some products within the BCS Class 1. In Europe biowaivers in general and biowaivers per BCS are covered both in the note for guidance on the investigation of bioavailability and bioequivalence (EMEA 2001). The EMEA guidance accepts biowaivers only when different strengths are manufactured by the same manufacturer and the same manufacturing process (Yu et al. 2002).

Recently, a panel of experts (Polli et al. 2004) supported the possibility of biowaivers for BCS Class 1 drugs and the potential for further BCS extensions, particularly biowaivers for at least some Class 3 drugs whose formulations exhibit very rapid dissolution.

It has been postulated that it may be possible to link Disc Intrinsic Dissolution Rates (DIDR) to the BCS solubility classification. There are problems associated with the equilibrium solubility measurement and excess of drug is required and guidelines are not sufficiently clear. Yu et al (2004) determined the DIDRs of 6 low solubility and 9 high solubility drugs and compared to their BCS solubility class membership. The test showed a strong relationship between DIDR and BCS

classification with 0.1 mg/min/cm^2 as a class boundary unless the dose is extremely high or low where discrepancies may exist between solubility and DIDR methods. Authors concluded that more research was needed before DIDR can be considered to classify drugs instead of solubility (The United States Pharmacopeia and the National Formulary 2003; Yu et al. 2004).

1.3.2 Strategies to improve drug solubility

Various techniques have been used to improve drug solubility. When one particular technique does not give a satisfactory outcome, a combination of techniques should be considered.

Commonly used techniques to improve drug solubility include: salt formation (see section 1.3.3), alteration of the solid state: polymorphs, solvates and amorphous forms and the use of solubilising excipients. These include: pH adjusters, water-soluble organic solvents, medium-chain triglycerides, long-chain triglycerides, cyclodextrins (CDs) and phospholipids (Strickley 2004).

- *pH adjustment*: two-thirds of all drug entities have ionizable groups and act as weak electrolytes in aqueous solution (Stahl and Wermuth 2002). The solubility of a compound is greater in the ionized state than in the neutral. Adjusting the pH with NaOH of HCl or with a buffer such as citrate, acetate, phosphate or Tris, can often increase the solubility of the drug in a vehicle. For oral formulations, the pH should generally be within the range of 2-9. Weak acids can be solubilised at pHs above their pK_a values and weak bases can be solubilised at pHs below their pK_a.
- *Cosolvents*: as opposed to pH adjustment or salt formation, the use of cosolvents can be applied to the solubilisation of non-ionizable drugs. Following the principle of "like dissolves like", the polarity of water is reduced by mixing with other less-polar hydrophilic solvents and thus, increasing the solubility of non-polar, water-insoluble substances. Solubility of a cosolvent system typically increases logarithmically with the linear increase in the fraction of the organic solvent(s). Cosolvents are often used in combination of pH adjustment. The most commonly used cosolvents are: polyethylene-glycol-400 (PEG-400), propylene glycol, ethanol, glycerine, dimethylacetamide (DMA) and N-methyl-2-pyrrolydone (NMP). One disadvantage of cosolvent systems is their precipitation behavior when diluted with water or aqueous body fluids. Precipitation can occur resulting in reduced bioavailability. Also cosolvents often show concentration-dependant tolerability issues.

- *Complexation*: Complexation using cyclodextrins (CDs) is a well-known approach. CDs are a family of cyclic oligosaccharides, the most common being α, β, and γ, consisting of 6-8 D-glucopyranosyl units, presenting a hydrophilic outer surface and a lipophilic cavity to which a hydrophobic guest molecule can complex (Szente and Szejtli 1999). Natural CDs have limited applications due to their limited aqueous solubility. Chemically modified CDs, such as hydroxypropyl-β-cyclodextrin (HPβCD), can have a much greater solubility. CDs normally combine to form a 1:1 complex. The binding constant, the intrinsic solubility of the drug, the dose requirement for the formulation and maximum amount of CD that the formulation can accommodate are important parameters in development (Rao and Stella 2003). Complexation with CDs has been used in combination with cosolvents (Faucci and Mura 2001) and with salt formation in the case of flurbiprofen for transdermal delivery (Maitre et al. 2007). Disadvantages of CDs include: owing to the high molecular weight of the CDs, the application is usually limited to drugs of high potency; strict correlation between the structure of the guest molecule and cavity size of the CD molecule; limited solubility of the CD in water, therefore, limited maximum concentration that can be achieved; and if binding constant is too high, CDs can affect significantly absorption-metabolism-excretion/elimination (ADME) parameters (Miller et al. 2006).
- *Surfactants and micelles*: surfactants are mainly used for three reasons: to increase wettability, to increase the dissolution to prevent drug precipitation from formulation and to increase solubilisation through micellisation. Micelles are colloidal dispersions that form spontaneously, under certain concentrations, from ambiphilic or surface-active agents (surfactants), molecules of which consist of two distinct regions with opposite affinities toward a given solvent such as water. Micelles form when the concentration of these ambiphiles is above the critical micelle concentration (CMC). They consist of an inner core of assembled hydrophobic segments and an outer hydrophilic shell serving as a stabilizing interface between the hydrophobic core and the external aqueous environment. Micelles solubilise, within their core, molecules of poorly soluble, non-polar drug entities. The advantages of micellisation are several: (i) when compared to cosolvents, micelles have a lower tendency to precipitate on dilution, (ii) the stability of the drug can be increased by micelle formation and (iii) side-effects are often reduced. Some forms of micellar systems can avoid, due to their small size, not only rapid renal exclusion but also uptake by the reticuloendothelial system. The latter allows longer therapeutic level in blood and less frequent readministration. (Yamamoto et al. 2001). Disadvantages of micellar systems, on the

other hand, include: toxicity associated with surfactants, even with low concentrations, with non-ionic surfactants being the least toxic; often the drug absorption capacity of the micelle is too small and the extent of the solubilising effect is too low and surfactants may also change the pharmacokinetics of the coadministered drug. Micelles are, however, one of the most useful drug delivery techniques. A combination of micelle and cosolvents or complexation has been reported in few studies. In general, this strategy did not provide significant synergistic effects on solubilisation and they were dependant on the type and concentration of complexing agents, surfactant and cosolvent (Kawakami et al. 2004; Kawakami et al. 2006a).

- *Emulsions and microemulsions:* unlike micelles, an emulsion is a liquid system in which one liquid is dispersed in another immiscible liquid, usually in droplets, with emulsifiers to stabilize the dispersed system. In contrast to conventional emulsions, microemulsions, with much smaller droplet diameters, are thermodynamically more stable. If a poorly water-soluble drug is relatively lipophilic, it can be solubilised in an emulsion where it dissolves in the oil phase. In terms of reaching high dosing concentrations, these vehicles are often superior to other approaches such as pH adjustment, cosolvents and micelles. The formation of microemulsions usually involves oil, water, surfactant and cosurfactant. The role of the cosurfactant (which is not mandatory) is to increase the interfacial fluidity by penetrating into the surfactant film. Lipid emulsions have a significant impact on the coadministered drug by the digestion of the oil component *in-vivo* (Cuine et al. 2007). For example, danazol solubilisation was markedly affected by lipase-mediated digestion and a reduction in lipid (and an increase of surfactant) content resulted in increased drug precipitation. Consequently, the bioavailability of danazol decreased significantly when the lipid content in the formulation was reduced.
- *Nanosuspensions*: a nanosuspension is a submicron colloidal dispersion of pure drug particles, which possess a large surface area for enhanced dissolution. Following the Noyes-Whitney equation:

$$\frac{dC}{dt} = \frac{DS(C_s - C)}{h}$$

where:

dC/dt = dissolution rate

D = diffusion coefficient

S = surface area

h = diffusion layer thickness

C_s = saturated solubility

C = concentration of the drug in bulk solution

A reduction in particle size from 10 μm to 200 nm increase the surface area by 50-fold, which may have a profound effect on drug solubility. Particle size reduction can significantly affect bioavailability of dissolution rate-limited drugs (Liversidge and Cundy 1995). Nanoparticles are typically produced by wet milling, homogenization or precipitation techniques. They are thermodyanamically unstable, with particle regrowth being common, and surface stabilizers are required to maintain particle size. The most commonly used excipients are celluloses, Pluronics®, polysorbates and povidones (Liversidge and Cundy 1995). Nanosuspensions do not work well for basic drugs with highly pH-dependant solubility. When administered orally, the nanoparticles of the basic drugs dissolve in the stomach, only to precipitate out in uncontrolled particles again (Peagram et al. 2005).

1.3.3 Salt formation

Salt formation is a simple way of modifying the properties of a drug having ionisable functional groups in order to overcome some undesirable characteristic of the parent drug. An active pharmaceutical ingredient often has suboptimal physicochemical or biopharmaceutical properties that can be overcome by pairing a basic or acidic drug molecule with a counterion to create a salt version of the drug. Physicochemical characteristics of a drug can be dramatically altered by salt formation (Berge et al. 1977; Bighley et al. 1996). Around 50% of drugs are administered as salts (USP 2006). If the free acid or base is a water-soluble solid with a high melting point, preparing a salt is often unnecessary (Stahl and Wermuth 2002).

Salts are formed when compound that is ionised in solution forms a strong ionic interaction with an oppositely charged compound leading to the precipitation of the salt form. The counterions are attracted by intermolecular coulombic forces. These interactions change the potential energy landscape and lead to stronger interaction between the charged active pharmaceutical ingredient and polar aqueous solvents, which can result in enhanced dissolution rates and higher apparent solubility on physiological timescales, resulting in increased drug delivery rates *in vivo*. For the salt to be dissolved the solvent must overcome the crystal lattice energy of the solid and create space for the solute. Thus, the solubility of the salt depends on its polarity, lipophilicity, ionisation potential and size. A salt's solubility also depends on the properties of the solvent and solid, such as the crystal packing and the presence of solvates.

The advantages and disadvantages of salt formation for manipulation of drug properties are summarised in Table 1.1:

Table 1.1Advantages and disadvantages of salt formation (adapted from Kumar, 2008)

Advantages	Disadvantages
• Altered solubility and dissolution rate • Controlled-release potential • Improved thermal, hydrolytic and photostability • Reduced hygroscopicity • Improved permeability • Improved organoleptic properties • Improved drug efficacy • Reduced pain on injection • Altered melting point resulting in improved milling and formulation properties • Ease of purification and handling • Improved compactability • Extended patent protection	• Decreased percentage of active content • Increased potential for formation of solvates and polymorphs • Reduced dissolution rate or solubility for hydrochloride salts in gastric fluid • Increased chance of poor solid-state stability at the microenvironment pH of the salt e.g. precipitation of the free acid in the gastrointestinal environment. • Corrosiveness of salts, resulting in tabletting problems • Possible dissociation of hydrochloride and hydrobromide salts, resulting in the release of hydrohalide gas or reaction with excipients or process-related chemicals • Additional step in synthesis of medicinal product • Only suitable for ionisable compounds

A large number of different salt forms are potentially available for application as the counterion. A lack of planning could result in many failures and may cause loss of time and substance. A well formulated decision tree will help scientists to choose a suitable salt for development in an efficient and timely manner.

The following criteria are desirable for a particular salt form:

- High aqueous solubility, over a wide pH range, depending on the intended pharmaceutical profile
- High degree of crystallinity
- Low hygroscopicity, for consistent performance
- Optimal chemical and solid-state stability under accelerated conditions

A serious deficiency in any of these characteristics should exclude the salt for further development. Other influential criteria are:

- Limited number of polymorphs
- Ease of synthesis, handling and formulation development

The solubility product of a salt, $K_{sp,}$ needs to be taken into account when predicting the solubility of a salt in a particular environment that contains other salts with a common counterion. A preliminary investigation of the pH-solubility profile with different counterions provides an indication of the counterions best suited to maximize the solubility. Marra-Feil and Anderson (1998), demonstrated that multiple counterions added in predetermined amounts so as not to exceed the solubility product K_{sp} of any salt, provided significantly higher solubility that any single counterion.

In spite of the abundance of available counterions, few are used frequently. USP (2006) showed that salt forms (56.15%) are generally preferred over free acid or base forms of a drug (43.85%). Hydrochloride (63%) and sodium (40%) salts remain the favourite counterions in salt formation with basic and acidic drugs, respectively. Because of the low solubility of many basic drugs, where pH_{max} (pH of maximum solubility of the salt) is very low, most common carboxylic acids do not form acceptable salts and it is anticipated that the use of relatively strong counterions will continue in the future. Similarly, 14 out of 19 salt forms of new chemical entities approved by the FDA from 1995 to 2006 are prepared with strong alkalis such as NaOH and KOH, and this trend is also expected to continue in the future (Serajuddin, 2007).

1.4 Selecting drugs and counterions

Carboxylic acids readily form salts with amine counterions. In this thesis, the selection of drugs and counterions was based on architectural and physicochemical properties, such as hydrogen bonding potential, to identify those parameters (such as molecular flexibility, hydrogen bonding network, preferred crystal lattice) that have an impact on mechanical properties.

Three different carboxylic acid drugs were selected for this study: flurbiprofen, gemfibrozil and diclofenac, similar in size but differing in shape and flexibility (see Fig 1.4).

Fig 1.4 Flurbiprofen, gemfibrozil and diclofenac molecules

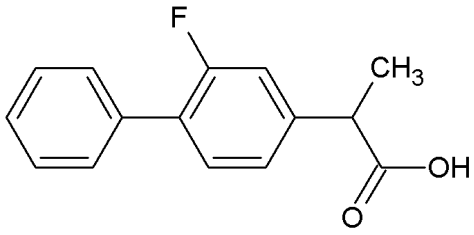

Flurbiprofen

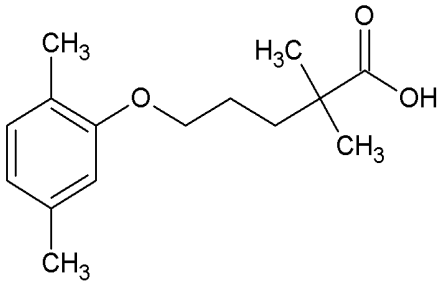

Gemfibrozil

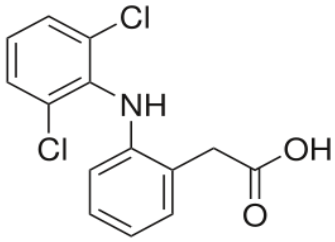

Diclofenac

Three different series of counterions were chosen: series number one, with increasing bulk and no hydroxyl groups to limit the hydrogen bonding potential: adamantamine (Adam), benzylamine (Benz), cylopropylamine (CProp), cyclobutylamine (CBut), cyclohexylamine (CHex); series number two, with tert-butylamine as the initial molecule and an increasing number of hydroxyl groups to complete the series: tert-butylamine (TBut), 2-amino-2-methyl-propan-1-ol (AMP1), 2-amino-2-methyl-1,3-propanediol (AMP2) and tromethamine (Tris) and finally a third series of alkanolamines: monoethanolamine (MEA), diethanolamine (DEA) and triethanolamine (TEA) (see Fig 1.5). All counterions are commercially available.

In 1987, the German BGA, the Federal Health Authority, recommended to the manufacturers of cosmetics to stop using secondary amines in cosmetics as neutralising and alkalising agents, reasoning that these amines might react with the N-oxides of the atmosphere to form absorbable nitrosamines. In view of this recommendation, it appears advisable to avoid such counterions, e.g. diethanolamine, diethylamine, N',N-dibenzyl-1,2-ethylenediamine (benzathine) and piperidine.

Figure 1.5 Structures of the selected counterions

Series 1

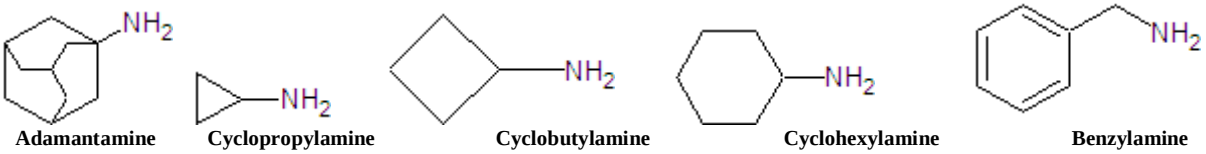

Adamantamine **Cyclopropylamine** **Cyclobutylamine** **Cyclohexylamine** **Benzylamine**

Series 2

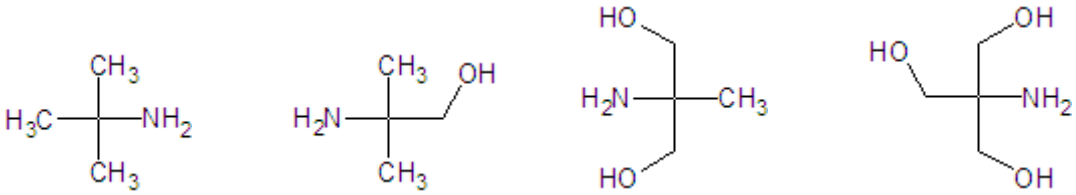

Tertbutylamine **AMP1** **AMP2** **Tris**

Series 3

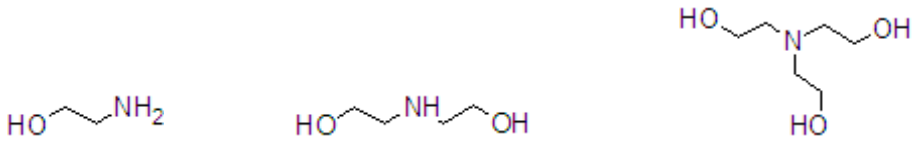

MEA **DEA** **TEA**

In 1984, the German BGA had initiated an action directed towards reducing the use of triethanolamine in pharmaceuticals. Later, this action was extended to nitrosable amines as neutralising or alkalising agents in pharmaceuticals. According to the current approval practice in Germany, drug products for internal use must not contain nitrosable amines, while those are tolerated in products for external use, with the constraint that the nitrosamines content of the starting material does not exceed 50 ppm. This applies to secondary amines. Moreover, in Switzerland the IKS banned triethanolamine and its salts from use in pharmaceuticals for internal drug products and those for external/topical and for parenteral use in humans. The decision came into effect in 1992 for all products for internal use (Anonimous 1991).

Despite the undesirability of the nitrosable amines as counterions, from a toxicological perspective, the decision to include them in this study was based on architectural grounds only. The idea was to explore relationships between crystal structure and physicochemical and mechanical properties and

establish general rules regarding which architectural parameters of counterions provide salts with favorable physiochemical and mechanical properties.

1.5 Mechanical properties

The relationships among compaction pressure, tensile strength, and solid fraction are critical to understanding and characterizing the compaction process. The faces of the three-dimensional plot shown in Fig 1.6 reflect the relationship among tabletability, compressibility, and compactability (Sun and Grant 2001c).

Fig 1.6 Three-dimensional relationship among compaction pressure, tensile strength, and solid fraction for a hypothetical material. Adapted from (Tye et al. 2005)

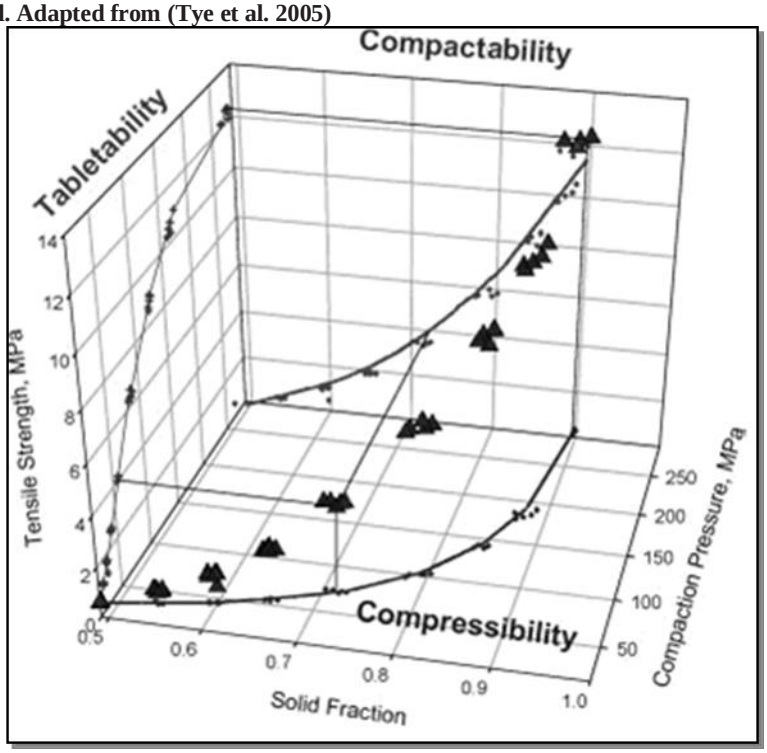

- *Tabletability* is the capacity of a powdered material to be transformed into a tablet of specified strength under the effect of compaction pressure (Joiris et al. 1998). Tabletability describes the effectiveness of the applied pressure in increasing the tensile strength of the tablet and demonstrates the relationship between the cause, i.e. the compaction pressure, and the effect, i.e. the strength of the compact.

- *Compressibility* is the ability of a material to undergo a reduction in volume as a result of an applied pressure (Joiris et al. 1998). Compressibility indicates the ease with which a powder bed undergoes volume reduction under compaction pressure and is represented by a plot showing the reduction of tablet porosity with increasing compaction pressure.
- *Compactability* is the ability of a material to produce tablets with sufficient strength under the effect of densification (Joiris et al. 1998). Compactability shows the tensile strength of tablets normalized by tablet porosity. In many cases, the tensile strength of a tablet decreases exponentially with increasing porosity.

The tensile strength of a compact is the direct result of its solid fraction. However, the relationship between applied pressure and the resulting tensile strength is more indirect.

1.5.1 Tabletting process

During the tabletting process, the powder mass must form a coherent compact that stays intact upon ejection out of the die. The consolidation mechanisms involved are influenced by the physicochemical nature of the material and the surface area of the contact points. The predominant consolidation mechanisms are listed below:

1. Mechanical theory: as the particles undergo deformation, the particle boundaries intertwine to form mechanical bonds.
2. Intermolecular forces: van der Waals forces bond the molecules at the newly sheared surfaces of the particle boundaries.
3. Liquid-surface film theory: thin liquid films form at the surface which bond particles together. The energy of compression causes melting or solution at the surface of the particle interface with subsequent solidification of crystallisation thus resulting in bonded surfaces.

After compression and consolidation the powder must be able to withstand the stresses of decompression and ejection. The same factors that impact on the compression process play a role during decompression. After application of the maximum compression force, tablets undergo elastic recovery. While the tablet is in the die, elastic recovery only occurs in the axial direction. If the elastic recovery is significant tablets may cap or laminate. Tablets that do not cap or laminate are able to relieve stress by plastic deformation. Since plastic deformation is a time-dependant process, fracture during deformation is affected by the rate of decompression, as the tablets are not able to relieve the stresses created in the process. In general, lower decompression rates result in stronger tablets.

After decompression the tablet remains in the die. Tablet ejection forces are described in three stages:

1. The initial ejection peak force required to break the tablet adhesion to the die wall.
2. Forces required to push the tablet up the wall die. This force is usually lower than the previous one.
3. Declining forces as tablet emerges from the die.

There are a number of challenges during tablet dosage form development that can impact on critical quality attributes (see Table 1.2):

Table 1.2 Problems during the tabletting process

*Tablet hardness**	*Sticking**	Potency
*Friability**	*Scale up**	Content uniformity
*Excipient selection**	*Disintegration**	Weight variation
Blend uniformity	*Drug Release/Dissolution**	*Capping**
Segregation	Stability	*Lamination**
*Machine speed effects**	*Powder flow**	

In italics*, those significantly affected by mechanical properties

1.5.2 Factors affecting tensile strength

A number of parameters can affect the tensile strength of the resulting compact.

1.5.2.1 Force of compression

As the compression force increases, tensile strength of tablets also increases then it may level into plateau or for some compounds even result in lamination or capping of tablets. At large pressures disintegration time can increase with increasing compression force as the pores within the tablet become smaller. This is more significant for plastic materials, such as aspirin, Avicel, or some forms of lactose (Bateman 1987).

1.5.2.2 Tabletting speed

It is well known that compression speed can have significant effects on the compaction properties of pharmaceutical powders. This is a challenge during scale up and technology transfer when tabletting speeds are significantly increased compared to speeds used in drug characterization stages. The tabletability and compressibility of some materials were observed to be dependent on the compression

speed whereas the compactability of all materials tested was essentially independent of tabletting speed (Tye et al. 2005). It is therefore proposed that the compactability profile (tensile strength vs. solid fraction) is a predictor that is independent of tabletting speed and can be used to predict tablet strength during formulation development and scale up. It is believed that this time dependency of tabletability and compressibility arises from stress relaxation after compaction for materials undergoing primarily plastic deformation. For these materials, consolidation decreases as speed increases (Armstrong and Govan 1988). However, compaction of brittle materials is less speed dependent because fragmentation is rapidly achieved and prolonged exposure to the force has a more limited effect on tablet properties.

1.5.2.3 Particle size

Reports on the influence of particle size on tabletting are conflicting. For most powdered pharmaceuticals, compaction of smaller particles results in stronger tablets because the smaller particles provide a larger total area for bonding than larger particles (McKenna and McCafferty 1982; Sun and Grant 2001a). However, the effects of the initial particle size on the strength of tablets depend on the mechanical properties of the materials. For example, dicalcium phosphate and sucrose undergo extensive fragmentation under pressure, and their tablet strength is independent of variations in particle size (Alderborn and Nystroem 1982). For sodium chloride, tablet strength increases with increasing particle size because of the formation of strong bonds in the form of solid bridges (Alderborn and Nystroem 1982).

Sun et al. (2001a) observed that the tensile strength of L-Lysine tablets, prepared by compacting smaller crystals, reached a plateau value at a lower compaction pressure than for larger crystals because of the greater compressibility of the smaller crystals. At any given pressure, larger crystals formed tablets of lower tensile strength. However, the effects of particle size on tensile strength appeared less significant when the particle size was greater than 595 µm. In explanation, the fragmentation of larger crystals under pressure reduces the effects of differences in initial particle size.

Compaction speed has also been found to play an important role in determining the effects of initial particle size on tensile strength. At slower compaction speeds, larger sodium chloride particles lead to higher tensile strength. However, when the compaction speed is increased, the tensile strength of compacts comprising larger particles is lower than that of smaller particles (Sheikh-Salem and Fell

1982). For lactose, variation in tensile strength due to differences in initial particle size, are reduced as the compaction speed is increased, because the more extensive particle fragmentation of the starting material minimizes the impact of the initial differences in particle size (Sheikh-Salem and Fell 1982).

Milling and sieving are the most common methods employed for obtaining particles of different sizes. However, smaller particles obtained by milling and sieving contain more defects, corresponding to a lower crystallinity. Generally, lower crystallinity improves the binding properties of a powder because amorphous materials are not well-ordered and they contain a large amount of free volume and the lack of a long range network. Consequently, plastic flow increases the bonding area and results in stronger tablets (Hüttenrauch 1983).

Particle size dispersity has no influence on the evolution in tablet porosity and tensile strength during compression. However, the spread in particle size had a significant and complex influence on the short-term post-compaction increase in tablet tensile strength (Fichtner et al. 2005).

1.5.2.4 Granulation

Granulation aids in increased plastic deformation of the solid, which leads to higher speed dependence of the tablet consolidation. Indeed, more pressure is required to be applied to granulated systems in order to attain a specified porosity as the speed of compression is increased (Armstrong and Govan 1988). In pharmaceutical industry it is common to add binders after dry granulation to compensate for the loss in tensile strength. However, this practice can negatively affect the powder flowability and can cause segregation of the final blend upon processing or storage.

For the effect of solid state parameters on mechanical properties see section 1.6.2.

1.6 Crystal engineering

The rapidly growing field of crystal engineering is still in its formative stages. Crystal engineering is a form of supramolecular synthesis, where individual synthons are discrete molecules that use molecular recognition through intermolecular interactions to form supramolecular entities. Supramolecular chemistry is defined as the chemistry of molecular species generated by the formation of non-covalent interactions. The role of hydrogen bonding is critical in this area (Leiserowitz 1976; Leiserowitz and Nader 1977; Desiraju 2002; Desiraju 2005; Desiraju 2007). The

key is to identify robust hydrogen bonded synthons that behave predictably in different chemical environments. This "synthon robustness" is more common among ionic supramolecular hydrogen bonded synthons than in synthons occurring in organic molecules (Banerjee et al. 2006). A subgroup of the supramolecular synthons is the "supramolecular heterosynthon", which is defined as a supramolecular synthon between unlike but complementary functional groups. A robust, ionic, supramolecular heterosynthon exists for (R-NH_3^+)·(R'-COO^-), ammonium carboxylate salts. In such structures, hydrogen bonding motifs occur in rings. In an analysis of the carboxylate-ammonium H-bonding patterns in the Cambridge Structural Database (CSD) (Allen and Motherwell 2002), it was revealed that the $R_4^3(10)$ column, using graph-set notation (Bernstein et al. 1995), also known as Type II column (Nagahama et al. 2003), was the most commonly occurring pattern in these salts (75/126), whereas, the alternative sequence of alternating $R_4^2(8)$ and $R_4^4(12)$ columns, also known as Type III columns (Nagahama et al. 2003) (see Fig 1.7), was the second most common (26/126). Two dimensional layers built up with $R_6^5(16)$ rings are the third most common network (19/126). When type II columns are joined by hydrogen bonds, then the 2-D resulting network is type V and, similarly, type VI networks are made up of joined Type III columns (see Fig 1.7).

Co-crystalisation constitutes a selective route to the concerted design of pharmaceutical compounds with desired pharmacokinetic and physical properties. Co-crystals are defined as a multi-component crystal that is formed between two compounds that are solids under ambient conditions, where at least one co-crystal former is molecular. Co-crystals may also play a role in modulating the physical properties of an API, including stability, solubility and dissolution (Remenar et al. 2003; Childs et al. 2004; McNamara et al. 2006). Co-crystal formation has also been used as a strategy to improve mechanical properties (see section 1.6.3).

1.6.1 Crystallography definitions

Crystal lattice refers to the regular spaced pattern resulting when atoms, molecules, or ions are arranged to form a crystal.

The space group of a crystal is a description of the symmetry of the crystal, and can have one of 230 types. A set of symmetry operations, also called point groups, like rotations or reflections, can leave a point fixed while moving each atom of the crystal to the position of an atom of the same kind. That is,

an infinite crystal would look exactly the same before and after any of the operations in its point group. There are 32 crystallographic point groups.

A lattice system is a class of lattices with the same point group. In three dimensions there are seven lattice systems:

1. Triclinic

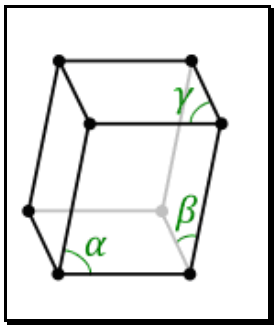

$\alpha \neq \beta \neq \gamma$ $a \neq b \neq c$

2. Monoclinic

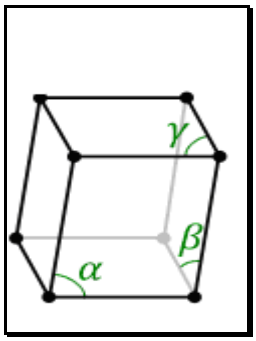

$\alpha \neq 90°\ \beta, \gamma = 90°$ $a \neq b \neq c$

3. Orthorhombic

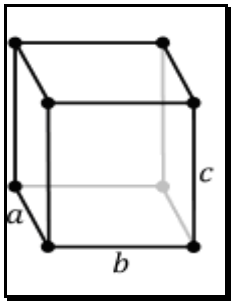

$\alpha = \beta = \gamma$ $a \neq b \neq c$

4. Tetragonal

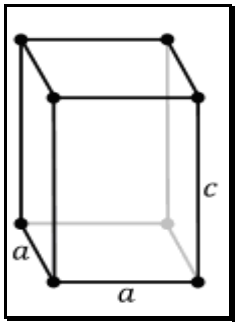

$\alpha = \beta = \gamma = 90°$ $a = b \neq c$

5. Rhombohedral

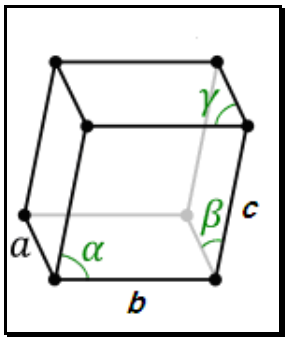

$\alpha = \beta = \gamma \neq 90°$ $a = b = c$

6. Hexagonal

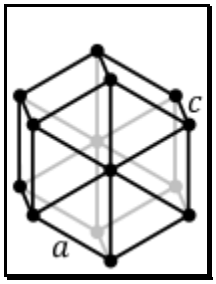

$\alpha = \beta = 90°$ $\gamma = 120°$ $a = b \neq c$

7. Cubic

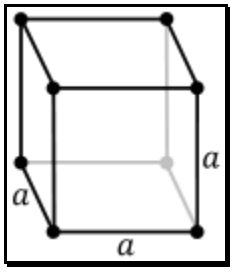

$\alpha = \beta = \gamma = 90°$ $a = b = c$

The space group is a combination of the translational symmetry of a unit cell including lattice centering, the point group symmetry operations of reflection, rotation and improper rotation (also called rotoinversion), and the screw axis and glide plane symmetry operations. The combination of all these symmetry operations results in a total of 230 unique space groups describing all possible crystal symmetries. The Hermann–Mauguin notation is used to represent the symmetry elements in point groups, plane groups and space groups. For example, the space group $P3_121$, exhibits primitive centering of the motif (once per unit cell), with a threefold screw axis and a twofold rotation axis.

1.6.2 Polymorphism

Many pharmaceutical solids can exist in different physical forms. Polymorphism is the ability of a drug substance to exist as two or more crystalline phases that have different arrangements and/or conformations of the molecules in the crystal lattice (Grant 1999). Polymorphs differ not only in the mode of packing but also in molecular conformation, also known as *conformational polymorphism*. Sometimes the same crystal cell has been seen with different molecular conformation (Bernstein 1987). Conformational polymorphism is normally observed only when the energy difference between the two lowest-energy conformers is small (Reutzel and Etter 1992).

Amorphous solids consist of disordered arrangements of molecules and do not possess a distinguishable crystal lattice. Solvates are crystalline solid adducts containing either stoichiometric or non-stoichiometric amounts of a solvent incorporated within the crystal structure. If the incorporated solvent is water, the solvates are also commonly known as hydrates.

Polymorphs and/or solvates of a pharmaceutical solid can have different chemical and physical properties such as melting point, chemical reactivity, apparent solubility, dissolution rate, optical and electrical properties, vapor pressure, and density. These properties can have a direct impact on the processability of drug substances and the quality/performance of drug products, such as stability, dissolution, and bioavailability. A very well known case of this is the ritonavir case; two years after the launch of Norvir® (an antiretroviral used in HIV treatment), some batches failed a dissolution specification. Investigation of this phenomenon revealed the existence of a crystal form of ritonavir other than the one already known (Form I). This new crystal form was designated as Form II, thermodynamically more stable and much less soluble, which potentially could have resulted in lower bioavailability and lack of efficacy (Bauer et al. 2001). These batches never reached the market.

Fig 1.7 One-dimensional type II and III versus two-dimensional type V and VI networks

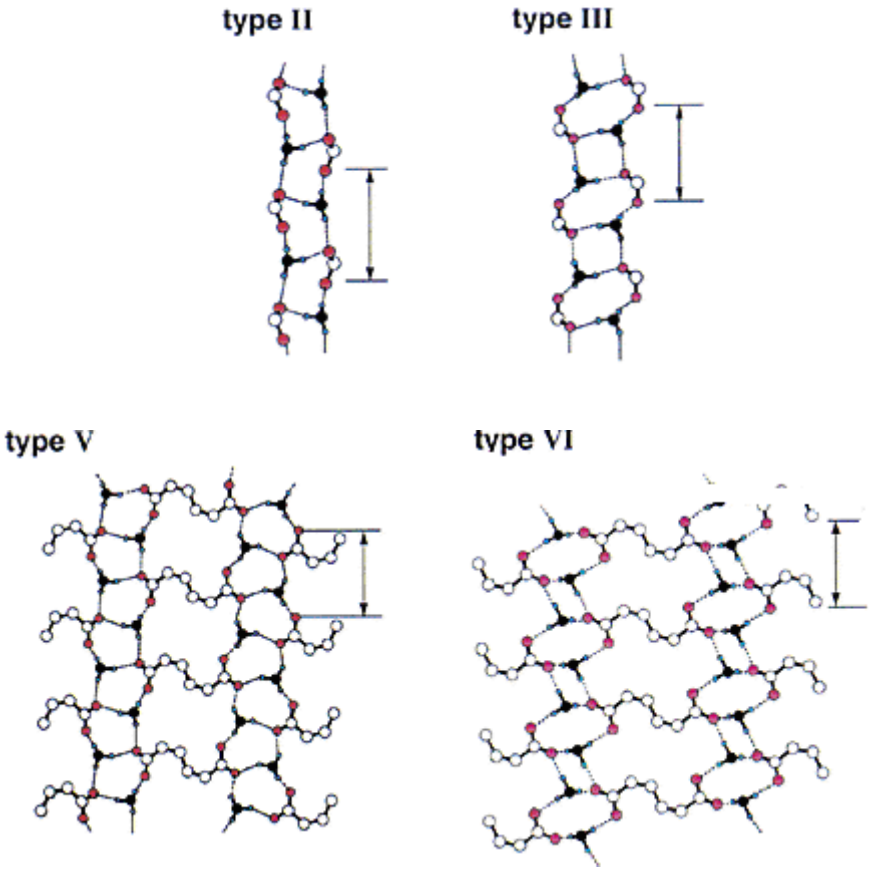

A metastable pharmaceutical solid form can change crystalline structure or solvate/desolvate in response to changes in environmental conditions, processing, or over time. The most stable polymorphic form of a drug substance is often used because it has the lowest potential for conversion from one polymorphic form to another while the metastable form may be used to enhance the bioavailability. Solid-state reactions include solid-state phase transformations, dehydration/desolvation processes, and chemical reactions. One polymorph may convert to another during manufacturing and storage, particularly when a metastable form is used. Since an amorphous form is thermodynamically less stable than any crystalline form, inadvertent crystallisation from an amorphous drug substance may occur as a consequence of the higher mobility and ability to interact with moisture. In addition, phase conversions of some drug substances are possible when exposed to a range of manufacturing processes (Brittain and Fiese 1999). Milling/micronization operations may result in polymorphic form conversion of a drug substance. In the case of wet granulation processes, where the usual solvents are aqueous, one may encounter a variety of interconversions between anhydrates and hydrates, or between different hydrates.

The selection of a polymorph of known stability is particularly important in the development of a stable formulation (Byrn 1982; Brittain 1999). Polymorphs are patentable and increasingly regulatory agencies require the identification of polymorphs in the formulation. Since polymorphs exhibit certain differences in physical properties (e.g., powder flow and compactability, apparent solubility and dissolution rate) and solid state chemistry (reactivity) attributes that relate to stability and bioavailability, it is essential that the product development and the review process pay close attention to this issue. This scrutiny is essential to ensure that polymorphic differences (when present) are addressed via design and control of formulation and process conditions to physical and chemical stability of the product over the intended shelf-life, and bioavailability/bioequivalence.

1.6.3 Solid state and mechanical properties

It is well known that physical and physicochemical properties of a substance such as mechanical properties, solubility or stability, etc. are directly linked with the characteristics of the corresponding crystals, i.e. the crystalline structure. Many drugs can exist in different polymorphic forms, but even isomorphic forms can have different crystal habits. Crystal habit is the description of the shape, size and appearance of the crystal and this can also affect the physical properties of the product. Compacts made from paracetamol in thin plate-like crystals exhibited higher elastic recoveries and elastic energies than compacts of the same polymorph of polyhedral crystals indicating that they underwent less plastic deformation during compression. Similarly with ibuprofen, the polyhedral crystal habit obtained from crystallisation from ethanol exhibited the better compression force/hardness profiles than the needles obtained from hexane (Garekani et al. 1999a; Garekani et al. 1999b).

Many pharmaceutical processes can induce changes in the material such as, creation of *amorphous regions* or *defects in the crystalline lattice*. One important difference between the two types of disorder is that while amorphous regions necessarily involve assemblies of molecules crystal defects can be as small a single dislocated molecule.

The amorphous form of pharmacologically active materials has received considerable attention because, in theory, this form represents the most energetic solid state of a material and thus it should provide the biggest advantage in terms of solubility and bioavailability. Using the amorphous form is a well known strategy to improve drug solubility (Hancock and Zografi 1997). The impact of amorphous versus crystalline state on mechanical properties is less clear. Shebatu and Alderborn

(1999) found that amorphous lactose produced tablets of higher tensile strength than crystalline lactose whereas Hancock, Carlson et al. (2002) found that compacts of a crystalline model drug were more ductile, less brittle and less elastic than those made from the amorphous form, but there were no major differences in the tensile strength.

Crystal defects on the other hand, represent imperfections in the crystal structure of the material. Also, impurities can be incorporated into the crystal lattice during crystallization, or which are taken up by the crystal from the vapor phase. The impurity interacts with the neighboring host molecules in a way which is different from the interaction between a host molecule and the surrounding host molecules creating defects. Defects can be further sub-categorized into point defects, line defects, planar defects and bulk defects. Point defects are the smallest; they do not extend in space in any dimension and at most involve a few atoms. Line defects, as the name indicates, are linear regions around which some atoms of the crystal lattice are misaligned. They are also known as dislocations and are a result of crystal lattice misalignment. Planar defects on the other hand occur where the crystallographic direction of the lattice changes. This happens mainly when two crystal nuclei grow and meet (grain boundary). In contrast to the other types, bulk defects are unique in the sense that they are essentially voids. These are small regions where crystal lattice vacancies accumulate. A defect, regardless of its type, retains a significant degree of the anisotropy of the original crystal, is localized in the crystal lattice and affects only a few molecules.

Regardless of the nature of disorder (amorphous or crystal defects), its presence results in what is characterized by its higher free energy. The impact of disordered cannot be overemphasized. The mechanical properties (Duddu and Grant 1995; Longuemard et al. 1998), dissolution rate (Burt and Mitchell 1981; Duddu and Grant 1995; Longuemard et al. 1998), surface energy (Carvajal and Staniforth 2006), moisture sorption (Kawakami et al. 2006b) and degradation rate (Dunitz 1995; Shalaev et al. 1997).

1.6.4 Slip planes

Slip planes correspond to the regions of weakest interaction between adjacent planes in the crystal lattice and have been used to explain differences in mechanical properties between polymorphs (Sun and Grant 2001c), hydrate/anhydrates (Sun and Grant 2004; Joiris et al. 2008) and structurally related molecules (Feng and Sun 2007) and co-crystals. Slip planes allow slippage of one layer over the adjacent one, enabling greater plastic deformation to produce stronger tablets.

The differences in the tabletting performance of sulfamerazine polymorphs in powder form has been explained by differences in their crystal structures, specifically by the slip planes in Form I and their absence in Form II. The slip planes in polymorph I provide greater plastic deformation of the particles during compaction, which favors the formation of tablets that are stronger for Form I than for Form II (Sun and Grant 2001c). In the case of paracetamol, unlike the monoclinic form, orthorhombic paracetamol is suitable for the direct compression process. The crystalline structure accounts for its better compression behavior, because of the presence of sliding planes (Joiris et al. 1998).

The greater compactability of plate-shaped L-lysine monohydrochloride dihydrate (LMH) when compared to prism-shaped LMH is related to favorable orientation of the slip planes in the tablet, corresponding to greater plasticity under load despite being the same phase (Sun and Grant 2001b).

Tabletting performances of anhydrate and monohydrate crystals of p-hydroxybenzoic acid were compared. The results suggested that the water of crystallisation in crystals of p-hydroxybenzoic acid monohydrate acts as a lubricant that facilitated easier plastic deformation of hydrate crystals than of anhydrate crystals, thereby conferring better tabletting performance. Water molecules in the p-hydroxy-benzoic acid monohydrate crystals assume a space-filling role, which increases the separation of the layers. This effect allowed easier slip between layers and provided greater plasticity of the crystals, which increased the interparticulate bonding area under the same compaction pressure. The greater bonding strength that results was reflected in greater tensile strength of the p-hydroxy-benzoic acid monohydrate compacts at zero porosity (Sun and Grant 2004). Similarly for naproxen sodium anhydrous, di- and tetrahydrate, the interposition of water molecules between sodium naproxen molecules weakened intermolecular bonds, and these sites can behave like sliding planes under compression. Such structural changes may explain the improved compression behaviour and modified densification mechanism according to the amount of associated water (Joiris et al. 2008).

An investigation of the relationship between the slip planes and the tabletting performance of the crystals of methyl, ethyl, n-propyl, and n-butyl 4-hydroxybenzoate (parabens) was conducted (Feng and Sun 2007). The absence of slip planes in the methyl paraben crystal resulted in significantly poorer tabletting performance than the other three parabens. While slip planes were present in the crystals of ethyl, propyl, and butyl parabens, they exhibited different plasticity. Under the same compaction pressure, tablet tensile strength was higher for crystals with higher plasticity. The results

confirmed that high levels of plasticity, which can result from the presence of slip planes in the crystal lattice, plays a critical role in the formation of strong and intact tablets by means of powder compaction.

Co-crystal formation has also been used as a strategy to improve mechanical properties. By the formation of a 1:1 co-crystal of caffeine and methyl gallate, powder compaction properties could be profoundly improved. The selection criterion for co-crystals exhibiting superior compaction properties was the presence of slip planes in crystal structure. Tabletability of caffeine was acceptable at <150 MPa compession pressure. However, at >180 MPa, severe lamination of caffeine tablets suddenly occurred. Tablet tensile strength dropped sharply at >240 MPa. In contrast, the tabletability of the co-crystal was excellent over the entire pressure range. Tablet tensile strength of the co-crystal was ~2 times that of caffeine at <200 MPa, and the ratio gradually increased with increasing pressure, e.g., ~8 fold at 350 MPa. Poor tablet tensile strength was always associated with high elastic recovery and low plasticity (Sun and Hou 2008).

1.7 Aims and objectives

The aim of this study was to form different series of amine salts of acidic drugs and to establish predictive relationships between architectural characteristics and physicochemical and mechanical properties of the salts.

Salt formation is a well known strategy to improve drug solubility but it has not been explored as a strategy to improve mechanical properties. A better understanding of which factors of the solid state can have an influence on the mechanical properties of pharmaceutical powders can help to optimise and reduce cost of tablet manufacturing.

For this purpose, three different carboxylic acid drugs were selected: flurbiprofen, gemfibrozil and diclofenac, similar in size but varying in flexibility and shape. Three different series of counterions were also chosen: one with increasing bulk and no hydroxyl groups to limit the hydrogen bonding potential; a second one with increasing number of hydroxyl groups and finally a third series, related to the latter in number of hydroxyl groups but with different molecular shape and flexibility.

The objectives of this thesis were to:

- Form salts of the three drugs with the selected counterions

- Perform thermal and solubility studies of the salts using a range of techniques.
- Study the mechanical properties of the salts using a compaction replicator.
- Obtain single crystals of X-ray quality to determine the crystal structure.
- Investigate a possible predictive relationship between the mechanical properties and the crystal structures.

2 Materials and methods

2.1 Materials

Salts were prepared using flurbiprofen, gemfibrozil and diclofenac. Flurbiprofen was obtained from Aesica (Cramlington, England), gemfibrozil was obtained from DiPharma (Italy) and diclofenac sodium was obtained from Sigma-Aldrich. Tert-butylamine (TBut), 2-amino-2methyl-1propanol (AMP1), 2-amino-2-methyl-1,3-aminopropanediol (AMP2), tromethamine (Tris), monoethanolamine (MEA), diethanolamine (DEA), triethanolamine (TEA), adamantamine (Adam), benzylamine (Benz), cyclopropylamine (CProp), cyclobutylamine (CBut) and cyclohexylamine (CHex), were obtained from Sigma-Aldrich. All materials were of pharmaceutical grade. Acetonitrile and methanol of HPLC grade were supplied by Fisher (Loughborough, UK).

2.1.1 Salt preparation

The general method of salt preparation was adapted from Anderson and Conradi (1985). Each counterion (0.01 moles) was accurately measured using a Sartorious balance; each material was dissolved in 40 ml of acetonitrile, except those counterions that were already in liquid form. Solutions were added together and the precipitate was recovered by vacuum filtration. If precipitate did not form immediately, the solution was stored at -4 °C overnight. Products were dried at 40 °C under vacuum using a Gallenkamp vacuum oven for 12h

All salts were recrystallised from methanol and allowed to evaporate. The powders were stored in sealed containers until use.

In the case of FDEA, a thick gel was obtained. Different solvents were tried with the same result. It was observed that after some weeks it crystallised and so samples were stored under ambient conditions until crystallisation was complete.

In the case of diclofenac salts, the free acid was first obtained by dissolving diclofenac sodium in water and lowering the pH using hydrochloric acid. The precipitate was recovered by vacuum filtration and dried at 40 °C under vacuum using a Gallenkamp vacuum oven. Diclofenac salts were prepared by dissolving diclofenac acid and counterions in methanol. In the case of mono- , diethanolamine and Tris salts of diclofenac, acetone was used as solvent as described in the literature regarding those crystal structures available in the Cambridge Structural Database to minimise the risk

of polymorphism (Castellari and Ottani 1995; Castellari and Ottani 1996; Castellari and Ottani 1997a).

2.1.2 Confirmation of salt formation

2.1.2.1 Yield and purity

The amount of acid in each salt was compared to the theoretical ratio. One hundred mg of each salt was weighed, placed in a 100 ml class A volumetric flask and made up to volume with the same solvent used as the mobile phase to give a 1 mg/ml solution. Methanol:water 80:20 was used for FTris and FAMP1 and the diclofenac series, and acetonitrile:water 65:35 was used in all the other cases. The solution was analysed then by HPLC (see 2.3.1.2) to determine the concentration. Experiments were performed in triplicate.

2.1.2.2 Fourier Transform Infrared Spectroscopy (FTIR)

FTIR was used to confirm the transformation from carboxylic acid to a carboxylate salt. Infrared (IR) spectroscopy exploits the fact that molecules have specific frequencies at which they rotate or vibrate corresponding to discrete energy levels (vibrational modes). IR spectroscopy provides a qualitative fingerprint check for the identity of drugs and polymorphs. IR is rarely used for quantitative analysis.

Carboxylic acids exist predominantly as hydrogen bonded dimers in condensed phases. The protonated carboxylic acid yields absorption bands corresponding to a carbonyl stretch between 1690 and 1750 cm^{-1}. On deprotonation, the band shifts to a lower energy as its vibrational mode becomes coupled to that of the other oxygen, giving rise to an asymmetric feature between 1540 and 1650 cm^{-1} (Silverstein et al. 1991), for carboxylate salt absorption is lower than that for the carboxylic acid because of resonance (Fig 2.1). In the carboxylate anion, the electrons are delocalised and the C=O bond has less of a double character requiring less energy to stretch.

Because of the potential in qualitative fingerprint check FTIR was also used to discard pressure-induced polymorphic changes in compacts prepared for intrinsic dissolution studies and mechanical testing.

Fig 2.1 Resonance in the carboxylate anion

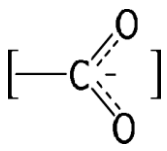

2.1.2.2.1 Equipment

A Unicam Mattson 3000 FTIR was used to analyse the samples and confirm salt formation. Galaxy software was used to interpret the results.

Pressure-induced polymorphic changes were ruled out by analysing the powder and compacts using attenuated total reflectance (ATR) mode on a Nexus FTIR system (ThermoNicolet, Cambridge, UK). Spectra were recorded from 4000 to 700 cm-1 using 64 sample/background scans and 4.0 cm-1 resolution.

2.1.2.2.2 Method

Fot the Unicam Mattson 3000 FTIR approximately 1 mg of sample was ground to a fine powder in a mortar together with 100 mg of KBr. The sample was placed in the die and subjected to 8 tonnes of pressure for 6 min to form a thin translucent disc.

The Nexus FTIR system does not require any specific sample preparation and recrystallised samples were used in analysis.

2.1.2.3 Nuclear Magnetic Resonance (NMR)

NMR was used to confirm salt formation and the proton count of the expected 1:1 salts. NMR is based on a property that magnetic nuclei have in a magnetic field and applied electromagnetic (EM) pulse or pulses, which cause the nuclei to absorb energy from the EM pulse and radiate this energy back out. The energy radiated back out is at a specific resonance frequency which depends on the strength of the magnetic field and other factors. The most common and sensitive nucleus is H^1. Proton NMR spectra of most organic compounds are characterized by chemical shifts in the range +12 to -4 ppm and by spin-spin coupling between protons. The integration curve for each proton reflects the abundance of the individual protons. The chemical shift, δ, describes the dependence of nuclear magnetic energy levels on the electronic environment in a molecule. The more a proton is shielded by its environment, the lower the δ value. Spin-spin coupling arises from the interaction of different spin states through the chemical bonds of a molecule and results in the splitting of NMR. Such coupling between pairs of nuclear spins is an important feature that is responsible for hyperfine structure in atomic spectra.

The reference point is taken as 7.25 ppm relative to tetramethylsilane (TMS) as this is the frequency at which the residual proton in chloroform absorbs. The area of each signal is proportional to the number of protons absorbing radiation.

Hydrogen in the carbon next to the carbonyl group usually come between 3.5-4 ppm in carboxylic acids, whereas in carboxylates they appear at lower chemical shifts (3.3-3.8 ppm).

2.1.2.3.1 Equipment

The samples were analysed using a Bruker AC 250 NMR operating at a frequency of 250 MHz. The number of performed scans was 16 with an acquisition time of 3 seconds.

2.1.2.3.2 Method

A small sample of drug was dissolved in deuterated dimethyl sulfoxide (DMSO) and filtered prior to analysis.

2.1.2.4 Powder X-ray diffraction (XRPD)

Max von Laue, in 1912, discovered that crystalline substances act as three-dimensional diffraction gratings for X-ray wavelengths similar to the spacing of planes in a crystal lattice. X-ray diffraction is now a common technique for the study of crystal structures and atomic spacing.

The interaction of the incident rays with the sample produces constructive interference (and a diffracted ray) when conditions satisfy Bragg's Law ($n\lambda=2d \sin\theta$). This law relates the wavelength of electromagnetic radiation to the diffraction angle and the lattice spacing in a crystalline sample. These diffracted X-rays are then detected, processed and counted. By scanning the sample through a range of 2θ angles, all possible diffraction directions of the lattice should be attained due to the random orientation of the powdered material. Conversion of the diffraction peaks to d-spacings allows identification of the crystal specimen because each material has a set of unique d-spacings. Typically, this is achieved by comparison of d-spacings with standard reference patterns.

X-ray powder diffraction is widely used for characterization of pharmaceutical materials. Applications include:

- Crystallinity determination: amorphous materials produce broad background signal instead of sharp peaks
- Quantification of polymorph mixtures

- Determination of unit cell dimensions
- Measurement of sample purity

2.1.2.4.1 Equipment

XRPD patterns were recorded on a PW 1729 Philips (Netherlands) 1983 (Cu anode operated at 35 kV and 40 mA).

2.1.2.4.2 Method

XRPD patterns were recorded at room temperature (25 °C). The samples were scanned from 5 to 80° two theta at a rate of 1.5° min^{-1}.

2.2 Thermal methods

2.2.1 Differential Scanning Calorimetry (DSC)

DSC was used to investigate the melting behaviour of all salts and carboxylic acids. The power compensation method relies on relies on sample and empty reference pans having separate heaters. Sample and reference are maintained at the same temperature and resulting in different amounts of heat being supplied to each specimen. The difference in power output to the heaters is monitored.

Single components can exhibit the following thermal behaviours: melting, crystallisation, boiling, sublimation, dehydration, desolvation, solid–solid transitions, glass transitions and polymorphic transitions. A standard DSC scan for an amorphous compound undergoing a glass transition (T_g), crystallisation (T_c), melting (T_m) and degradation is shown in Fig 2.2.

The purity of a crystalline compound can also be calculated from the enthalpy of fusion and the melting temperature using the van't Hoff equation. Requirements for purity determinations are low scanning speeds:

$$T_s = T_e - \frac{RT_e^2 X}{\Delta H_0 F_i}$$

where:

T_s is the sample temperature at equilibrium (K)

T_e is the melting temperature of the pure component (K)

R is the gas constant (8.314 J/mol/K)

X is the molar fraction of the impurity

ΔH_0 is the enthalpy of fusion of the pure compound (J/mol)

F_i is the fraction of the sample molten at T_s.

Fig 2.2 Thermal transitions of a compound

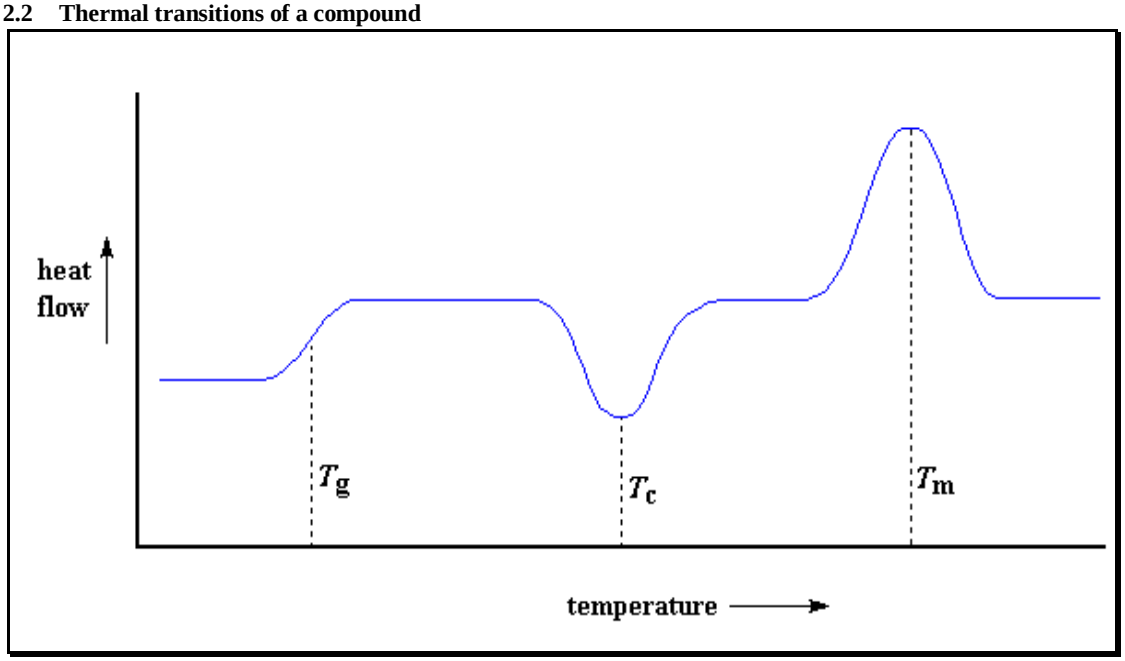

Quantification of crystallinity is possible with DSC. In the case of formulation of crystalline drugs, some conversion to the amorphous form can occur during processing, such as wet granulation, milling and compaction. This can have an important impact on the dosage form, in terms of both the chemical and physical stability of the compounds. In DSC scans, crystallisation can be observed as an exothermic transition, and samples that undergo crystallisation during heating necessarily have some amorphous content. However, there are amorphous compounds that do not recrystallise. The amount of energy released on crystallisation is related to the lattice energy of the crystalline compound, and thus DSC can be used to quantify the crystallinity of lyophilised or milled pharmaceutical compounds.

Similarly, many drugs and excipients can be made amorphous, either by quench cooling from above the melting temperatures or by techniques such as lyophilisation or spray drying. Amorphous materials can be characterised by their glass transition temperature. The glass transition temperature

may be important to define the propensity of amorphous compounds to crystallise at certain temperatures.

DSC can be a used for rapid screening of excipients in drug–excipient compatibility studies. There are several advantages in using DSC to evaluate drug–excipient compatibility.

DSC can be used as a quick stability screening method in conjunction with chromatographic techniques in degradation, decomposition and stability determinations. The advantage of DSC is the speed of the measurements and the small amount of sample that is required.

Crystalline materials may take-up water as part of their crystalline lattice or water may be associated in tunnels between the molecules of the lattice or associated such as in the case of clathrates. The nature of the water can be measured by subambient DSC and their stoichiometry can be calculated.

The selection of a polymorph of known stability is particularly important in the development of a stable formulation. Polymorphs are patentable and increasingly regulatory agencies require the identification of polymorphs in the formulation. DSC should not be used routinely for the quantification of different polymorphs, but it can be used to identify presence of different polymorphs of mixtures of them, for example, when batches have been manufactured differently.

2.2.1.1 Equipment

All thermal analysis measurements were performed on a Diamond DSC fitted with an Intracooler 2P-cooling unit (Perkin-Elmer). All measurements were performed under a nitrogen gas purge at a flow rate of 20 ml/min. The instrument was calibrated for temperature and heat flow using indium as a standard.

2.2.1.2 Method

Samples were weighed using a Kern 770 five decimal place balance and encapsulated into closed aluminium pans (Perkin-Elmer) and subsequently pressed to ensure a tight seal. Sample of 2–5 mg were used. Samples were run at a scan rate of 10 °C/min to a maximum of 250 °C or a temperature exceeding the melting point. All experiments were performed in triplicate.

Data acquisition and analysis were performed using the Pyris Manager software.

2.2.2 Thermogravimetric analysis (TGA)

TGA can be used in conjunction with DSC to calculate the material:solvent ratio in a solvate/hydrate. It uses a thermobalance, which allows for ongoing monitoring of sample weight as a function of temperature. TGA is most useful when materials incorporate solvent into their crystal lattice to form solvates/hydrates. On heating, the solvent is usually released at a discrete temperature or, if desolvation is a multistage process, at a series of discrete temperatures. TGA allows calculation of the stoichiometric weight of the solvent.

When a solvent/water participates in a linked hydrogen bond network, then the loss of the solvent typically results in a major change in the crystal structure and starts at a higher temperature than the previous case. Typically, when the solvent is not a direct participant in a hydrogen bond network, the void volume that would be present if the solvent was removed from this crystal forms channels that run parallel to the longest dimension of the crystal morphology. The solvent/water is usually lost through the smallest crystal surfaces. If the void volumes created by removing the solvent do not form channels in the crystals, then the rate of solvent lost would be lower, because there is no direct path for the solvent to escape from the crystal (Adeyeye and Brittain 2008).

TGA can be used in decomposition vaporisation studies but this is rarely used in pharmaceutical applications as drugs and excipients are not normally heated to decomposition temperatures, the important exception being dehydration reactions.

2.2.2.1 Equipment

A Perkin Elmer Thermal Analysis TGA 4 was used.

2.2.2.2 Method

Approximately 3 mg of sample was accurately weighed and placed in the aluminium basket. Analysis was carried out under nitrogen conditions and a heating rate of 10°C/min from 50-250°C.

2.3 Solubility and dissolution studies

2.3.1 High Pressure Liquid Chromatography (HPLC)

HPLC was the technique used to separate, identify and quantify the compounds in the solubility and dissolution studies. The solvent is forced through the column under high pressures. It allows you to use small particle size for the column packing material which gives a much greater surface area for

interactions between the stationary phase and the molecules flowing past it. This allows a much better separation of the components of the mixture. Reversed phase HPLC is the most common form of HPLC used. The column silica is modified to make it non-polar by attaching long hydrocarbon chains to its surface. A polar solvent is used. Polar molecules in the mixture will therefore spend most of their time moving with the solvent.

The time taken for a particular compound to travel through the column to the detector is known as its retention time. This time is measured from the time at which the sample is injected to the point at which the display shows a maximum peak height for that compound. Different compounds have different retention times. For a particular compound, the retention time will vary depending on:

- Pressure used
- Nature of the stationary phase
- Composition of the solvent
- Temperature of the column

Ultra-violet (UV) absorption is a common method of detecting substances that pass through the column. Many organic compounds absorb UV light of many wavelengths. The amount of light absorbed is proportional to the amount of the compound passing through the column.

2.3.1.1 Equipment

The HPLC system comprised a Hewlett-Packard Agilent 1100 system with G1312A Binary Pump, G1313AALS Auto-injector, G1316A COLCOM column section and a G1314A VWD variable wavelength detector. The HPLC was controlled by Chemstation software which runs on Windows 2000.

2.3.1.2 Method

Calibration and sample dilutions were made with the solvent mixture (65:35, acetonitrile: water for gemfibrozil and most of flurbiprofen series, and 80:20, methanol:water for FTris, FAMP1 and the diclofenac series); each drug was freely soluble in the relevant mix. Linear regression analysis was performed on a plot of standard concentration against a peak area and the resultant equation of the line was used to calculate the sample concentration from the response. In the case of FTris and FAMP1 salts, precipitation was observed when diluted in the mobile phase and a mixture of 80:20, methanol: water was used instead.

Working standards were prepared by serial dilution of a stock solution to produce samples in the range of 0.001-3.0 mg/ml. Calibration curves (see Figs 2.3-6). The chromatographic conditions were:

Drug:	**Flurbiprofen**
Injection volume:	1 µl
Mobile phase:	acetonitrile:water, 65:35
	methanol:water, 80:20
Wavelength:	250 nm
Flow rate:	1 ml/min
Runtime:	6 min
Column:	Thermo ODS-2-Hypersil 150 mm x 4.6 mm 5µm

Drug:	**Gemfibrozil**
Injection volume:	1 µl
Mobile phase:	acetonitrile:water, 65:35
Wavelength:	276 nm
Flow rate:	1 ml/min
Runtime:	5 min
Column:	Thermo ODS-2-Hypersil 150 mm x 4.6 mm 5µm

Drug:	**Diclofenac**
Injection volume:	1 µl
Mobile phase:	Methanol :water, 80:20
Wavelength:	274 nm
Flow rate:	1 ml/min
Runtime:	4 min
Column:	Thermo ODS-2-Hypersil 150 mm x 4.6 mm 5µm

Two parameters are important when constructing a calibration curve; the detection limit, LOD, the lowest concentration of a substance level that can be determined to be statistically different from an analytical blank o absence of substance and the quantification limit, QOL, is the limit at which the difference between two different values can be detected. They can be calculated as follows:

LOD and LOQ may be calculated based on the residual standard deviation of the regression line (SD) and the slope of the calibration curve (S) according to the equation:

$$LOD = \frac{3SD}{S}$$

Similarly:

$$LOQ = \frac{10SD}{S}$$

Fig 2.3 Flurbiprofen calibration curve with acetonitrile:water, 65:35 as mobile phase

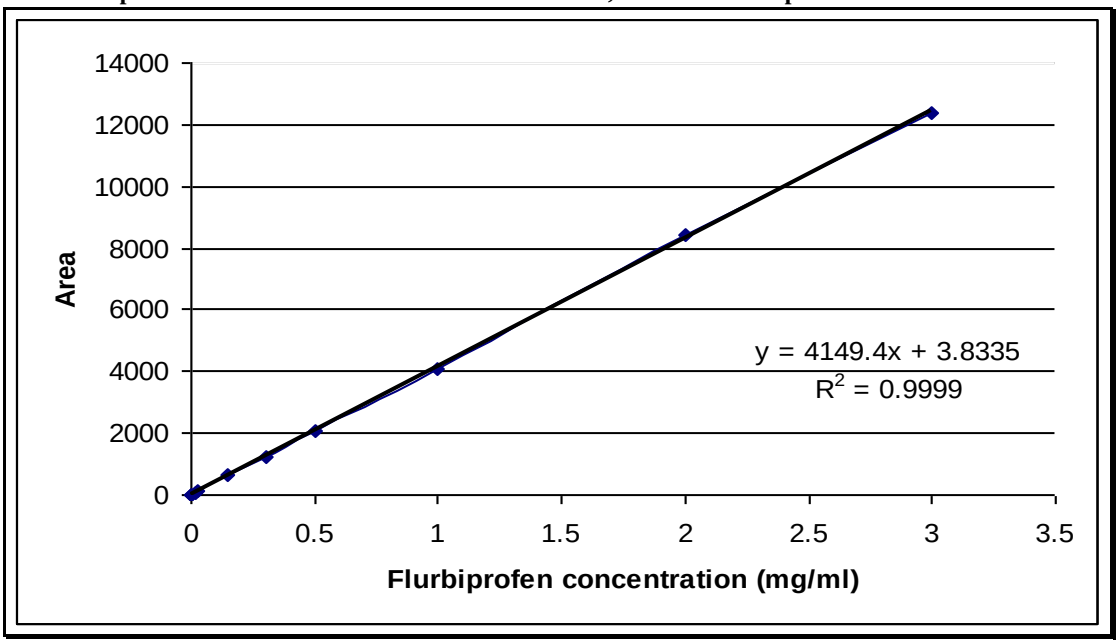

Detection limit	0.013 mg/ml
Quantification limit	0.043 mg/ml

Fig 2.4 Flurbiprofen calibration with methanol:water, 80:20 as mobile phase

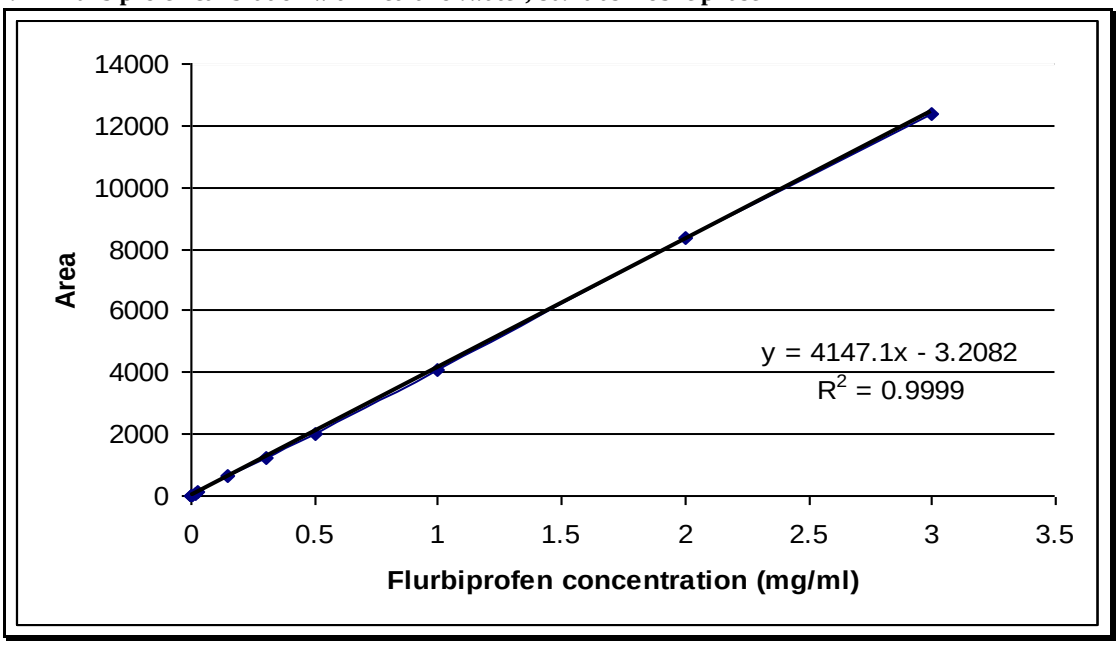

Detection limit	0.012 mg/ml
Quantification limit	0.041 mg/ml

Fig 2.5 Gemfibrozil calibration curve in acetonitrile:water, 65:35 as mobile phase

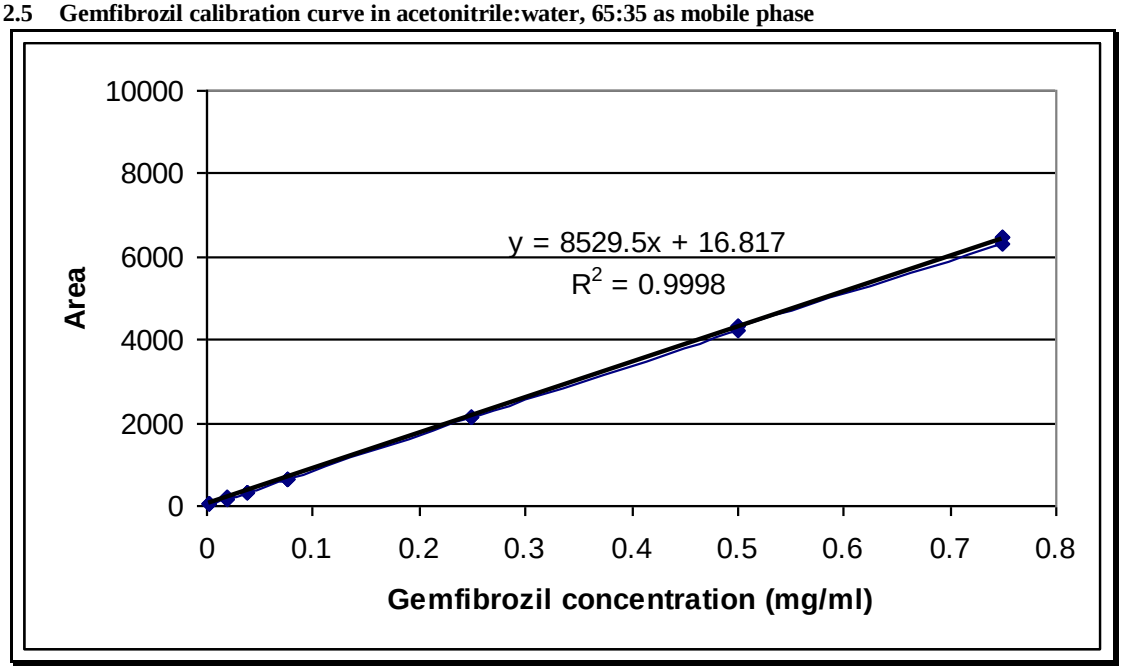

Detection limit	0.039 mg/ml
Quantification limit	0.13 mg/ml

Fig 2.6 Diclofenac calibration with methanol:water, 80:20 as mobile phase

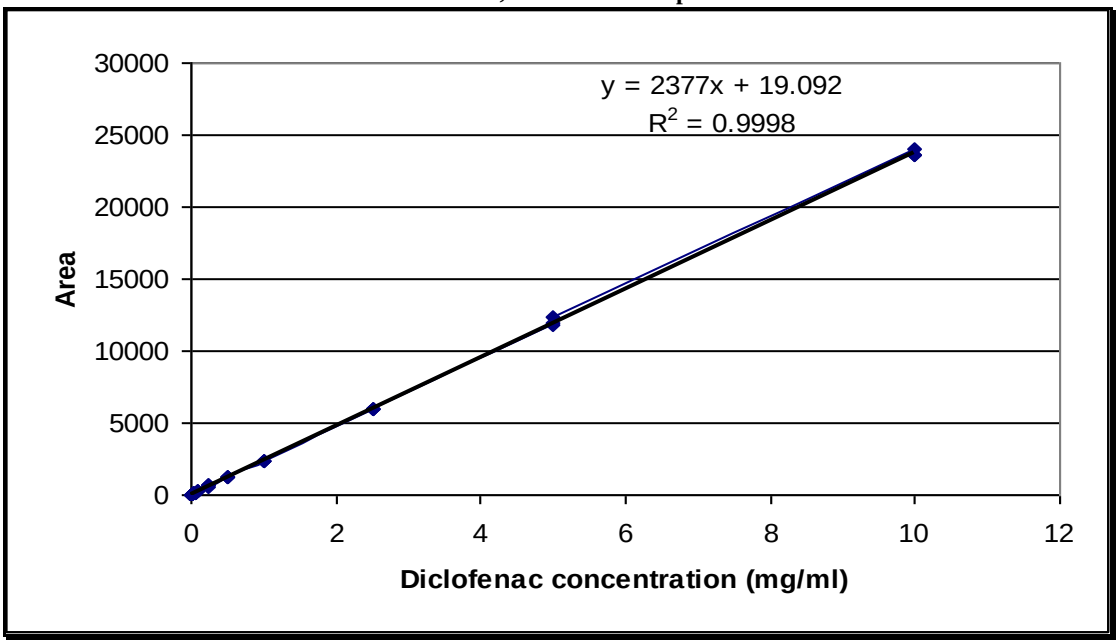

Detection limit	0.021 mg/ml
Quantification limit	0.071 mg/ml

2.3.2 Salt solubility

The aqueous solubility of an acidic or basic drug as a function of pH dictates whether the compound will form suitable salts or not and, if salts are formed, what some of their physicochemical properties

might be. pH–solubility interrelationships also dictate what counterions would be necessary to form salts, how easily the salts may dissociate into their free acid or base forms, what their dissolution behaviour would be under different GI pH conditions, and whether solubility and dissolution rate of salts would be influenced by common ions.

When a salt is added to water, the resultant solution can be neutral, acidic or basic. Interaction between the ions of the salt and the ions of water is called hydrolysis. Salts can be classified in 4 categories:

- Salts of strong acids and strong bases
- Salts of strong acids and weak bases
- Salts of weak acids and strong bases
- Salts of weak acids and weak bases

In the case of salts in this study, i.e, a weak acid with moderate to strong bases, these salts completely ionise in aqueous solution and the hydrolysis reaction results in a basic solution:

$$AB \rightarrow A^- + B^-$$

The conjugate anion A^- interacts with one molecule of water to form the molecular acid and hydroxide ion, resulting in alkaline solution:

$$H_2O + A^- \rightarrow AH + OH^-$$

The combined reaction is given by:

$$AB \rightarrow A^- + B^-$$

$$\updownarrow$$

$$AH + OH^-$$

The equilibrium expression is defined by:

$$K_b = \frac{[AH][OH^-]}{[A^-]} = \frac{K_w}{K_a}$$

$$pH = \frac{1}{2} pK_w + \frac{1}{2} pK_a + \frac{1}{2} \log[A^-]$$

where $[A^-]$ would be the solubility of the salt in water.

Fig 2.7 shows a schematic diagram for the pH–solubility interrelationship of a free acid and its salt form, which may be expressed by two independent curves, one where the free acid is the saturation or

equilibrium species at a pH below pH_{max}, and the other where the salt is the equilibrium species at pH above pH_{max}. When the free acid is the equilibrium species, it converts to a salt only if it is equilibrated with a solution at a pH above pH_{max} by adding a sufficient quantity of an alkali or counterion.

When the aqueous medium, at a given pH, is saturated with the free acid, the total solubility (S_T) at that pH may be expressed as:

$$S_T, acid\,(pH < pH_{\max}) = \frac{K_a}{[AH]+[A^-]} = [AH]+\left(1+\frac{K_a}{[H_3O]}\right) = [AH]\left(1+10^{\,pH-pK_a}\right)$$

$$S_T, salt(pH > pH_{\max}) = [A^-]+[AH] = [A^-]\left(1+\frac{[H_3O^+]}{K_a}\right) = [A^-]\left(1+10^{\,pk_a-pH}\right)$$

Fig 2.7 pH solubility profile of a free acid and its salt (adapted from Stahl, (2002))

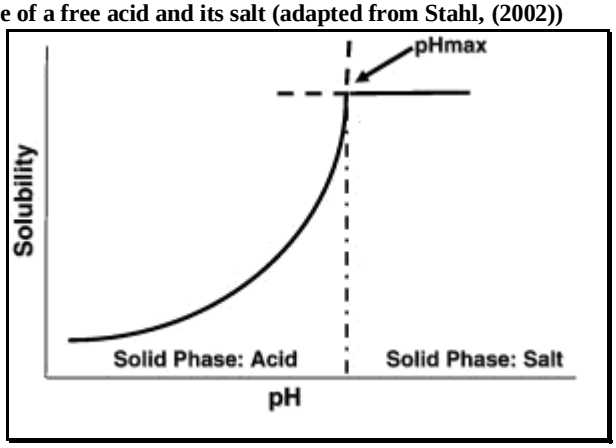

The point where both curves intersect is called the pH_{max}, the pH of maximum solubility. Only at the pH_{max} do the solid phases of both species coexist. At pH< pH_{max}, the solid phase comprises free acid and at pH> pH_{max} the solid phase comprises the salt. Interconversion from the salt to the free acid form or *vice versa* may occur if the pH shifts from one side of the pH_{max} to the other. There are numerous reports in the literature indicating that these equations are, in general, followed for solubilities of free acids and their salts (Anderson and Conradi 1985; Ledwidge and Corrigan 1998; O'Connor and Corrigan 2001a; O'Connor and Corrigan 2001b; Li et al. 2005). In all cases, salts had higher solubilities than their corresponding free acids, although solubilities of different salt forms of a particular acid can vary.

Intrinsic solubility, S_0, is defined as the solubility of the unionised form of a drug. A simple relationship between pH_{max}, pK_a, intrinsic solubility and salt solubility can be applied to a specific salt of a monoprotic compound:

$$pH_{\max} = pK_a + \log \frac{S_0}{\sqrt{K_{sp}}}$$

K_{sp} is related to the constant solubility achieved on the salt plateau and depends on the identity of the salt. Because S_0 and pK_a depend on the properties of the drug, not on those of the counterion, this equation can be used to describe the pH at which the maximum solubility is achieved. This is useful for pharmaceutical compounds because it can be used to ensure that the region of maximum solubility corresponds to the physiologically relevant pH range, or that the solubility of a solution formulation is governed by the desired solid form. Nonetheless, raising K_{sp} is perhaps the most valuable method for enhancing the solubility of pharmaceutical compounds because, unlike changes in S_0 and pK_a, it does not require any alteration to the molecular structure with the potential to adversely affect the pharmacological activity (see Fig 2.8).

It is generally accepted that the difference between the pK_a of the drug and the counterions should be at least 2-3 units. This is meant to make the proton transfer energetically favourable. When the pK_a of the counterion is not significantly different from the drug, a solid complex may form but it can rapidly disproportionate in an aqueous environment. In the case of salt forms of acidic drugs, the counterion must also bring the pH to a higher level than the pH_{max} to reach the salt plateau, at which the solubility of the salt prevails over the solubility of the free acid or base.

Although it can be simple to enhance solubility by exploiting the K_{sp}, unfortunately the opposite effect can also be achieved if ionised molecules in solution encounter counterions with which they form a less soluble salt. Similarly, excess counterion can drive the drug out of solution though the common ion effect (Serajuddin et al. 1987; Li et al. 2005).

2.3.2.1 Equipment

A Variomag electronic multipoint magnetic stirrer set at 500 rpm was used.

2.3.2.2 Method

Saturated aqueous solubilities were determined under ambient conditions (average 20-21 °C). Excess solid was added to around 15 ml of water and stirred for 48 hours. The experiment was performed in

triplicate and 5 ml was extracted with a plastic syringe and pH was measured. The sample was filtered though a 0.45 μm PTFE syringe filter and diluted 1:1 with mobile phase. Samples were analysed by HPLC.

2.3.3 Intrinsic Dissolution Rate (IDR)

Intrinsic dissolution is the measurement of the rate of drug dissolution per area of dissolving surface; while intrinsic rates greater than 1 mg/min/cm^2 suggest negligible problems with a dissolution rate limiting step in absorption, rates below 0.1 mg/min/cm^2 indicate the likelihood of such problems (The United States Pharmacopeia and the National Formulary 2003). It is measured using a compacted disc of a drug in aqueous buffer.

Fig 2.8 Effect of relevant parameters on pH_{max}, on alkali and their salts (Stahl, 2002)

A number of theories on the dissolution of solids have been proposed (Leeson and Carstensen 1974; Carstensen 1980; Grant and Higuchi 1990). However, the simple diffusion model (see Fig 2.9) may be adequate to describe the dissolution behaviour of most pharmaceutical solids. The diffusion layer model assumes that a thin film of saturated solution of concentration, C_s, exists at the interface of the dissolving solid and the dissolution medium.

Fig 2.9 Diffusion layer model of drug dissolution (Stahl and Wermuth 2002)

The dissolution rate is controlled by the diffusion rate of solute molecules from this thin saturated film into the bulk solution. By keeping the volume of the solvent large with respect to the saturation point, sink conditions are approximated. Sink conditions are the main experimental parameter to be controlled during dissolution testing, that is, C_b<10% of C_s.

For weak acids and bases the pH of the diffusion layer is especially important. Increasing C_s is an effective way of improving the dissolution rate of a drug. For example, if the particle size of a drug is decreased by a factor of 5, the surface area *S* increases by 5 times and, consequently, the dissolution rate also increases by a factor of 5. There is a limit to the extent of particle size reduction using conventional techniques such as milling (about 2-3 μm). On the other hand, salt formation may be able to increase C_s to 2 orders of magnitude, for example, and the dissolution rate would increase by a similar factor (Serajuddin 2007).

The USP chapter on Intrinsic Dissolution recommends that the test material is compressed with a bench-top tablet press for 1 min at the minimum pressure to form a non-disintegrating compacted tablet (The United States Pharmacopeia and the National Formulary 2003). Compression at 3.3 tonnes is sufficient for many organic crystalline compounds. The compression pressure plays an important role in the test; if it is too low, a non-disintegrating tablet may not be obtained and if it is too high, it may induce polymorphic changes. Drugs can undergo polymorphic transformations when subjected to temperature as well as pressure changes and other processing parameters (Byrn 1982).

The determination of IDR is a very simple procedure. IDR, along with permeability, is a rate phenomenon instead of an equilibrium phenomenon. It might be expected to correlate more closely with *in vivo* drug dissolution dynamics than solubility. Comparison of the aqueous solubility of various salts with the free form alone may not provide an indication of which form would result in optimal dissolution behaviour. The dissolution of a salt can be equal, higher or lower than that of the free form depending on the micro-environmental pH at the surface of the dissolving solid. However, the relative superiority of a salt over the free form may not be obvious from the IDR studies, because of the differences in the self-buffering capacity of the salt and the free form.

Dissolution methods are based on the USP (The United States Pharmacopeia and the National Formulary 2003):

1. *USP-1,* the rotating basket: Adopted in 1970 and was the first official method. It consists of a 1 inch diameter by 1-3.8 inch high stainless-steel mesh wire basket rotated at constant speed of 25-150 rpm. It is immersed in 900 ml of dissolution medium in a flask of 1000 ml capacity. The medium is kept at a constant temperature of 37 degrees by means of a suitable water bath. Other types of basket exist for specific applications. See Fig 2.10.
2. *USP-2,* the paddles method. It was originally developed in 1969. The USP specifications are identical except that the paddle is substituted for the rotating basket. Some of the dimensions and tolerances for the paddle are critical if consistent results are to be obtained from flask to flask. The USP specifies that the paddle must rotate smoothly without significant wobble. See Fig 2.11.

Fig 2.10 USP-1 Rotating basket method

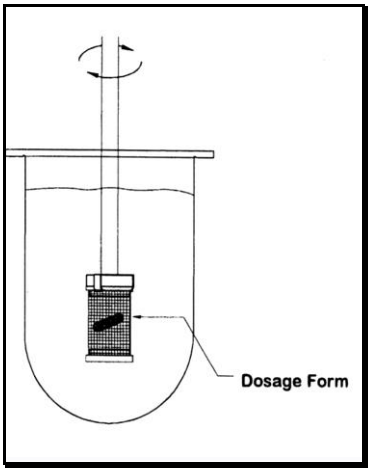

Fig 2.11 USP-2 Paddles method

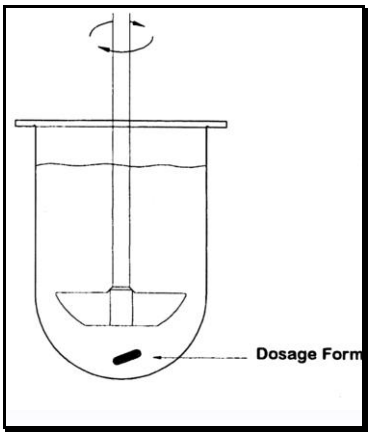

Commercially available IDR apparatus often consist of a die in which cylindrical compacts can be prepared where one face of the compact is exposed. Shaw (2001) developed an alternative method of IDR measurement that used poly-tetra-fluoroethylene (PTFE) disc holders. The PTFE holders fit the discs that were fixed in place with paraffin wax and one surface of the disc was exposed.

2.3.3.1 Equipment

A Hanson SEII 6-flask dissolution test station was used equipped with 1 litre round bottomed flasks and paddles. Discs were prepared using a Specac KBr press and 13 mm die abd placed in PTFE holders, which was based on the method described by Shaw (2001).

2.3.3.2 Method

Disodium hydrogen orthophosphate and citric acid for pH 4.5 and 6.8 buffer preparation were obtained from Sigma-Aldrich (Poole, UK).

The tablets were made using a pressure of 3 tonnes on a powder weight of 0.001 moles with a 1 min dwell time and 24 h recovery time. Infrared analysis was performed on every tablet to eliminate pressure induced polymorphic changes. At least 3 replicates were made of each compound. Tablets were carefully attached to PTFE holders so that no paraffin was present on the face of the tablet. Paddles were positioned 3 cm above the disc holder. It is important that stirring conditions are not causing a turbulent flow, as it can result in elevated dissolution rates (Emara et al. 2009).

Samples were taken using disposable 5 ml syringes at 10, 20, 30, 50, 70 and 90 min. Samples were filtered using 0.45 μm syringe filters and 0.5 ml diluted with 0.5 ml of mobile phase to be analyzed by HPLC. The remainder was returned to the dissolution bath. In the case of FMEA, FTEA and

FAMP2 it was observed that the disc dissolved completely within 20-25 min and closer sampling points were chosen at 5, 10, 15, 20, 25 and 30 min.

2.4 Crystallography

2.4.1 Crystal growing techniques

In order to produce high quality single crystals, the sample needs to be reasonably pure. While recrystallisation is a standard technique for purifying chemicals since the growing crystals exclude impurities, such impurities are likely to impede growth on certain faces leading to small size and distorted crystal morphology. Glassware should be clean but not obsessively cleaned. Dust particles often provide nucleation sites for crystal growth.

The most commonly used methods for growing X-ray quality crystals are:

- *Slow evaporation:* Saturated or nearly saturated solution is prepared and the container left open to allow evaporation.
- *Slow cooling:* This is useful for solute-solvent systems which are less than moderately soluble and the solvent's boiling point is less than 100 °C. A saturated solution of the compound is prepared where the solvent is heated to just boiling point or just below it. The vessel is transferred to a Dewar flask containing hot water (heated to a temperature of a couple of degrees below the solvent boiling point). The water level should exceed the solvent level in the vessel, but should not exceed the height of the vessel. Solution is left to cool very slowly and crystal will form.
- *Vapour diffusion:* This method is good for milligram amounts of material. A solution of the substance is prepared using a solvent, S1, and placed in a vessel. A second solvent, S2, is placed in a closed beaker. S2 is chosen such that when mixed with S1 the solute will become less soluble. The test tube containing S1 is then placed in the beaker and the beaker is sealed. Slow diffusion of S2 into S1 will cause crystals to form. If S2 is more volatile than S1 the solvent level will increase and prevent microcrystalline crusts from forming on the sides of the vessel (see Fig 2.12).

Fig 2.12 Vapour diffusion method for crystal growing

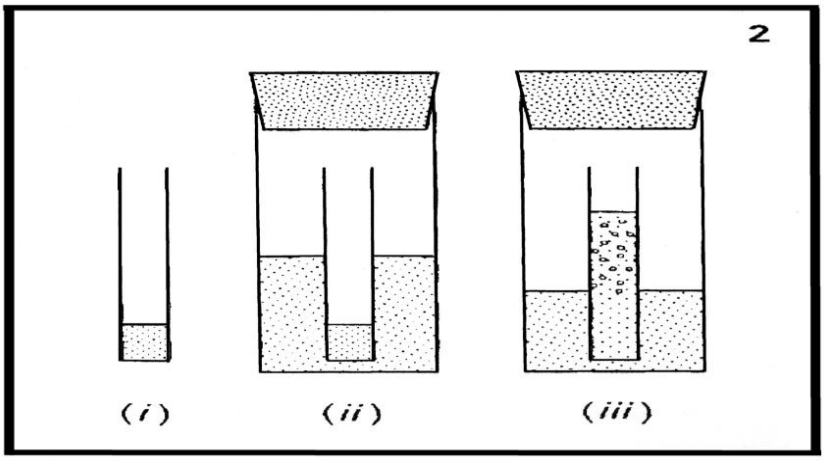

- *Liquid diffusion:* This method also is good for milligram amounts of materials which are sensitive to ambient conditions. Solute is dissolved in S1 and place in a vessel. A second solvent, S2, is slowly dribbled into S1 so that S1 and S2 form discreet layers. The density of S2 has to be greater than S1 (see Fig 2.13).
- *Sublimation:* Useful for volatile, air sensitive crystals. A sample has to be sealed under vacuum into a glass tube and placed the tube into an oven for a few days or weeks. Larger crystals tend to grow at the expense of smaller ones. The tube can be placed close to one end of the furnace so that there is a mild temperature gradient.

Fig 2.13 Liquid diffusion method for crystal growing

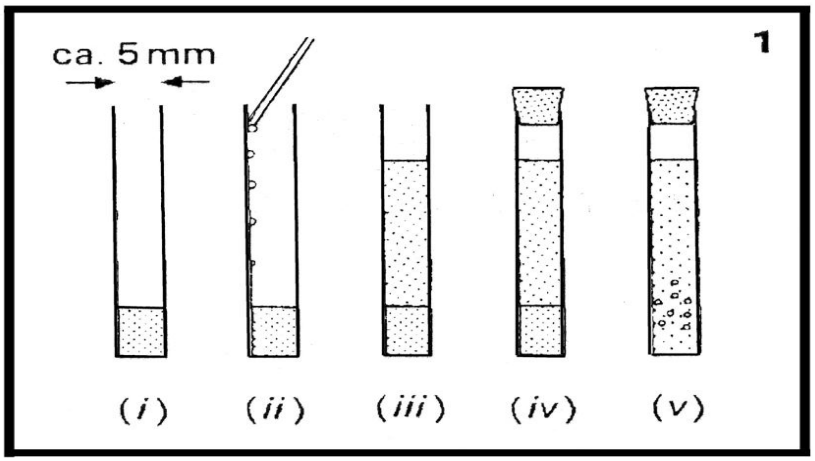

2.4.1.1 Method

All single crystals in this thesis were obtained by slow evaporation from methanol or acetonitrile. In the case of FDEA, crystals suitable for X-ray diffraction were obtained from the resultant gel on storage. Whereas FTris polymorph I was obtained by recrystallising from methanol, single crystals of FTris polymorph II were obtained by recrystallising 3 g of polymorph I in 50 ml of a 40:60 warm solution of MeOH:Acetonitrile, allowing it to cool down and maintaining at -20 °C for 24h.

2.4.2 Crystal structure determination

Crystal structure determination relies on the ability of the crystal, irradiated with a parallel beam of X-ray or neutrons, to produce diffracted beams which can be measured.

2.4.2.1 Method

Data for FDEA were collected locally on a Enraf-Nonius CAD-4 diffractometer using graphite monochromated Mo Kα whereas the rest were collected on a Bruker Nonius X8-Apex2 CCD diffractometer at the EPSRC National Crystallography Service. Beamline I19 at the Diamond synchrotron was used to collect data on FAMP1, FTris I and FCProp. All structures were solved by direct methods and refined by full-matrix least squares using the program SHELXL-97. The non-hydrogen atoms in FDEA were refined independently with anisotropic displacement parameters. Most of the hydrogen atoms appeared in difference Fourier maps. All other hydrogen atoms for FDEA and all hydrogens for the rest of structures were placed at calculated positions and refined using a riding model with isotropic displacement parameters.

2.5 Mechanical properties

Pharmaceutical development scientists should have a sound, scientific understanding of the properties of materials and their role and impact in product development. During the overall tabletting process there are many challenges significantly influenced by mechanical properties.

1. Evaluation of deformation behaviour and compressibility:

Compressibility is the ability of a material to undergo volume reduction under pressure. Both deformation behaviour and compressibility can be assessed using a range of techniques. These techniques include measurement in changes in bed porosity during compression, effect of punch velocity in compression, strain-stress sensitivity index, stress-strain relaxation, various tablet indices,

stress transmission during compression, work involved in compaction, compaction force versus time profiles and elastic recovery during multiple compression.

The deformation characteristic of a material can be elastic, plastic or brittle fracture or a combination of all of them. Elastic deformation is time independent and reversible, whereas plastic deformation refers to the permanent deformation of a material. Plastic deformation facilitates the formation of permanent particle-particle contact regions during compaction. Because of the time-dependant nature of the plastic flow, plastically deforming materials produce higher yield pressures as the punch speed increases (Roberts and Rowe 1985). The force applied on a compact divided by the surface area is called "stress" and the magnitude of the induced dimensional change is called "strain". Hook's law denotes the plot of the stress-strain plot and the proportionality constant between them is given by the Young's modulus.

$$\sigma_d = \varepsilon E$$

where:
E = Young's modulus
ε = deformation strain
σ_d = deformation stress

During tabletting changes in bed porosity occur as force is applied. This volume reduction can be calculated using the Heckel Equation:

$$Ln(1/1-D) = KP + A$$

where:
D = relative density of the compact in die at pressure P
K and A = regression coefficients of the linear portion of the curve. The reciprocal of K is P_y, the mean yield pressure, which represents the minimum pressure to deform a material.

The Heckel equation is applicable to all plastically deforming materials but deviation from linearity at low pressures suggests other densification mechanisms, such as brittle fracture. As the compression process consists of several stages, it may seem unrealistic to look for one relatively simple formula with few parameters covering the entire compression process. It is, therefore, generally agreed that the mathematical models fit the data in either the initial or the final stage of the densification process.

As the density during compression is varying in the tablet, it must be expected that the different stages of the process overlap with each other. This makes it difficult or impossible to point out distinct regions where only one type of deformation — plastic, elastic or brittle — is dominating. A review of the apparent yield pressures published in the literature for Avicel® PH 101 (Paronen 1986; Roberts and Rowe 1987; Yu et al. 1989) and paracetamol (Humbert-Droz et al. 1983; Podczeck and Wenzel 1989) show considerable differences. Considering the relatively narrow region where the apparent yield pressures are observed, these variations are too large to give a satisfactory and general valid material constant. It is important to note that the Heckel plot and derived parameters are extremely sensitive to small errors in the experimental conditions and variations such as the true density values (Sonnergaard 1999), maximum pressure (Paronen 1986; Rees and Tsardaka 1994; Konkel and Mielck 1997). In an interlaboratory investigation on compression simulators (Bateman et al. 1989), the apparent yield pressures differed by up to 10%.

2. Evaluation of compactability and tablet strength

Compactability is the ability of a material to yield a compact with adequate strength. Compactibility is an intrinsic property of the material. If the solid fraction is known, then tablet strength can be determined. Compactability and mechanical strength are assessed by measurement of deformation hardness, compression force versus tablet strength, tensile strength, friability, indentation hardness, tabletting indices and by measurement of mechanical moduli and constants, for example beam bending, fracture mechanics and single crystal microindentation techniques.

In pharmaceutical practice, tensile strength is usually measured by diametral compression involving failure of the tablets. Radial tensile, σ_x, strength is given by the relationship:

$$\sigma_x = 2F / \pi D^2$$

Where:

F = force required to break the tablet

D = is the diameter of the tablet

A comparison of radial and axial stress is indicative of the bonding strength in two directions and may provide information about the lamination and capping tendencies of the material (Alderborn and Nystroem 1984).

Compaction simulators have facilitated compression studies using very small amounts of material under conditions relevant to the full-scale machine operation.

2.5.1 3-point bending test

Young's moduli of the gemfibrozil salts were determined using a three-point beam test as reported by Roberts, Rowe *et al.* (1991) and Bassam, York *et al.* (1990). The purpose was to investigate the compression characteristics of compacts of 100% drug and salt. The beam test is a geometrically simple specimen of 7 x 20 x 1 mm easily made and readily loaded. Load alignment problems are eliminated by the use of a simple fixture or jig in which the beam is supported on and loaded though smooth hard cylindrical rollers. The beam can have any cross-sectional shape, but for convenience, sections with at least one plane of symmetry are preferred. The rectangular cross-section is generally easy to make. Typically, the length of the beam should be at least 10 times the cross sectional dimension. Fracture occurs when the maximum stress, σ, equals the tensile fracture stress of the material.

Fig 2.14 Schematic representation of the three point single beam test

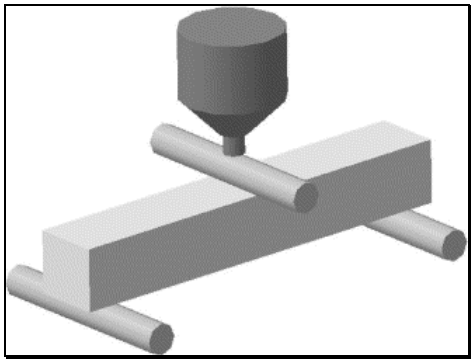

For a rectangular beam *Flexural Strength* (MPa) is given by the expression:

$$\sigma = \frac{3 \times d \times F}{2 \times w \times t^2}$$

And the *Elastic Modulus* (MPa):

$$E = \frac{d^3 \times m}{4 \times w \times t^3}$$

where:

d = the support span (mm)

F = load at a given point on the load deflection curve (N)

w = width of the beam (mm)

t = Thickness of the beam (mm)

m =Slope of the tangent to the initial straight-line portion of the curve (N/mm)

E_0 is the *Young's modulus* at zero porosity, which is calculated by the extrapolation of the exponential polynomial. Young's modulus is indirectly determined for powders because the specimen used always involves pores. Young's modulus provides a means of quantifying the elastic behaviour.

The relationship between the measured elastic modulus and E_0, is given by the Sprigg's equation:

$$E = E_0 \exp^{-bP}$$

Where:

E = measured elastic modulus at porosity P and

b = a constant.

The Spriggs equation is an empirical relationship between porosity and E but its applicability is restricted over a narrow, typically low porosity range (Kachrimanis and Malamataris 2004).

The true densities, ρ_t, of the salt powders were determined using a helium pycnometer. The desired thickness of the tablets for a solid fraction of 0.85 was calculated using the equation:

$$SF = \frac{\rho_c}{\rho_t}$$

Where:

ρ_c = density calculated from the dimensions of the compact (*weight / (length x width x thickness)*.

Disadvantages of this method are that the results of the testing method are sensitive to specimen and loading geometry and strain rate.

2.5.1.1 Equipment

Beams were prepared sing a Specac KBr press. G&F Press Tools Ltd, Brierley Hill, West Midlands, constructed a hardened steel die that was made of a piece of steel with a 20 x 7 mm hole in the centre. The bottom die face had a 2 mm elevation and the top longer shaft had 20 mm so that there was a 1 mm gap when the die was complete. An additional longer shaft was manufactured to aid the ejection

of the beam from the die. Elastic modulus was measured using a Hounsfield S-Series machine. Tinius Olsen designed a three-point bend jig for testing typical 20 x 7 mm wafers. The Linear Displacement Unit (LDU) was required to measure the displacement accurately. The 5 N load cell used to calculate the elastic modulus.

2.5.1.2 Method

Beams were prepared compacting 203 ± 1 mg of powder so that the final weight of the beams would be 200 ± 3 mg. The dimensions of the die were 20 mm in length and 7 mm in width. Compaction was carried out using a hydraulic press with compaction pressure range between 0.75 -3.5 tonnes with a 1 min dwell time and 24 h recovery time. Pressure induced polymorph transformation was ruled out by IR. Decompression in the die was uniaxial and ejection of the beams was carried out in a controlled manner at a rate to minimise the risk of structural failures such as cracks, capping and lamination. Broken or fractured beams were discarded.

2.5.2 Stylcam 100R

The Stylcam is a rotary press compaction replicator is a facility to perform compaction analysis on APIs and formulated products. Its main use is to replicate production tablet presses and to predict the performance of formulations at full scale production. Different force-time-profiles can be obtained from the Stylcam 100R, which can be useful to characterise the packing mechanism. Ductile materials show time dependency therefore very low dwell times with high speed production presses can yield softer tablets. Possible scale up issues could arise. Early compaction information allows the formulator to make possible changes to the formulation to enhance its performance and minimise possible issues during production. Characterization can determine properties predictive of processed formulations and/or API performance and aids in early formulation, process selection and optimization i.e. it can identify the procedures amenable to compaction, such as dry vs. wet, granulation vs. direct mixing, milling conditions, evaluation of different tablet tooling shape. Early API characterization is important when a high drug loading is expected and the Stylcam can assess the critical level of excipients needed for successful tabletting operations. Currently there is a Stylcam 200R Simulator, a single-punch press used to duplicate and analyze precompression, compression, and ejection phases in industrial tablet-production presses under identical conditions to those of a unit producing up to 300,000 tablets per hour

The Stylcam makes tablets using up to 50 kN compression force at a user specified speed. It can measure upper and lower punch displacement, upper and lower pre/main compression force, ejection

force and take-off force. The obtained information can be displayed in a range of scientific plots and reports, such as force-hardness, force-thickness, Heckel, etc.

It is important to note that the Heckel plot and derived parameters are extremely sensitive to small variations in the experimental conditions and variations such as the true density values (Sonnergaard 1999) and maximum pressure (Paronen 1986; Rees and Tsardaka 1994; Konkel and Mielck 1997). In an interlaboratory investigation on compression simulators (Bateman et al. 1989), the apparent yield pressures differed by up to 10%.

The Stylcam 100R seems to be a useful tool for characterising tabletting properties of powders, except for the Heckel's model probably due to an unadapted equation of deformation and a lack of accuracy of the displacement transducers (Michaut et al. 2009). However, these limitations relate to applications when used as a compaction simulator. In this study, the Stylcam 100R was used as a compaction replicator. The performance of the upgraded Stylcam 200R has been reported and it has the capacity to simulate various force-time-profiles of different rotary tablet presses by realizing several speeds and different lags between pre and main compaction (Busignies et al. 2010).

2.5.2.1 Method

Tablets containing 400 mg of drug or salt were prepared using a Stylcam 100R compression replicator.

Compression forces were measured with stain gauges located on the upper and lower punch holders, with an accuracy of 10N. The accuracy of punch displacement, measured with LVDT's on the punch holders, was 0.01mm.

Standard Euro D tools, 11.28mm round flat- faced punches were fitted. A direct cam profile was used for the study. Displacement sensors were zeroed prior to measurement following instruction via the Analis software, using a 2mm gauge block. The height of the bottom punch at the point of ejection was measured using a micrometer, (between 0.02 and 0.06mm) and accounted for by the controlling software, at this point the bottom punch displacement was zeroed. A 2mm gauge block was inserted between the upper and lower punch. A small force is applied and the upper punch displacement is zeroed.

The machine deformation (including punch deformation) was taken into account. Machine and punch deformation is performed by the compaction of a non deformable 5mm metal block by increasing the force applied to it by hand. (between 0 and 5000daN). For each force, the punch separation was measured. The data obtained for compact thickness displayed by the software is the 'corrected thickness' allowing for this deformation.

For external lubrication, 5% w/v magnesium stearate slurry was used. For direct comparison between the different salts a Solid Fraction (SF) of 0.85, which is typical of pharmaceutical tablets (Hancock et al. 2003) was targeted. Mass, thickness and crushing strength of the tablets were measured immediately after ejection with scales (B104), a micrometer (CA17, Mitutoyo, Japan) and a tablet strength tester (Tablet tester, HT1). A minimum of six replicates were performed.

The true densities, ρ_t, of the salt powders were determined using a Accupyc 1330 v103helium pycnometer. The helium pycnometer allows measuring the volume and true density of solid objects, without damaging samples. This is accomplished by employing Archimedes' principle of fluid displacement and Boyle's law that suggests that for a fixed amount of an ideal gas kept at a fixed temperature, pressure and volume are inversely proportional. The displaced medium in this application is a gas (helium) which can penetrate the finest pores, thereby assuring maximum accuracy.

The desired thickness of the tablets for a solid fraction of 0.85 was calculated using the equation:

$$SF = \frac{\rho_c}{\rho_t}$$

Where:

ρ_c = density calculated from the dimensions of the compact (weight / π x r^2 x thickness).

After a load is removed, some of the total deformation is recovered. The degree of change in compact thickness after decompression as pressure is removed is indicative of the elastic recovery.

Elastic Recovery (ER) which starts after decompression and can finish several days after is defined as:

$$ER = \frac{T - T_{\min}}{T_{\min}}$$

where:

T = thickness measured after relaxation

T_{min} = minimum height of the tablet under load

Elastic recovery can be measured in die or out of die. In die measurements do not allow axial recovery.

3 Flurbiprofen

Flurbiprofen is a white crystalline powder which is practically insoluble in water (0.034 mg/ml, Tavorvipas 2002, 0.024 mg/ml Maitre 2007) and freely soluble in alcohol (Martindale 2007). It is a weak acid (pK_a = 4.22) that contains a biphenyl group with a fluorine atom in ortho position (see Fig 3.1). Flurbiprofen is a relatively rigid molecule as the coplanar conformation for any biphenyl with a single ortho-substituent, X, has maximum destabilization from the steric interaction of X with the nearer ortho-hydrogen on the second phenyl ring and maximum stabilization from the π–π interaction of the two rings. The overall lowest energy conformation for the biphenyl will be somewhere between these extremes. The twist angle increases with a heavier atom, from 42.5º for biphenyl to 45.1º for 2-fluoro (Grein 2002).The diphenyl angles of flurbiprofen acid structures (flurbiprofen acid polymorphs plus neutral flurbiprofen molecules in cyclodextrins) from the Cambridge Structural Database (CSD) reveals an average twist angle of 53.17º ± 0.24.

Fig 3.1 Flurbiprofen structure

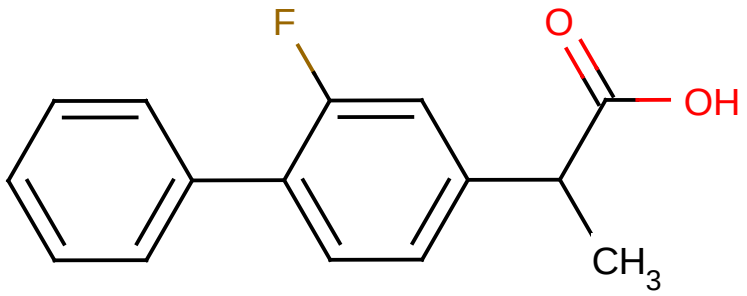

Therapeutically, it belongs to the non-steroidal anti-inflammatory drugs (NSAIDs), a group of structurally unrelated organic acids that have analgesic, anti-inflammatory, and antipyretic properties. NSAIDs are inhibitors of the enzyme cyclo-oxygenase, and so directly inhibit the biosynthesis of prostaglandins and thromboxanes from arachidonic acid. There are two forms of cyclo-oxygenase

(COX), COX-1, which is the constitutive form of the enzyme, and COX-2, which is the form induced in the presence of inflammation. Inhibition of COX-2 is therefore thought to be responsible for at least some of the analgesic, anti-inflammatory, and antipyretic properties of NSAIDs whereas inhibition of COX-1 is thought to produce some of their toxic effects, particularly those on the gastrointestinal tract. Most of the NSAIDs currently available for clinical use inhibit both COX-1 and COX-2, although selective COX-2 inhibitors such as celecoxib are now available.

NSAIDs are used for the relief of mild to moderate pain, minor febrile conditions and for acute and chronic inflammatory disorders such as osteoarthritis, rheumatoid arthritis, juvenile idiopathic arthritis, and ankylosing spondylitis. Indometacin and some other NSAIDs are used to close patent ductus arteriosus in premature neonates. Some NSAIDs are applied topically for the relief of muscular and rheumatic pain, and some are used in ophthalmic preparations for ocular inflammatory disorders.

The commonest adverse effects of NSAIDs are generally gastrointestinal disturbances, such as gastrointestinal discomfort, nausea, and diarrhoea; these are usually mild and reversible but in some patients peptic ulceration and severe gastrointestinal bleeding may occur.

CNS-related adverse effects include headache, vertigo, dizziness, nervousness, tinnitus, depression, drowsiness, and insomnia. Hypersensitivity reactions may occur occasionally and include fever, angioedema, bronchospasm, and rashes. Hepatotoxicity and aseptic meningitis, which occur rarely, may also be hypersensitivity reactions. Some patients may experience visual disturbances. Haematological adverse effects of NSAIDs include anaemias, thrombocytopenia, neutropenia, eosinophilia, and agranulocytosis.

Some NSAIDs have been associated with nephrotoxicity such as interstitial nephritis and nephrotic syndrome; renal failure may be provoked by NSAIDs especially in patients with pre-existing renal impairment. Haematuria has also occurred. Long-term use or abuse of analgesics, including NSAIDs, has been associated with nephropathy.

Fluid retention may occur, rarely precipitating heart failure in susceptible patients.

The following flurbiprofen-containing products are currently marketed in the UK: Froben 50 and 100 mg tablets, Froben 200 mg slow release capsules and Ocufen eyedrops. All of these formulations contain the sodium salt of the drug.

3.1 Salt confirmation

3.1.1 Recovery

The flurbiprofen ratio in the salt was compared to the theoretical ratio. One hundred milligrams of each salt was weighed and placed in a 100 ml class A volumetric flask and made up to volume with appropriate mobile phase to give a 1 mg/ml solution. Methanol:water 80:20 was used for F-Tris and F-AMP1 and acetonitrile:water 65:35 was used in all the other cases. The solution was analysed then by HPLC. Experiments were performed in triplicate.

Table 3.1Recovery of flurbiprofen salts

	% content Experimental (Average ± SD)	**% content Theoretical**	**Salt recovery**
FAdam	60.55 ± 0.12	61.76	98.04%
FBenz	69.47 ± 0.11	70.00	99.14%
FCProp	79.99 ± 0.17	81.05	98.69%
FCBut	76.75 ±0.20	77.45	99.09%
FCHex	61.33 ± 0.09	61.75	99.31%
FTBut	76.50 ± 0.78	76.96	99.40%
FAMP1	72.50 ±0.18	73.30	98.90%
FAMP2	68.60 ± 0.06	70.00	98.00%
FTris	69.57 ± 0.76	69.98	99.40%
FMEA	79.73 ± 0.56	80.70	98.79%
FDEA	69.72 ± 0.27	70.21	99.30%
FTEA	62.12 ± 0.13	62.24	99.80%

With a recovery of >98%, this method of salt formation was considered satisfactory in producing a reasonable yield, with little wastage and acceptable level of purity.

3.1.2 Fourier Transform Infrared Spectroscopy (FTIR)

FTIR was used to confirm the transformation from carboxylic acid to a carboxylate salt.

Protonated carboxylic acids yield absorption bands corresponding to a carbonyl stretch between 1690 and 1750 cm^{-1}. On deprotonation, it shifts to a lower energy as its vibrational mode becomes coupled to that of the other carboxylic oxygen, giving rise to an asymmetric feature between 1540 and 1650 cm^{-1} (Silverstein et al. 1991). The frequency for caboxylate salt absorbance is lower than that for the carboxylic acid because of resonance. Salt formation could be established by the shift of the carboxylic acid peak from 1684 cm^{-1} (Silverstein et al. 1991; Palomo et al. 1999) to characteristic bands of carboxylic acid salts, at 1650–1550 and 1440–1335 cm^{-1} (Socrates 1994) and absorption at 3350–3150 cm^{-1}, attributable to NH_3^+ stretching of solid amine salts (Socrates 1994). This method has previously been used by O'Connor and Corrigan (2001b) to confirm salt formation.

The infrared spectra for flurbiprofen and the FMEA (see Figs 3.2 and 3.3) salt are included here as typical examples and the spectra for other salts are included in Appendix A.

Fig 3.2 FTIR scan for flurbiprofen

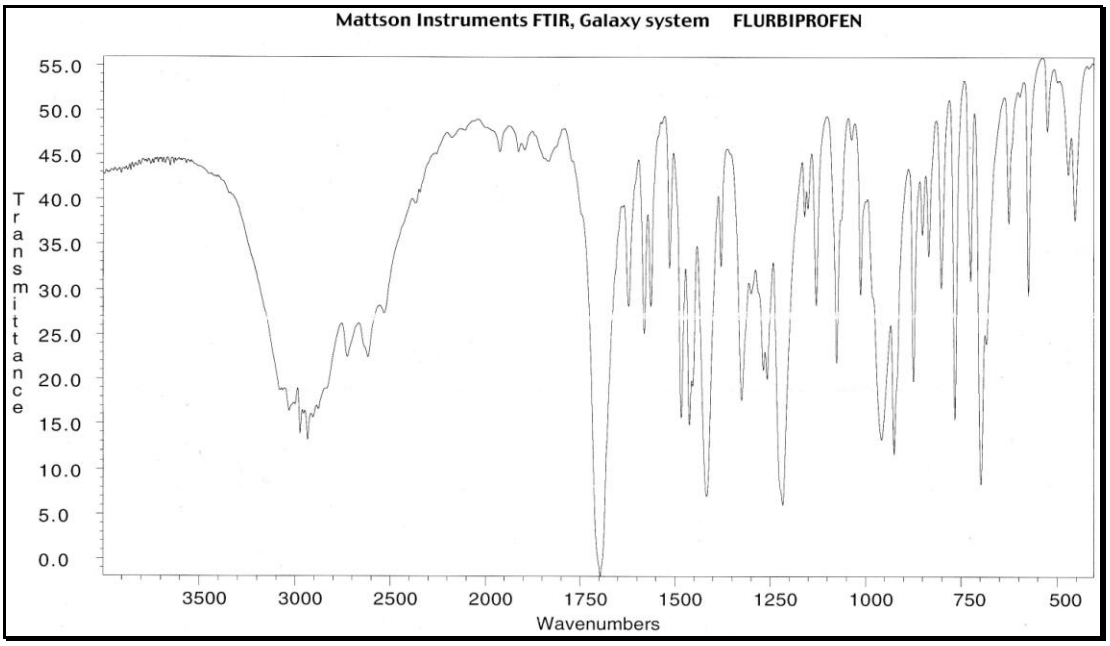

Fig 3.3 FTIR scan for FMEA salt

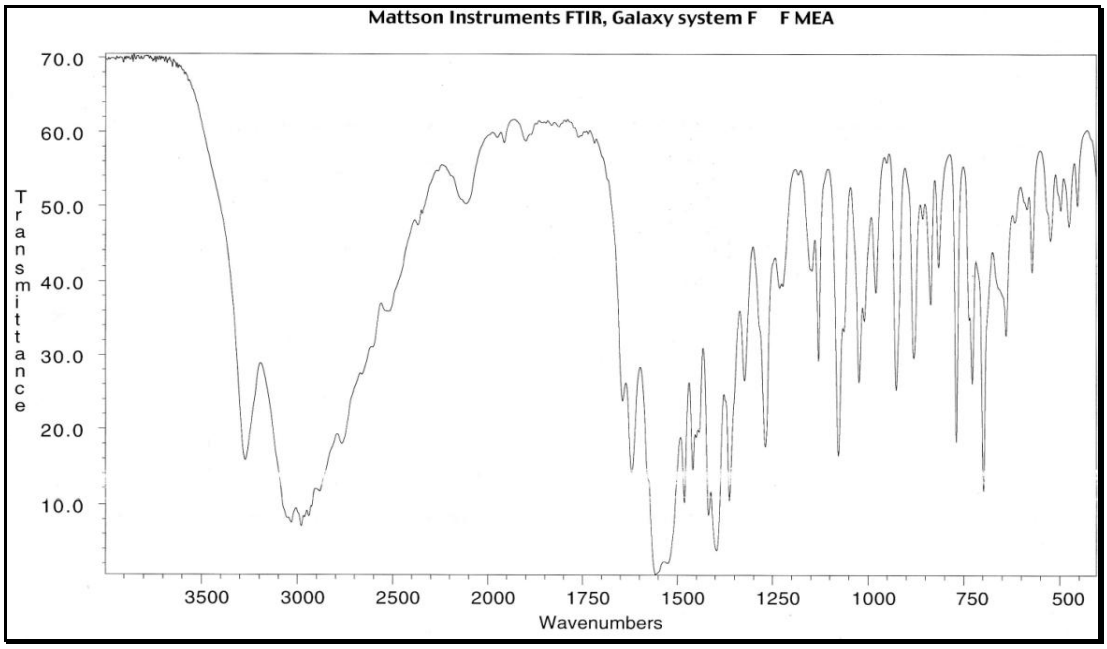

The signal at 1700 cm^{-1} in the flurbiprofen spectrum was attributed to a stretching of the C=O group in the carboxylic acid in the case of flurbiprofen acid. The peak shifts to 1550 cm^{-1} in the FMEA salt. The absorption peak between 3350-3150 cm^{-1} is attributable to NH_3^+ stretching in amine salts and is only present in salt form below.

A broad peak at approximately 2100 cm-1 can be observed in FMEA which is not present in neither the carboxylic acid scans nor the salts with tertiary amines (FTEA, DTEA, GTEA). It is possible that this peak is only present in $(R\text{-}NH_3^+)\bullet(R'\text{-}COO^-)$ salts with primary and secondary amines

3.1.3 Nuclear Magnetic Resonance

The NMR spectra accounted for every hydrogen atom in the expected molecules. NMR spectra for flurbiprofen (Fig 3.4) and FMEA (Fig 3.5) are included here and the NMR spectra for the rest of the salts are in Appendix B.

Salt confirmation is strengthened by the change in chemical shift of the proton attached to the carbon next to the COOH group upon salt formation. In the case of flurbiprofen and its monoethanolamine salt the chemical shift is 3.61 ppm and 3.41 ppm respectively.

3.2 Thermal studies

3.2.1 Methods

DSC and TGA methods were used as described in sections 2.2.1.2 and 2.2.2.2 respectively.

3.2.2 Results and discussion

Melting points are summarised in table 3.2. An example of a DSC scan of flurbiprofen is shown in Fig 3.7. The rest are attached in Appendix C. There was no evidence of any hydrate/solvate formation in any of the salts. Desolvation of any bound solvent would be observed as a multistage process using TGA, at a series of discrete temperatures This was also confirmed by the lack of weight loss observed in TGA around 100 degrees and the gradual decline in weight for all salts after the melting point of the salt.

Fig 3.4 NMR scan for flurbiprofen

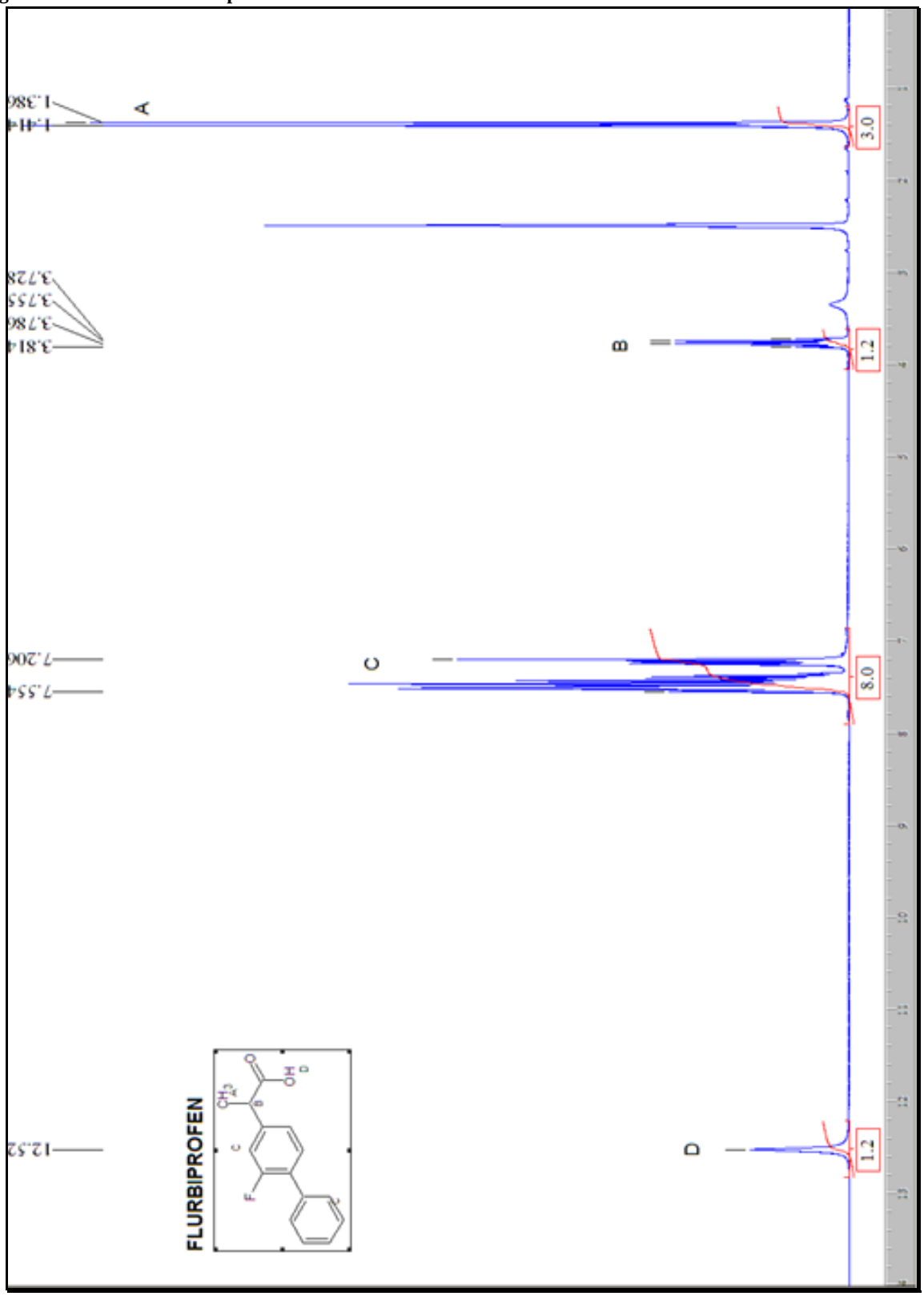

Fig 3.5 NMR scan for FMEA

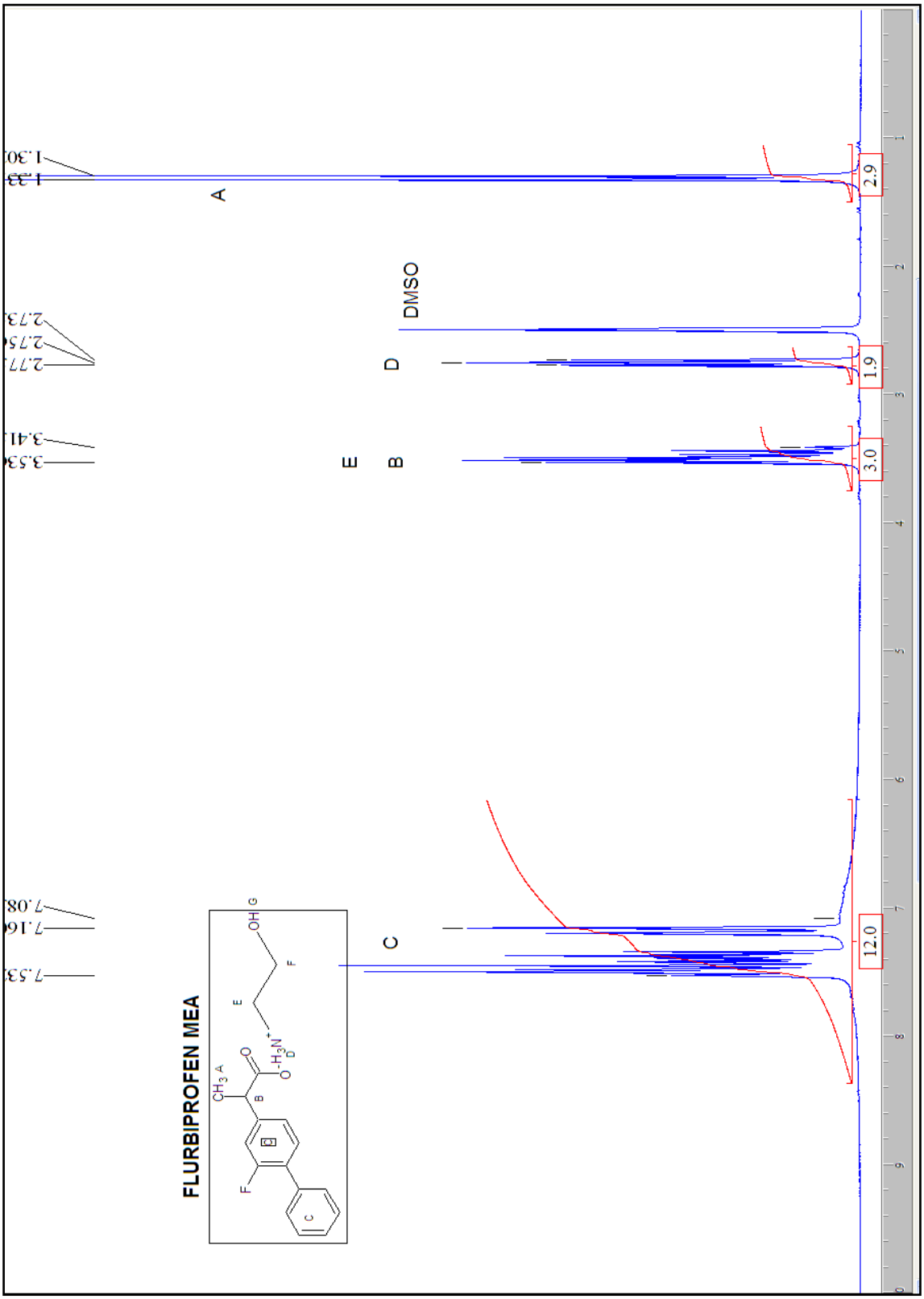

The obtained melting point for flurbiprofen (116.58°C, see Fig 3.6) is in line with those reported in the literature; 115 °(Grzesiak and Matzger 2007). The melting points of some of the salts studied have also been reported in the literature; FMEA, 108°C, FDEA, 60°C and FTEA 101° (Maitre et al. 2007) and FTBut, 183.0°, FAMP1, 151.2°, FAMP2, 119.0° and FTris, 148°(Anderson and Conradi 1985). FTBut melting point differs slightly and is probably related to thermal instability by evaporation of the amine near the melting point.

Table 3.2Melting points for flurbiprofen and salt series (n=3; mean±s.d.)

Drug	Melting point (°C)
Flurbiprofen	116.58 ± 1.00
FAdam	252.75 ± 0.91
FBenz	133.24 ± 0.33
FCProp	136.14 ± 1.00
FCBut	166.63 ± 1.11
FCHex	215.14 ± 0.41
FTBut	202.68 ± 0.57
FAMP1	154.09 ± 0.60
FAMP2	120.24 ± 0.48
FTris I	156.01 ± 0.49
FTris II	147.73 ± 0.42
FMEA	109.21 ± 0.36
FDEA	56.89 ± 1.36
FTEA	100.98 ± 0.50

Fig 3.6 DSC thermogram for flurbiprofen

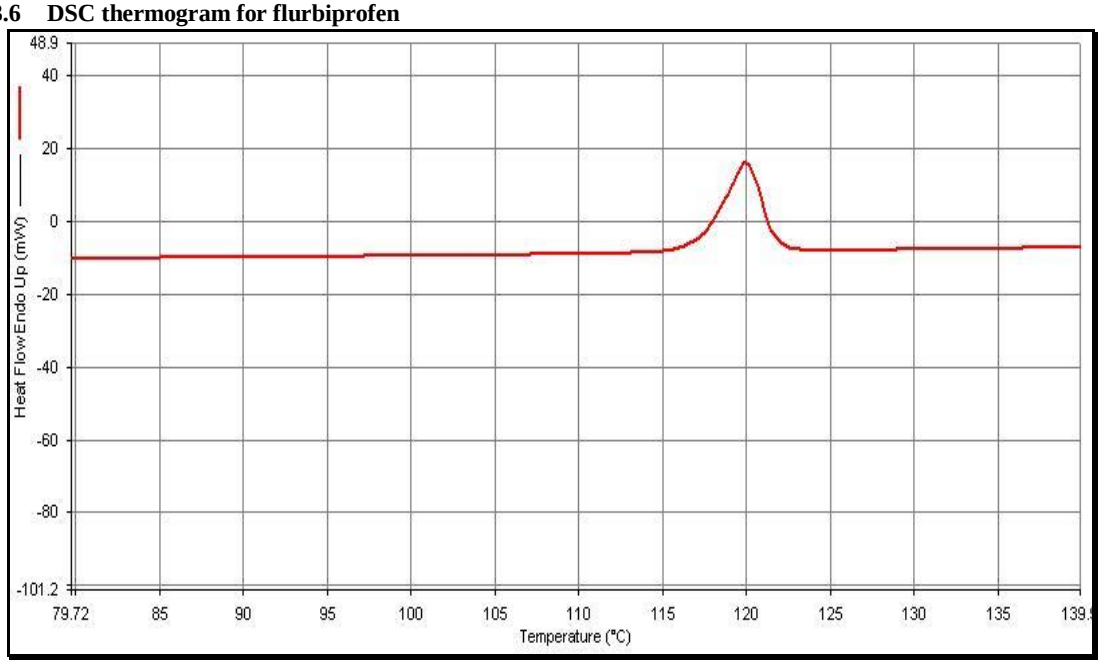

Fig 3.7 DSC thermogram for FMEA

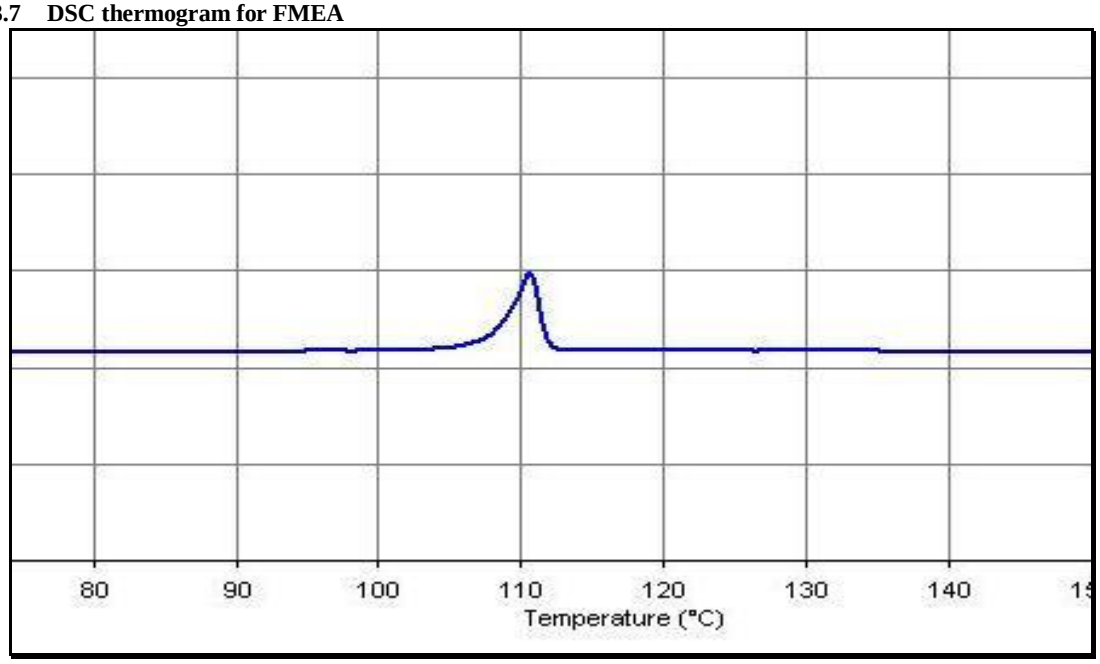

Previous publications (Agharkar et al. 1976; Anderson and Conradi 1985; Rubino 1989) have indicated that the solubilities of certain groups of salts exhibit an inverse relationship with melting point. Conversely, Gu and Strickley (1987) concluded that no simple solubility-melting point relationship could be established. O'Connor and Corrigan (2001b) reported a trend between the melting point and the logarithm of the solubility and between the inverse of the melting point and the logarithm of the solubility. There is no obvious simple correlation (R=0.1632) between the meting point and the saturated solubility values of this data set (see Fig 3.8).

Anderson and Conradi (1985) reported a strong correlation between the melting point and the $\log K_{sp}$ of different flurbiprofen salts. A similar correlation was achieved in this study (Fig 3.9). The solubility product K_{sp} is a constant proportional to the relationship between solid and dissolved states of a salt at saturation. K_{sp} was calculated from the saturated solubilities and they were not corrected for ionic strength:

$$A_n B_m \rightarrow nA^+ + mB^-$$

$$K_{sp} = \left[A^+\right]^n \times \left[B^-\right]^m$$

Fig 3.8 Relationship between solubility (mg/ml) and melting point (°C) of flurbiprofen salts

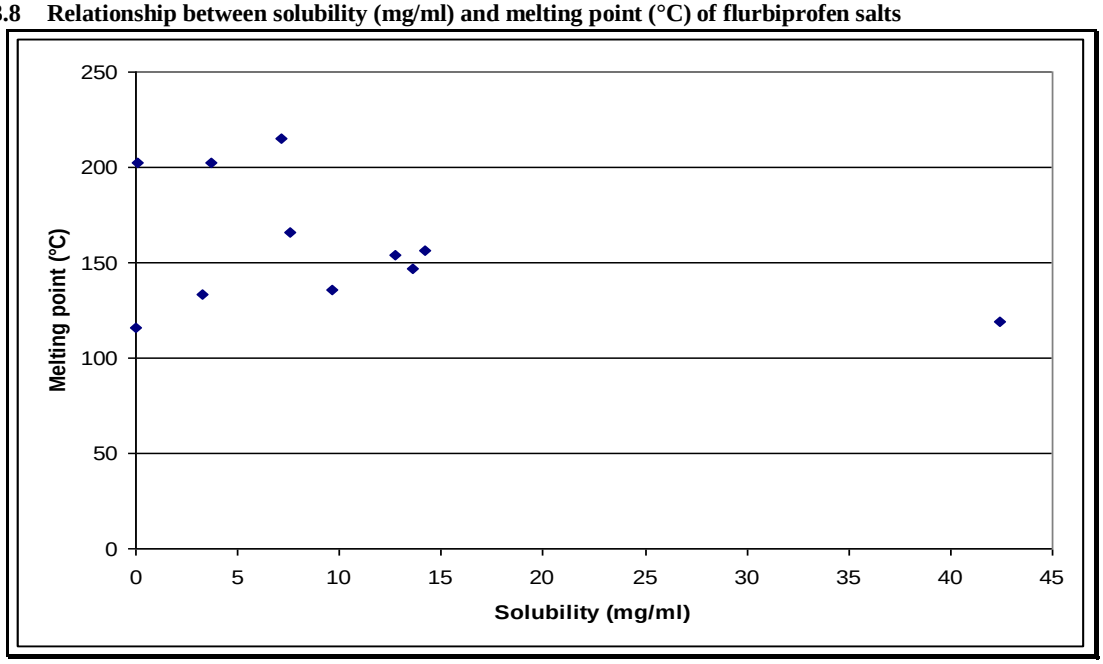

Fig 3.9 Relationship between solubility product (K_{sp}) product and melting points (ºC) for flurbiprofen and its salts

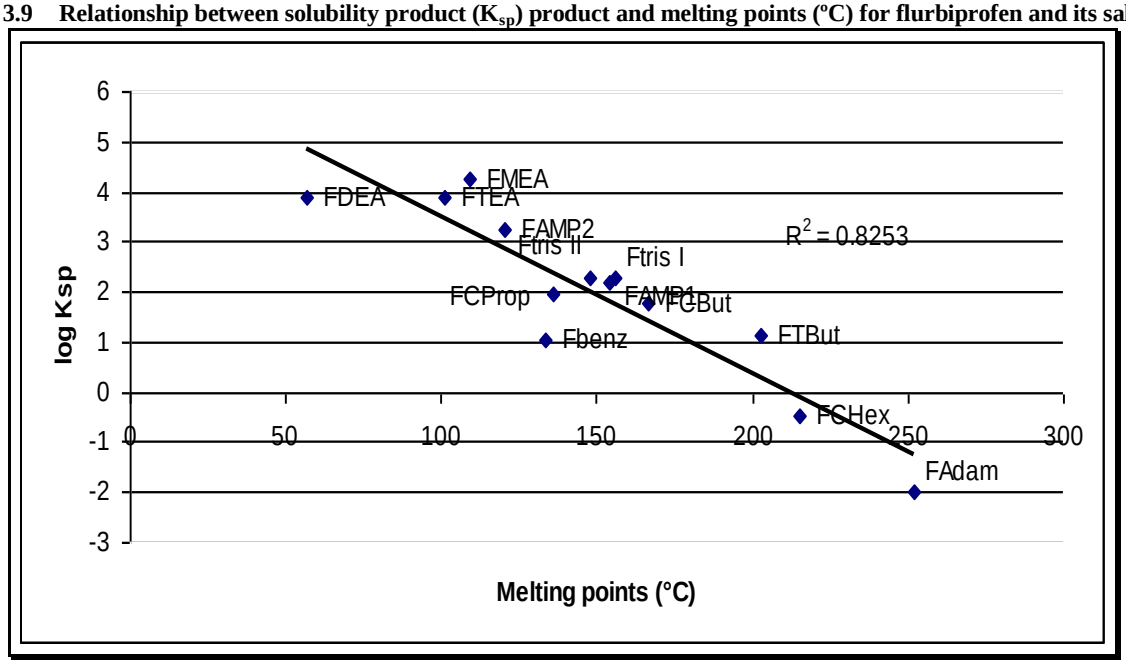

In an analysis of the carboxylate-ammonium H-bonding patterns seen in the Cambridge Structural Database, it was revealed that the $R_4^3(10)$ column, using graph-set notation (Bernstein et al. 1995), also known as Type II columns (Nagahama et al. 2003), was the most commonly occurring pattern in these salts (75/126), whereas, the alternative sequence of alternating $R_4^2(8)$ and $R_4^4(12)$ columns,

also known as Type III (Nagahama et al. 2003) columns, was the second most common (26/126). Two dimensional layers built up with $R_6^5(16)$ rings were the third most common network (19/126).

It is believed that type II columns are more stable than type III and the type of hydrogen bonded column has an effect on the melting points, with those salts having Type II columns being higher than those of Type III. This phenomenon has been observed previously in the melting behaviour of seven isomers of inositols (Simperler et al. 2006) and chiral ammonium naphthalene carboxylate salts (Lemmerer et al. 2008b). These studies by Simperler (2006) and Lemmerer (2008b) focus on paired salts of chiral compounds so that the influence of additional parameters are minimised. For the salt series investigated in this thesis, only FAdam and FCProp display type III columns (see section 3.4.3) and so conclusions are limited. However, if FCProp (type II) is compared to FCBut (type III), as they are close in morphology and they share the same space group P21/n, there is a higher melting point for FCBut (166 ºC) compared to FCProp (133ºC). With different counterions many other structural/molecular parameters may come into play and it would be interesting to include further examples to investigate this relationship further.

The FTris polymorphic system was studied more closely. Hyper DSC was used to study this phenomenon. The method was different to the previous general one. Three different scan rates were used: 100, 300 and 500 °C/min. In all cases temperature was held at 20 °C for 1 min, then heated from 20 °C to 190 °C, cooled from 190 °C to 0 °C, held again at 0 °C for 1 min and finally reheated from 0 °C to 190 °C.

In the first heating step, the onset of the melting peak of FTris I was at around 153.76 °C for 100 °C/min, 156.80 °C for 300 °C/min, 154.62 °C for 500 °C/min (Fig 3.10). The onset of the melting peak of FTris II in the first heating step was 144.89 °C for 100 °C/min, 145.44 °C for 300 °C/min, 146.89 °C for 500 °C/min (Fig 3.11). In the second heating step, all the curves showed similar behaviours. There was a glass transition between 30-40 °C, followed by recrystallisation, then a melting peak. For FTris I, the onset of the melting peak was 142.12 °C for 100 °C/min, 145.81 °C for 300 °C/min, 145.04 °C for 500 °C/min. For FTris II, the onset of the melting peak was 140.20 °C for 100 °C/min, 143.93 °C for 300 °C/min, 147.95 °C for 500 °C/min. In the second heating step at 100 °C/min, there was a small exothermic peak observed around 115 °C for both FTris I and form II which was not seen at other heating rates.

Fig 3.10 Flurbiprofen tris salt form I at heating rate of 100 °C/min, 300 °C/min and 500 °C/min

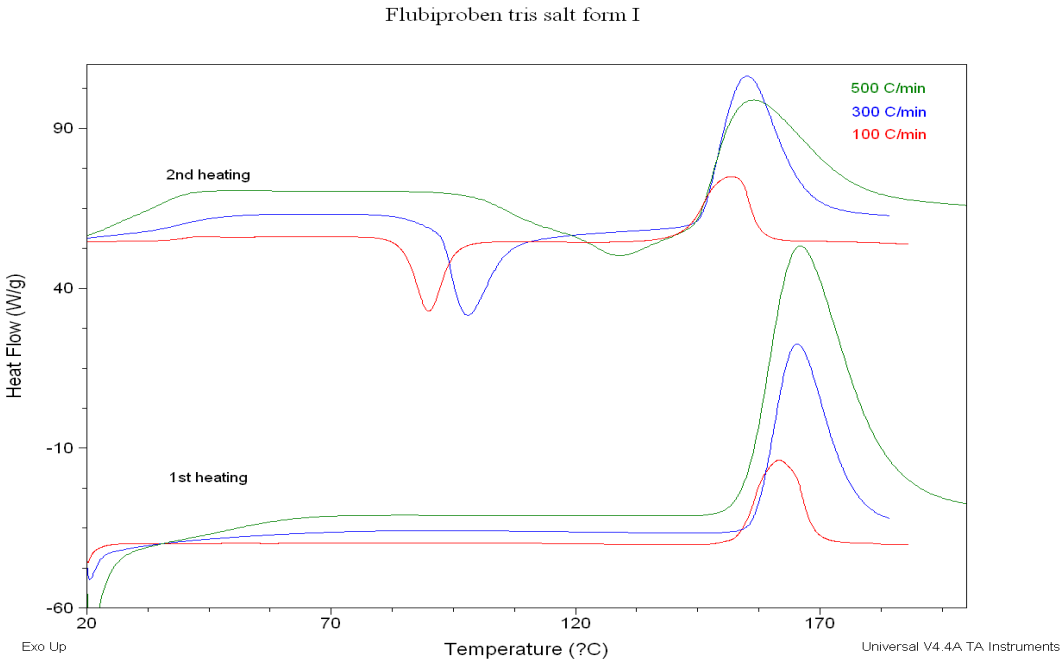

Fig 3.11 Flurbiprofen tris salt form II at heating rate of 100 °C/min, 300 °C/min and 500 °C/min

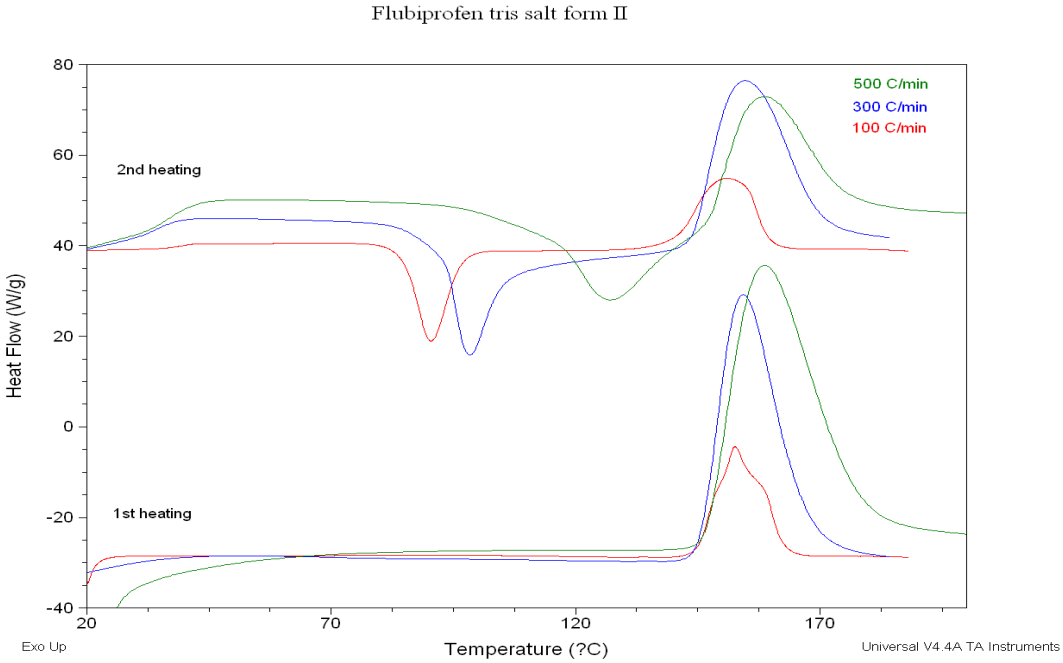

The main approaches used to assess thermodynamic stability relationships of polymorphs are based on thermodynamic rules according to Burger and Ramberger (Burger and Ramberger 1979). While

the former distinguishes between monotropic and enantiotropic systems, the latter in addition to this allows for calculation of the transition temperature. The *heat of fusion rule* states that in an enantiotropic system the higher melting polymorph will have the lower heat of fusion and if the higher melting polymorph has the higher heat of fusion the system is monotropic. If the melting points of the polymorphs differ by more than 30 °C then the rule may not be valid and the higher melting polymorph could have the higher enthalpy of fusion in an enantiotropic system. The *heat of transition rule* states that if an endothermic transition is observed between the two forms, then both forms are enantiotropic. No endothermic transition temperature was observed between both crystal forms.

Enthalpies of fusion for FTris polymorphs were calculated as per Table 3.3.

Table 3.3Enthalpies of fusion of FTris polymorphs (J/g)

	Heating rate (°C/min)	Enthalpy 1st heating (J/g)	Enthalpy 2d heating (J/g)
FTris I	100	157.24	123.01
	300	158.06	147.15
	500	183.75	109.84
FTris II	100	151.86	124.39
	300	165.14	136.25
	500	154.55	90.67

The available data makes it difficult to determine the thermodynamic relationship between both polymophs. At 500°C, the enthalpies of fusion of FTris I and FTris II are 183.75 J/g and 154.55 J/g. This fact and the lack of endothermic transition between both forms suggest a monotropic relationship between the polymorphs.

3.3 Solubility and dissolution studies

3.3.1 Saturated solubility

Saturated solubility in water was calculated at ambient temperature 21±1 °C for all the flurbiprofen series.

3.3.1.1 Materials

All materials were prepared as described in section 2.1.1.

3.3.1.2 Method

Saturated solubility was determined following the method described in section 2.3.2.2.

3.3.1.3 Results and discussion

The saturated aqueous solubilities of flurbiprofen and its salts are presented in Table 3.4. Solubility experiments were performed in triplicate.

Table 3.4 Saturated solubility and pH of flurbiprofen salts in aqueous solution at 21 °C (n=3, SD)

	Solubility (mg/ml)	Solubility (mM)	pH
Flurbiprofen	0.015 ± 0.003	0.06	3.20 ± 0.02
FAdam	0.10 ± 0.02	0.41	5.10 ± 0.01
FBenz	3.25 ± 0.07	13.30	7.37 ± 0.01
FCProp	9.64 ± 1.45	39.46	7.01 ± 0.20
FCBut	7.61 ± 1.89	31.11	6.75 ± 0.08
FCHex	0.57 ± 0.03	2.33	7.10 ± 0.01
FTBut	3.72 ± 0.05	15.22	6.25 ± 0.01
FAMP1	12.71 ± 0.15	52.03	6.95 ± 0.01
FAMP2	42.46 ± 0.11	173.83	8.06 ± 0.01
FTris I	14.16 ± 0.71	57.97	6.85 ± 0.01
FTris II	13.57 ± 0.37	55.55	7.37 ± 0.01
FMEA	-	-	-
FDEA	-	-	-
FTEA	-	-	-

Saturated solubility was improved in all cases by salt formation. Each counterion increased the flurbiprofen aqueous solubility from a minimum of 250- to nearly 9000-fold. In the case of flurbiprofen salts of the alkanolamines, solubility was greatly increased to values up to >200 mg/ml however, they formed thick gels in water which were, difficult to handle and solubility values were difficult to measure.

The obtained solubility for flurbiprofen acid is in line with the reported literature data at 25 °C (i.e., 0.034 mg/ml (Tavornvipas et al. 2002) and 0.024 mg/ml (Maitre et al. 2007). Solubilities of some of the salts above have also been reported in the literature and are in line with these results: FAdam, 0.10 mg/ml, FTBut, 3.17 mg/ml, FAMP1, 13.92 mg/ml, FTris, 16.85 mg/ml except for FAMP2, 219.83 mg/ml, which is considerably higher (Anderson and Conradi 1985). The difference in the solubility of FAMP2 can possibly be explained because at this range of pH values in theoretical pH-solubility diagram, small pH variations can cause large changes in solubility (see Fig 3.12). For a basic drug, avitriptan, the solubilities of the salts were similar if structurally similar counterions were used (Serajuddin 2002). However, the FTBut-FAMP1-FAMP2-FTris series of flurbiprofen salts show a lack of relationship between solubility and increasing number of hydroxyl groups. O'Connor and

Corrigan (2001a) found the same lack of simple correlation between solubility and increasing number of hydroxyl groups for the same series of diclofenac differing by a factor of as much as >100-fold.

There is a correlation between the saturated aqueous solubility and the theoretical pH solubility profile for flurbiprofen (see Fig 3.12). An intrinsic solubility value of 5.0 x 10^{-5} M was used (Anderson and Conradi 1985) to calculate the theoretical pH solubility profile according to the equation:

$$pK_a = pH - \log \frac{S - S_0}{S_0}$$

As expected the higher the pH of the obtained saturated solution the higher the solubility.

Fig 3.12 Saturated solubility versus pH of flurbiprofen and its salts. Theoretical pH solubility profile for flurbiprofen shown in pink

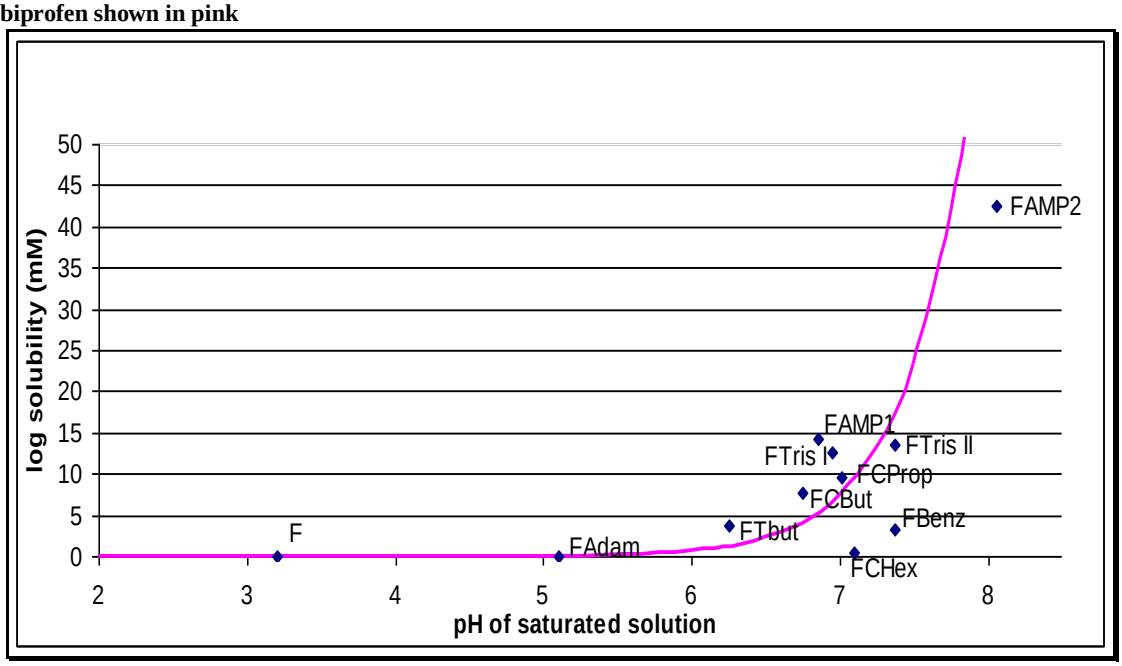

Self-association has been postulated as the reason why compounds with rigid aromatic structures and alkyl chains have lower solubilities and this is probably the explanation for the relatively low solubility of FCHex and FBenz, both containing rigid alkyl aromatic and alkyl chains. They are believed to typically associate by non-micellar processes (л-л stacking and van der Waals interactions) involving face-to-face stacking (Florence and Attwood 1998).

3.3.2 Dissolution studies

3.3.2.1 Materials

All materials were obtained as described in section 2.1.1.

3.3.2.2 Method

Method was followed as described in 2.3.3.2.

3.3.2.3 Results and discussion

It was observed that high compression forces resulted in more fragile discs prone to lamination and it was determined that a pressure of 3 tonnes was the optimum to produce coherent non-disintegrating discs. Fourier transformed infrared spectroscopy (FTIR) was used on the surface of all tablets to discard pressure-induced polymorphic changes.

The mass dissolved (mg) was plotted against time (see Figs 3.13-3.20). IDRs for flurbiprofen and its salts showed linear profiles and IDRs were measured successfully (see Table 3.5). The IDR was calculated dividing the gradient of the resulting regression line by the surface area (1.327 cm^2) of the exposed drug.

Table 3.5 IDR for flurbiprofen and its salts at 37°C. n=3

Material	IDR (mg/min/cm^2)		Correlation coefficient (R^2)	
	pH = 4.5	pH = 6.8	pH = 4.5	pH = 6.8
Flurbiprofen	0.06	0.33	0.9311	0.9979
FTBut	0.03	0.28	0.9255	0.9984
FAMP1	0.02	1.64	0.9837	0.9945
FAMP2	0.04	10.42	0.6998	0.9999
FTris I	0.06	0.81	0.9719	0.9989
FTris II	0.06	0.78	0.9898	0.9942
FMEA	0.11	16.71	0.8888	0.9972
FTEA	0.06	14	0.6361	0.9986

While regression values at pH 6.8 are > 0.99, they are very poor for at pH 4.5, with values as low as 0.69 for FTEA. This is explained by the fact that at pH = 4 there is significant conversion to free acid and once the entire drug at the surface converts to the free acid, the IDR corresponds to that of flurbiprofen. Conversion to the free acid was confirmed by running DSC on samples of the tablet surface. Because of this, when a second polymorphs of FTris was discovered, IDR measurement was

limited to the more relevant pH 6.8 only. No significant difference in intrinsic dissolution values of FTris I and II was found. Both polymorphs could not be distinguished based solely on solubility and dissolution methods.

FMEA, FTEA and FAMP2 discs dissolved rapidly at pH 6.8 and sampling time was changed to once every 5 minutes. Only the points before reaching plateau were used for gradient calculation.

Fig 3.13 Intrinsic Dissolution Rate (IDR) of F at pH 4.5 and 6.8 at 37°C (n=3)

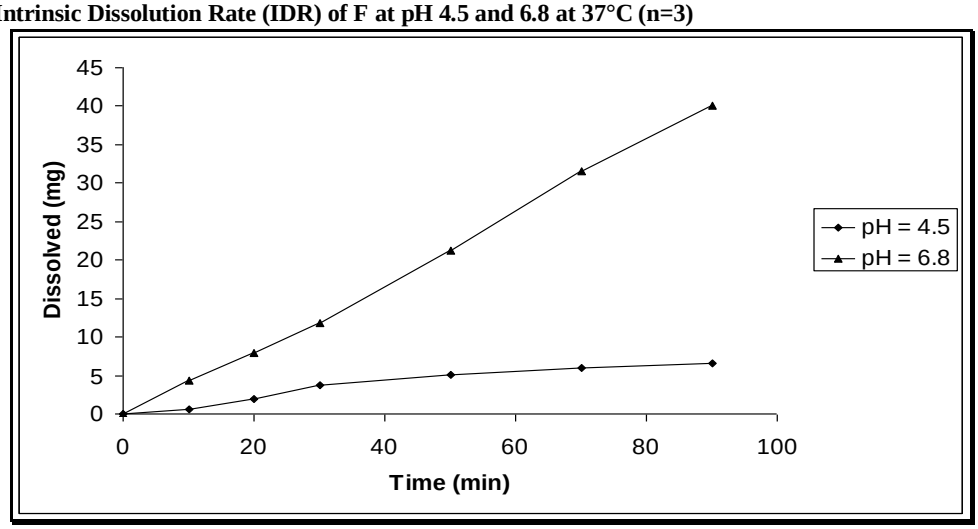

Fig 3.14 Intrinsic Dissolution Rate (IDR) of FTBut at pH 4.5 and 6.8 at 37°C (n=3)

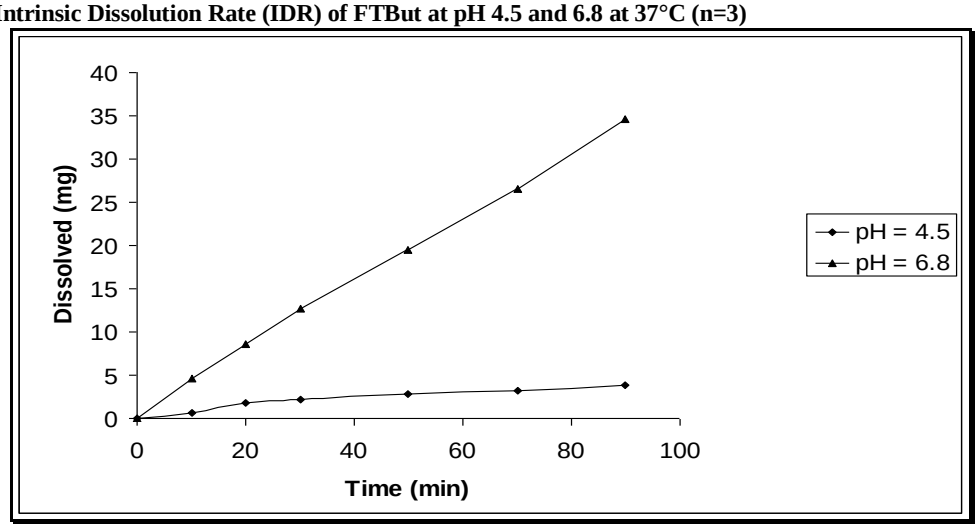

Fig 3.15 Intrinsic Dissolution Rate (IDR) of FAMP1 at pH 4.5 and 6.8 at 37°C (n=3)

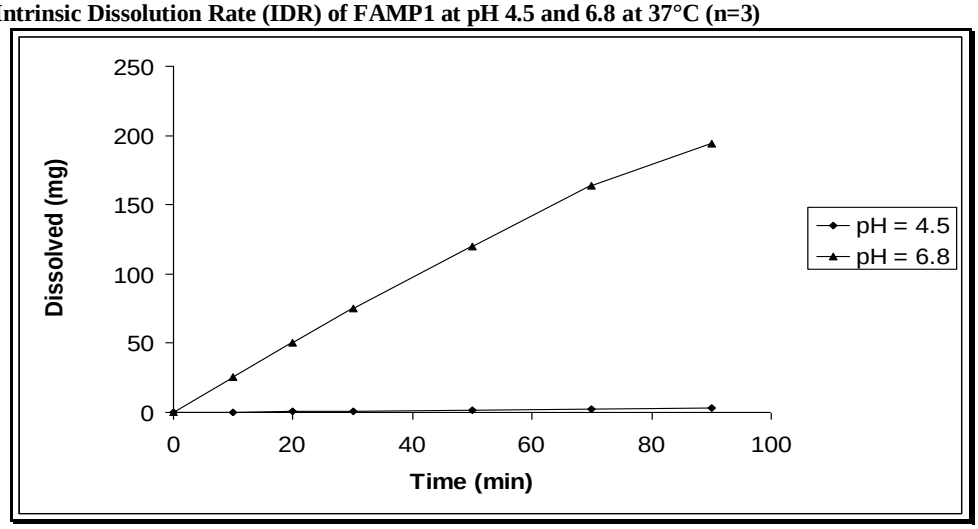

Fig 3.16 Intrinsic Dissolution Rate (IDR) of FAMP2 at pH 4.5 and 6.8 at 37°C (n=3)

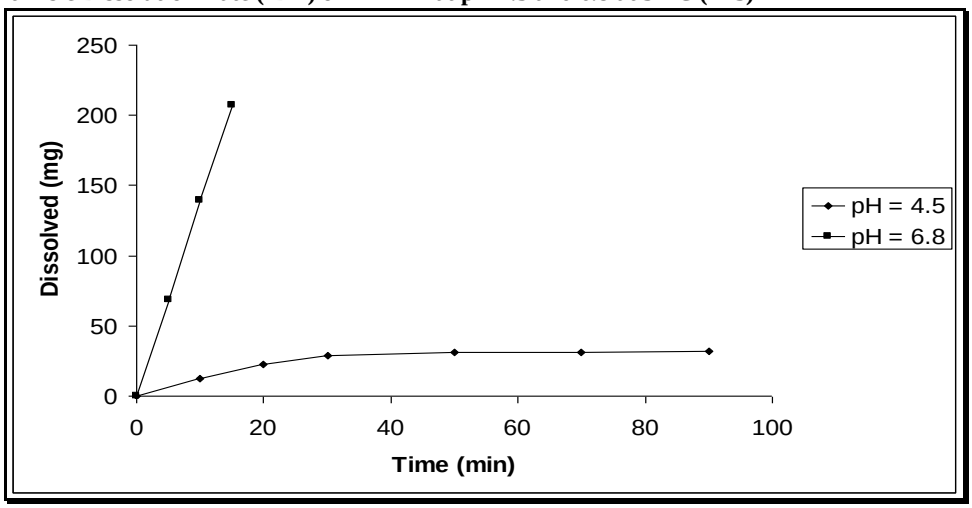

Fig 3.17 Intrinsic Dissolution Rate (IDR) of FTris I at 6.8 at 37°C (n=3)

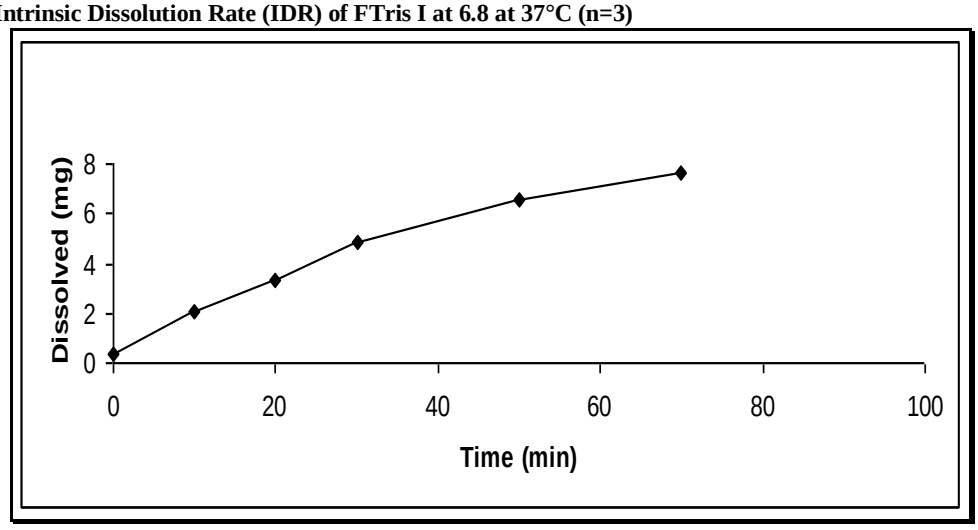

Fig 3.18 Intrinsic Dissolution Rate (IDR) of FTris II at 6.8 at 37°C (n=3)

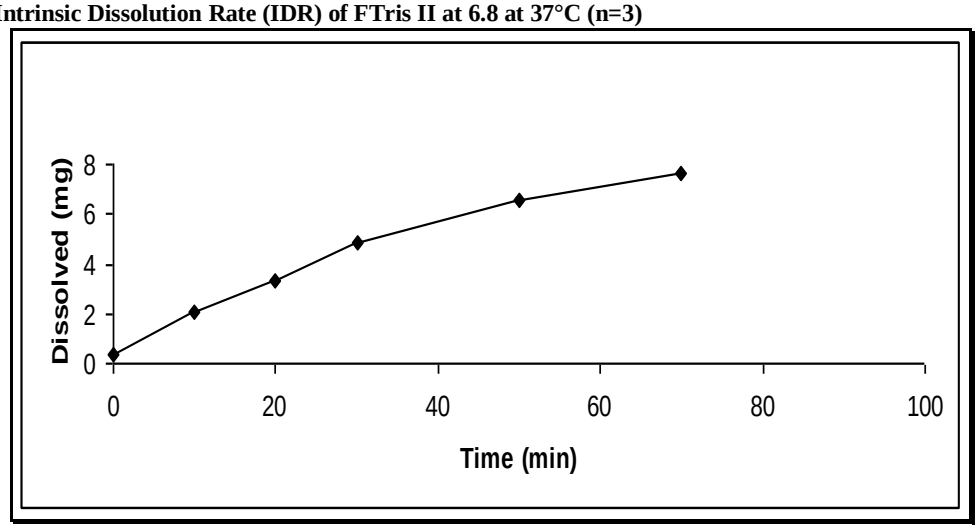

Fig 3.19 Intrinsic Dissolution Rate (IDR) of FMEA at pH 4.5 and 6.8 at 37°C (n=3)

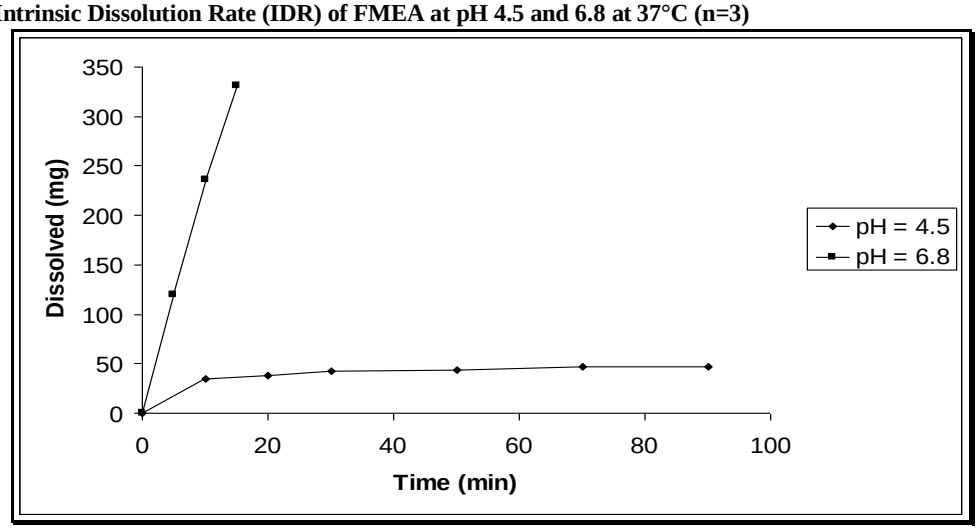

Fig 3.20 Intrinsic Dissolution Rate (IDR) of FTEA at pH 4.5 and 6.8 at 37°C (n=3)

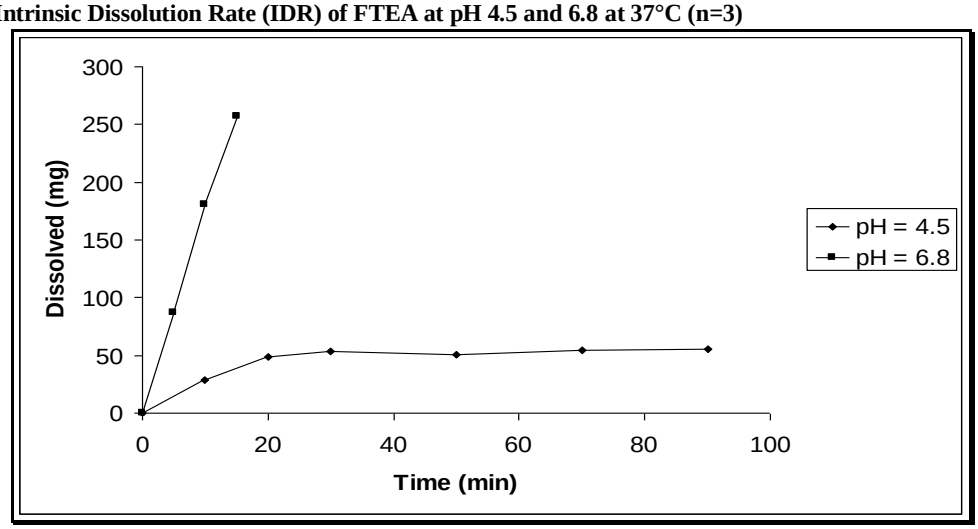

There is a correlation (R^2 = 0.9081) between saturated solubility and IDR at pH 6.8 (see Fig 3.21).

Fig 3.21 Relationship between saturated solubility and IDR at pH = 6.8

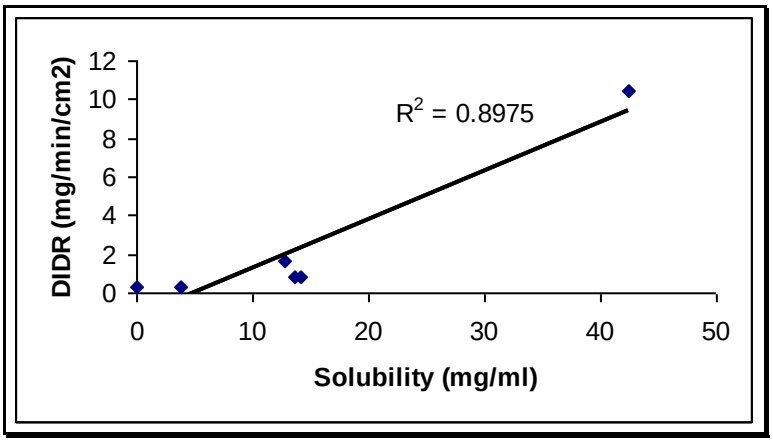

3.4 Crystal structure analysis

3.4.1 Materials

All salts were prepared as described in section 2.2.1.

3.4.2 Methods

3.4.2.1 Crystal growth

Most crystals were obtained by recrystallising from methanol. In the case of FDEA, crystals suitable for X-ray diffraction were obtained from the resultant gel on storage. Whereas FTris polymorph I was obtained by recrystallising from methanol, single crystals of FTris polymorph II were obtained by recrystallising 3g of polymorph I in 50 ml of a 40:60 warm solution of MeOH:Acetonitrile, allowing it to cool and maintaining at -20°C for 24h.

3.4.2.2 Crystal structure determination

Data on FDEA were collected locally whereas the remainders were collected at the EPSRC National Crystallography Service. Beamline I19 at the Diamond synchrotron was used to collect data on FAMP1, FTris I and FCProp. Structures were solved by direct methods and refined by full-matrix least squares.

3.4.3 Results and discussion

In an analysis of the carboxylate-ammonium hydrogen bonding patterns reported in the Cambridge Structural Database (CSD), it was revealed that the $R_4^3(10)$ column, using graph-set notation (Bernstein et al. 1995), was the most commonly occurring pattern in these salts (75/126). This $R_4^3(10)$ notation indicates a sequence of 10-membered rings with 4 hydrogen bond donors (2 per ammonium group) and 3 acceptors (one carbonyl oxygen accepting 2 hydrogen bonds).

The cation, R-NH_3^+, has the three N–H bonds of the –NH_3^+ group as hydrogen bond donors, and the anion, R'-COO^-, has the two oxygen atoms of the carboxylate group as hydrogen bond acceptors. The structure comprises chains of alternating molecules of flurbiprofen and the counterions along the b-axis, with each pair of adjacent molecules in this chain linked by an N–H···O hydrogen bond. Each carboxylate oxygen atom of flurbiprofen is the acceptor in an N–H···O hydrogen bond within such a chain, and the –NH_3^+ group of the counterion contributes two N–H bonds to the chain. The remaining N–H bond of the –NH_3^+ group forms an N–H···O hydrogen bond to a carboxylate oxygen atom of a molecule in an adjacent chain, thus effectively providing a cross-link between adjacent chains. Pairs of adjacent chains are exclusively cross-linked to each other, and do not form cross-links to any other chain. As shown in Fig 3.22, the cross-linked pairs of hydrogen-bonded chains resemble a ladder-like arrangement, with the chains representing the frame of a ladder and the cross-links representing the rungs of the ladder. The two chains of the ladder and an adjacent pair of rungs give rise to a hydrogen-bonded ring, which is designated $R_4^3(10)$ in graph set notation.

These columns are also called type-II columns by Kinbara et al. (1996) and are shown schematically in Fig 3.22. They occur even more frequently with increasing robustness if the cation containing the ammonium group is chiral.

The alternative sequence of alternating $R_4^2(8)$ and $R_4^4(12)$ columns, also known as type III columns (Nagahama et al. 2003), was the second most common (26/126) chain arrangement in the database. Two dimensional layers, built up with $R_6^5(16)$ rings, are the third most common network (19/126). When type II columns are joined by hydrogen bonds, then the 2-D resulting network is type V and, similarly, type VI networks are made up of joined Type III columns.

Figs 3.22a and 3.22b **Type II and type III hydrogen bonded columns**

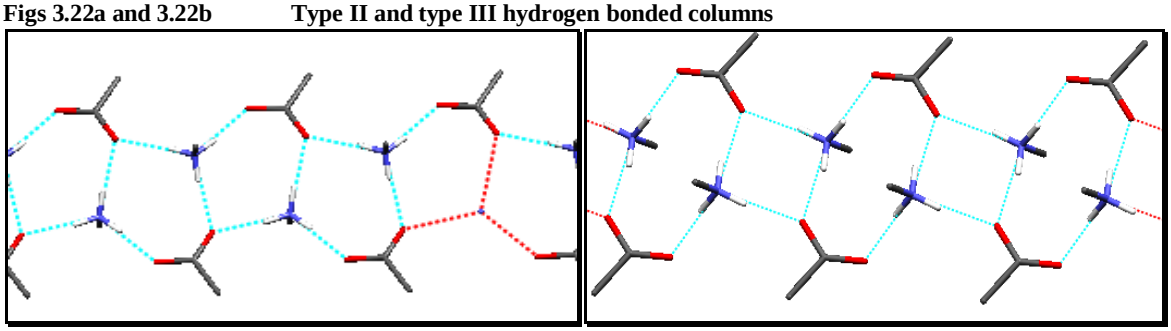

Table 3.6 **Crystal parameters and particle size for flurbiprofen acid and its salts (part 1)**

F	***FAdam***	***FBenz***	***FCProp***	***FCBut***	***FCHex***
Triclinic,	Orthorhombic,	Monoclinic,	Monoclinic,	Monoclinic,	Monoclinic,
P-1	$Pna2_1$	$P2_1$	$P2_1/n$	$P2_1/n$	$P2_1/n$
Z = 2	Z = 8	Z = 2	Z = 4	Z = 4	Z = 4
a = 9.315 Å	a = 39.350 Å	a = 10.7639 Å	a = 6.1055 Å	a = 14.4870 Å	a = 14.7991 Å
b = 12.738 Å	b = 6.3973 Å	b = 6.6034 Å	b = 15.9502 Å	b = 6.0590 Å	b = 6.3014 Å
c = 5.823 Å	c = 16.9976 Å	c = 13.1004 Å	c = 16.3340 Å	c = 19.5570 Å	c = 19.7845 Å
α = 83.0	α = 90	α = 90	α = 90	α = 90	α = 90
β = 107.2	β = 90	β = 90.912	β = 97.666	β = 92.340	β = 91.273
γ = 107.0	γ = 90	γ = 90	γ = 90	γ = 90	γ = 90
R_{int} = not reported	R_{int} = 5.8%	R_{int} = 4.5%	R_{int} = 7.7%	R_{int} = 10.3 %	R_{int} = 5.2%
PS = 36.80 µm	PS = 9.74 µm	PS = 36.17 µm	PS = 26.39 µm	PS = 33.48 µm	PS = 54.36 µm

Table 3.6 **Crystal parameters and particle size for flurbiprofen acid and its salts (part 2)**

FTBut	***FAMP1***	***FAMP2***	***FTris I***	***FTris II***	***FDEA***
Monoclinic,	Monoclinic,	Triclinic,	Triclinic,	Triclinic,	Triclinic,
$P2_1/n$	$P2_1/c$	P-1	P-1	P-1	P-1
Z = 4	Z = 4	Z = 2	Z = 2	Z = 4	Z = 2
a = 15.9343 Å	a = 16.133 Å	a = 6.1928 Å	a = 10.0028 Å	a = 6.1930 Å	a = 6.758 Å
b = 6.2903 Å	b = 6.270 Å	b = 9.5205 Å	b = 11.1012 Å	b = 9.9421 Å	b = 8.920 Å
c = 19.1949 Å	c = 18.852 Å	c = 15.1359 Å	c = 16.5792 Å	c = 14.6846 Å	c = 15.426 Å
α = 90	α = 90	α = 82.627	α = 84.389	α = 93.937	α = 80.920
β = 114.705	β = 114.883	β = 87.874	β = 78.857	β = 90.032	β = 80.130
γ = 90	γ = 90	γ = 89.058	γ = 88.253	γ = 90.718	γ = 86.230
R_{int} = 10.94%	R_{int} = 6.9%	R_{int} = 6.6%	R_{int} = 11.3%	R_{int} = 5.1%	R_{int} = 5.9%
PS = 36.35 µm	PS = 45.16 µm	PS =38.72 µm	PS = 38.48 µm	PS = 24.21 µm	PS = 66.95 µm

In the flurbiprofen series, type II columns were observed for FBenz, FCBut, FCHex and FTBut, whereas the less frequent type III columns are only seen in FAdam and FCProp structures. FAMP1 constitutes a weak example of Type V network as the two-dimensional network is kept together by weak hydrogen bonds (see section 3.4.3.8). FAMP2 and both FTris polymorphs have different but related one- and two-dimensional hydrogen bonding networks respectively.

3.4.3.1 Flurbiprofen

Monocarboxylic acids, R-COOH, which are either non-chiral or racemic form, usually contain hydrogen bonded pairs. If the R group is small, the molecules may interlink by single O-H···O bonds to form a chain motif in which the O-H···O bond is almost linear, the C=O···H-O- is around 130°, and the O-H proton donor lies in the plane of the carbonyl system O=C<, to which it is hydrogen bonded. Mono carboxylic acids with chiral residues and which are enantiomeric show some tendency to form a hydrogen bonded chain motif along a two-fold screw axis. The angular geometry of this O-H···O bond shows considerable variation and seems to be dependent upon the van der Waals forces between the R groups along the hydrogen bonded chains (Leiserowitz 1976).

Flurbiprofen is a racemic carboxylic acid having a single chiral centre. So far three different forms have been identified but only crystal structures of form I and III have been determined (Flippen and Gilardi 1975; Grzesiak and Matzger 2007) and they both form dimers. Form I is the thermodynamically stable crystal form from absolute zero to its melting point and is monotropically related to forms II and III. The melting points are 113-114 °C for form I, 92 °C for form II, and 87 °C for form III (Henck and Kuhnert-Brandstatter 1999). Form I of flurbiprofen was used in this study, which comprises non-hydrogen bonded chains of dimers.

Fig 3.23a Crystal structure of flurbiprofen form I (P-1)

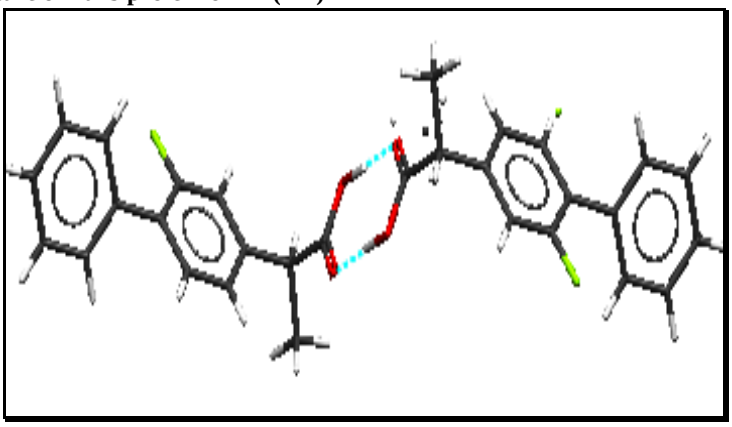

Fig 3.23bCrystal structure of flurbiprofen form I (P-1)

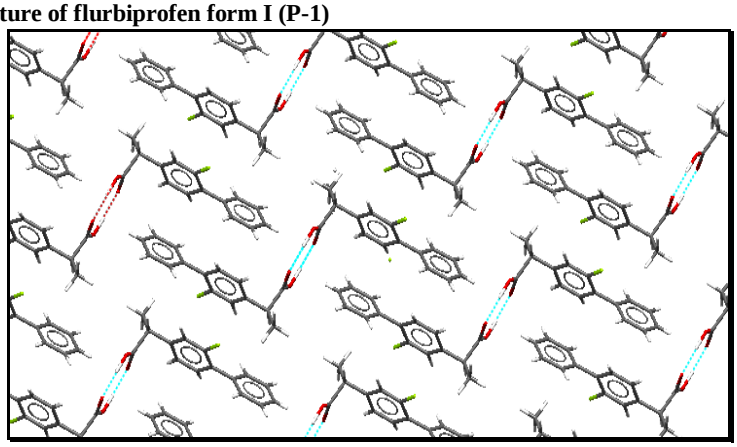

3.4.3.2 Flurbiprofen adamantamine

Flurbiprofen adamantamine (FAdam) forms hydrogen bonded ladders with NH_3^+ groups as donors and COO^- groups as acceptors. The ladders consist of alternating $R_4^2(8)$ and $R_4^4(12)$ rings, also known as Type III columns (Nagahama et al. 2003). The columns are not hydrogen bonded to adjacent columns and there are no van der Waals forces between them.

Fig 3.24aCrystal structure of flurbiprofen adamantamine ($Pna2_1$)

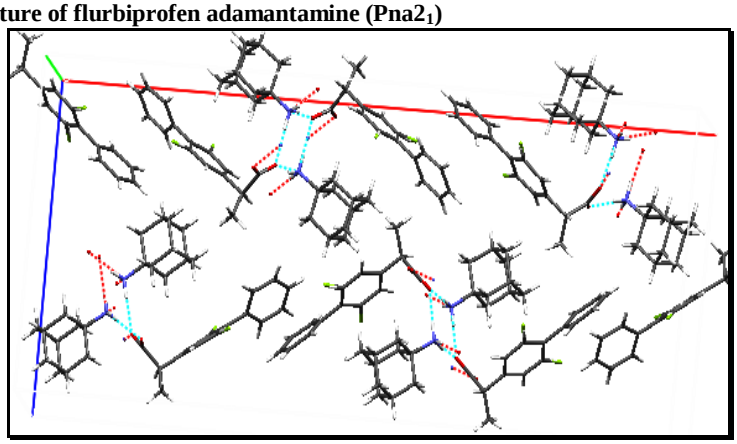

Fig 3.24bCrystal structure of flurbiprofen adamantamine ($Pna2_1$)

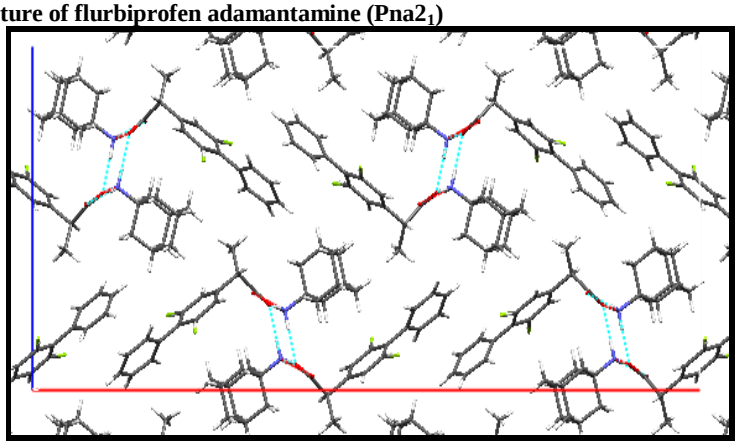

3.4.3.3 Flurbiprofen benzylamine

Flurbiprofen benzylamine (FBenz) forms identical infinite ladders formed by N-H···O hydrogen bonds with successive $R_4^3(10)$ rings. These Type II columns arrange themselves in layers with the benzene rings of flurbiprofen facing outwards and the counterions inside the layers. Neither the columns, nor the resulting layers, are hydrogen bonded.

Fig 3.25a and 3.25b **Crystal structure of flurbiprofen benzylamine ($P2_1$)**

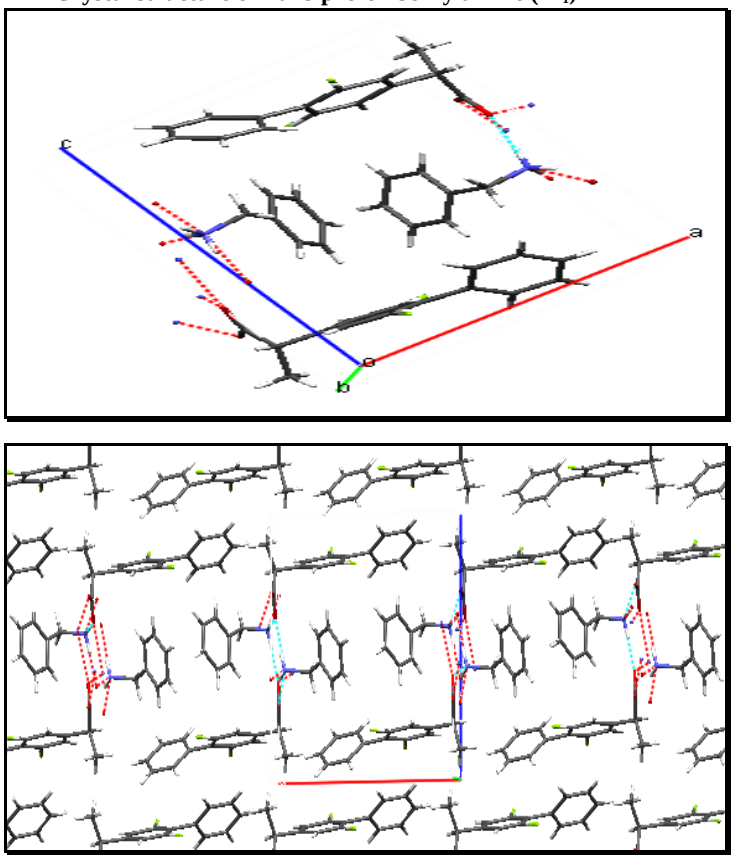

3.4.3.4 Flurbiprofen cylopropylamine

Flurbiprofen cyclopropylamine (FCProp) constitutes the second example of type III columns in this series with alternating $R_4^2(8)$ and $R_4^4(12)$ rings. These columns are arranged in zigzagged layers that are not hydrogen bonded. The methyl groups in flurbiprofen are disordered with no effect on the overall hydrogen bonding network.

Fig 3.26a and 3.26b **Crystal structure of flurbiprofen cyclopropylamine ($P2_1/n$)**

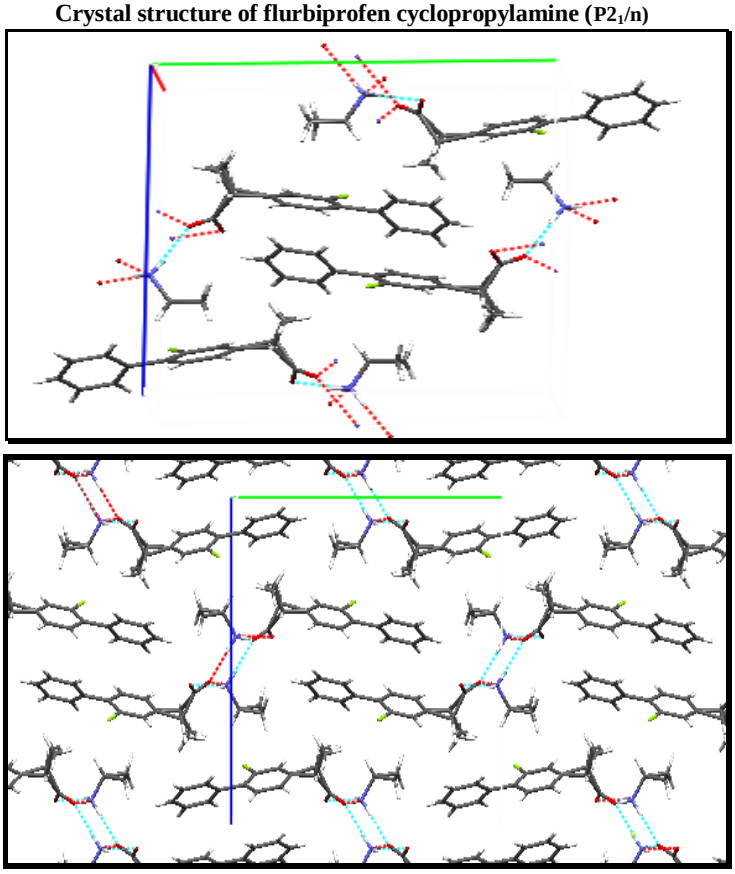

3.4.3.5 Flurbiprofen cyclobutylamine

The crystal packing of flurbiprofen cyclobutylamine (FCBut) resembles that of FBenz but has a different space group ($P2_1/n$ vs. $P2_1$). Type II columns of $R_4^3(10)$ rings are observed. These Type II columns arrange themselves in layers with the benzene rings of flurbiprofen in the outside and the counterions inside. Neither the columns nor the resulting layers are hydrogen bonded.

Fig 3.27a Crystal structure of flurbiprofen cyclobutylamine ($P2_1/n$)

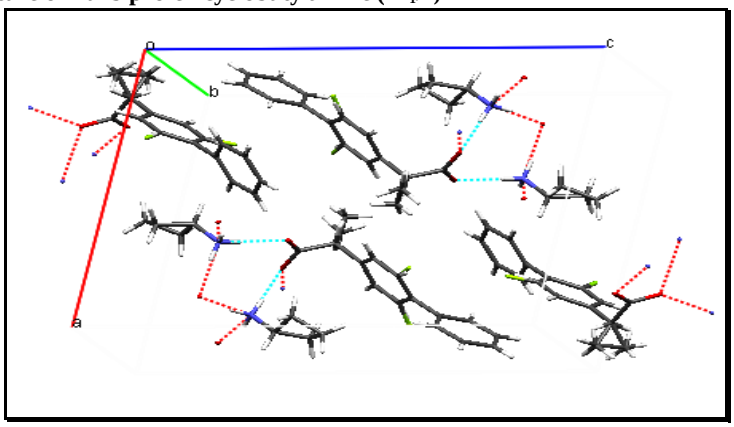

Fig 3.27bCrystal structure of flurbiprofen cyclobutylamine ($P2_1/n$)

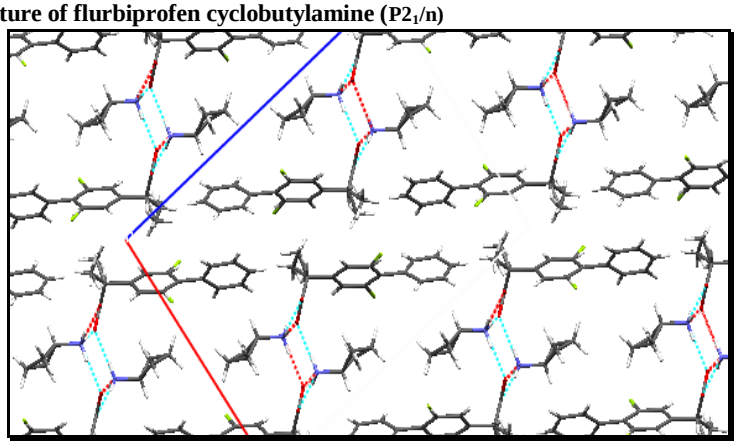

3.4.3.6 Flurbiprofen cyclohexylamine

Flurbiprofen cyclohexylamine (FCHex) also exhibits virtually identical packing to that seen in FBenz and FCBut; typical type II columns of successive $R_4^3(10)$ rings. Type II columns arrange themselves in layers with the benzene rings of flurbiprofen facing outwards and the counterions inwards. Neither the columns nor the resulting layers are hydrogen bonded. There are two kinds of disorder in this structure: almost 50:50 disorder in the positioning of the methyl group in the isopropyl moiety, showing little discrimination between enantiomers; and approximately 2:1 disorder in the position of the fluorine atom arising from a 2-fold rotation of the benzene ring.

Fig 3.28aCrystal structure of flurbiprofen cyclohexylamine ($P2_1/n$)

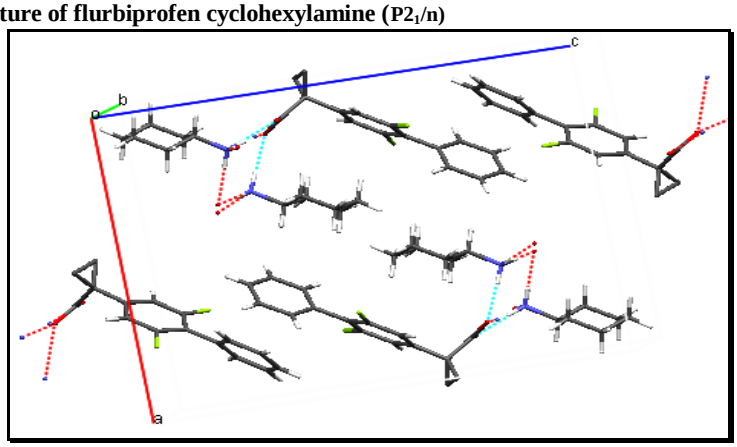

Fig 3.28b Crystal structure of flurbiprofen cyclohexylamine ($P2_1/n$)

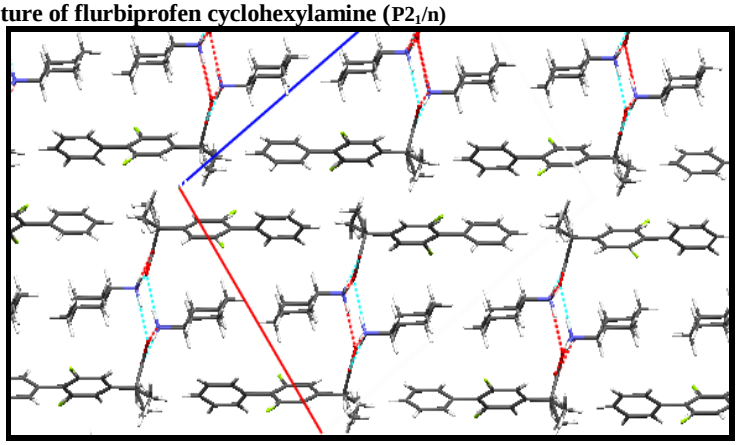

3.4.3.7 Flurbiprofen tert-butylamine

In flurbiprofen tert-butylamine (FTBut), donation of hydrogen bonds from $^{+}NH_3$ to OCO^{-} forms the ladders built out of $R_4^3(10)$ rings previously described for FBenz, FCBut and FCHex. In FTBut, the columns do not arrange themselves in straight parallel layers. Adjacent columns intercalate their biphenyl groups leaving a zigzagging interplanar space free of hydrogen bonds.

Fig 3.29a Crystal structure of flurbiprofen tert-butylamine ($P2_1/n$)

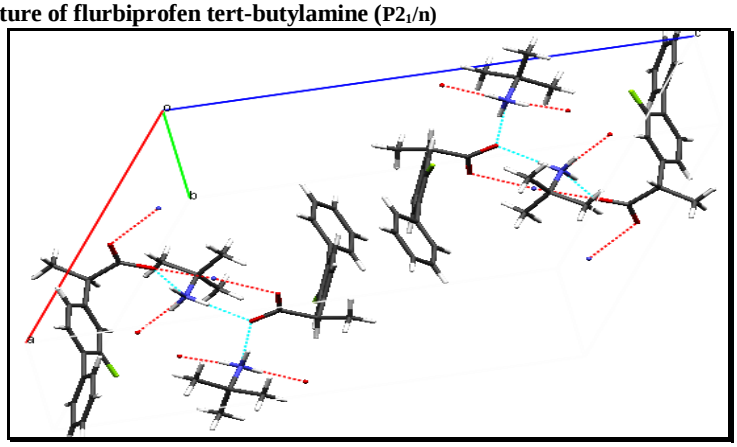

Fig 3.29bCrystal structure of flurbiprofen tert-butylamine ($P2_1/n$)

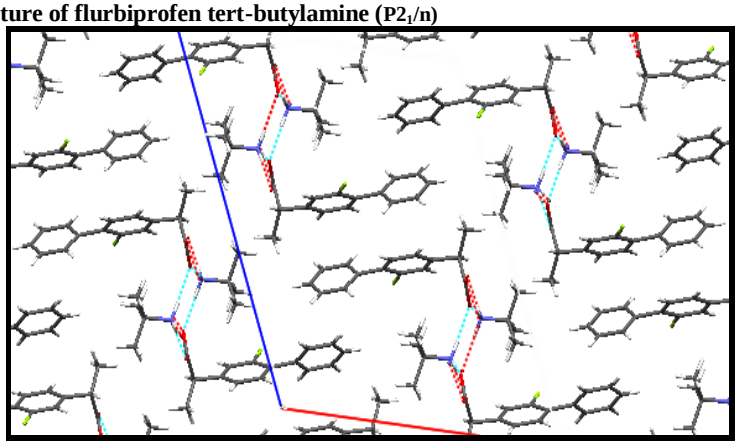

3.4.3.8 Flurbiprofen 2-amino-2-methylpropanol salt (FAMP1)

The structure described for FTBut remains unchanged after substitution with one OH group in FAMP1 as the OH group is disordered and behaves as a weak hydrogen bond acceptor. Disorder is observed in the hydroxyl group with 2 alternative positions: one hydroxyl position does not form a hydrogen bond and the other hydroxyl group, with a O···O distance of 3.034 Å makes a weak hydrogen bond. Generally, distances of <3 Å can be interpreted as hydrogen bonds (Steiner and Saenger 1995). In the distance region of 3-3.6 Å, the probability of a hydrogen bond decreases with increasing distance.

When Type II columns are hydrogen bonded they form a two-dimensional network called type V network. In FAMP1, we observe a case of weak Type V network due to the cross linking provided by the long hydrogen bonds of the disordered hydroxyl group.

Fig 3.30aCrystal structure of flurbiprofen AMP1 ($P2_1/c$)

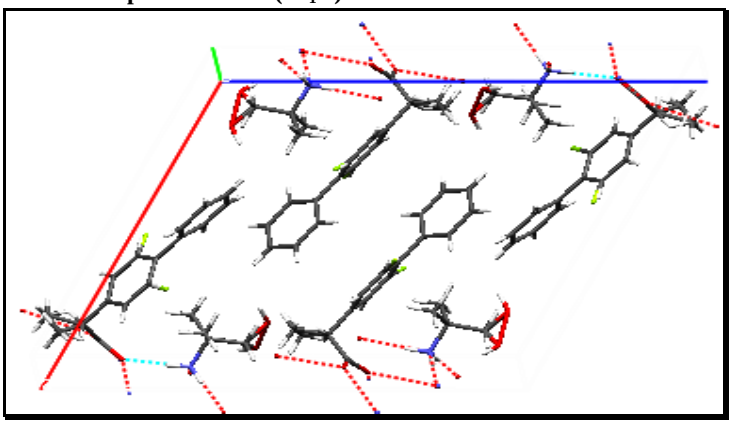

Fig 3.30bCrystal structure of flurbiprofen AMP1 ($P2_1/c$)

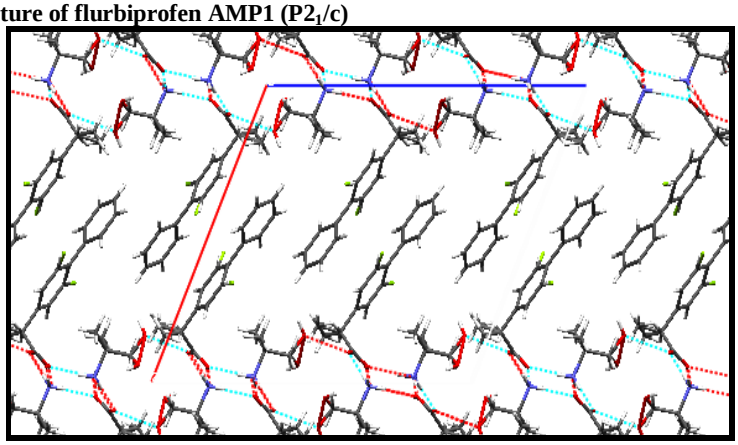

3.4.3.9 Flurbiprofen 2-amino-2methyl-1,3-propanediol (FAMP2)

Adding a second OH group to the counterion, as in FAMP2, changes the pattern fundamentally. Simple HNH···OCO···HNH···OCO hydrogen bonds still form a charge-assisted C(6) infinite chain traversing the entire crystal, but in addition cations deploy one NH and one OH hydrogen atom in hydrogen bonds to one anion forming a ring, $R_2^2(9)$. The other OH group links intermolecularly to the first one while NH finds OCO^- $R_3^2(9)$. The third amino H atom pairs with OH as acceptor in the $R_2^2(10)$ centrosymmetric dimer. This pattern results in a 1-D network of parallel, non-hydrogen-bonded, columns.

Fig 3.31aCrystal structure of flurbiprofen AMP2 (P-1)

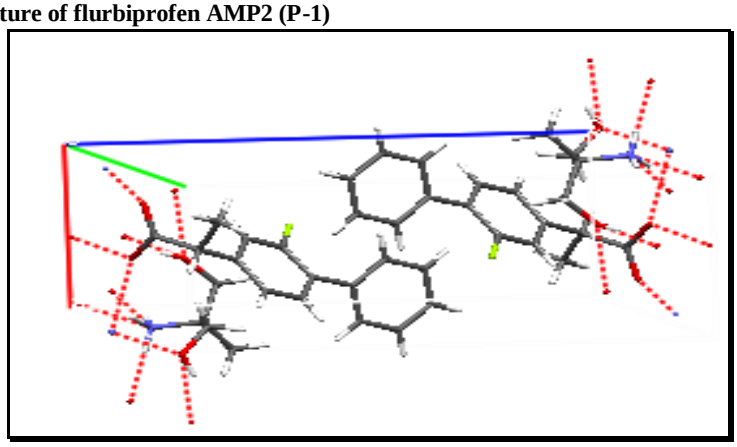

Fig 3.31bCrystal structure of flurbiprofen AMP2 (P-1)

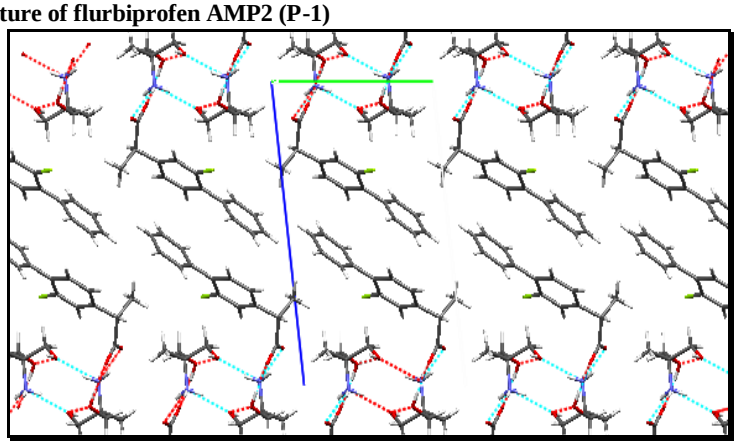

3.4.3.10 Flurbiprofen tris form I (FTris I)

Two polymorphic forms of FTris were identified. Crystals of FTris form I have Z' = 2 in a triclinic cell; independent ions are related by pseudosymmetry and show disorder. Each carboxylate O atom accepts only one hydrogen bond, and the C(6) chain has disappeared. Each N atom is within 2.79-2.91 Å of four oxygen atoms but can only donate three hydrogen bonds. The twist angle in the biphenyl moiety of F in this molecule is 55° and 61° here but 44-46° in the other structures.

Fig 3.32aCrystal structure of flurbiprofen Tris I (P-1)

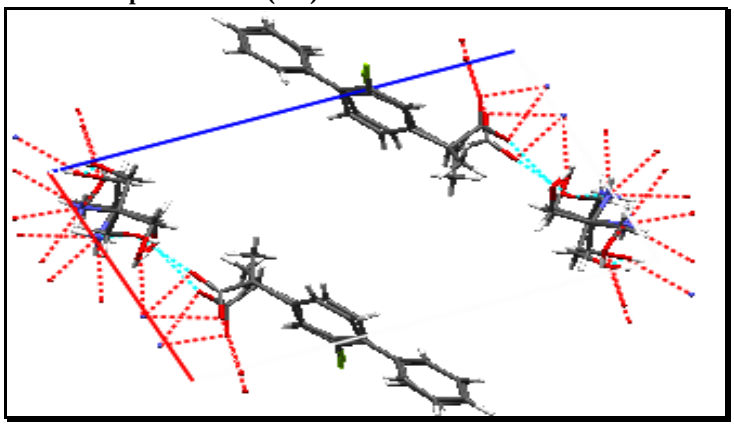

Fig 3.32a Crystal structure of flurbiprofen Tris I (P-1)

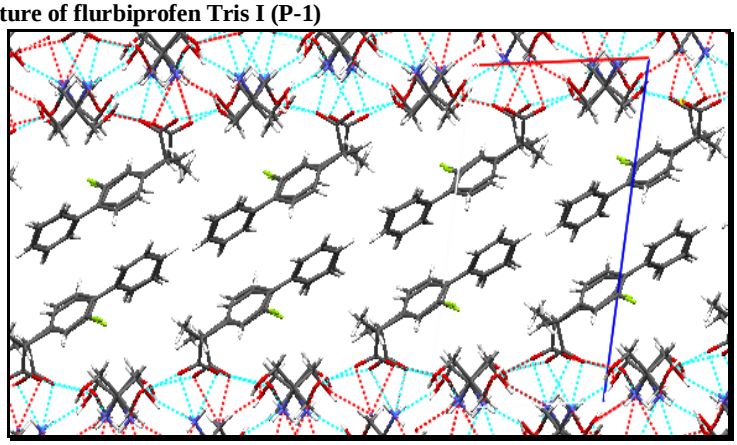

3.4.3.11 Flurbiprofen tris form II (FTris II)

Form II is well ordered with similar hydrogen bonds to those in FAMP2. In particular, the C(6) chain persists. The additional hydroxyl group donates a hydrogen bond to the carboxylate O linking the columns to form a two dimensional layer.

Fig 3.33a and 3.33b Crystal structure of flurbiprofen Tris II (P-1)

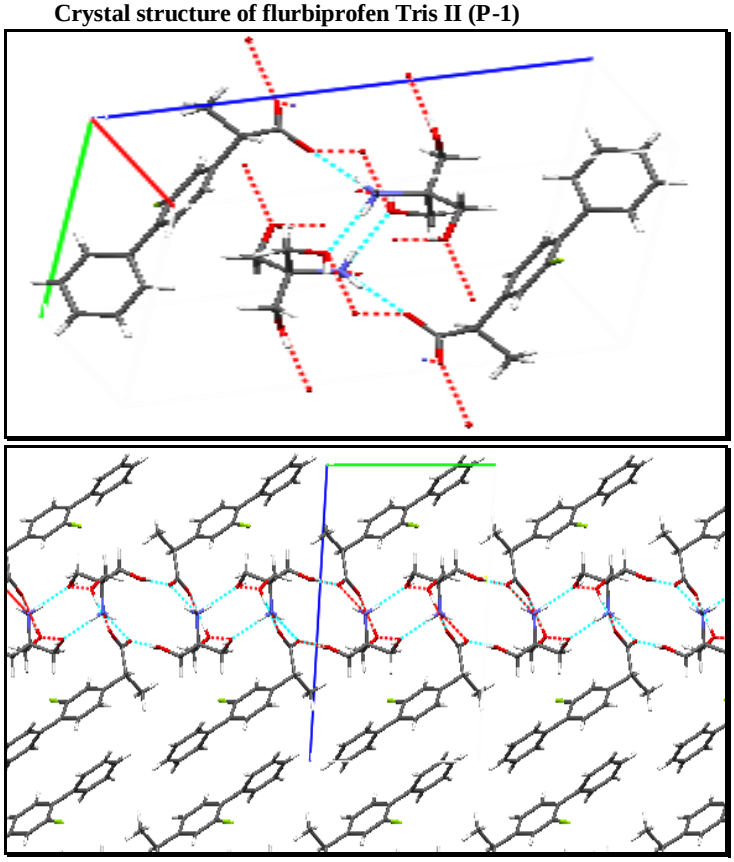

3.4.3.12 Flurbiprofen diethanolamine (FDEA)

The diethanolamine cation has disorder in one hydroxyethyl group. The hydrogen bonds form no extended motif. Two anions and two cations using NH^{3+} and COO^{-} functionality create a discrete $R_4^4(12)$ ring. Instead of linking adjacent rings, one ethanolamine OH donates a hydrogen bond to the same carboxylate O atom already accepting from NH, thus appending $R_2^1(7)$ rings to either side of the main ring. The other ethanolamine OH can link to a carboxylate O atom across the large ring but is disordered. Hydroxyl O atoms accept no hydrogen bonds from NH or OH donors. There is no cross-linking between these 2:2 unit.

Fig 3.34a and 3.34b **Crystal structure of flurbiprofen diethanolamine (P-1)**

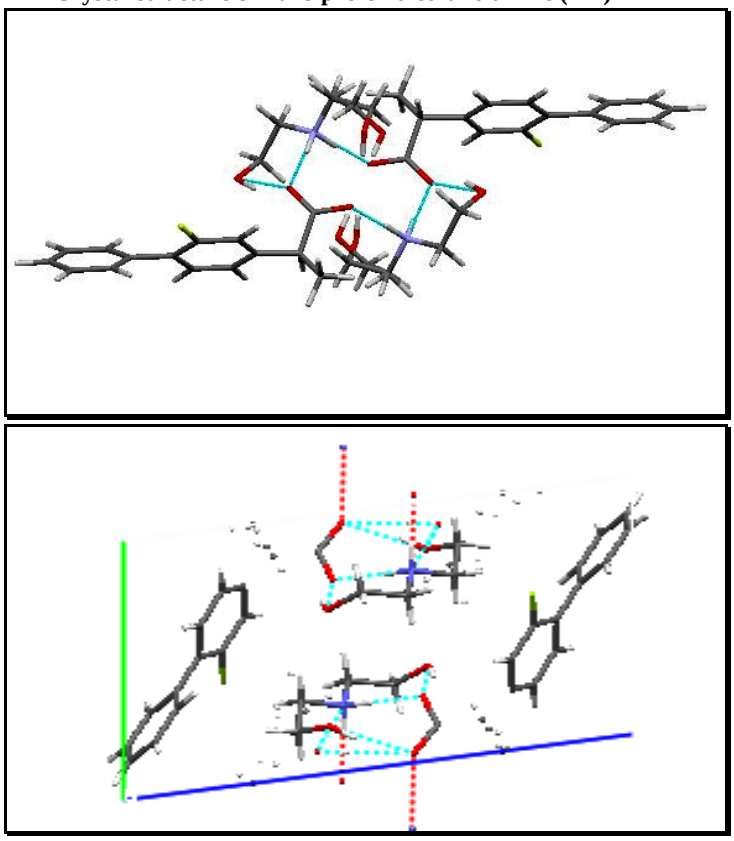

3.5 Mechanical properties

3.5.1 3-point bending test

3.5.1.1 Materials

Salts were prepared as in section 2.2.1. A sieved fraction between 96 – 250 μm was selected for use in mechanical testing.

3.5.1.2 Method

As described in 2.5.1. True density values were calculated using a Accupyc 1330v1.03 helium pycnometer.

3.5.1.3 Results

True density values for flurbiprofen salts are summarised in Table 3.7.

Table 3.7True density values for flurbiprofen and its salts (n = 5, SD)

	True Density (g/cm^3)
F	1.2940 ± 0.0008
FAdam	1.2279 ± 0.001
FBenz	1.2572 ± 0.0013
FCProp	1.2381 ± 0.07
FCBut	1.2213 ± 0.007
FCHex	1.2403 ± 0.0001
FTBut	1.2160 ± 0.003
FAMP1	1.2388 ± 0.002
FAMP2	1.3163 ± 0.0005
FTris I	1.3411 ± 0.0011
FTris II	1.3575 ± 0.002
FMEA	1.3109 ± 0.003
FDEA	1.2874 ± 0.002
FTEA	1.3874 ± 0.0011

It can be observed that, in general, true density is higher for salts containing hydroxyl groups and is highest for those salts with 3 hydroxyl groups (FTEA and FTris I and II). It is likely that the higher number of hydroxyl groups is related to more hydrogen bonding and therefore, better packed network.

Elastic moduli versus porosity are represented in Fig 3.35 and all Young's moduli are summarized in Table 3.8.

A low Young's modulus means that the material is more prone to elastic deformation. With the exception of FTris I, the obtained Young's moduli are in line with those of other pharmaceutical material reported in the literature using the 3-point bending test (see Table 3.9).

Table 3.8 Young's Moduli (E_0) and flexural strength (σ) at SF = 0.85 for flurbiprofen drug and its salts (n=6)

	E_0 (GPa)	σ (MPa)
F	3.54	3.55
FTBut	5.58	6.86
FAMP1	5.42	5.12
FAMP2	17.56	6.29
FTris I	994.80	0.76
FTris II	2.79	4.62
FMEA	5.66	6.58
FTEA	17.31	6.96

Fig 3.35 Young's modulus versus porosity

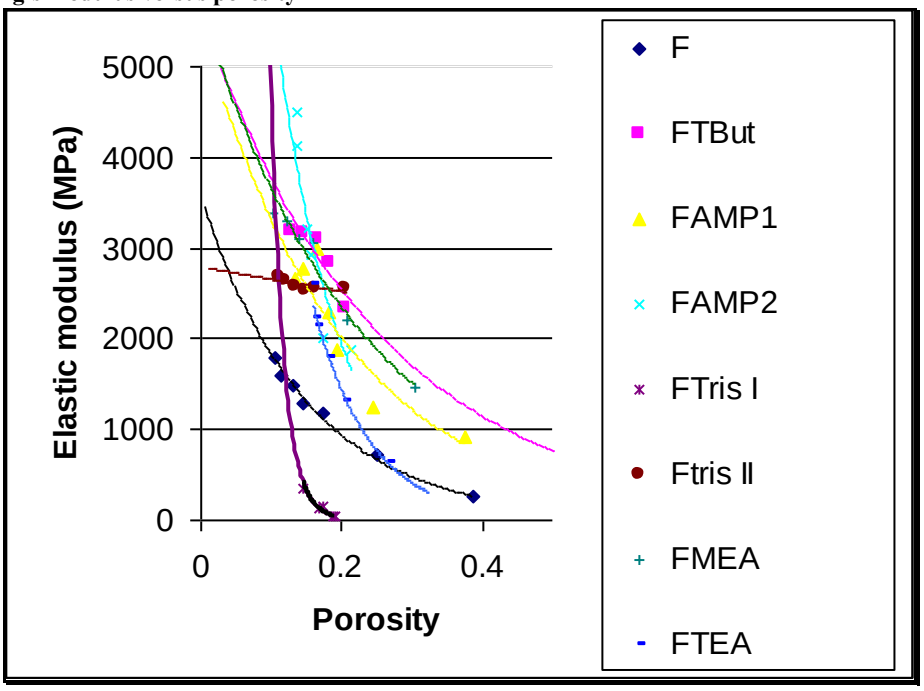

As can be seen from the Table 3.8, Young's modulus varies between polymorphic pairs due to differences in the packing motifs. Better packing and the three-dimensional nature of the hydrogen

bond network manifested itself in higher Young's modulus in the case of sulfanilamide β compared to sulfanilamide γ (Roberts and Rowe 1996). Similarly, in FTris polymorphic pair there are appreciable differences in Young's modulus. Polymorphic pairs with conformational differences can result in different mechanical properties. In fact, the Young's modulus of FTris I differs from all the others.

With the exception of FTris I, prior to breakage point, elastic deformation was the deformation mechanism observed for all materials. In FTris I deformation was plastic as observed in the post-peak regions of the stress-strain profile. All materials exhibited a sharp decline in stress after fracture whereas in FTris I the stress declined gradually after fracture. This is reflected in the abnormally high Young's modulus. When the fragments can be rebuilt into the original pellet/compact this has been used as a criterion for discrimination of elastic failure mode (Frechette 1990). Fragments of FTris I compact were flattened or deformed which made reconstruction of the compact impossible, suggesting a ductile nature. Crack initiation and propagation are essential to fracture. The manner in which the crack propagates through the material gives great insight into the mode of fracture. In ductile materials, the crack moves slowly and is accompanied by a large amount of plastic deformation. The crack will usually not extend unless an increased stress is applied. On the other hand, when dealing with brittle materials, cracks spread very rapidly with little or no plastic deformation.

FTris I was a difficult material with which to work. During compact preparation, visually appreciable recovery started soon after ejection, often accompanied by deformation and bending of edges especially at higher compaction pressures. This high elastic recovery resulted in weaker compacts as reflected in the low tensile strength values. It is suspected that due to this troublesome elastic recovery compact bonding was impaired resulting in a less coherent compact.

This model is highly idealized. The assumption of monosized powder distribution within the specimen and identical powder arrangement are required by the model and are clearly violated due to the non-uniform particle size distribution and irregular stacking. Measurements of deformation are unidirectional and therefore non-isotropic. Additionally, it was observed that the test was very sensitive to problems derived from handling e.g. specimen defects or positioning. It can be observed in Table 3.9 that different values of elastic modulus for aspirin have been reported (7.45 vs. 1.84 GPa). Nevertheless, the 3-point bending test has proved to be a useful method to distinguish those materials where plastic deformation and fracture predominates over brittle fracture, such as FTris I.

Table 3.9Young's modulus of pharmaceutical materials as determined by the 3-point bending test (Roberts et al. 1991; Podczeck 2001)[1,2]

Drug/excipient	Young's modulus (GPa)
Theophylline	12.93
Paracetamol	11.65
Caffeine	8.73
Sulfadiazine	7.70
Aspirin[1]	7.45
Aspirin[2]	1.84
Tolbutamide	5.22
Ibuprofen	5.02
Testosterone propionate	3.16
Phenylbutazone	3.33
Carbamazepine III	13.19
Carbamazepine I	3.67
Sulfathiazole III	14.59
Sulfathiazole I	10.55
Sulfanilamide β	10.66
Sulfanilamide γ	6.34

3.5.2 Compaction replication

Compaction properties of flurbiprofen salts were determined using the Stylcam 100R (Medelpharm, Bourge-en Bresse, France) with acquisition software (Analis version 2.01.27, Medelpharm). Stylcam 100R is a compression replicator, designed to allow compaction analysis on APIs and formulated products. Its main use is to replicate production tablet presses and to predict the performance of formulations at full scale production.

3.5.2.1 Materials

All flurbiprofen salts were obtained as described in section 2.2.1. A sieved fraction between 96 – 250 μm was selected for use in mechanical testing.

3.5.2.2 Method

Method was followed as described in 2.5.2.1.

3.5.2.3 Results and discussion

The following values of yield pressure (P_y) and elastic recovery where recorded (see Table 3.10).

The yield pressure values recorded correspond to soft to moderately hard materials where the main consolidation mechanism is fragmentation, plastic or elastic deformation or a combination of all three (see Fig 3.36). Brittle materials, such as dibasic calcium phosphate dihydrate, acetaminophen and lactose, compress mainly by fragmentation. Ductile materials such as microcrystalline cellulose and starch compress mainly by plastic deformation (Rowe et al. 1996). It is well known that fragmentation and plastic deformation occur with all materials and it is the extent of the two processes taking place during compression that determines the volume reduction mechanism of a given material.

It is important to highlight FDEA, with a P_y value of 6.81 MPa, which was a completely plastic material and the tablet crusher would literally sink in the compact. This is in line with the practically absent elastic recovery after ejection.

Table 3.10 **Yield Pressure (MPa) and elastic recovery (%) for flurbiprofen salts**

	Yield pressure, P_y (MPa)	**Elastic recovery (%)**
Flurbiprofen	62.97	2.80
FAdam	140.42	6.86
FBenz	41.14	5.50
FCProp	41.10	6.42
FCBut	58.08	4.24
FCHex	66.22	4.27
FTBut	72.73	10.80
FAMP1	90.12	4.59
FAMP2	96.54	3.91
FTris I	90.66	"8.36"
FTris II	98.32	5.07
FMEA	69.17	4.35
FDEA	6.81	0.50
FTEA	102.03	2.52

Capping and lamination occur when the bonds within a tablet cannot withstand the elastic recovery during decompression. Reducing compression pressure and reducing decompression speed, within practical limits or increasing the binder or moisture content may be an option to overcome tablet

failure by capping and lamination. It is generally accepted in practice that elastic recovery values exceeding 10% can result in the above problems. All the elastic recovery values are within the acceptable range with the exception of FTris I, which could not be measured but was visually appreciable after ejection. For this reason, it was difficult to obtain compacts of a specific thickness. When preparing the compacts, instead of aiming for the target thickness of 3.51 mm, which would result in tablets of 0.85 solid fraction, compacts of 3.40-3.45 mm were made and thickness was measured constantly after ejection until it reached the desired thickness by relaxation and tensile strength was then measured without delay.

Fig 3.36 Typical Yield Pressure, P_y (MPa) values of pharmaceutical materials. Adapted from (Alderborn and Nystroem 1996)

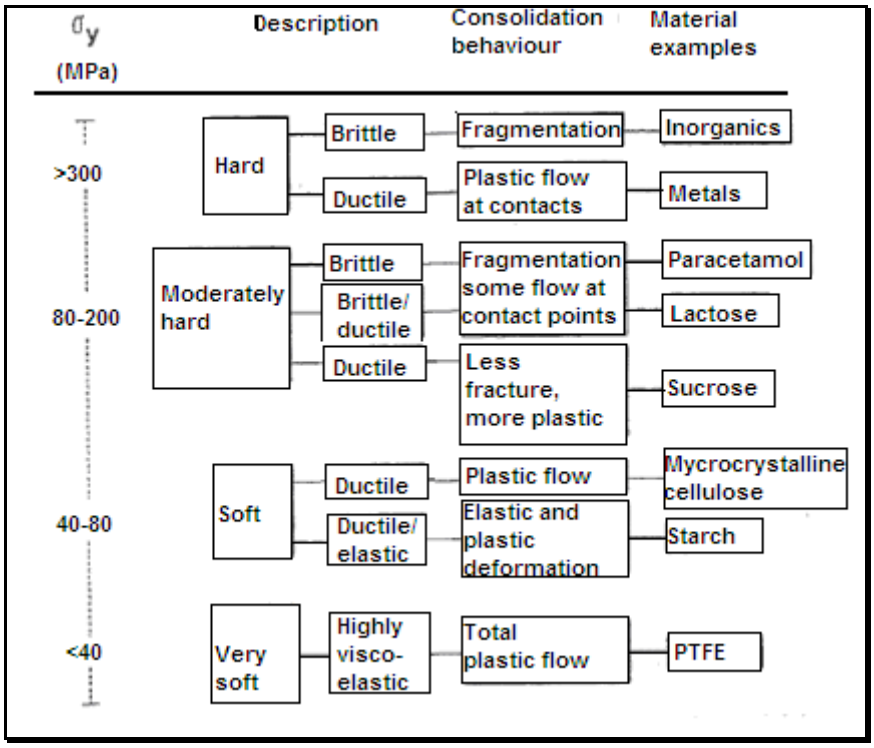

Tensile strength values of flurbiprofen and its salts are presented in Fig 3.37 and Table 3.10.

Initial observations are that, with the exception of FTris I, at 0.85 solid fraction, all the salts that contain hydroxyl groups exhibit tensile strengths above 1 MPa, a value generally regarded as acceptable, and higher than those of salts with no potential for hydrogen bonding.

To simplify the interpretation of the results, the series was divided into subgroups with structural similarities to facilitate identification of the impact of crystal/molecular structure on the mechanical properties.

Fig 3.37 Tensile strength for flurbiprofen salt series at SF=0.85. (n=6; mean±s.d.)

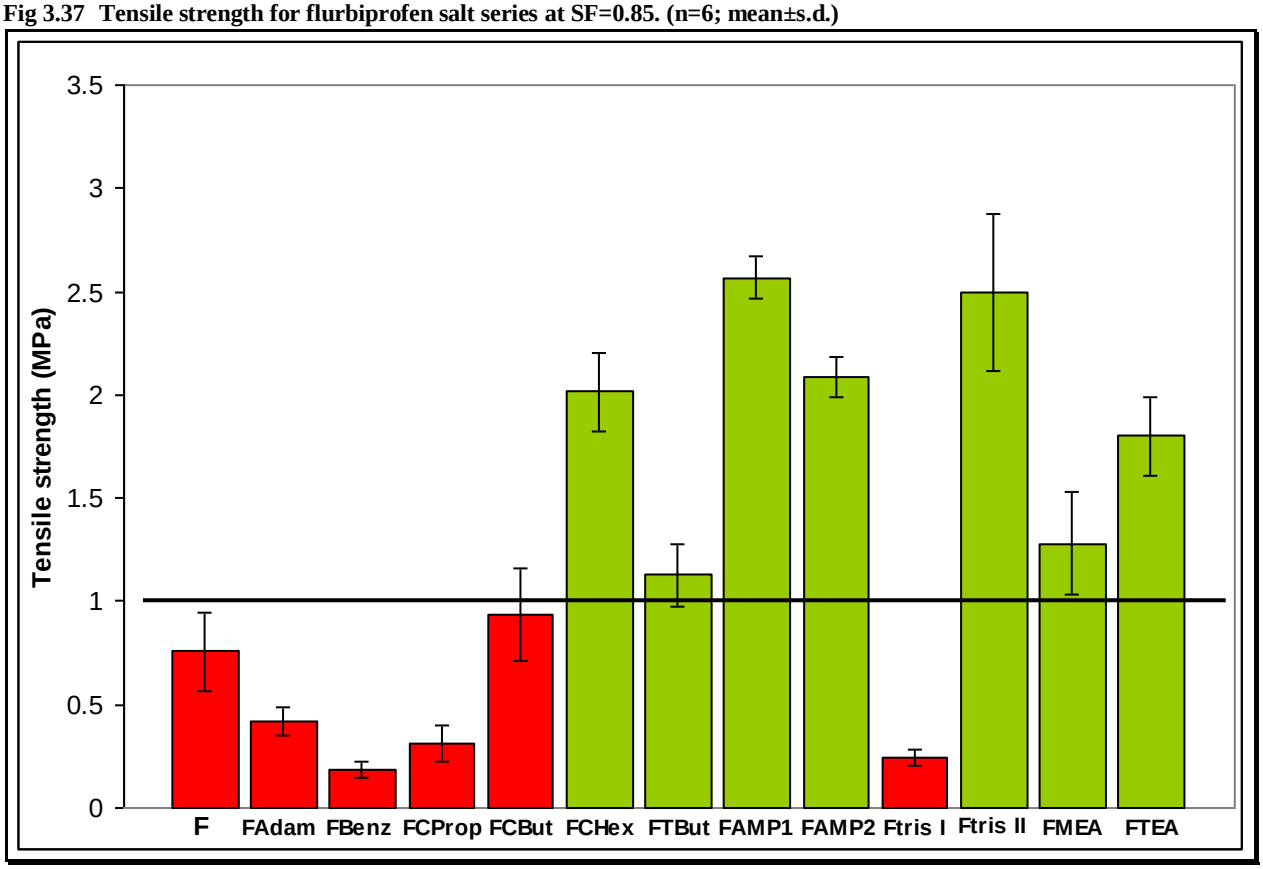

Table 3.10 Tensile strength values for flurbiprofen salts (MPa) (n=6; mean±s.d.)

	F	FAdam	FBenz	FCBut	FCProp	FCHex	FTBut	FAMP1	FAMP2	FTris I	FTris II	FMEA	FTEA
TS, n= 6, (MPa)	**0.76**	**0.42**	**0.19**	**0.93**	**0.31**	**2.02**	**1.13**	**2.57**	**2.09**	**0.24**	**2.49**	**1.28**	**1.80**
SD	0.19	0.07	0.04	0.22	0.09	0.19	0.15	0.10	0.09	0.04	0.38	0.25	0.22

3.5.2.3.1 FBenz-FCHex-FTBut

All three salts share the same one-dimensional, more frequently occurring $R_4^3(10)$ columns (Lemmerer 2008). See section 3.4.3.

The presence of *slip planes* is another motif common to these three salts. Slip planes correspond to the regions of weakest interaction between adjacent planes and have been used to explain differences in mechanical properties between polymorphs (Roberts and Rowe 1996; Sun and Grant 2001c), hydrate/anhydrates (Sun and Grant 2004; Joiris et al. 2008) and structurally related molecules (Feng and Sun 2007). Slip planes allow slippage of one layer over the adjacent one, enabling greater plastic deformation to produce stronger tablets. These crystallographic planes can also be identified by visualization of crystals characterized by stacking layers of high molecular density and often strengthened by two-dimensional hydrogen bonding network.

Apart from sharing the same hydrogen bonding pattern, these three salts have rather similar crystal parameters (see Table 3.6 for crystal parameters).

The arrangement of the columns differs among the three salts. In FBenz and FCHex the columns are arranged in straight layers with the ($R\text{-}NH_3^+$)•(R'-COO-) heterosynthon inside and the flurbiprofen biphenyl towards the outside, allowing a straight slip plane free of hydrogen bonds. In FCHex the nearest interlayer distance is of 2.803 Å for a C-H contact, which exceeds, van der Waals contacts, however, in FBenz, the layers are profusely cross-linked by van der Waals forces (see Fig 3.40) with distances of 3.078 Å and 2.801 Å for C-F contacts and 2.137 Å for H-F contacts. In FTBut, the columns intercalate originating wide interlayer space of zigzagging nature, where shortest interplanar distance is 3.558 Å for a C-C contact, which comfortably exceeds van der Waals distances.

Fig 3.38 Crystal arrangement in FCHex

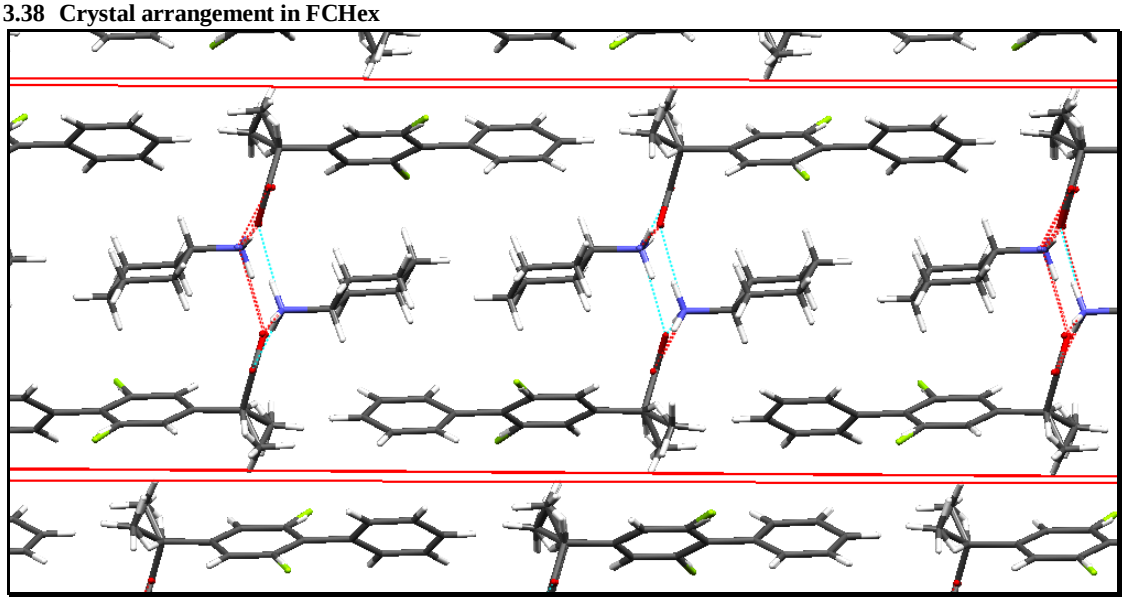

Fig 3.39 Crystal arrangement in FBenz

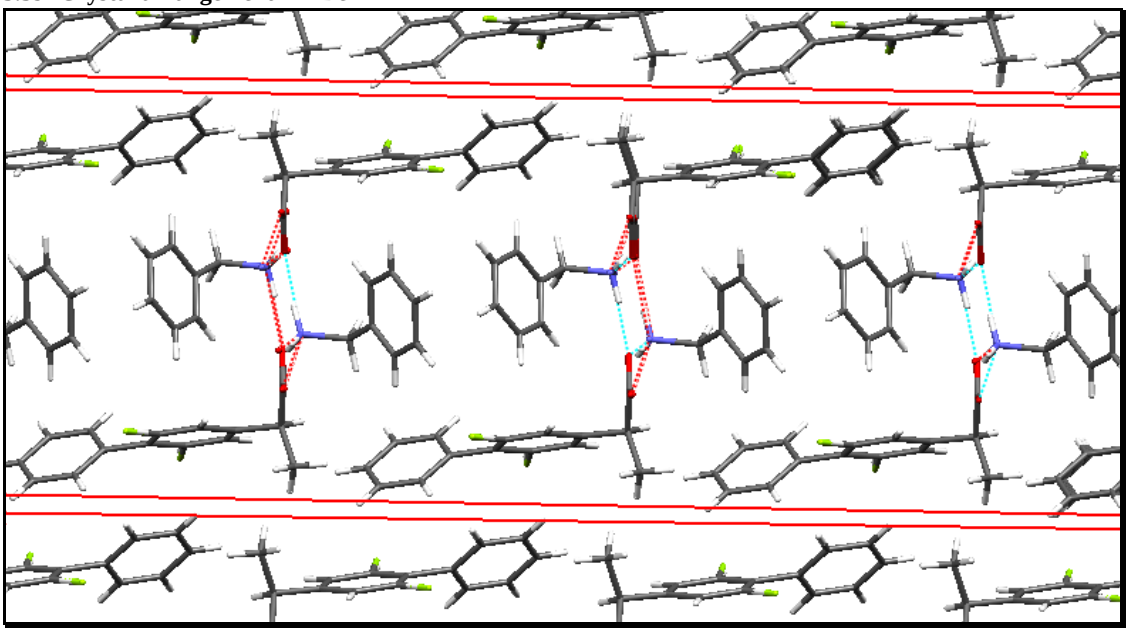

Fig 3.40 Crystal arrangement in FBenz showing van der Waals interactions

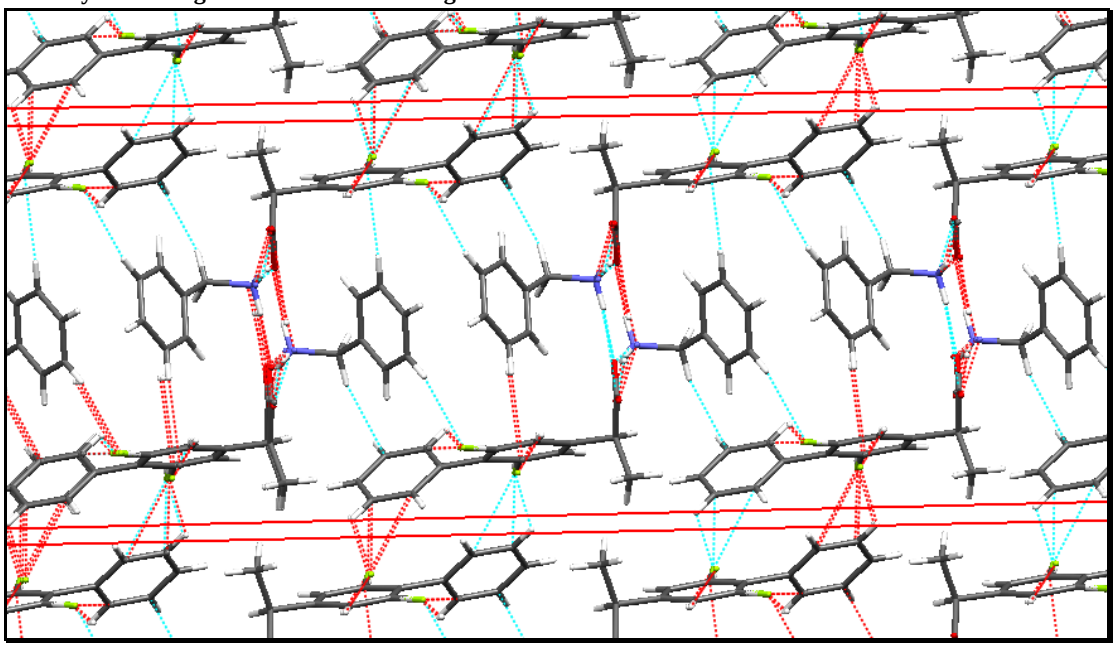

Fig 3.41 Crystal arrangement in FTBut

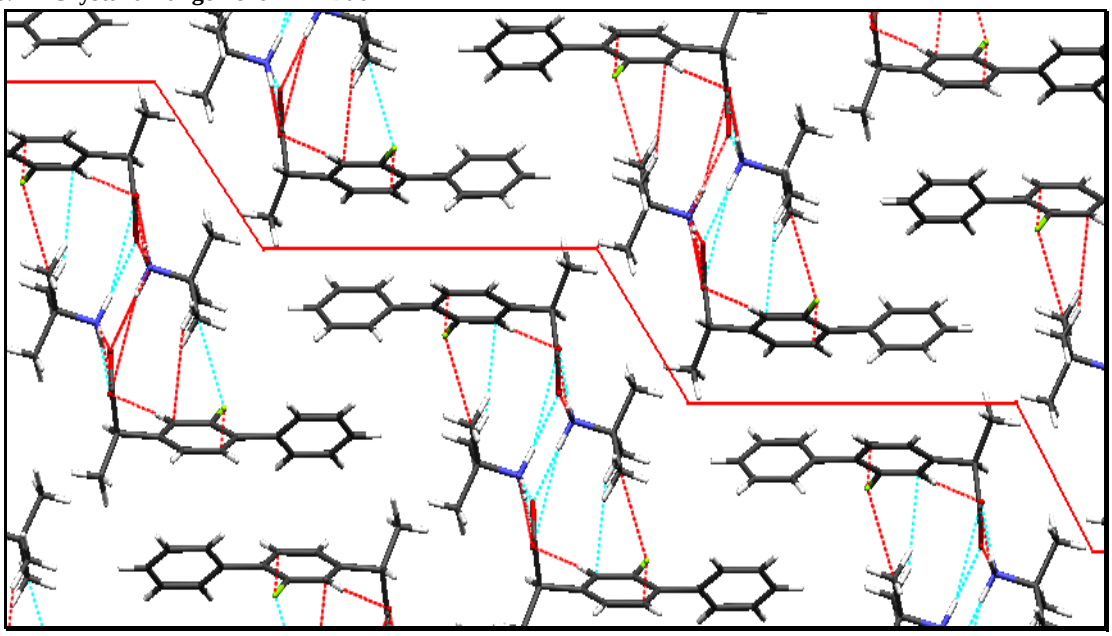

The mechanical properties of the three salts differ. FCHex, at solid fraction values of 0.85, produces strong tablets with shiny faces. With a value of 2.01MPa, the tensile strength exceeds the values generally regarded as acceptable (>1 MPa). FTBut makes tablets with smooth faces and a tensile strength of 1.12 MPa. FBenz produces tablets of reasonable appearance with brittle edges but the tensile strength is the lowest at 0.19 MPa, far from desirable values (See Fig 3.37 and Table 3.10).

The interlayer space in FBenz, though non hydrogen-bonded, is profusely cross-linked by van der Waals forces and consequently it exhibits the lowest plasticity. Van der Waals interactions hold the layers together resulting in a non-functional *slip plane* and preventing the plastic deformation necessary to create the interparticulate bonding. This results in weak tablets with brittle edges. The slip plane has previously been defined as the presence of flat non hydrogen-bonded interlayer space in previous studies with polymorphic forms I and II of sulfamerazine (Sun and Grant 2001c). Van der Waals forces are weak bonds, generally not greater than 1 kcal/mol, whereas hydrogen bond strength can range between 1-5 Kcal/mol. Considering FBenz, this is an example of non hydrogen-bonded layers that results in a non-functional slip plane due to the presence of profuse van der Waals forces. This may prove that even though weak, van der Waals forces can be as potent as hydrogen bonds in limiting plastic deformation of a material subjected to compaction if present in great number.

After observing this example, we can redefine a *slip plane* as interlayer spaces free of hydrogen bonds or van der Waals forces. A wide straight slip plane is better than a zigzagging one. The wider interlayer distance in FTBut is offset by the zigzagging nature of it because the layers interlock and slip between layers is more restricted within the crystals. Consequently, FTBut exhibits lower plasticity than FCHex.

3.5.2.3.2 FTris polymorphic system

The identification of two different polymorphs for the FTris salt afforded the opportunity to investigate mechanical properties of a polymorphic pair with conformational differences. As for the 3-point bending test, the polymorph I of FTris behaved in an unusual manner. Experience with other flurbiprofen salts in the series, had shown that the elastic recovery always occurred during the decompression and ejection phases of the process. In the case of FTris I, visually appreciable elastic recovery, which at higher compaction pressures often ended up in crumbling of the tablet, took place for several minutes after ejection of the tablet. For this reason, it was difficult to obtain tablets of a specific thickness. Instead of aiming for a thickness of 3.51 mm, which would result in tablets of 0.85 solid fraction, tablets of 3.40-3.45 mm were made and thickness was measured constantly after ejection until it reached the desired thickness by relaxation and tensile strength was then measured without delay. As expected FTris I provided tablets of very low tensile (0.24 MPa) strength whereas FTris II gave strong tablets with shiny faces with tensile strengths well exceeding the generally accepted value of 1 MPa (2.49 MPa) (see Table 3.10)

Despite a different hydrogen bonding pattern, the general crystal packing of both FTris I and II was similar with both exhibiting hydrogen-bonded 2-D layers, slightly more dense in FTris I, projecting biphenyl groups to the interlayer space, which was free of H-bonds in both cases. The resulting slip plane was not straight and was slightly wider in the case of FTris II. The shortest distances between layers being 2.398 Å for FTris I for and 2.451 Å for in FTris II both for H-H contacts.

Table 3.12 **Torsion angles between benzene rings (º).**

	Torsion angle benzene rings (º)
Ftris I conformer 1	52.33
Ftris I conformer 2	62.16
Ftris II	43.68

A more detailed analysis of the FTris system showed that it possessed conformational polymorphism, which is evidenced in the differences in the torsion angles between both benzene rings of flurbiprofen. Polymorph I, interestingly, has two different conformers in the same unit cell that also have different torsion angles.

Fig 3.42 Crystal arrangement of FTris I

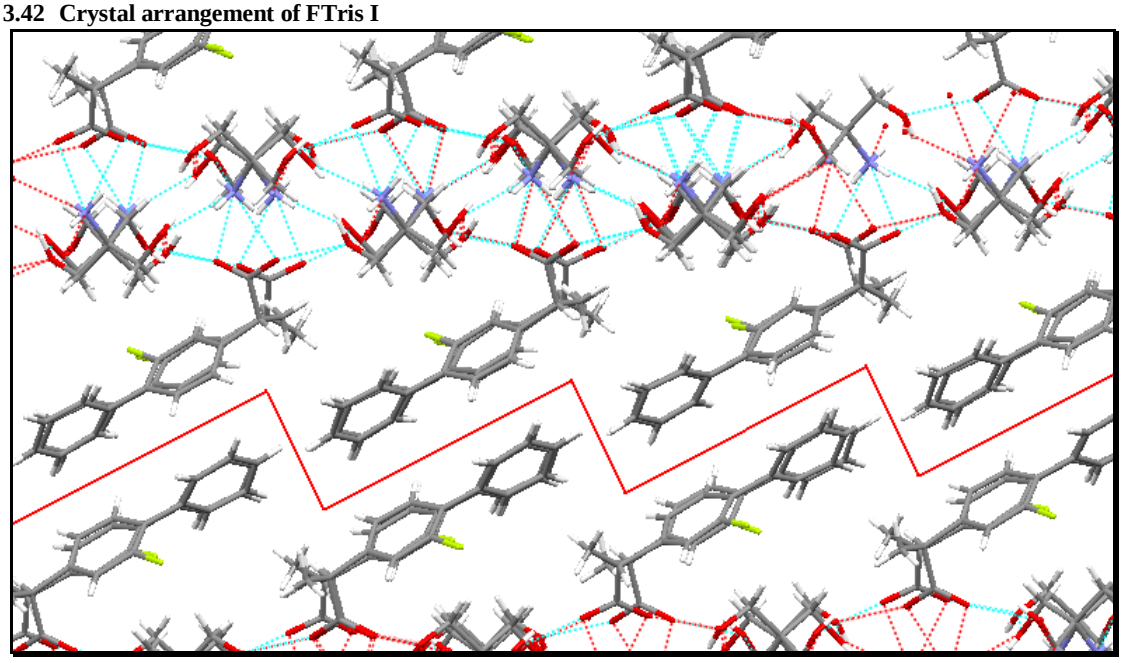

Fig 3.43 Crystal arrangement of FTris II

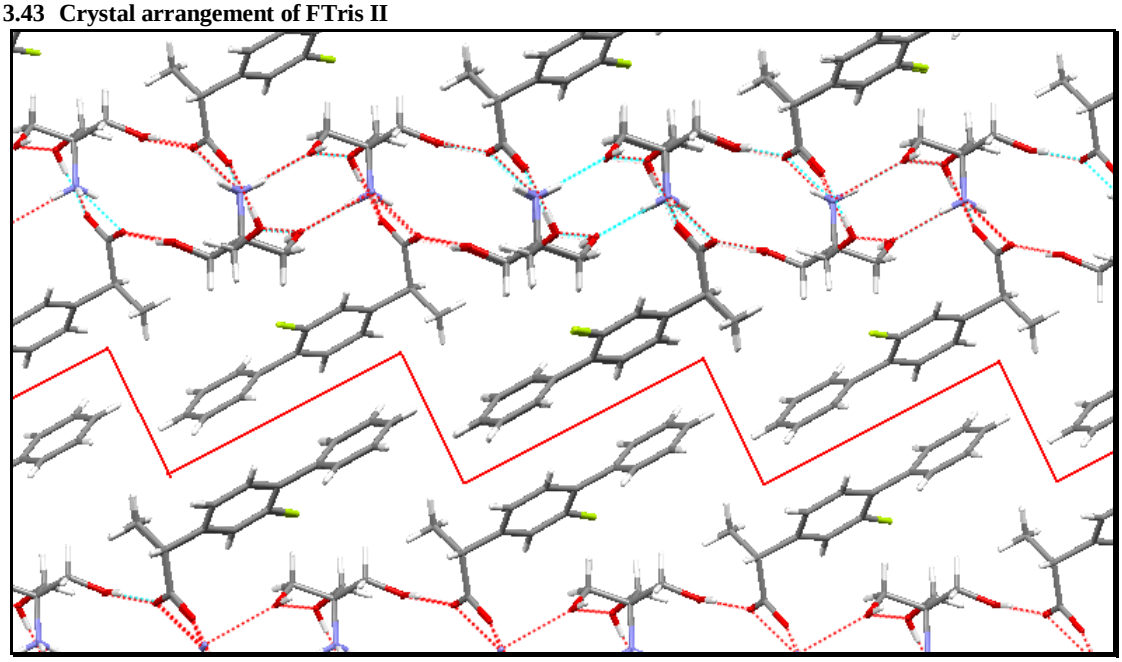

The Cambridge Structural Database has been used to carry out studies on conformational preferences focusing on specific molecular fragments than were then compared with conformations computed for gas-phase model molecules using *ab initio* methods (Allen et al. 1996; Allen and Motherwell 2002). The following general rules were found:

- Crystal structure conformations are generally a good indicator of conformational preferences. They lie close to an energy minimum
- High-energy conformers are rarely observed in crystal structures.

A typical exception to this general rule is non-substituted biphenyls (Brock and Minton 1989). Here planar, or near planar, conformations appear to be favoured in crystal structures, despite having energies of *ca* 6 kJ/mol above the gas-phase minimum energy conformation which exhibits a twist angle of 44.4 ± 1.2º (Almenningen et al. 1985). This near 45º twist angle is explained as a competition between the repulsion of the ortho hydrogens, favouring a 90º twist angle, and the π-electron delocalization effect, preferring coplanar arrangement.

It has been observed for chlorinated biphenyls that non-ortho substituted biphenyls behave similarly to their biphenyl parent; the phenyl groups can easily rotate around the central C-C bond, owing to the lower energy barrier to rotation (<2 kcal/mol) (Arulmozhiraja et al. 2002). In a study with no

ortho substituents, Brock and Minton (1989) found no structures with twist angles > 60º and very few with angles >50º.

Ortho substituted biphenyls (such as flurbiprofen) therefore have a relatively high torsion angle (φ). Using high-level Hartree-Fock and density functional calculations, the twist angles and energies of ortho substituted biphenyls, with halogen atoms, were investigated. The twist angle increased with a heavier atom, from 42.5º for biphenyl to 45.1º for 2-fluoro (Grein 2002) substituted structures. As expected the optimized twist angle increases with heavier halogen atoms and so does the energy required to force the molecule into a coplanar conformation (φ = 0). This can be explained based on steric reasons alone. However, some molecules are capable of forming intermolecular interactions that are sufficiently strong to compete with intramolecular forces and induce strained conformations.

With a twist angle of 62.16º, conformer 2 of FTris I has twist angles equivalent to that of 2-bromo diphenyl, 63.6º (Grein 2002), whereas conformer 1 also exhibits a rotational angle larger than expected (53.33º). A plot of the diphenyl angles of neutral flurbiprofen structures from the Cambridge Structural Database and the 9 salts in this series reveals that, in the solid state, the twist angle is greater in neutral than anionic moieties, with an average of 53.17 ± 0.24º for neutral flurbiprofen versus 44.46 ± 2.71º for anionic forms.

Fig 3.44 Flurbiprofen interplanar angles (º)

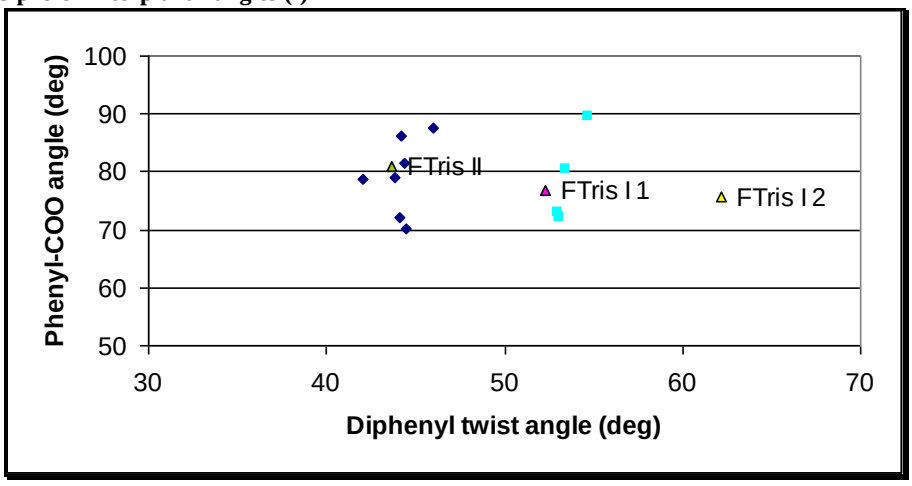

In the case of FTris II the twist angle is 43.68º, in line with the 44.46º ± 2.71 for anionic forms. However, in FTris I, both conformers 1 and 2 exhibit different twist angle values. There are no flurbiprofen salts with a diphenyl angle >46º. Both conformers of FTris I are at the moment exceptional examples of larger rotational angles.

All these factors play against stability, and polymorph I displays poor mechanical properties, producing weak compacts with troublesome elastic recovery. Intermolecular interactions in the crystal packing of FTris I are sufficiently strong to induce a strained conformation. This strained conformation makes the compound oppose plastic deformation and exhibit high elastic recovery. This may also suggest that more coplanar biphenyl structures display better mechanical properties.

3.5.2.3.3 FCBut

On initial interpretation, the mechanical properties of FCBut are disappointing. FCBut forms rather coherent tablets with tensile strength not reaching desirable values (0.93 MPa). When comparing the crystal parameters to those of FCHex, they appear to be extremely similar, with both crystallising in $P2_1/n$ and sharing similar cell dimensions (see Table 3.10).

They both exhibit one-dimensional Type II columns of $R_4^3(10)$ hydrogen bonded rings. The columns arrange themselves in layers, with the $(R\text{-}NH_3^+)$•(R'-COO-) heterosynthon inside and the biphenyl groups outside, allowing a wide straight slip plane free of H-bonds or van der Waals interactions. The slip plane is slightly narrower for FCHex as determined by the nearest contacts (2.806 Å vs 2.817Å).

Fig 3.45 Section vision along b axis of flurbiprofen cyclobutylamine

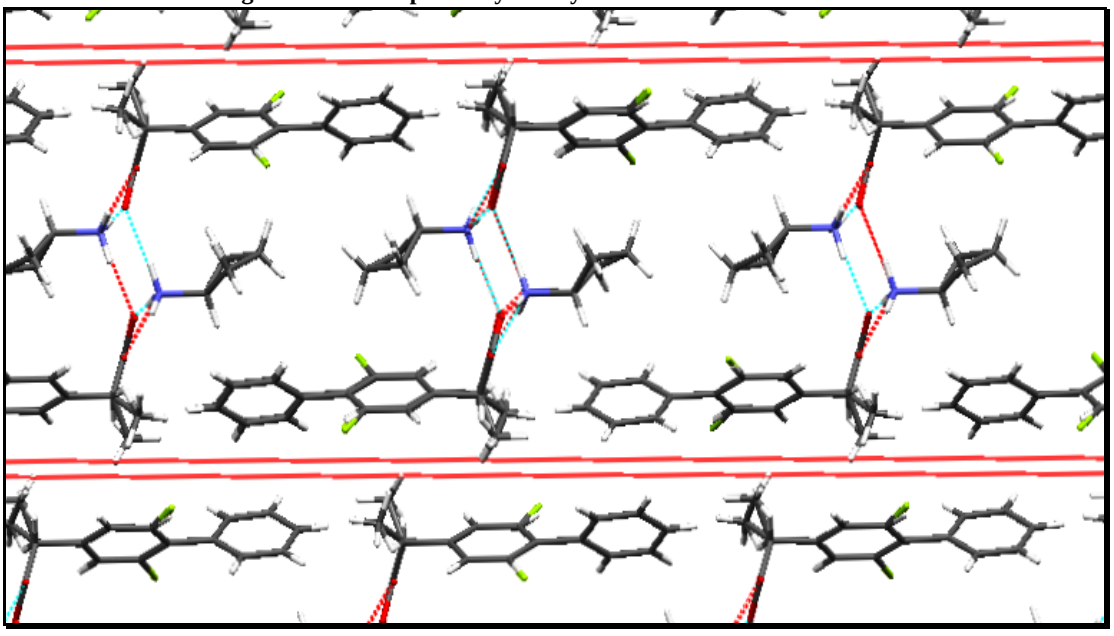

Fig 3.46 Section vision along b axis of flurbiprofen cyclohexylamine

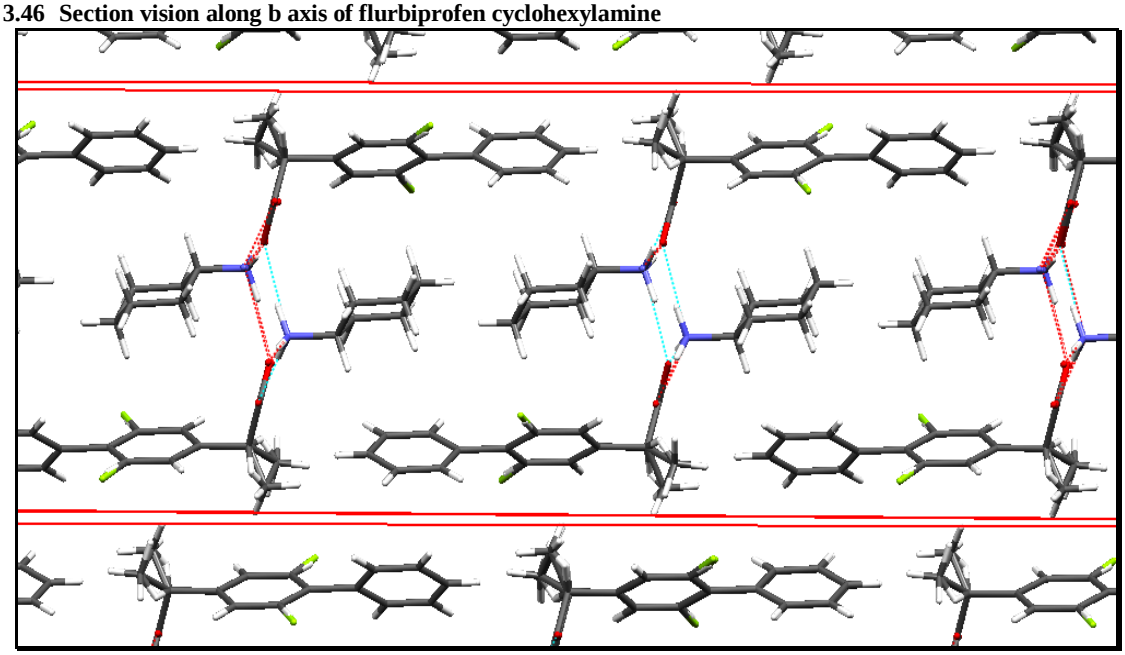

Due to the presence of a wide straight plane, the tensile strength of tablets would be expected to be similar and high. Such is the case for FCHex, with a tensile strength of 2.01 MPa, however, for FCBut it does not exceed 1 MPa (0.93 MPa).

Fig 3.47 Flurbiprofen cyclobutylamine. Nearest interlayer contacts in slip plane.

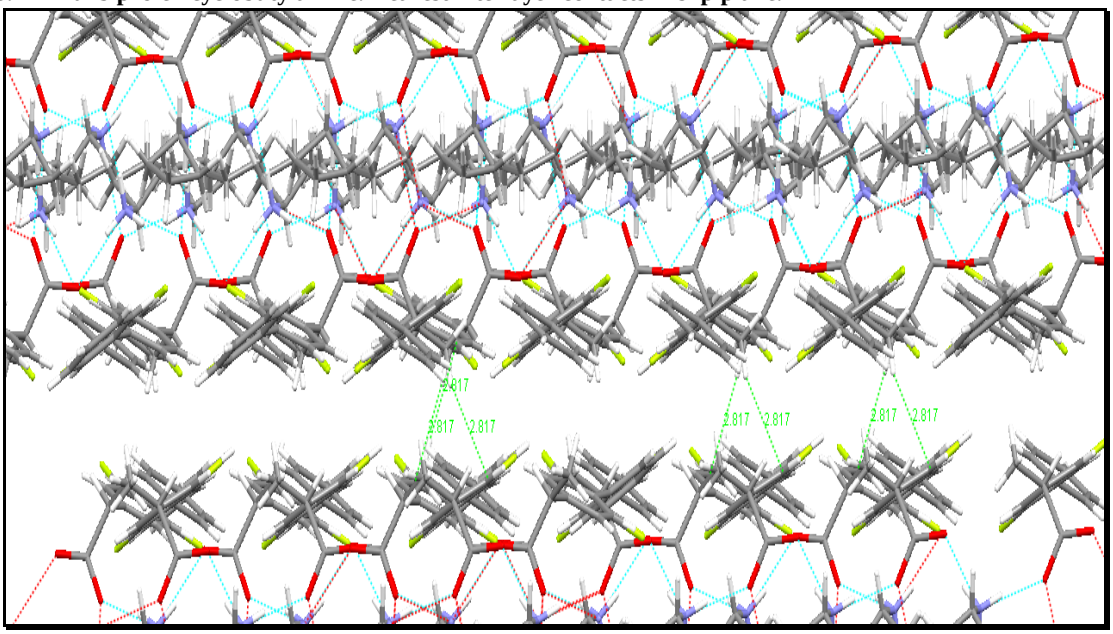

Fig 3.48 Flurbiprofen cyclohexylamine. Nearest interlayer contacts in slip plane.

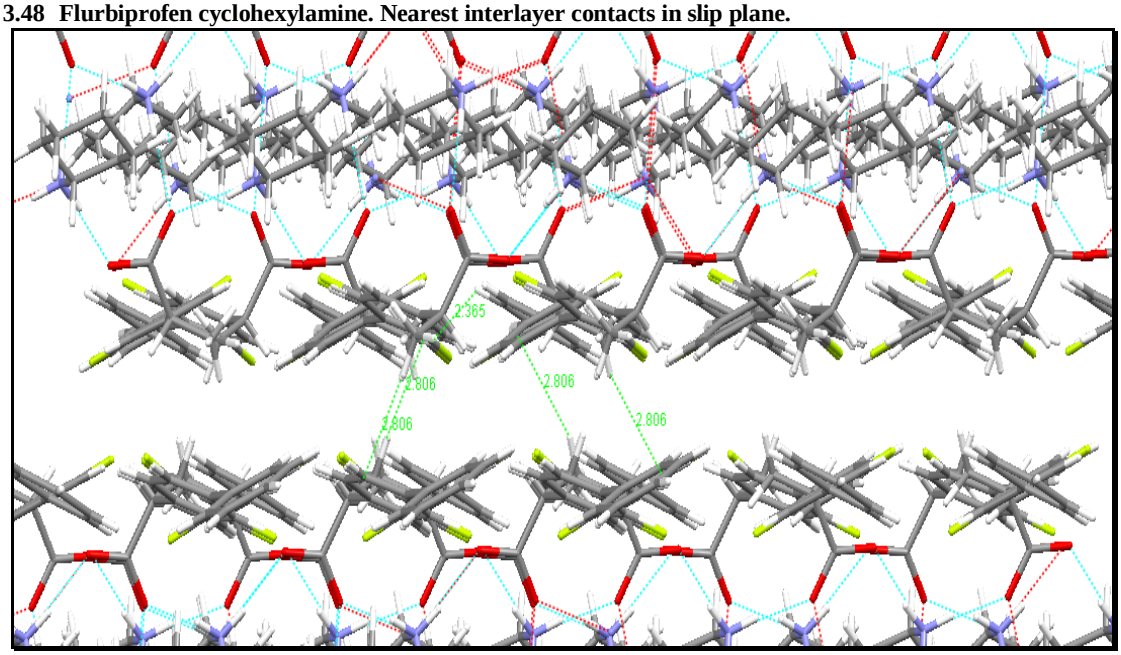

Similarly to the FTris polymorphic system, the torsion angles were studied and FCBut constitutes another exception to the preferred conformation rules above. With a torsion angle of 50.43º, it falls slightly outside the expected 44.46 ± 2.71º range for anionic flurbiprofen moieties. Although it is not as extreme a deviation as the 62.16º of FTris I, this slightly strained conformation still compromises mechanical properties.

3.5.2.3.4 Type II versus Type III columns

Mechanical properties of those structures with Type II $R_4^3(10)$ columns and type III sequence of alternating $R_4^2(8)$ and $R_4^4(12)$ rings were studied.

FAdam and FCProp are the only two examples in this series that contain Type III columns and they have orthorhombic and monoclinic space groups respectively. For the purpose of comparing Type II versus Type III hydrogen bonded columns FBenz was excluded, on the basis of van der Waals interactions that render the slip plane non-functional.

In both salts, type III columns arrange themselves in a parallel manner and are not hydrogen bonded, as expected by the lack of chemical groups with hydrogen bonding potential. The columns are also free of van der Waals interactions.

Fig 3.49 Type III columns in flurbiprofen cyclopropylamine (section view)

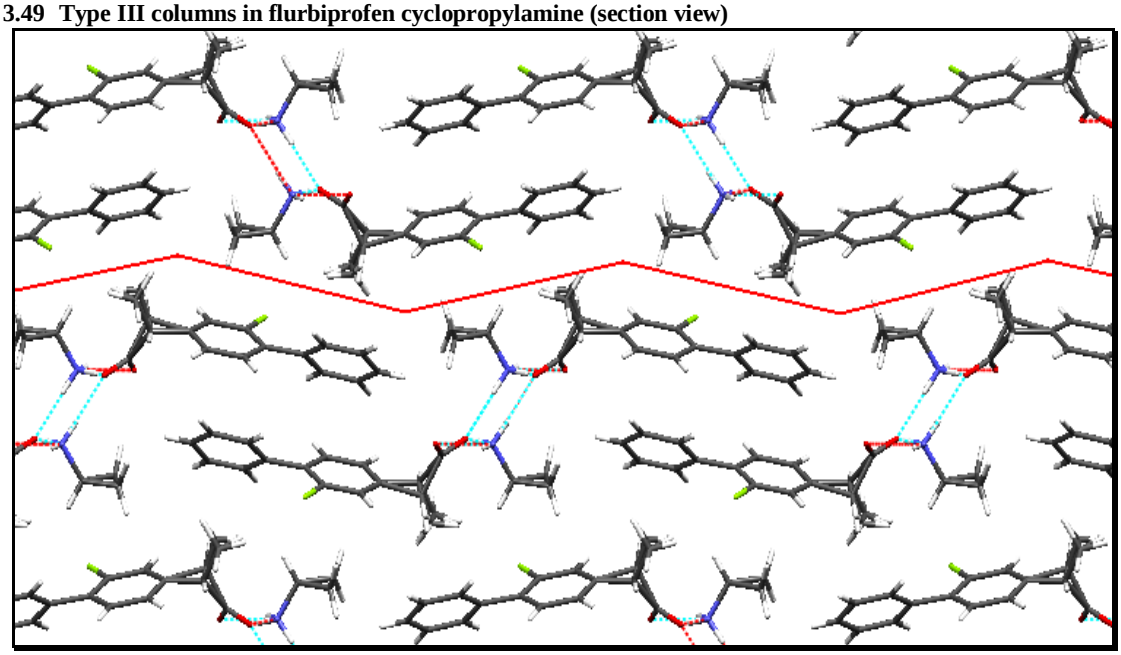

At the usual 0.85 solid fraction, it was observed that salts containing type II columns have higher tensile strength than those with type III columns (see Table 3.10). Even FCBut, with the mechanical difficulties of a strained biphenyl conformation, has higher tensile strength than any compact formed from salts with aType III column.

Fig 3.50 Type III columns in flurbiprofen adamantamine (section view)

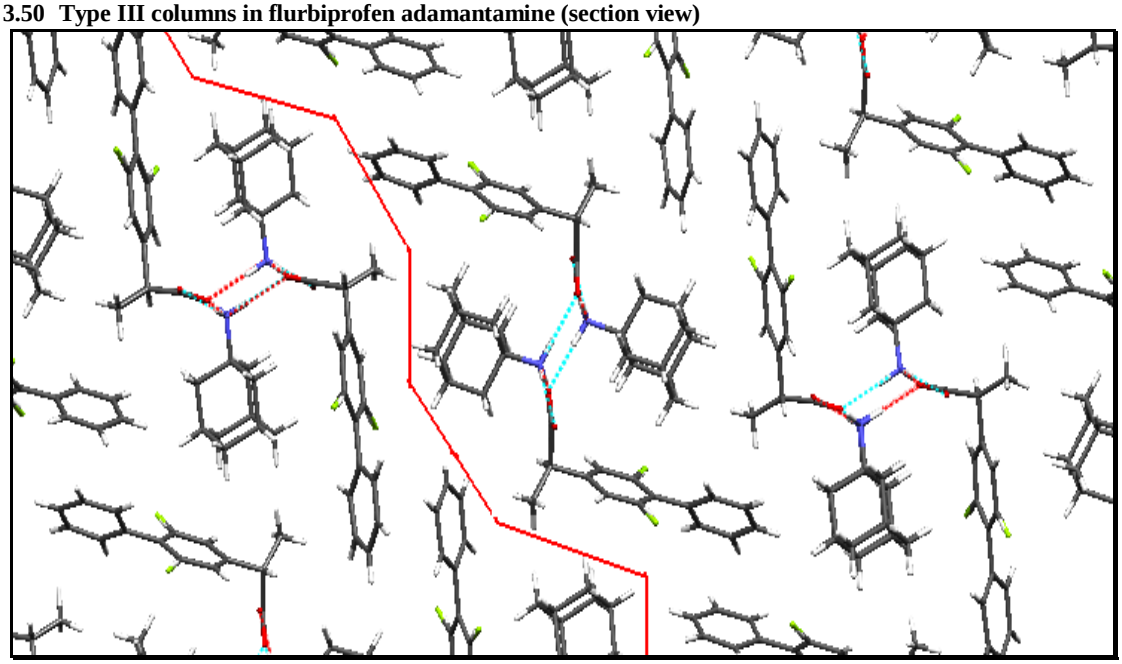

3.5.2.3.5 2-D versus 1-D hydrogen bonded networks

- *Type II versus Type V hydrogen bonding*

When type II columns are joined by hydrogen bonds, then the 2-D resulting network is type V and, similarly, type VI networks are made up of joined type III columns. Unfortunately, no type VI network was determined in this study. FAMP1 is the only candidate to display a type V 2-D network. The disorder of the hydroxyl group limits its ability as hydrogen bond former as it does not form hydrogen bonds in one position and just a weak one in the alternative position resulting in a weak two-dimensional type V network (see section 3.4.3.8).

The general network of FAMP1 shows hydrogen bonded columns projecting the biphenyl groups of the flurbiprofen towards the interlayer space. The layers are deeply interdigitated but are free of attractive van der Waals forces (seeFig 3.51).

When comparing the mechanical properties of salts with type II column arrangement with FAMP1 it was observed that tensile strength was higher for the two-dimensional hydrogen bonded network (see Table 3.10).

Fig 3.51 FAMP1 network

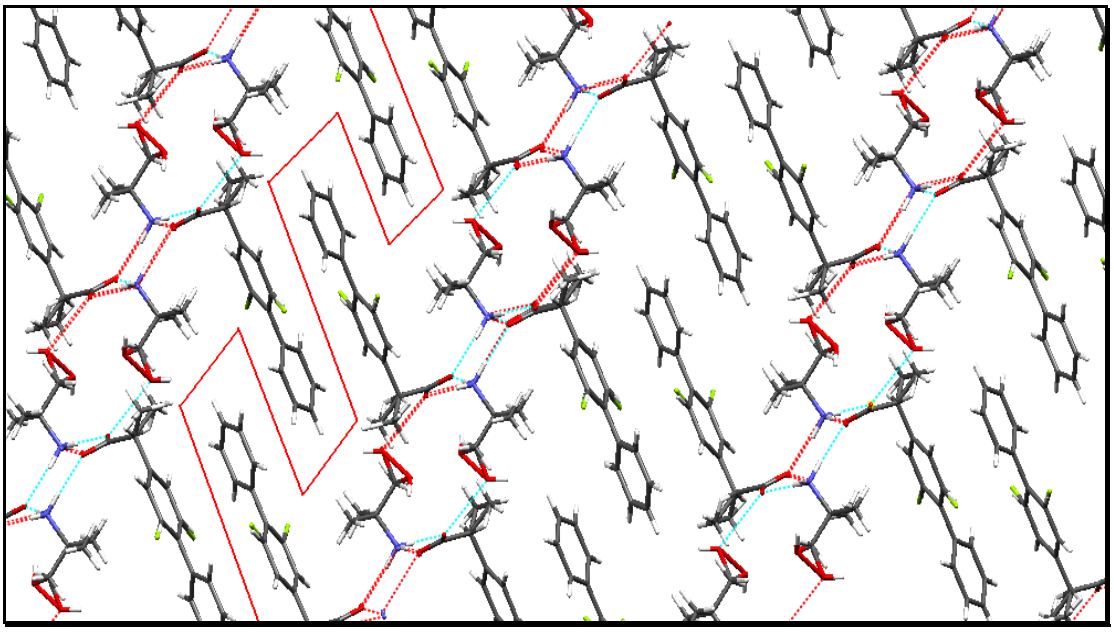

It was observed that for related hydrogen bonding networks, the one with a higher level of complexity (two- versus one-dimensional network) has stronger mechanical properties. It is believed that that the

more densely packed layers in one direction improve tabletability by reducing the attachment energy of the stacking layers. Despite the fact that the more interdigitating slip plane of FAMP1 could arguably result in more restrictions on the slipping of one layer over the next one, the 2-D stacked layers result in higher plasticity and stronger tablets.

- *FTris II versus FAMP2*

Neither FTris II nor FAMP2 exhibit any of the more frequent type II or type III hydrogen bonding motifs between NH_3^+ and COO^-. Nevertheless, FTris II possesses a higher level of the organization seen in FAMP2. In FAMP2, simple HNH···OCO···HNH···OCO hydrogen bonds still form a charge-assisted C(6) infinite chain traversing the entire crystal, but in addition cations deploy one NH and one OH hydrogen atom in hydrogen bonds to one anion forming a ring, $R_2^2(9)$. The other OH group links intermolecularly to the first one while NH finds OCO^- $R_3^2(9)$. The third amino H atom pairs with OH as acceptor in the $R_2^2(10)$ centrosymmetric dimer. This pattern results in a 1D network of parallel, non-hydrogen-bonded columns. FTris II is well ordered with similar hydrogen bonds to those in FAMP2. In particular, the C(6) chain persists. The additional hydroxyl group donates a hydrogen bond to the carboxylate O linking the columns to form a two dimensional layer (see Figs 3.52 and 3.53). The nearest contact points between layers correspond to 2.451 Å for FTris II and 2.378 Å for FAMP2, both for H-H contacts. This well exceeds the limits expected for Van der Waals contacts and affords another opportunity to examine mechanical properties of two-dimensional versus one-dimensional arrangements of related H-bonding networks.

There is a trend for FTris II producing stronger compacts than FAMP2 (2.49 MPa versus 2.09 MPa) (see Table 3.10).

Salts containing hydroxyl groups have the potential to form stacking layers of higher density and are strengthened by two-dimensional hydrogen bonding network. The possible mechanism for improved tabletability of two-dimensional versus one-dimensional networks may be that the higher density in one direction may decrease the attachment energy of the stacking layers improving plasticity.

Fig 3.52 One-dimensional arrangement in FAMP2

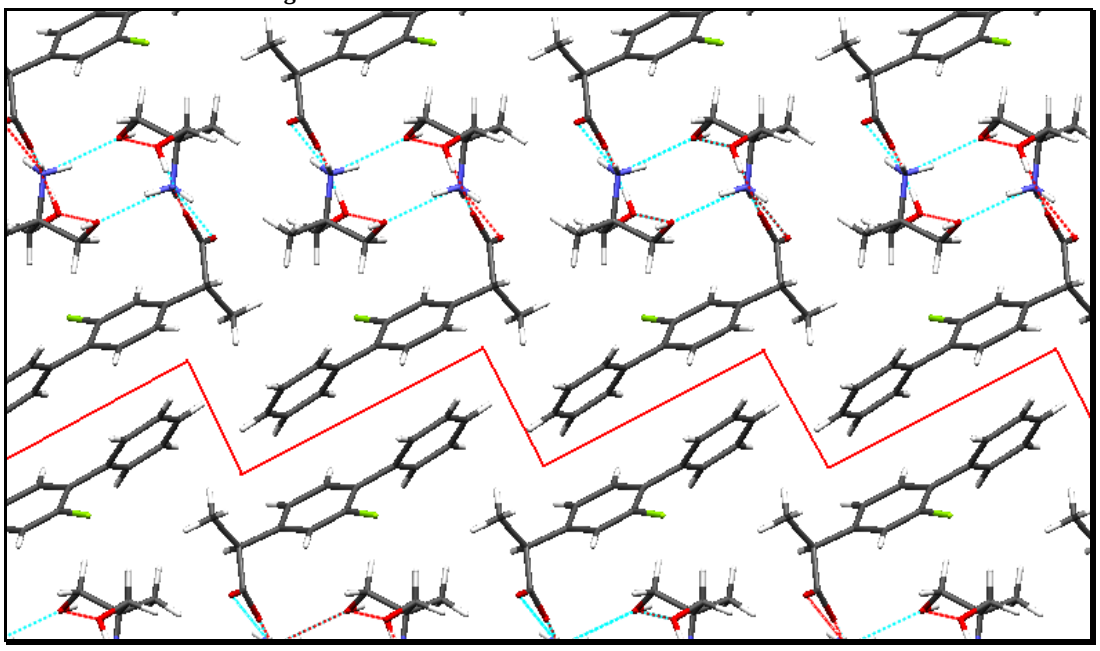

Fig 3.53 Two-dimensional arrangement in FTris II

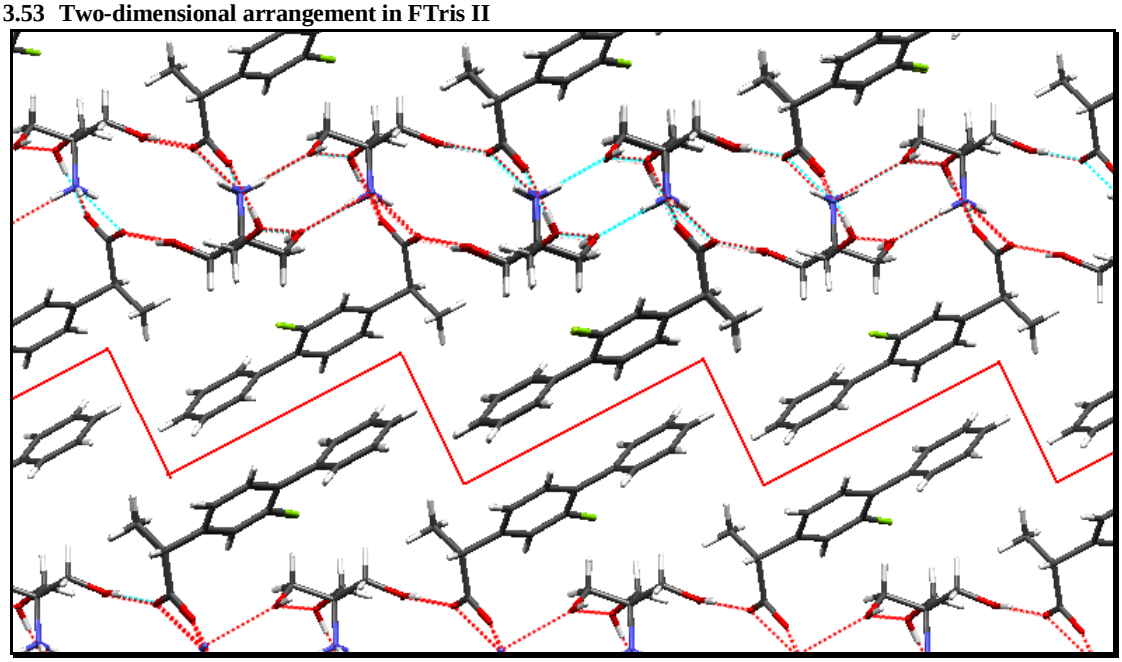

3.5.2.4 Conclusions

Mechanical tests from this series of flurbiprofen salts show that solid state can have an influence on the mechanical properties.

In general terms, presence of hydroxyl groups was associated with the formation of stronger compacts.

A slip plane is defined as a region of weakest interactions between layers. Presence of slip planes improved mechanical properties by allowing slip of one layer over adjacent ones. Absence of hydrogen bonds does not only determine the presence of a slip planes as van der Waals forces can restrict the slippage of one layer over the next one if they are present in high numbers.

Crystal structure conformations are generally a good indicator of conformational preferences as they lie close to an energy minimum. High-energy conformers are rarely observed in crystal structures. However, certain molecules/fragments adopt strained conformations and compromise mechanical properties. In particular with flurbiprofen salts, the rotational angle in the biphenyl group was critical to the mechanical properties of the salt, with more coplanar conformations resulting in stronger compacts.

The hydrogen bonding motif affects mechanical properties. Type II columns, already associated with thermal stability, produced stronger tablets that those salts with type II columns and two-dimensional type V networks produced stronger tablets than type II containing salts. Similarly, FTris II which possesses a higher level of complexity than FAMP2 (two- versus one-dimensional networks of related structures) was associated with an improvement in tensile strength.

4 Gemfibrozil

Gemfibrozil, 5-(2,5-Dimethylphenoxy)-2,2-dimethylpentanoic acid, is a non-halogenated phenoxypentanoic acid, structurally related to clofibrate (no longer commercially available in the UK) and clofibric acid (the active metabolite of clofibrate).

Fig 4.1 Gemfibrozil structure

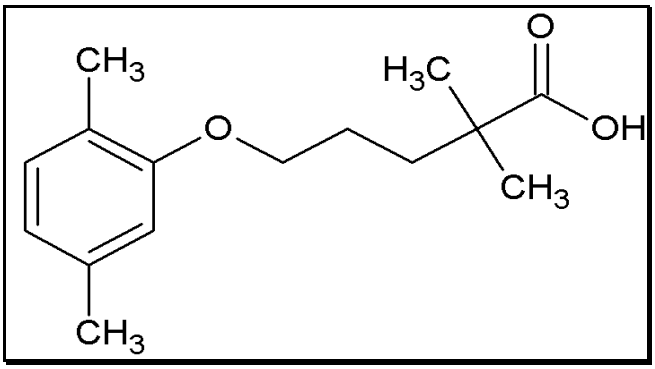

A white waxy crystalline solid, gemfibrozil is practically insoluble in water; soluble in alcohol, in methyl alcohol, dichloromethane and in chloroform. The drug has solubilities of 19 μg/ml (Parke-Davis 1982) in water and 100 mg/ml in alcohol (Rhodes 1986) at room temperature. It has a melting point of 58 to 71 °C.

Gemfibrozil is used to reduce total cholesterol and triglycerides in the management of hyperlipidaemia, including type IIa, type IIb, type III, type IV, and type V hyperlipoproteinaemias. It is also indicated for the primary prevention of ischaemic heart disease in hyperlipidaemic men: in the USA this use is restricted to type IIb patients who also have low HDL-cholesterol concentrations and who have not responded to dietary and other measures. The usual oral dose is 1.2 g daily in 2 divided doses given 30 minutes before the morning and evening meals. Alternatively, a single daily dose of 900 mg has been given 30 minutes before the evening meal.

Adverse effects of gemfibrozil are infrequent and generally mild. The commonest adverse effects are gastrointestinal disturbances including anorexia, nausea, and gastric discomfort. Other adverse effects reported to occur less frequently include headache, dizziness, vertigo, fatigue, skin rashes, pruritus, photosensitivity, alopecia, impotence, anaemia, leucopenia, and thrombocytopenia. Raised serum-aminotransferase concentrations have occasionally been reported. Elevated creatine phosphokinase concentrations during therapy may be associated with a syndrome of myositis, myopathy, and rarely

rhabdomyolysis; patients with hypoalbuminaemia resulting from nephrotic syndrome or with renal impairment may be at increased risk. Gemfibrozil should not be given with statins in patients with risk factors for myopathy. Gemfibrozil should not be given to patients with severe hepatic impairment or significant liver disease, gallstones or gallbladder disorders, or hypoalbuminaemic states such as nephrotic syndrome. It should be used with caution in renal impairment and is contra-indicated if creatinine clearance is below 15 ml/minute unless the patient is on dialysis

In the UK gemfibrozil is marketed as Lopid® (300 mg capsules and 600 mg film-coated tablets).

4.1 Salt confirmation

4.1.1 Recovery

The gemfibrozil ratio in the salt was compared to the theoretical ratio. One hundred milligrams of each salt was weighed and placed in a 100 ml class A volumetric flask and made up to volume with mobile phase to give a 1 mg/ml solution. Acetonitrile:water (65:35) was used as mobile phase. The solution was analysed then by HPLC. Experiments were performed in triplicate.

Table 4.1Recovery of gemfibrozil salts (n=3, SD)

	% content Experimental	% content Theoretical	Recovery of salt
GAdam	60.89 ± 0.07	62.00	98.16%
GBenz	69.88 ± 0.13	70.00	99.82%
GCProp	81.20 ± 0.09	81.41	99.74%
GCBut	77.02 ± 0.18	77.86	98.92%
GCHex	70.32 ± 0.03	71.61	98.19%
GTBut	76.95 ± 0.28	77.37	99.45%
GAMP1	72.83 ± 0.11	73.73	98.77%
GAMP2	69.13 ± 0.18	70.41	98.18%
GTris	66.77 ± 0.11	67.37	99.10%
GMEA	79.12 ± 0.16	80.37	98.44%
GDEA	69.37 ± 0.07	70.41	98.52%
GTEA	61.72 ± 0.08	62.64	98.53%

With a yield of >98%, this method of salt formation was considered satisfactory in producing a reasonable yield, with little wastage and acceptable level of purity.

4.1.2 Fourier Transform Infrared Spectroscopy (FTIR)

FTIR was used to confirm the transformation from carboxylic acid to a carboxylate salt.

The infrared spectra for gemfibrozil and GAdam salt are included here as typical examples and the spectra for other salts are included in Appendix A.

The signal at 1700 cm^{-1} in the gemfibrozil spectrum was attributed to a stretching of the C=O group of the carboxylic acid. As with flurbiprofen, we can observe the shift to 1550 cm^{-1} in the case of GAdam salt. The absorption peak between 3400 cm^{-1} is attributable to NH_3^+ stretching in amine salts and is only present in GAdam, not in gemfibrozil.

A broad peak at approximately 2100 cm^{-1} can be observed in GAdam which is not present in neither of the carboxylic acid scans nor in the salts with secondary or tertiary amines (FTEA, DTEA, GTEA, FDEA, DDEA). It is possible that this peak is only present in $(R\text{-}NH_3^+)\bullet(R'\text{-}COO^-)$ salts with primary and secondary amines.

Fig 4.2 FTIR scan for gemfibrozil

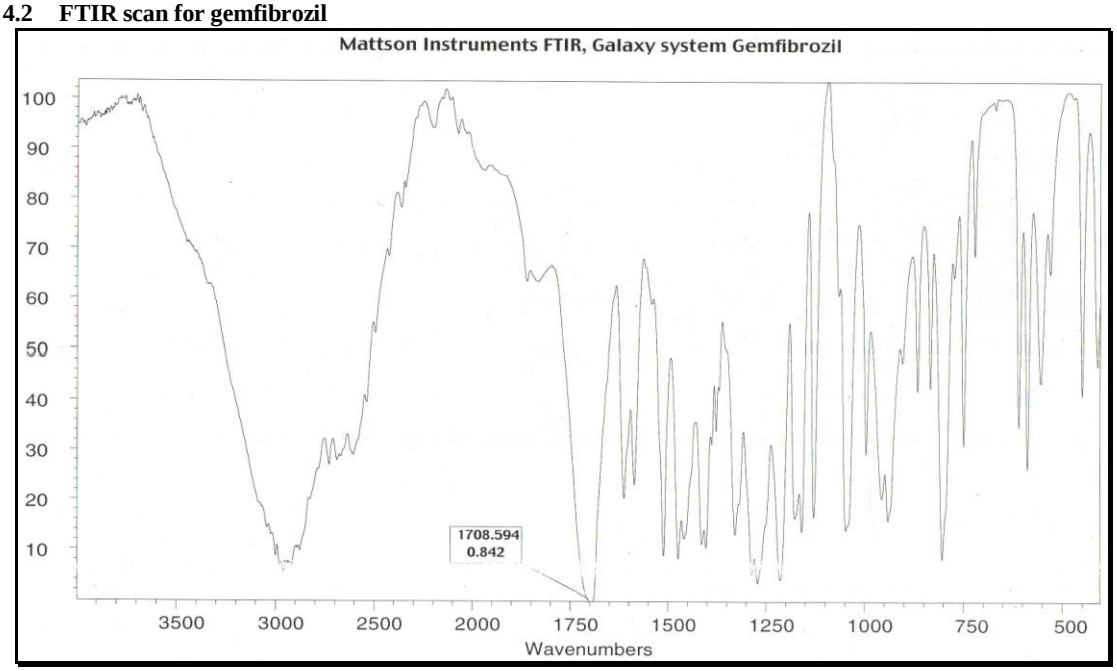

Fig 4.3 FTIR scan for GAdam salt

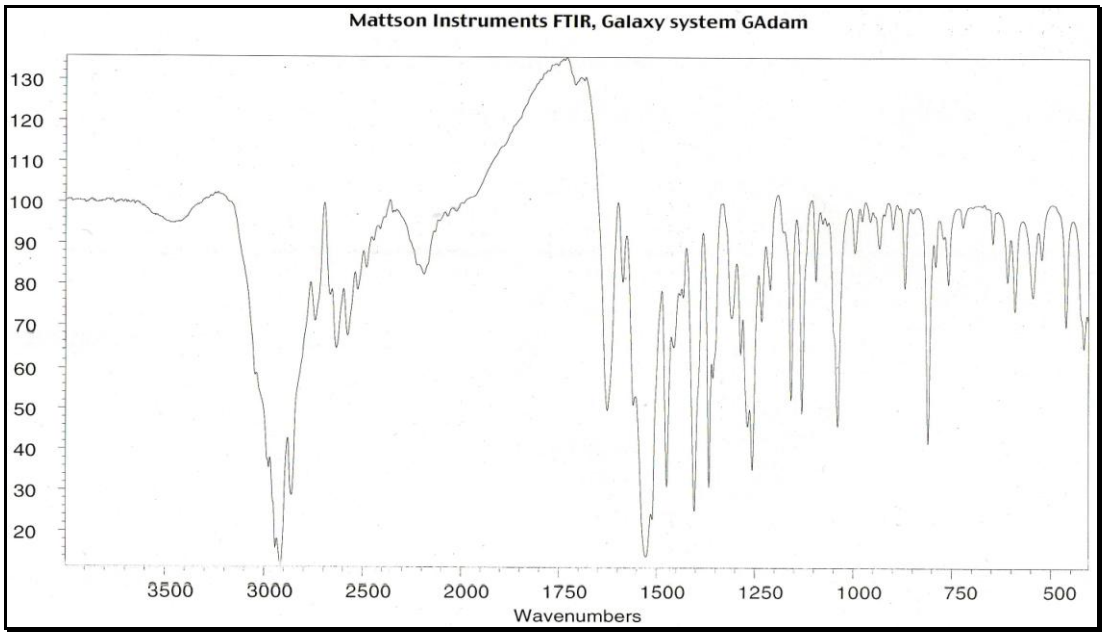

4.1.3 Nuclear Magnetic Resonance

The spectra accounted for every hydrogen atom in the expected molecules. It also confirmed the formation of 1:1 salts. In this case, there are no hydrogens attached to the carbon next to the carbonyl group, so salt formation can not be confirmed in the same manner as possible with flurbiprofen salts (see 3.1.3) NMR spectra for GAdam and GBenz salts are included here and the NMR spectra for the rest of the salts are in Appendix B.

4.2 Thermal studies

4.2.1 Material

All salts were obtained as described in section 2.1.1.

4.2.2 Methods

DSC and TGA methods were used as described in sections 2.2.1.2 and 2.2.2.2 respectively.

Fig 4.4 NMR scan for GAdam salt

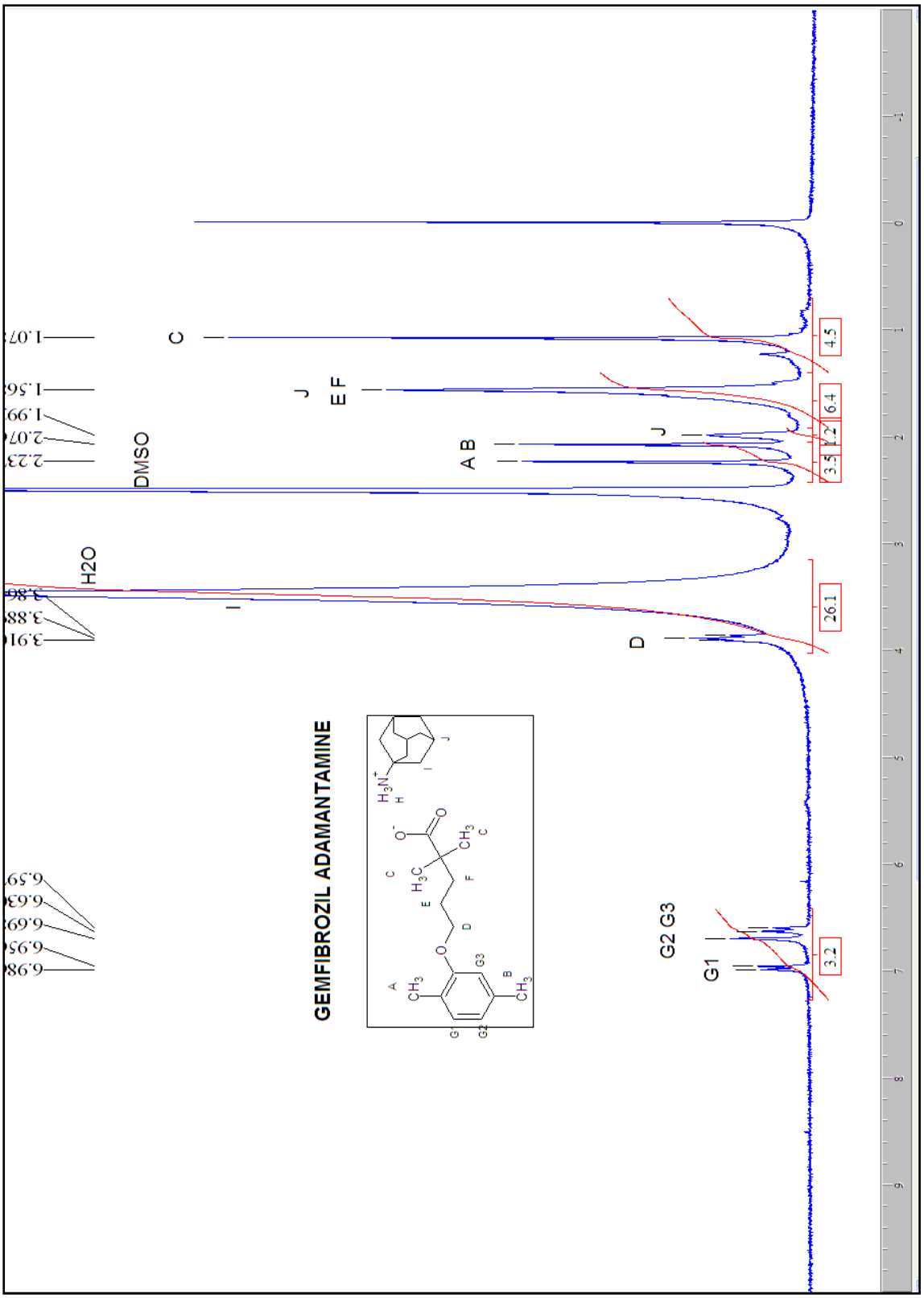

Fig 4.5 NMR scan for GBenz salt

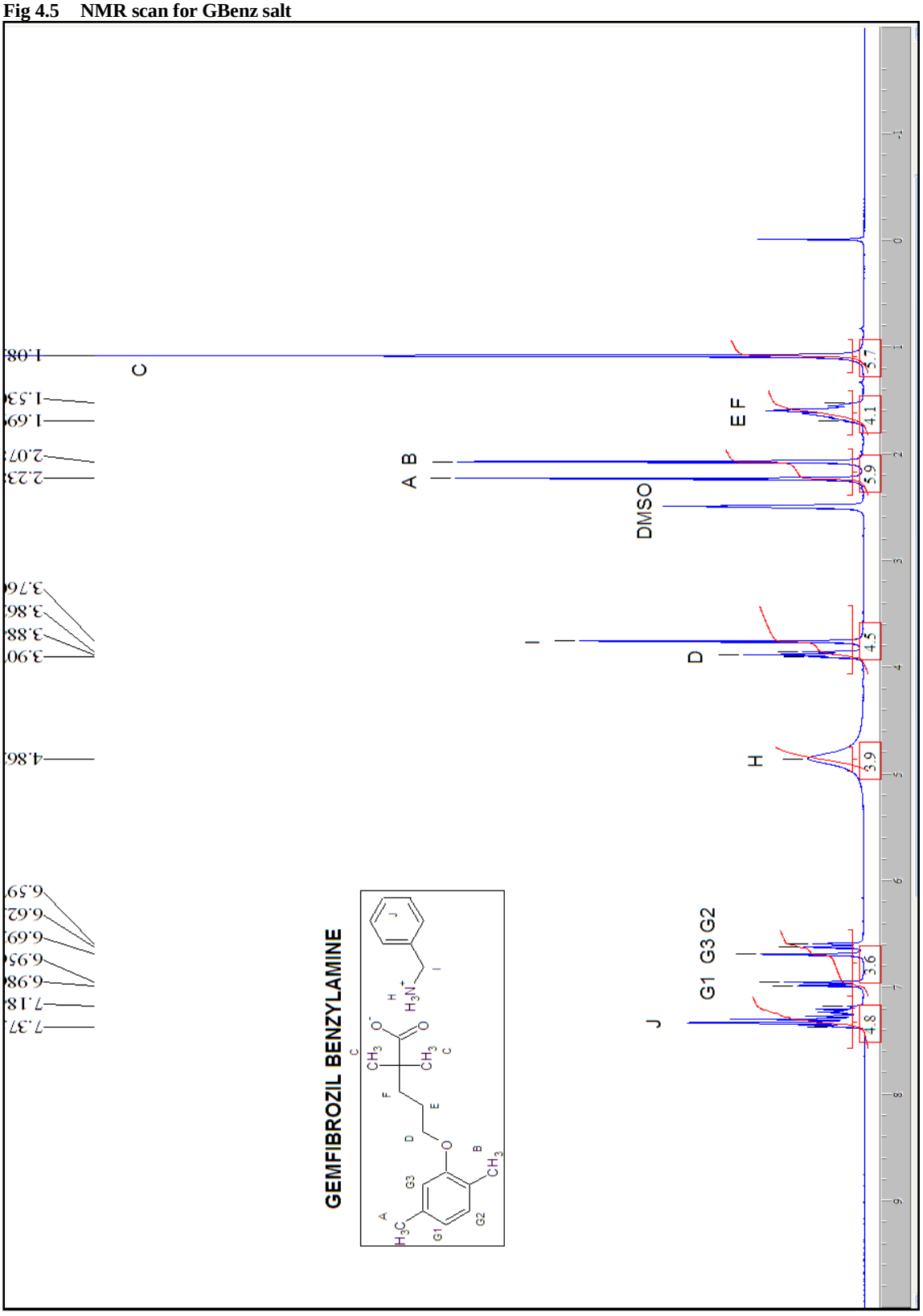

4.2.3 Results and discussion

Melting points are summarised in Table 4.2. An example of a DSC scan of gemfibrozil is shown in Fig 4.6. The rest are attached in Annex C. There was no evidence of any hydrate/solvate formation in any of the salts. Desolvation of any bound solvent would be observed as a multistage process using TGA, at a series of discrete temperatures This was also confirmed by the lack of weight loss observed in TGA around 100 degrees and the gradual weight loss for all salts after the melting point of the salt.

The endothermic peak in the DSC spectrum of gemfibrozil at 60.34°C (see Fig 4.6) shows the melting point of the material (enthalpy of fusion, 100.45 ± 5.27 J/g), in line with the value of 59.25°C reported in the literature (Aigner 2005). No degradation was observed up to 160°C. Melting points of any gemfibrozil salts have not been found in the literature.

Table 4.2Melting points for gemfibrozil and salt series (n=3, SD)

Drug	Melting point (°C)
Gemfibrozil	60.34 ± 0.54
GAdam	190.99 ± 1.02
GBenz	91.35 ± 1.36
GCProp	85.32 ± 0.30
GCBut	101.78 ± 0.87
GCHex	133.05 ± 0.38
GTBut	136.78 ± 4.47
GAMP1	101.79 ± 0.56
GAMP2	117.35 ± 0.36
GTris	119.22 ± 0.13

Fig 4.6 DSC thermogram for gemfibrozil

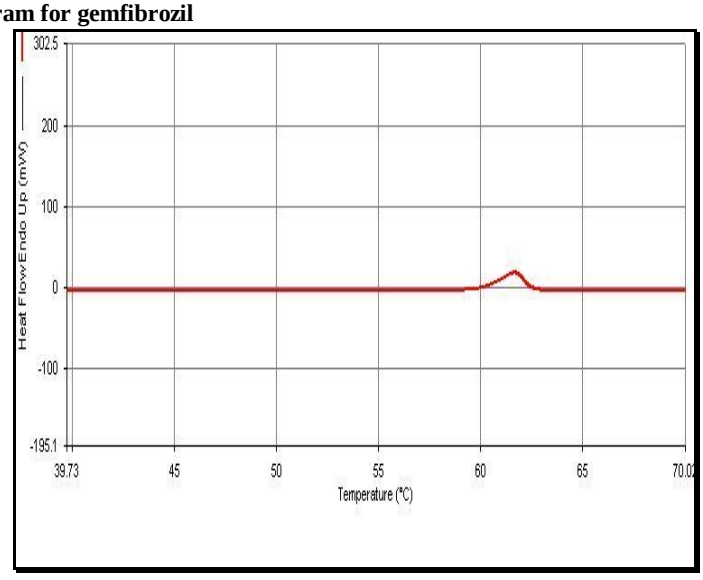

O'Connor et al. (2001b) characterized a range of diclofenac salts and examination of the data revealed reasonable correlation (R^2=0.7518, n=7) between the base and salt melting points. A very poor correlation was found between the amine counterions and gemfibrozil melting points (R^2=0.3218, n=8) and even poorer with flurbiprofen melting points (R^2=0.0363, n=8). However, in this study a reasonable correlation is found between the melting points of flurbiprofen and gemfibrozil salts (R^2=0.7645, n=10).

Fig 4.7 Melting points of flurbiprofen and gemfibrozil salts

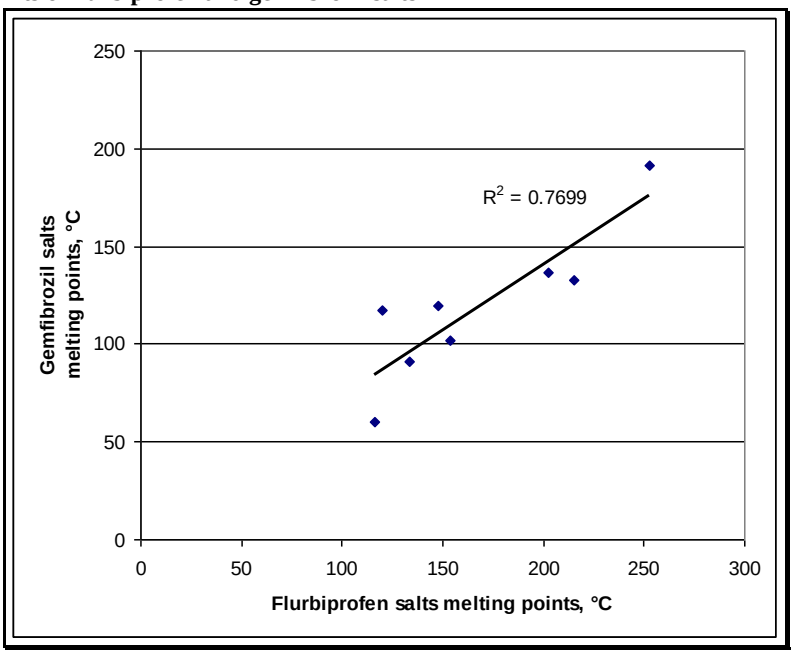

When trying to correlate melting point and solubility data for gemfibrozil salts, a simple correlation between the melting point and the saturated solubility can not be found as seen with flurbiprofen (see discussion in 3.2.2).

4.3 Solubility and dissolution studies

4.3.1 Saturated solubility

Saturated solubility in water was calculated for all the gemfibrozil series.

4.3.1.1 Materials

All materials were prepared as described in section 2.1.1.

4.3.1.2 Method

Saturated solubility was determined following the method described in section 2.3.2.2.

4.3.1.3 Results and discussion

The saturated aqueous solubilities of gemfibrozil and its salts are presented in Table 4.3.

Table 4.3 Saturated solubility and pH of final solution of gemfibrozil salts at 21° (n=3, SD)

	Solubility (mg/ml)	Solubility (mM)	pH
Gemfibrozil	< 0.039	<0.15	4.62
GAdam	0.19 ± 0.01	0.75	5.96
GBenz	1.73 ± 0.043	6.91	8.32
GCProp	4.28 ± 0.06	17.11	8.02
GCBut	4.28 ± 0.20	17.11	8.06
GCHex	3.20 ± 0.05	12.79	7.37
GTBut	11.03 ± 2.42	44.10	7.78
GAMP1	16.62 ± 2.36	66.43	7.89
GAMP2	25.2 ± 1.06	100.73	8.10
GTris	6.97 ± 2.46	27.86	7.6

Fig 4.8 Solubilities of flurbiprofen and gemfibrozil salts with the same counterions at 21°C

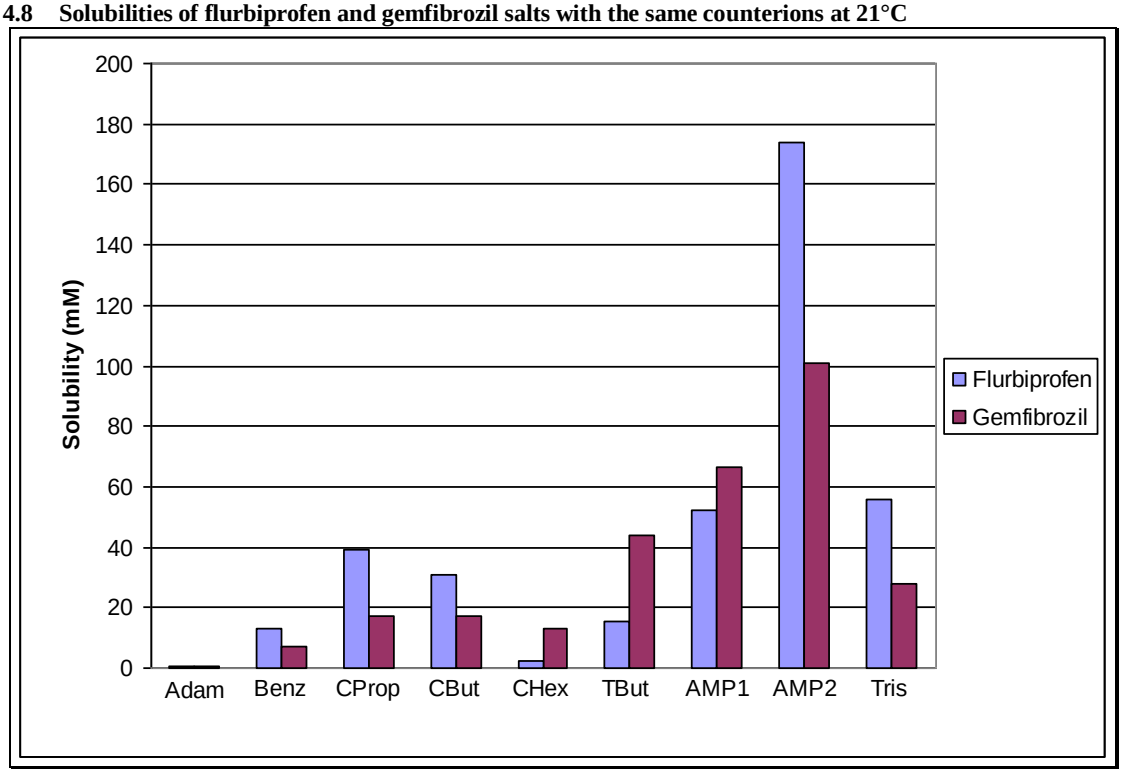

Solubility of gemfibrozil was below the detection limit (0.039 mg/ml) of the HPLC method. Values of 0.029 mg/ml (Hassan 2004) and 0.019 mg/ml (Parke-Davis 1982) have been published.

As expected, saturated solubility was improved in all cases by salt formation. Counterions increased the gemfibrozil aqueous solubility by over 500-fold. Comparing the solubilities of the salts of flurbiprofen and gemfibrozil, two drugs with comparable solubilities (literature averages: 0.12 vs. 0.10 mM, respectively), a similar trend is observed for the same counterions (see Fig 4.8).
Different strategies have been used to improve the solubility of gemfibrozil. Chen et al. (2010) demonstrated that the dissolution rate of micronized gemfibrozil, in simulated intestinal fluid, was enhanced by 5.5 times compared to that of the original compound by reducing the particle size of gemfibrozil was micronized from its original 14.3 to 5.8 μm. Inclusion complexes of gemfibrozil with cyclodextrins (CD) also improve solubility (Hassan 2004). On increase of the CD content, the solubility increases further. The 1:2 spray dried preparation gave the best results in simulated intestinal medium (a 716-fold solubility). Based on theoretical pH solubility profiles, solubility by salt formation in simulated intestinal fluid, SIFsp, as described in USP 26 (pH=6.8) would not exceed a 200-fold solubility (purely based on pH basis).

When representing the calculated saturated solubilities of the salts versus the obtained pHs, a correlation is observed between these values and the theoretical pH-solubility profile for gemfibrozil (see Fig 4.9): the higher the pH of the obtained saturated solution, the higher the solubility. An intrinsic solubility value of 3.2×10^{-5} M (Fernández et al. 2008) was used to calculate the theoretical pH solubility profile according to the equation:

$$pK_a = pH - \log \frac{S - S_0}{S_0}$$

The lower solubility:pH ratio of GCProp, GCBut and GBenz is likely to be due to self-association. Compounds having rigid aromatic structures and alkyl chains are believed to typically associate by non-micellar processes (л-л stacking and van der Waals interactions) involving face-to-face stacking (Florence and Attwood 1998).

Fig 4.9 Saturated solubility (mM) versus pH of gemfibrozil and its salts. Theoretical pH solubility profile for gemfibrozil shown in pink

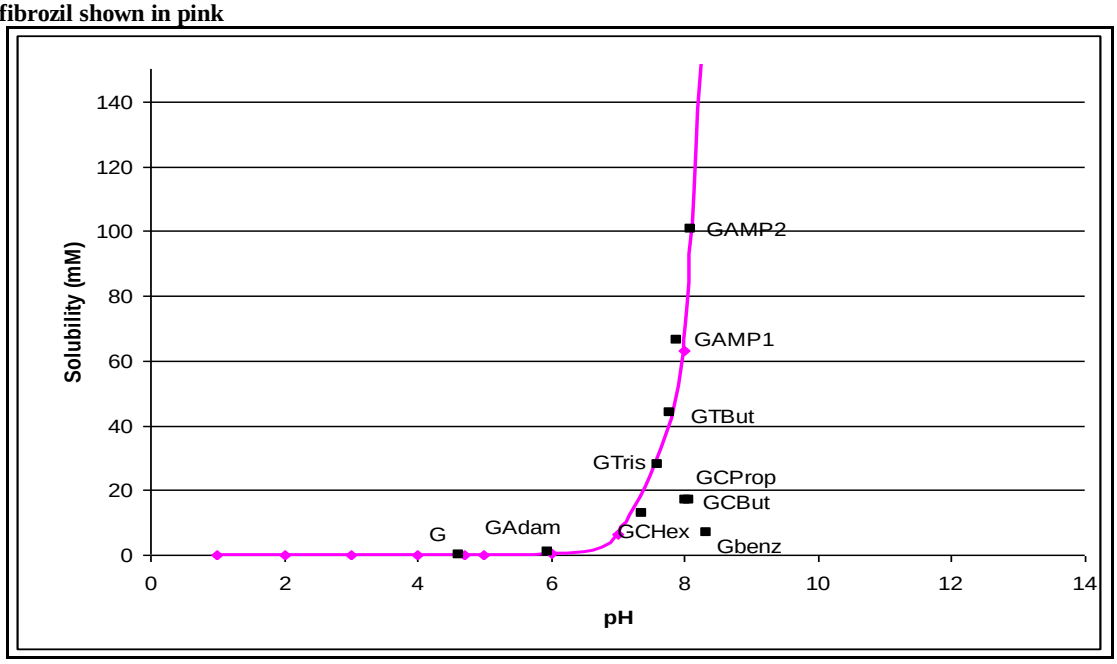

4.4 Crystal structure

4.4.1 Material

All salts were prepared as described in section 2.1.1.

4.4.2 Methods

4.4.2.1 Crystal growing

All crystals were obtained by slow evaporation from methanol.

4.4.2.2 Crystal structure determination

Crystal data were collected at the EPSRC National Crystallography Service. Beamline I19 at the Diamond synchrotron was used to collect data on GCProp. Structures were solved by direct methods and refined by full-matrix least squares. Mercury was the crystal structure visualizing program used to measure intermolecular contacts.

The following structures were already available in the Cambridge Structural Database (CSD): G, *XAPVOA*, GTBut, *GICHEG*, GAMP1, *GICHIK*, GAMP2, *GICHOQ* and GTris, *GICHEW* (Cheung et al. 2007).

4.4.3 Results and discussion

Only type II, $R_4^3(10)$ columns were observed in all gemfibrozil salts without hydroxyl groups. The less frequent type III columns were not observed in the gemfibrozil series, including the adamantamine salt, which resulted in Type III columns in the flurbiprofen equivalent (see section 3.4.3). All salts containing hydroxyl groups formed different assemblies. Interestingly, neither gemfibrozil nor the amine counterions of this series are chiral. In this series, it appears that hydrogen bonding pattern provides a means of creating chiral crystal structures from achiral molecules. The inherent chirality of this architecture comes from spatial disposition rather than the presence of chiral atoms, thereby illustrating an important aspect of the solid state. A chiral space group is one that contains only rotation or screw axes, such as P212121, which occurs in 3 of the salts: GAdam, GCBut and GTBut. The creation of chiral crystals from constituents that do not possess a chirality centre is a much studied phenomenon (Mateos-Timoneda et al. 2004; Matsuura and Koshima 2005). A survey of the 190,000 crystal structure data sets deposited in the CSD revealed that the statistical probability for the chiral crystallisation of achiral compounds was 8%, showing that chiral crystallisation is not an exceptionally rare phenomenon. It has been suggested that two-component molecular crystals have higher probabilities for the generation of chirality in the crystallisation of achiral compounds than those of single organic compounds (Matsuura and Koshima 2005).

Table 4.5 Crystal parameters and particle size for gemfibrozil acid and its salts

G	***GAdam***	***GCBut***	***GCHex***	***GTBut***
Monoclinic,	**Orthorhombic,**	**Orthorhombic,**	**Monoclinic,**	**Orthorhombic,**
$P2_1/n$	**$P2_12_12_1$**	**$P2_12_12_1$**	**$P2_1/n$**	**$P2_12_12_1$**
Z = 2	**Z = 4**	**Z = 4**	**Z = 4**	**Z = 4**
a = 14.8610 Å	**a = 6.5081 Å**	**a = 6.1793 Å**	**a = 9.4821 Å**	**a = 6.4481 Å**
b = 7.3640 Å	**b = 10.5426 Å**	**b = 9.3558 Å**	**b = 6.5170 Å**	**b = 9.6811 Å**
c = 27.948 Å	**c = 34.282 Å**	**c = 33.270 Å**	**c = 32.9176 Å**	**c = 33.0974 Å**
α = 90	**α = 90**	**α = 90**	**α = 90**	**α = 90**
β = 93.420	**β = 90**	**β = 90**	**β = 90.194**	**β = 90**
γ = 90	**γ = 90**	**γ = 90**	**γ = 90**	**γ = 90**
R_{int} = not available	**R_{int} = 8.5**	**R_{int} = 6.0**	**R_{int} = 4.4**	**R_{int} = 2.6**
PS = 37.34 µm	**PS = 52.84 µm**	**PS = 99.66 µm**	**PS = 69.67 µm**	**PS = 48.34 µm**

Table 4.5 Crystal parameters and particle size for gemfibrozil acid and its salts (continuation)

GAMP1	*GAMP2*	*GTris*	*GTEA*
Monoclinic,	Monoclinic,	Monoclinic,	Monoclinic,
C2/c	C2/c	$P2_1/c$	$P2_1/c$
Z = 8	Z = 8	Z = 4	Z = 4
a = 26.8776 Å	a = 27.0843 Å	a = 18.4999 Å	a = 18.0782 Å
b = 6.3695 Å	b = 6.3242 Å	b = 10.0377 Å	b = 7.1068 Å
c = 23.9178 Å	c = 22.8922 Å	c = 10.9957 Å	c = 18.5776 Å
α = 90	α = 90	α = 90	α = 90
β = 91.734	β = 92.277	β = 97.3784	β = 112.377
γ = 90	γ = 90	γ = 90	γ = 90
R_{int} = 2.7	R_{int} = 4.8	R_{int} = 4.2	R_{int} = 4.4
PS = 63.08 µm	PS = 28.95 µm	PS = 54.76 µm	PS = 59.36 µm

Molecular flexibility plays a role in space group choice. It appears that rigid molecules, particularly if they have mirror symmetry, have an increased chance of crystallisation in a non-centrosymmetrical space group. However, in conformationally flexible molecules where interconversion with the mirror image can be achieved through internal degrees of freedom, centrosymmetrical space groups are greatly preferred (Pidcock 2005).

4.4.3.1 Gemfibrozil

Monocarboxylic acids, like gemfibrozil, which are non-chiral almost invariably form hydrogen bonded pairs (Leiserowitz 1976). In this case, dimers are not hydrogen bonded.

Fig 4.10a Crystal structure of gemfibrozil ($P2_1/n$)

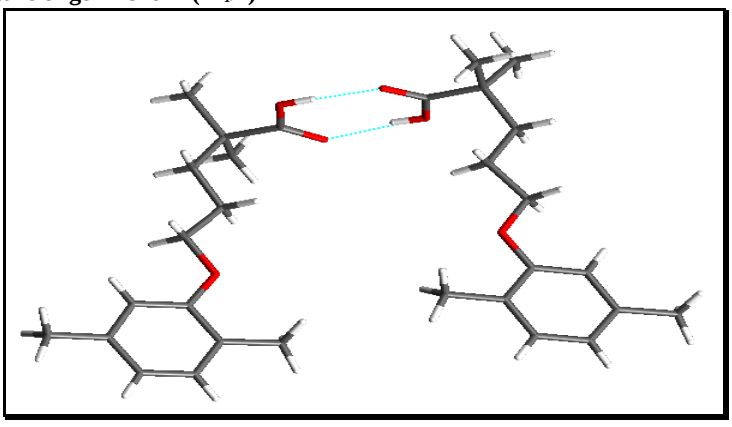

Fig 4.10bCrystal structure of gemfibrozil ($P2_1/n$)

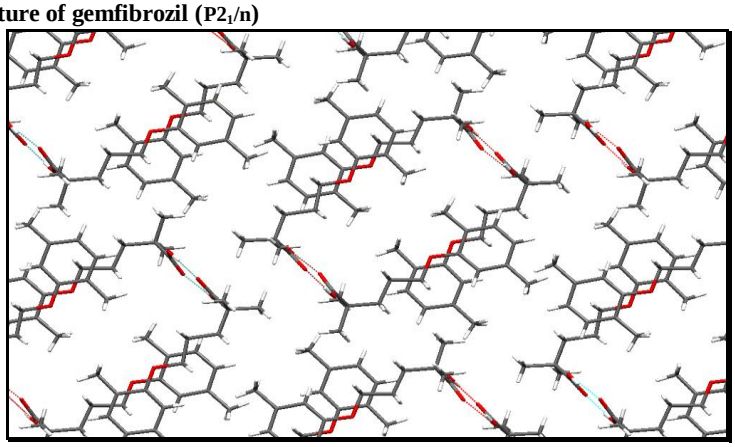

4.4.3.2 GAdam

Crystal structure analysis showed that in GAdam the three N–H bonds of the ammonium group NH_3^+ act as hydrogen bond donors, and the two oxygen atoms of the carboxylate groups accept hydrogen bonds, resulting in the Type II columns, $R_4^3(10)$. The columns arrange themselves parallel to each other in non-bonded layers projecting the benzyl groups which intercalate. The columns are not linked through van der Waals forces. Interestingly, FAdam, adopts the type III columns instead. It is possible that the preferred type II column (as observed in the CSD) is not formed with flurbiprofen due to steric hindrance between the bulky adamantyl group and the rigid benzyl ring close to the carboxyl groups in the flurbiprofen molecule.

Fig 4.11aCrystal structure of gemfibrozil adamantamine ($P2_12_12_1$)

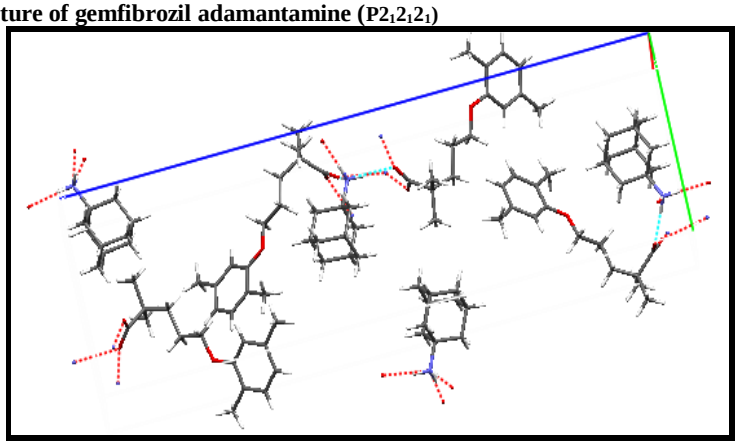

Fig 4.11bCrystal structure of gemfibrozil adamantamine ($P2_12_12_1$)

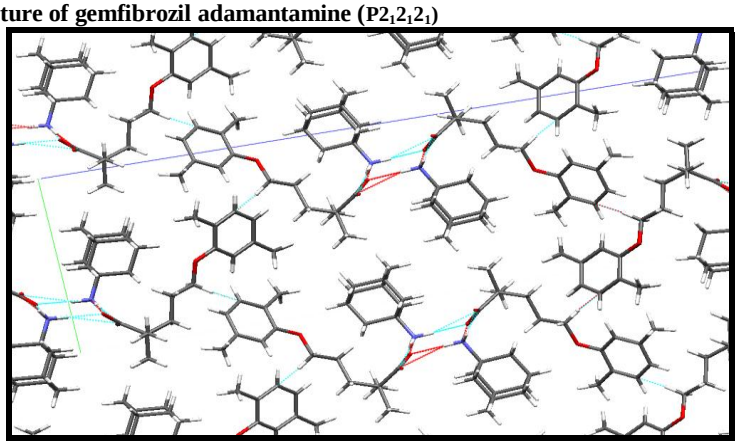

4.4.3.3 GCBut

Very similar to GAdam, in GCBut Type II columns R_4^3 are formed. The chains are cross-linked through van der Waals forces.

Fig 4.12aCrystal structure of gemfibrozil cyclobutylamine ($P2_1/n$)

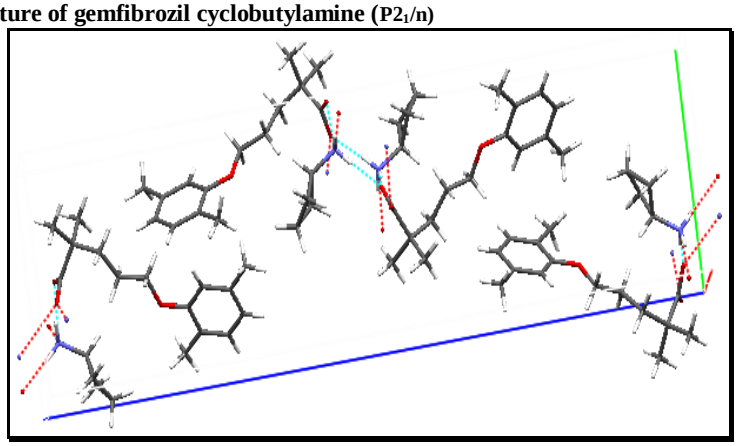

Fig 4.12bCrystal structure of gemfibrozil cyclobutylamine ($P2_1/n$)

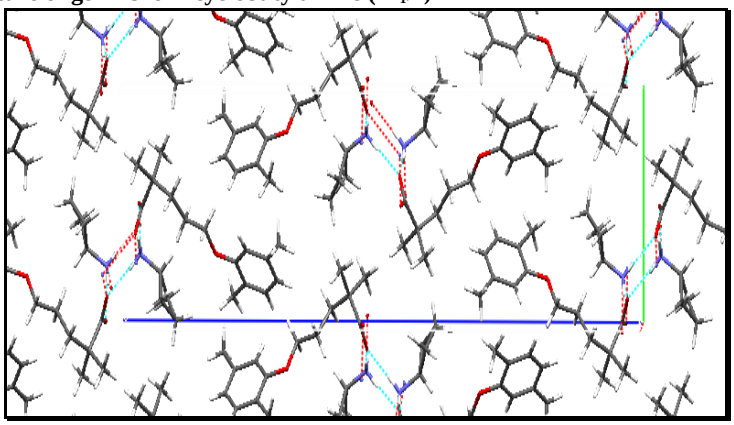

4.4.3.4 GCHex

GCHex ($P2_1/n$) displays the of $R_4^3(10)$ columns in a space group different to that of GAdam, GTBut, and GCBut. Columns are cross linked by van der Waals forces but only in one direction resulting in stacked layers.

Fig 4.13a Crystal structure of gemfibrozil cyclohexylamine ($P2_1/n$)

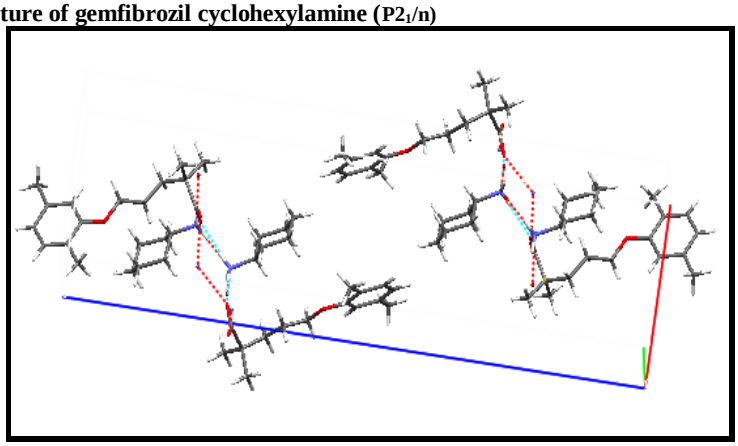

Fig 4.13b Crystal structure of gemfibrozil cyclohexylamine ($P2_1/n$)

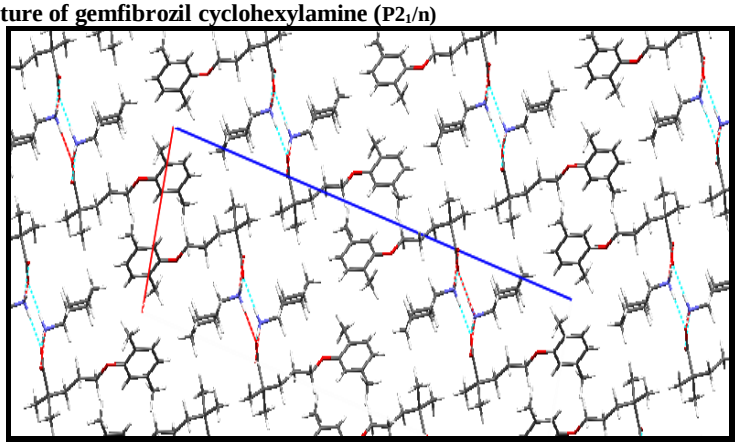

4.4.3.5 GTBut

GTBut shares the same structural arrangement with GCBut and GAdam of $R_4^3(10)$ columns. The columns not cross-linked by van der Waals forces.

Fig 4.14a Crystal structure of gemfibrozil tert-butylamine ($P2_12_1/2_1$)

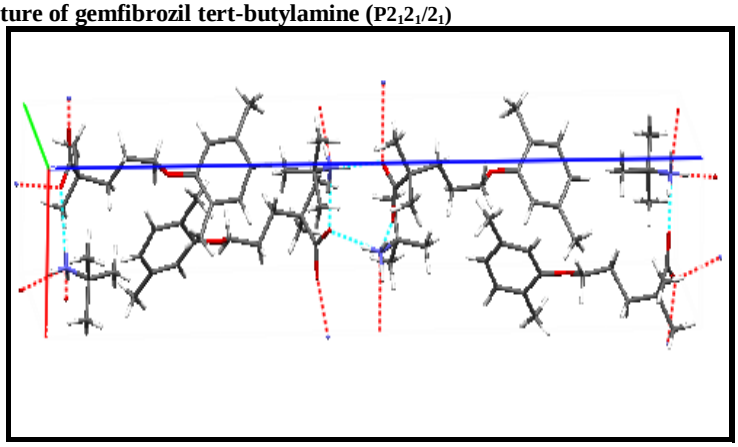

Fig 4.14b Crystal structure of gemfibrozil tert-butylamine ($P2_12_1/2_1$)

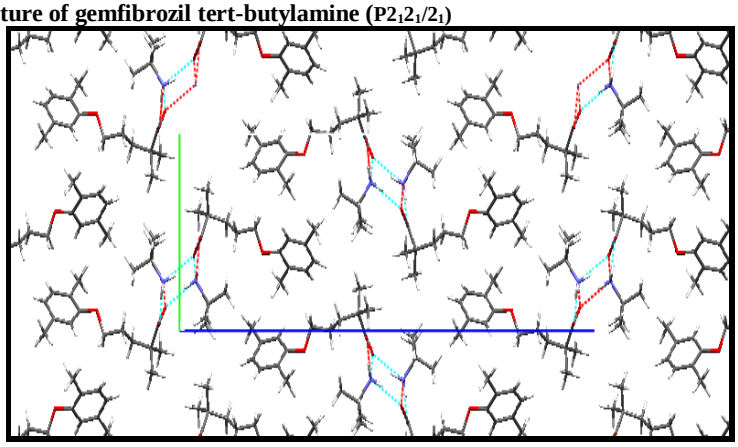

4.4.3.6 GAMP1

In the crystal structure GAMP1, the OH group provides additional potential for hydrogen bonding resulting in a two-dimensional Type V network. The structure contains chains of alternating molecules of gemfibrozil and AMP1 along the shortest unit cell axis, with each pair of adjacent molecules in the chain linked by an N–H···O hydrogen bond. As in the structure of GTBut, pairs of chains are cross-linked to each other to form a ladder type structure, but the cross-linking is different from that seen in GTbut. Thus, instead of the single N–H···O hydrogen bond that forms the rungs of the ladder in GTBut, the rungs of the ladder in GAMP1 involve a hydrogen bonding arrangement of the type N–H···O–H···O in which the O–H group is from a molecule of AMP1. For any given carboxylate group of gemfibrozil, only one oxygen atom is involved in a cross-linking interaction of this type. A given molecule of AMP1 acts as a hydrogen bond donor in N–H···O and O–H···O interactions that are formed to the same carboxylate group of AMP1 (but to different oxygen atoms of this carboxylate group), with the N–H···O hydrogen bond forming part of the chain along the b-axis and the O–H···O hydrogen bond forming part of the cross linking rung of the ladder (see Fig 4.15). A

hydrogen bonded ring is formed by the two chains of the ladder and an adjacent pair of rungs, and is designated as $R_6^6(16)$ in graph set notation. As in the structure of GAMP1, pairs of neighbouring chains are exclusively cross-linked to each other and do not cross-link to any other chain.

Fig 4.15 Schematic representation of the hydrogen bonding in gemfibrozil AMP1 ($P2_1/c$)

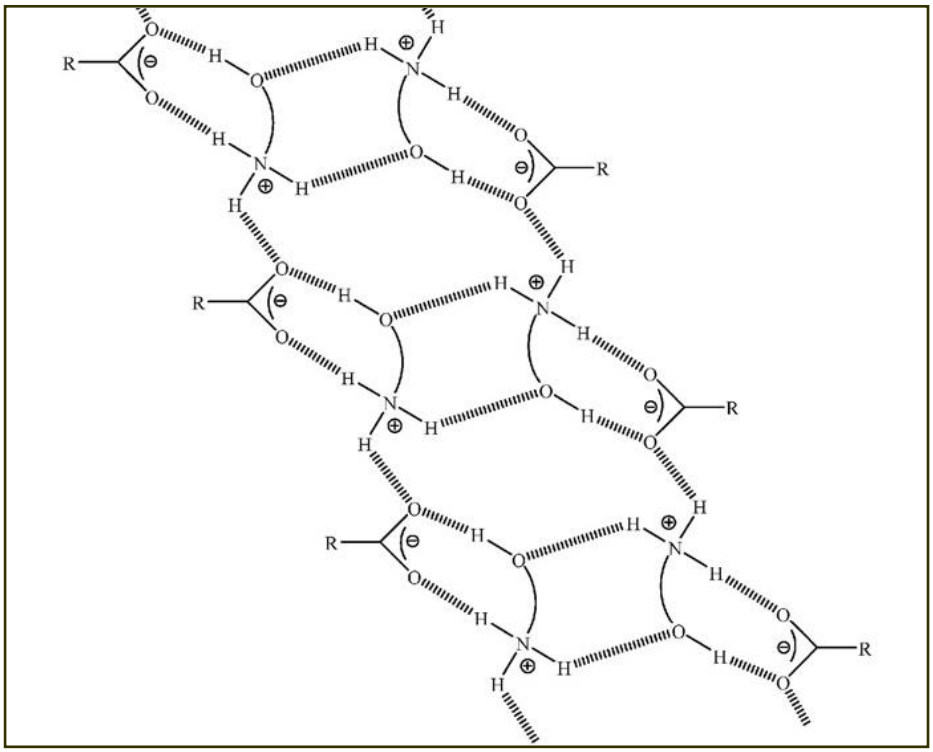

Sets of cross-linked chains interact with each other through van der Waals interactions.

Fig 4.16a Crystal structure of gemfibrozil AMP1 ($P2_1/c$)

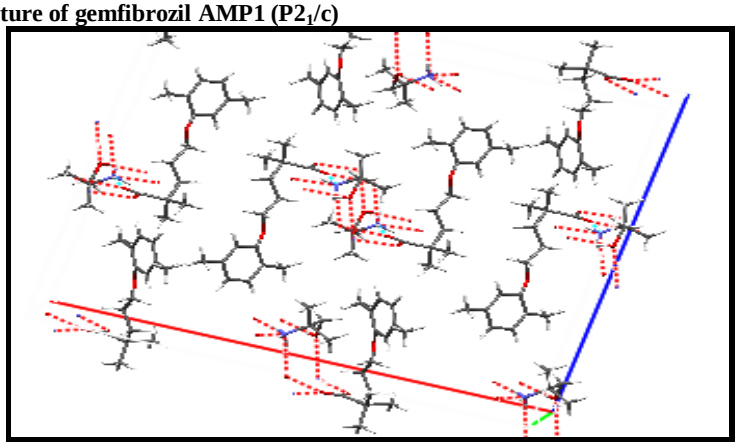

Fig 4.16bCrystal structure of gemfibrozil AMP1 ($P2_1/c$)

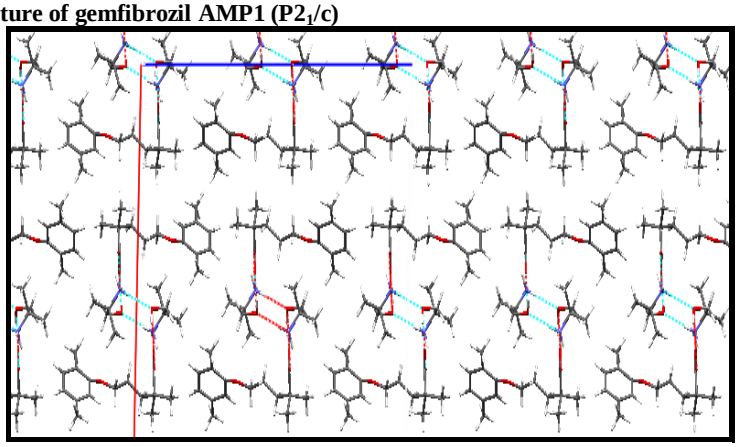

4.4.3.7 GAMP2

GAMP2 has two OH groups from the amine counterion, creating further opportunities for hydrogen bonding. Indeed, each of the five potential hydrogen bond donors (i.e. three N–H bonds and two O–H bonds) is involved in an N–H···O or O–H···O hydrogen bond. As in GTBut and GAMP1, hydrogen bonded chains are formed along the shortest unit cell axis, involving alternating molecules of G and AMP2. Within the chain, each pair of adjacent molecules is linked by an N–H···O hydrogen bond. Each carboxylate oxygen is involved in one N–H···O hydrogen bond within the chain, and two N–H bonds of each ammonium group are involved in the N–H···O hydrogen bonds within the chain. A ladder-type structure is again formed by cross-linking of neighbouring chains, but each cross-link involves a hydrogen bonding arrangement of the type N–H···O–H···O–H···O. For a given carboxylate group of gemfibrozil, only one oxygen atom is involved in a cross-linking interaction of this type, and for each ammonium group, one N–H bond is involved in such cross links. For a given cross-link, the two O–H groups are from different molecules of AMP2. The two chains of the ladder and an adjacent

Fig 4.17aCrystal structure of gemfibrozil AMP2 (P-1)

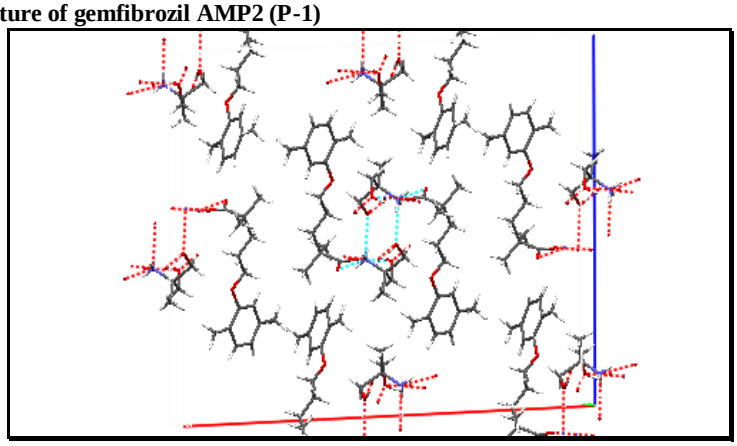

Fig 4.17bCrystal structure of gemfibrozil AMP2 (P-1)

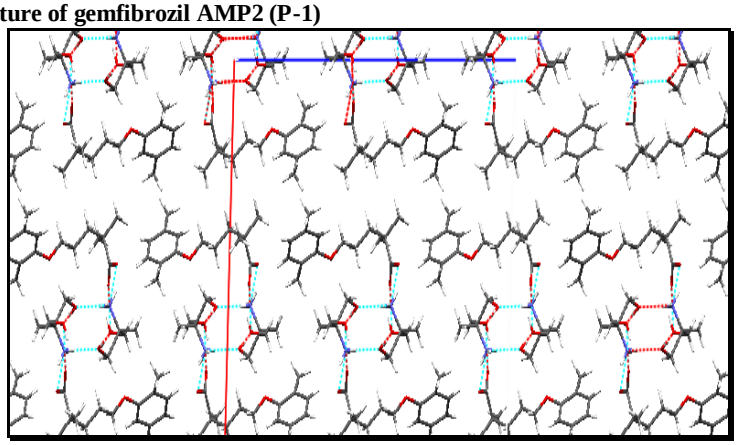

pair of rungs give rise to a hydrogen bonded ring, designated $R_8^8(20)$ in graph set notation. The rungs are not straight, but form a twisted path. As in the crystal structures of GTBut and GAMP1, pairs of neighboring chains are exclusively cross-linked to each other, and not to any other chain. Adjacent sets of cross-linked chains are in van der Waals contact with each other.

4.4.3.8 GTris

GTris contains three OH groups, in addition to the three N–H hydrogen bond donors, representing a total of six potential hydrogen bond donors. Each carboxylate oxygen receives one hydrogen bond from the same ammonium group of a tris molecule and another one from nearby tris hydroxyls. Those tris molecules are then hydrogen bonded to the first tris molecule through the remaining ammonium hydrogen and hydroxyl groups respectively (see Fig 4.18b).

Fig 4.18aCarboxylate·ammonium hydrogen bonding pattern in FTris I conformer 1 and GTris

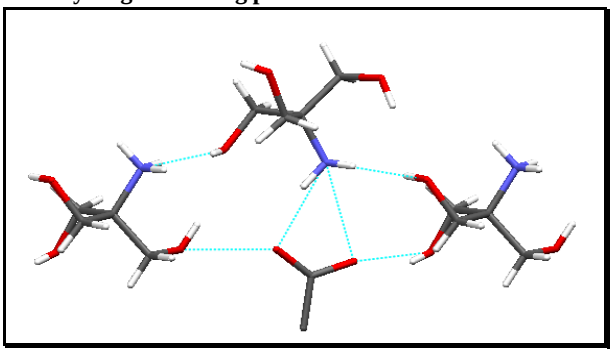

Fig 4.18bCarboxylate·ammonium hydrogen bonding pattern in FTris I conformer 1 and GTris

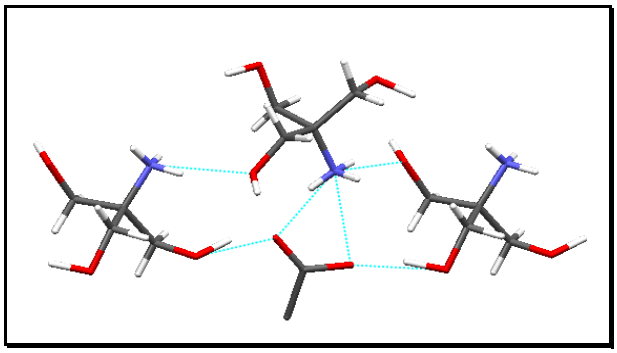

The numerous hydrogen bonding interactions give rise to extensively hydrogen-bonded sheets parallel to the *bc*-plane. The other (non-carboxylate) parts of the gemfibrozil molecules extend outwards from both faces of the sheet, and the region between adjacent sheets is dominated by van der Waals interactions between the gemfibrozil molecules. The arrangement of molecules in the crystal structure of GTris, which clearly differs substantially from those in GTBut, GAMP1 and GAMP2, resembles that of the conformer 1 of FTris I (see section 3.4.3.10).

Fig 4.19aCrystal structure of gemfibrozil Tris ($P2_1/c$)

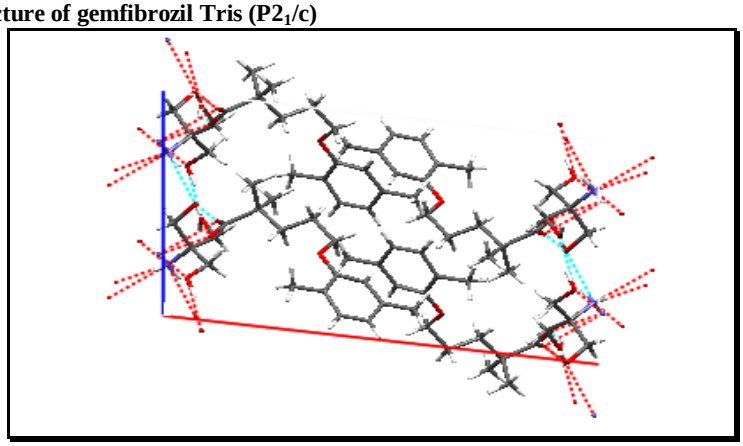

Fig 4.19bCrystal structure of gemfibrozil Tris ($P2_1/c$)

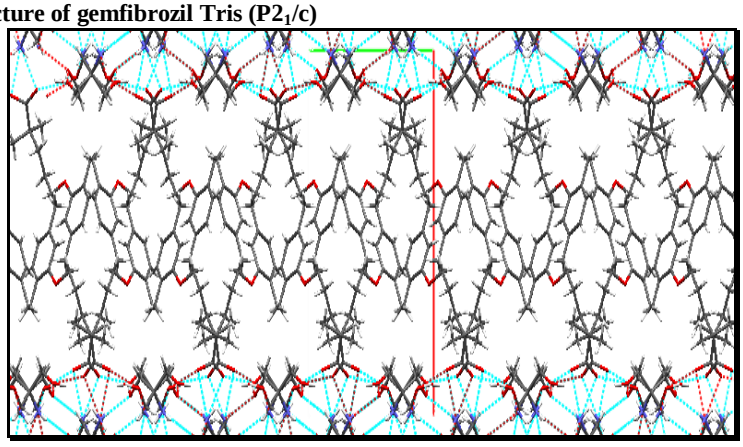

4.4.3.9 GTEA

Although GTEA is a salt-like adduct, apparently no electrostatic interaction, $NH^{+}\cdots O^{-}$, between the positively charged ammonium ions and the negatively charged acetate groups is observed. A salt adduct of the type carboxylate-hydroxyl is observed. This breaks Etter's first rule which states that all good proton donors and acceptors are used in hydrogen bonding (Etter 1990). It appears to be likely due to steric hindrance as the three hydroxyethyl arms surround the ammonium group. This type of bonding has been seen before with hydroxyethyl fragments and carboxylic acids (Dhanaraj and Vijayan 1987). In the four examples of salts between carboxylic acids and triethanolamine observed in the CCSD (*BEVMIY, BUZSUK, GAHJOO, TEKVAG*) they all form carboxylate-hydroxyl interaction type salts and in all of them the ammonium are so shielded by the hydroxyethyl arms that they do not take part in intermolecular interactions. The hydroxyl group also interacts via a hydrogen bond with the carboxylate group in GTEA, but in this case the ammonium group is not completely shielded and manages to donate a hydrogen bond to a neighbouring hydroxyl group.

Two triethanolamine molecules form a pair between the ammonium and one of the hydroxyl groups. The hydroxyl group involved in this pair and a second one donate then hydrogen bonds to each carboxylate of one gemfibrozil molecule and the third hydroxyl group donates a H-bond to a second gemfibrozil molecule. The resulting network exhibits hydrogen bonded layers with the gemfibrozil groups projected to the interlayer space. Layers are subject to van der Waals interactions.

Fig 4.20 Ammonium-hydroxyl salt between gemfibrozil and triethanolamine

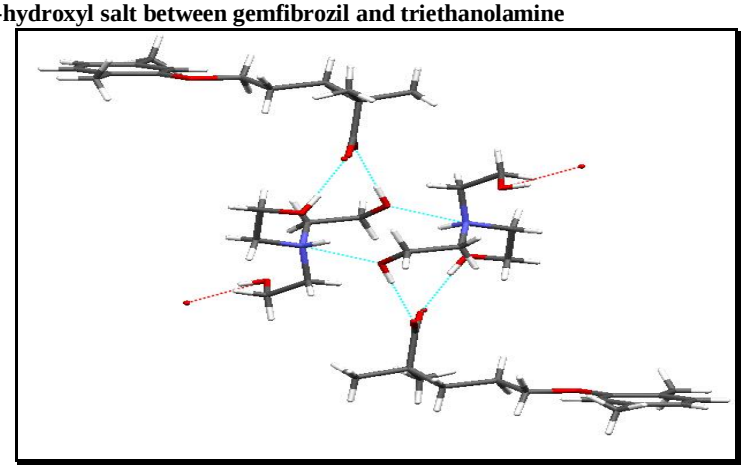

Fig 4.21a Crystal structure of gemfibrozil TEA ($P2_1/c$)

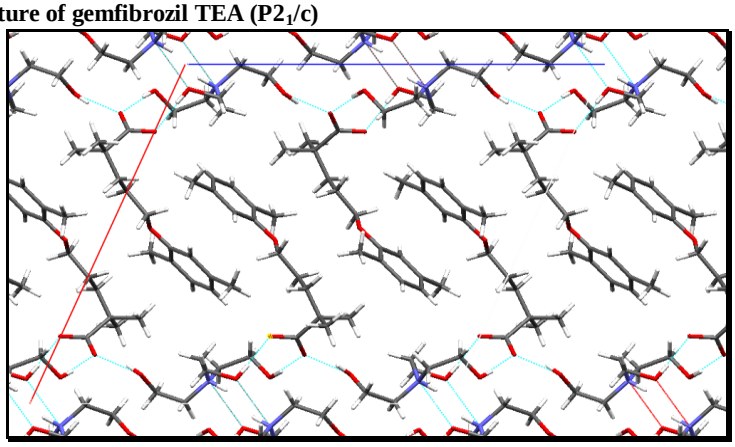

Fig 4.21b Crystal structure of gemfibrozil TEA ($P2_1/c$)

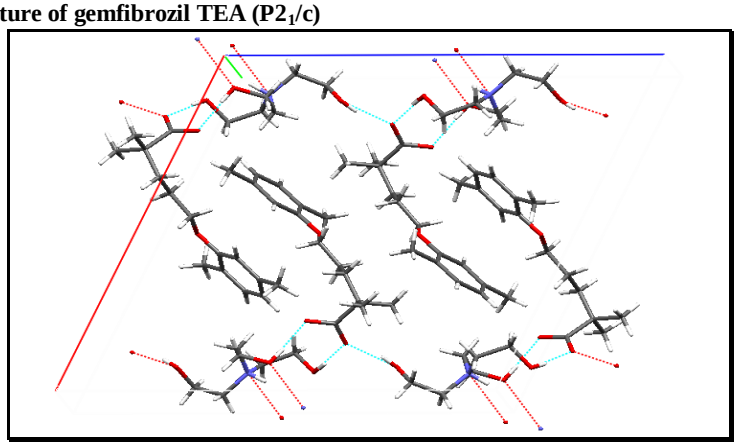

4.5 Mechanical properties

4.5.1 Compaction replicator

4.5.1.1 Materials

All gemfibrozil salts were obtained as described in section 2.1.1. A sieved fraction between 96 – 250 μm was selected for use in mechanical testing.

4.5.1.2 Method

A Stylcam 100R compaction replicator (Medelpharm, Bourge-en Bresse, France) with acquisition software (Analis version 2.01.27, Medelpharm) was used as detailed in section 2.5.2.1.

4.5.1.3 Results and discussion

For every salt, the true densities of the flurbiprofen salts are higher than the gemfibrozil equivalent (see also Table 3.7).

Table 4.6True density values for gemfibrozil and its salts (n = 5, SD)

	True Density (g/cm^3)
G	1.0895 ± 0.0006
GAdam	1.1368 ± 0.007
GBenz	1.1286 ± 0.002
GCProp	1.1378 ± 0.003
GCBut	1.1233 ± 0.002
GCHex	1.1413 ± 0.003
GTBut	1.0399 ± 0.002
GAMP1	1.1018 ± 0.005
GAMP2	1.2052 ± 0.003
GTris	1.2185 ± 0.003

The more flexible structure of gemfibrozil is not associated with better packing as expected. Therefore there must be other factors that turn gemfibrozil into a conformationally "locked" molecule resulting in less efficiently packed crystals. Examining the conformation of gemfibrozil in these salts it is observed that the aliphatic chain adopts a rather straight conformation in most cases. The angle between the planes formed by C5-C6-C7 and the benzyl ring does not exceed 15° with the exceptions of GTris (58.02°) and GTBut (63.12°) resulting in a L-shaped long molecule with the carbonyl group perpendicular to the chain. (see Figs 4.22 and 4.23 with gemfibrozil, the straightest, and GTBut the most convoluted of the structures in this series).

Fig 4.22 C5, C6 and C7 in gemfibrozil

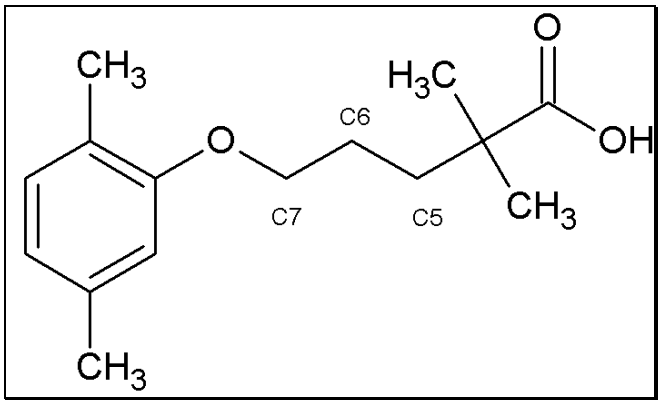

Fig 4.23a **L-shape conformation of gemfibrozil in the neutral molecule**

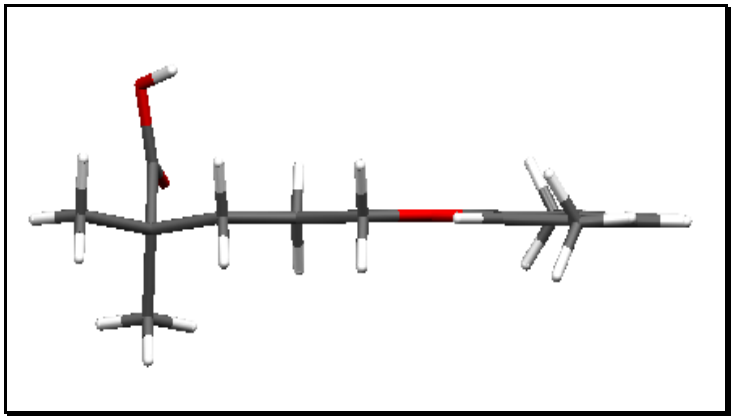

Fig 4.23bL-shape conformation of gemfibrozil in GTBut

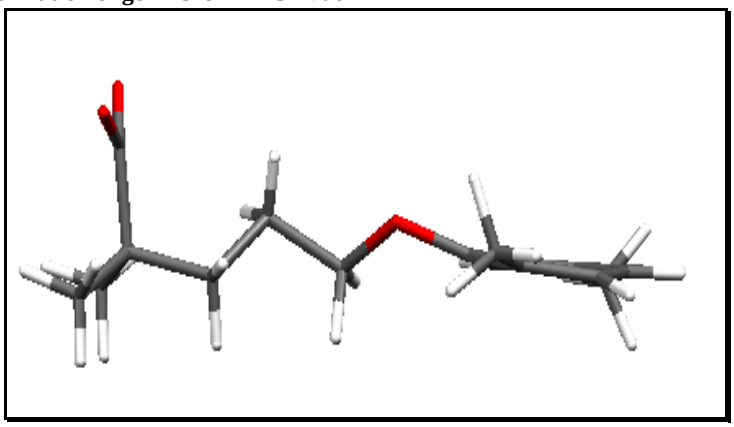

Table 4.7Yield Pressure (MPa) and elastic recovery (%) for gemfibrozil salts

	Yield Pressure, Py (MPa)	Elastic recovery
Gemfibrozil	37.16	5.06
GAdam	63.32	6.97
GBenz	47.66	3.73
GCProp	38.32	4.01
GCBut	51.82	4.26
GCHex	78.41	4.60
GTBut	38.22	8.84
GAMP1	36.78	7.31
GAMP2	60.66	9.77
GTris	100.72	7.78

Similar to results for the flurbiprofen salts, the observed yield pressure values correspond to values commonly seen in other pharmaceutical compounds where the consolidation mechanism is a mixture of plastic and elastic deformation (see Table 3.36). None of the compounds displayed troublesome elastic recovery.

Tensile strengths of gemfibrozil salts are summarized in Table 4.8 Overall, it can be observed that mechanical properties of gemfibrozil salts are considerably poorer that the equivalent flurbiprofen compounds. Few gemfibrozil salts exceed the desirable tensile strength value of 1 MPa. There is no significant difference in the hardness of the tablets between salts containing hydroxyl groups with different hydrogen bonding potential.

Fig 4.24 Tensile strength for gemfibrozil salt series at SF=0.85. (n=6)

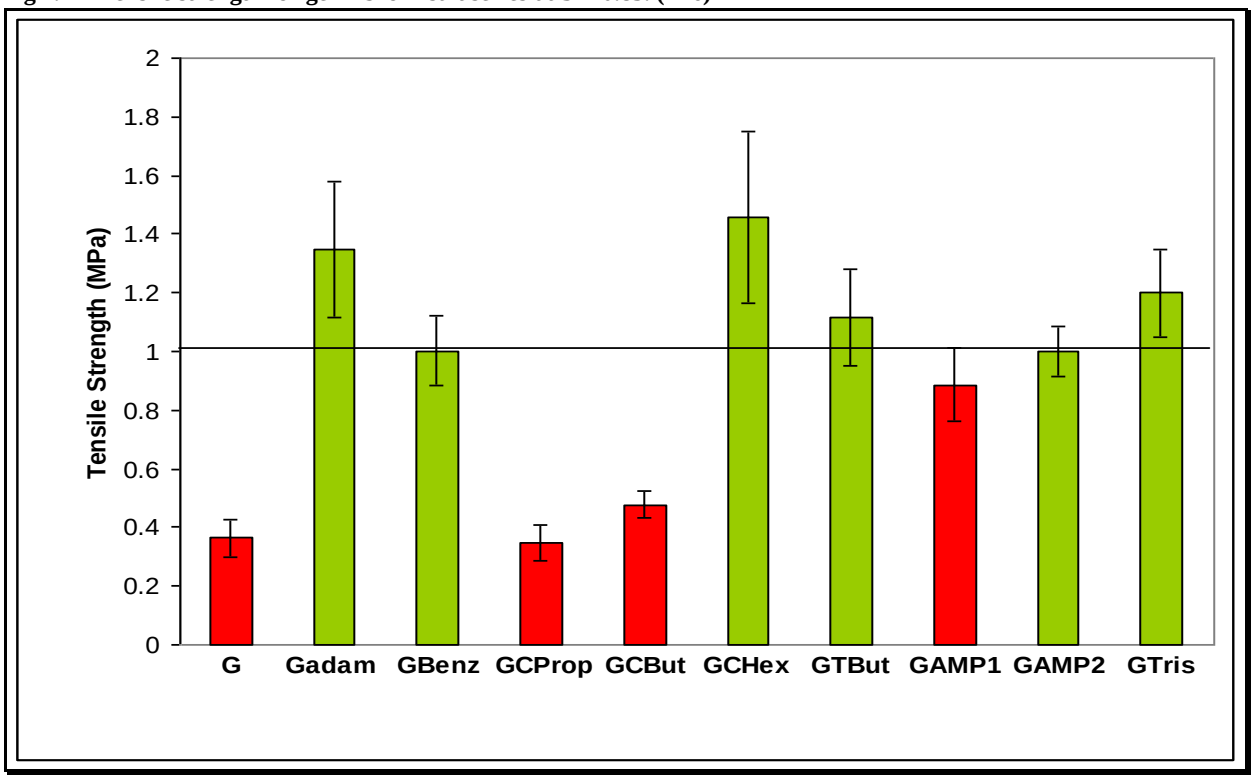

Table 4.8Tensile strength values for gemfibrozil salts (MPa) and SD (n=6)

	G	GAdam	GBenz	GCBut	GCProp	GCHex	GTBut	GAMP1	GAMP2	GTris
Tensile strength	**0.36**	**1.34**	**1.00**	**0.34**	**0.47**	**1.45**	**1.12**	**0.88**	**1.00**	**1.19**
SD	0.06	0.230	0.11	0.06	0.04	0.2	0.49	0.12	0.08	0.14

As the tensile strength is generally low, it is difficult to make comparisons but there are some tendencies if molecules with similar features are grouped together

4.5.1.3.1 Type II columns, GAdam-GCHex-GTBut-GCBut

All four salts share the same one-dimensional $R_4^3(10)$ hydrogen bonded columns.

On one hand there are GAdam, GCBut, GTbut, which also share the same space group ($P2_12_12_1$), and on the other there is GCHex, with space group $P2_1/n$. The first three give a very similar picture with the columns arranged parallel in layers projecting the long gemfibrozil residues to an interlayer space. Columns are cross-linked by van der Waals forces in GCBut only. The gemfibrozil groups are more densely interdigitated in GTBut. GCHex, on the other hand,has a similar arrangement to that observed in flurbiprofen salts of parallel columns arranged in layers where a straight and wide interlayer space, or *slip plane*, is generated where the nearest interlayer H-H contacts are 2.352 Å, which exceeds Van der Waals contacts.

Fig 4.25 Crystal arrangement in GAdam

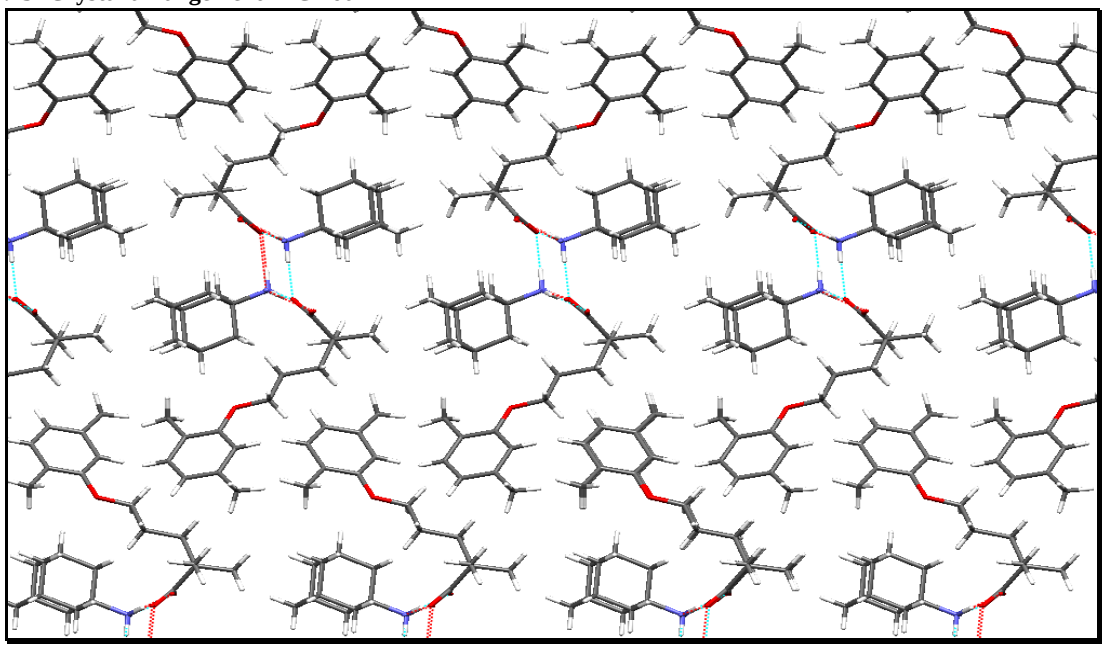

Fig 4.26 Crystal arrangement in GCBut. Van der Wals forces cross-link the columns

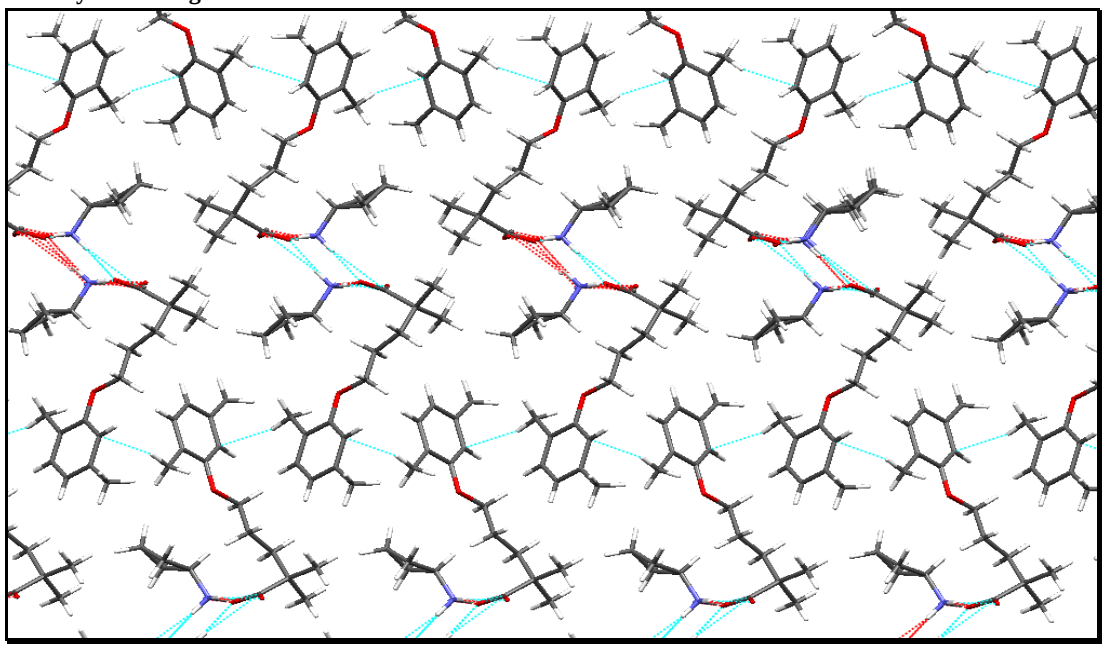

Fig 4.27 Crystal arrangement in GTBut

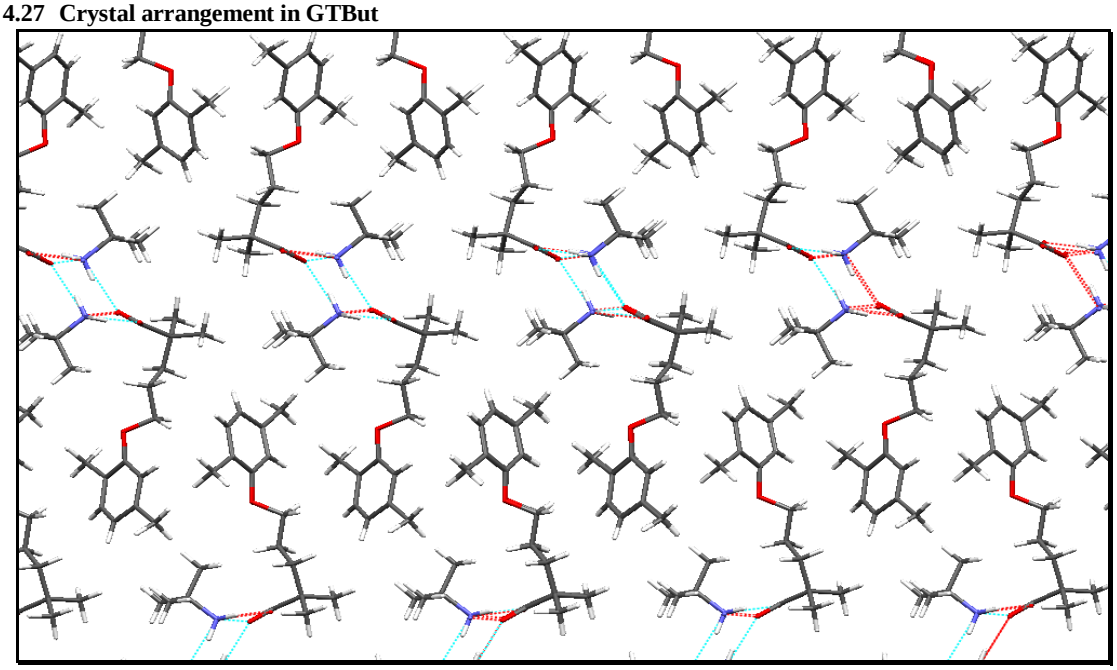

Fig 4.28 Crystal arrangement in GCHex

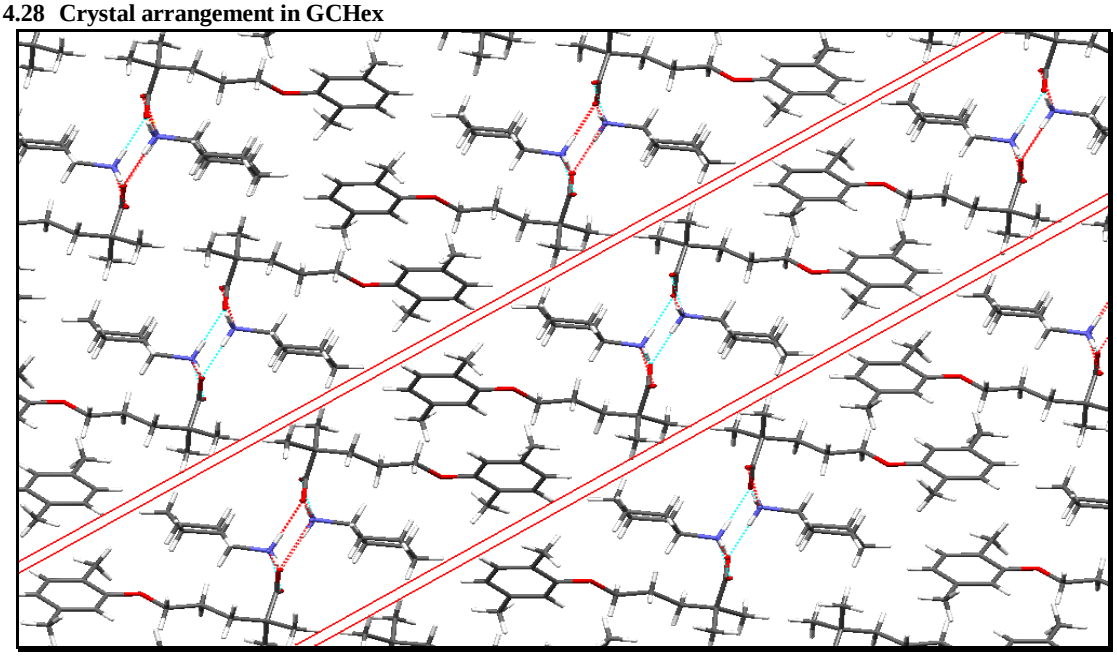

At solid fraction 0.85, the highest tensile strength values correspond to GCHex (1.45 MPa). Similar to the observations for the flurbiprofen series, wide and straight slip planes are associated with improved plasticity and result in stronger compacts.

When comparing GAdam, GCBut and GCHex, GCBut, in which $R_4^3(10)$ columns are cross linked by van der Waals forces, has the lowest tensile strength values (0.47 MPa), followed by GTBut (1.12 MPa). The lower tensile strength of the latter compared to GAdam (1.34 MPa), can be explained by the presence of more deeply interdigitating gemfibrozil residues in GTBut which makes slippage more difficult. In GAdam, not only is the interdigitation is not so dense, but the closest points are further also.

4.5.1.3.2 GTris

GTris exhibits a crystal structure similar to one of the conformers of FTris polymorph I (see Fig 4.18) but free of the conformational strain. A highly hydrogen bonded layer containing the ($R\text{-}NH_3^+$)•($R'\text{-}COO^-$) heterosynthon and the hydroxyl groups is observed. The gemfibrozil residues are projected into the interlayer space in an interdigitating fashion. The interlayer space is free of hydrogen bonds or van der Waals forces (see Fig 4.29 and Fig 4.30).

Fig 4.29 Highly hydrogen bonded layer in GTris

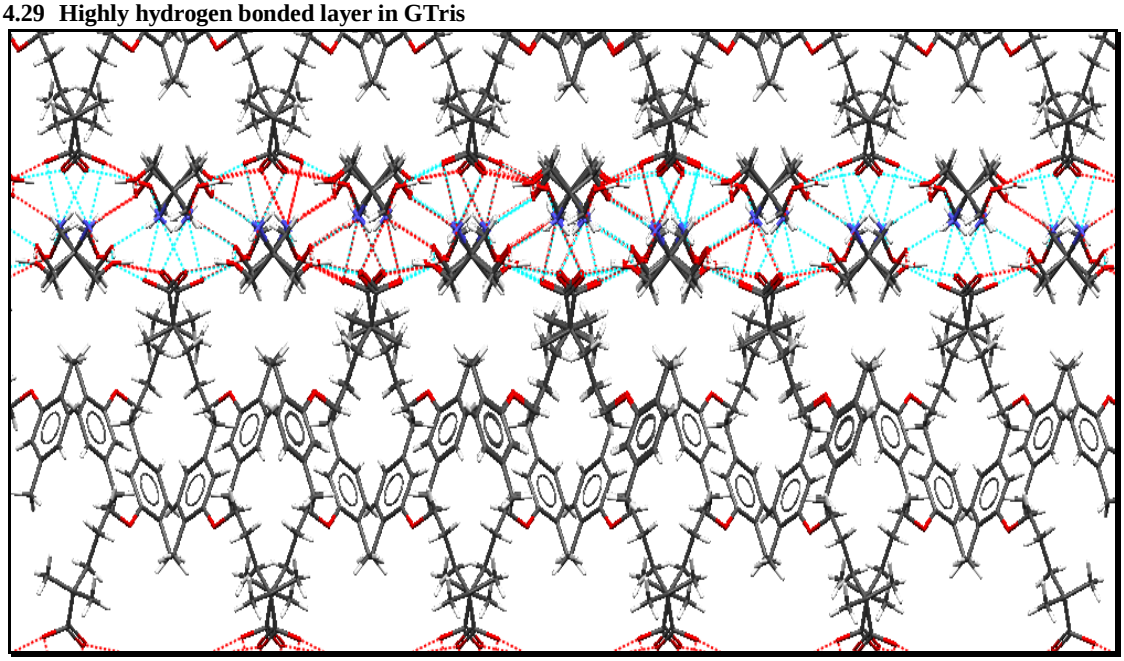

Fig 4.30 Interlayer space free of hydrogen bonds and van der Waals forces. Adjacent layer removed to aid visualisation

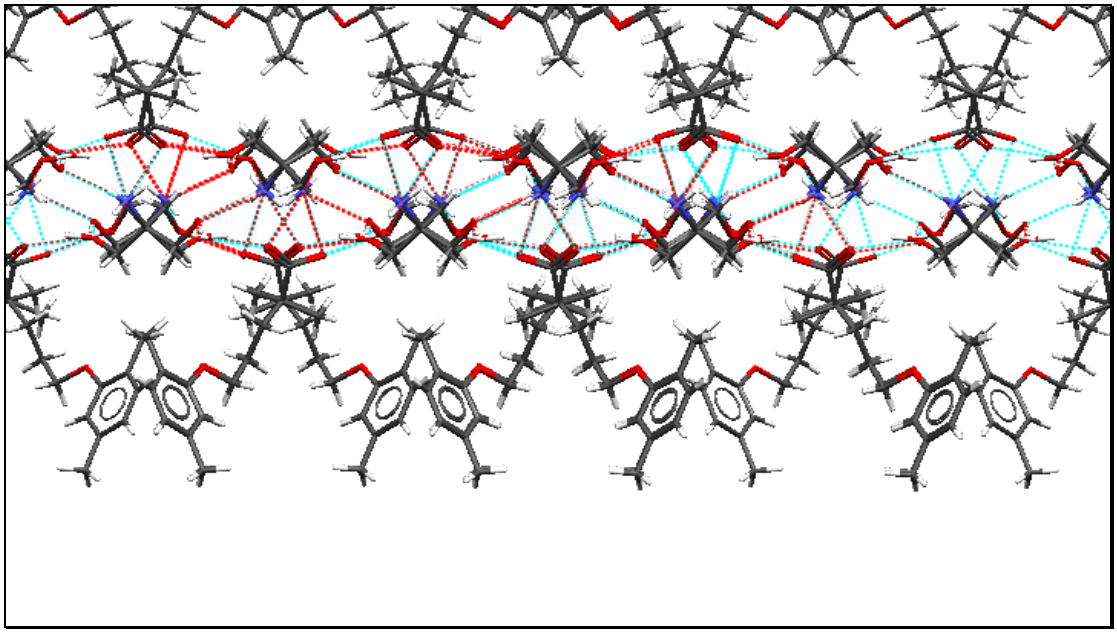

Considering the low tensile strength of the gemfibrozil salts, GTris gives compacts with reasonable tensile strength (1.20 MPa) despite the deeply interdigitating layers limiting plastic deformation to one dimension only. Once again, densely bonded layers are believed to reduce the attachment energy of the stacked layers, improving the slippage of one layer over the adjacent one. The combination of

highly hydrogen bonded two-dimensional layers and an interlayer space, is associated with a resultant higher tensile strength than expected.

4.5.1.3.3 GAMP1 and GAMP2

GAMP1 and GAMP share similarities both in their crystal parameters (see Table 4.9) and in the molecular network (See Figs 4.31 and 4.32). They both have two chains of the ladder where cross-linking of the chains involves an N–H···O hydrogen bond in GAMP1 and a hydrogen bonding arrangement of the type N–H···O–H···O–H···O in GAMP2. An adjacent pair of rungs gives rise to a hydrogen bonded ring, designated $R_6^6(16)$ in GAMP1 and $R_8^8(20)$ in GAMP2 in graph set notation.

The resulting general structure resembles that adopted by the Type II column-containing structures of FCHex, FBenz and FCBut, where columns arrange themselves in parallel layers, free of van der Waals contacts with drug molecules outside and the ammonium-carboxylate heterosynthon internalised. Nearest C-H contacts are 3.161 Å for GAMP1 and 2.930 Å for GAMP2.

Fig 4.31 Slip plane in GAMP1

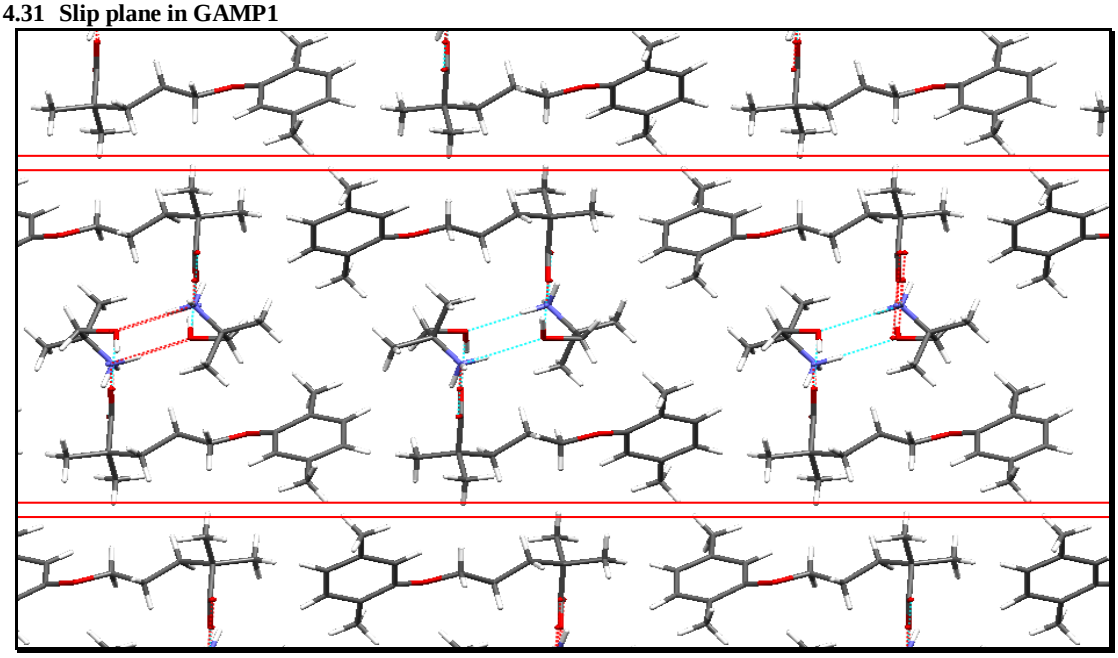

Tensile strength of GAMP1 and GAMP2 compacts area similar with a trend towards higher values for GAMP2 (1.00 vs. 0.88 MPa). This could probably be attributed to the extra hydrogen bonding (74 versus 60 hydrogen bonds in the unit cell) that lowers the attachment energy between the columns thus affording easier slippage.

Fig 4.32 Slip plane in GAMP2

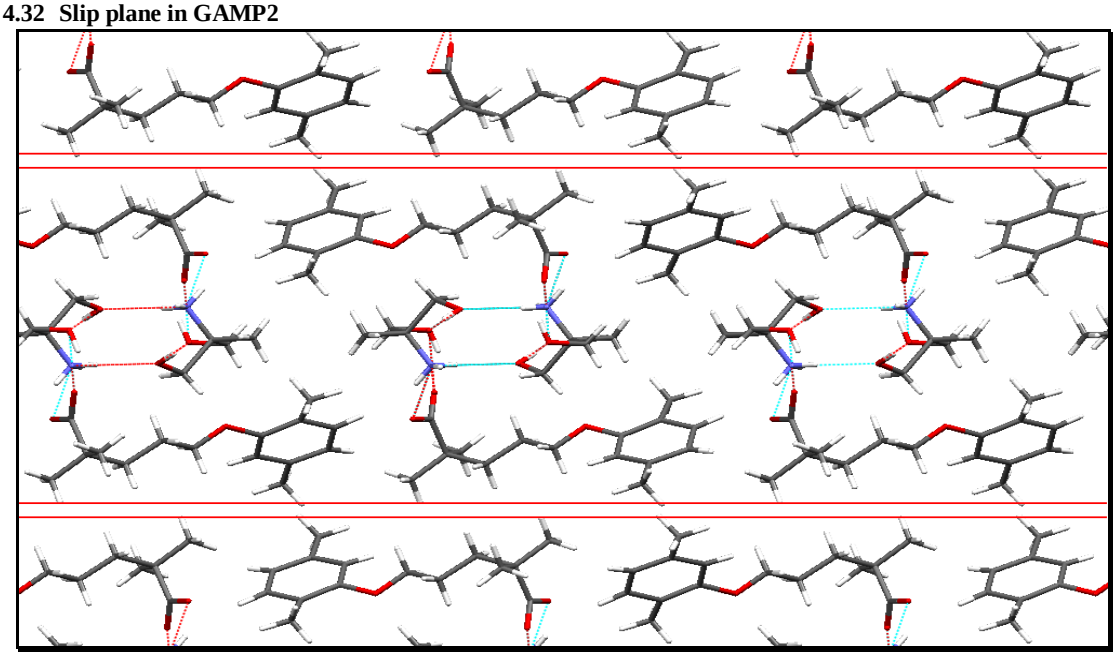

On the other hand, these tensile strength values are lower than that of GCHex, which contains type II columns arranged in similar layers with straight slip planes and even those type II columns with interdigitating slip planes (excluding GCBut where columns are cross-linked by van der Waals forces). It was observed in the flurbiprofen series that among the one-dimensional networks, Type II columns may be associated with higher tensile strength than Type III columns. It appears that in the gemfibrozil series Type II columns are also associated with higher values of tensile strength than other alternative columns arrangements as evidenced by the GAMP1 and GAMP2 examples.

4.5.1.4 Conclusions

The conclusions from the gemfibrozil series are in line with those reached in the flurbiprofen chapter (see section 3.5.2.4). Molecules exhibiting straight wide planes generally have higher tensile strength values than those with interdigitating planes. Not only hydrogen bonds, but Van der Waals forces also render potential slip planes ineffective. Two-dimensional networks are associated with the formation of stronger compacts with higher values corresponding to more densely bonded layers.

One additional point has been identified, that type II columns may provide stronger compacts than other one-dimensional networks rather than Type III columns in similar circumstances (presence of slip planes, straight/zigzagging nature of it and absence of van der Waals forces).

5 Diclofenac

Diclofenac is practically insoluble in water; soluble in alcohol. It has a solubility of 0.071 mg/ml with a resulting pH of 5.47 at 25°C (Ledwidge and Corrigan 1998). It has a melting point of 156° to 158 °C (Lund 1994; Merck 2010).

Fig 5.1 Diclofenac structure

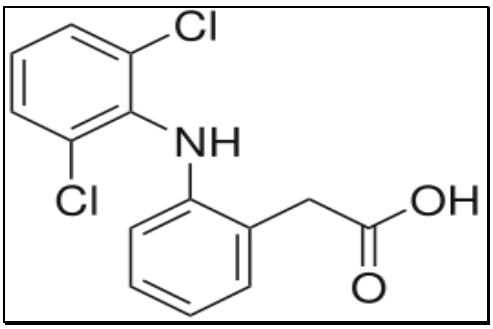

Diclofenac, 2-[(2,6-Dichlorophenyl)amino]benzeneacetic acid, is an NSAID (like flurbiprofen. It is used mainly as the sodium salt for the relief of pain and inflammation in various conditions, inducing topical application. It has also been used in some countries for the management of actinic keratoses. Eye drops of diclofenac sodium are used for the prevention of intra-operative miosis during cataract extraction, for the treatment of inflammation after surgery or laser treatment of the eye, for pain in corneal epithelial defects after surgery or accidental trauma, and for the relief of ocular signs and symptoms of seasonal allergic conjunctivitis.

The usual oral or rectal dose of diclofenac sodium is 75 to 150 mg daily in divided doses. In the UK the maximum dose regardless of route or indication is 150 mg daily; however, in the USA a maximum oral dose of 200 mg daily is allowed in the treatment of rheumatoid arthritis. Modified-release preparations of diclofenac sodium are available for oral use. Diclofenac has also been given in equivalent oral doses as the free acid in dispersible preparations for short-term treatment up to 3 months long. Diclofenac is also given orally as the potassium salt. Doses of the potassium salt are similar to those for diclofenac sodium. Diclofenac potassium is also used in the treatment of migraine in an initial dose of 50 mg taken at the first signs of an attack; an additional dose of 50 mg may be taken after 2 hours if symptoms persist. If necessary further doses of 50 mg may be taken every 4 to 6 hours to a maximum daily dose of 200 mg.

Diclofenac sodium may also be given by deep intramuscular injection into the gluteal muscle in a dose of 75 mg once daily or, if required in severe conditions, 75 mg twice daily. Diclofenac sodium may also be given as a continuous or intermittent intravenous infusion in glucose 5% or sodium chloride 0.9% (both previously buffered with sodium bicarbonate) or as a bolus intravenous injection.

Side-effects are similar to those of flurbiprofen (see Section 3)

In the UK diclofenac is marketed under various trade names as fast-dissolving tablets (potassium salt), immediate and modified release tablets, injections, suppositories and eye drops (sodium salts) and topical sprays and gels (diethylammonium salts). Diethylammonium salts have been used for dermal application more often than other diclofenac salts, due to its ambiphilic nature which enhances the solubility of the drug and penetration of the skin.

5.1 Salt preparation

All salts for which single crystals had to be obtained for structure determination were prepared recrystallising from methanol. The following salt structures were already available in the Cambridge Structural Database (CSD): DDEA, *ZIKPOY* (Castellari and Ottani 1995), DTEA, *TEKVAG,* (Castellari and Ottani 1996) and DTris, *TUDPIR (Castellari and Ottani 1997a).* These salts were prepared by recrystallising from the same solvents as described by their authors. Thus, DDEA and DTEA were recrystallised from acetone and DTris was recrystallised from methanol.

5.1.1 Recovery

The diclofenac ratio in the salt was compared to the theoretical ratio. One hundred milligrams of each salt was weighed and placed in a 100 ml class A volumetric flask and made up to volume with mobile phase to give a 1 mg/ml solution. Methanol:water, 80:20 was used as mobile phase. The solution was analysed then by HPLC. Experiments were performed in triplicate.

With a recovery of >98%, this method of salt formation was considered satisfactory in producing a reasonable yield, with little wastage and acceptable level of purity.

Table 5.1Recovery of diclofenac salts (n=3, SD)

	% content Experimental	% content Theoretical	Recovery of salt
DAdam	65.53 ± 0.12	66.19	99.01%
DBenz	72.77 ± 0.09	73.42	99.12%
DCHex	73.57 ± 0.11	74.91	98.22%
DTBut	79.38 ± 0.23	80.19	99.00%
DAMP1	76.52 ± 0.11	76.86	99.57%
DAMP2	72.33 ± 0.07	73.80	98.02%
DTris	69.93 ± 0.12	70.96	98.56%
DMEA	81.54 ± 0.13	82.90	98.37%
DDEA	72.92 ± 0.17	73.80	98.81%
DTEA	65.56 ± 0.08	66.50	98.59%

5.1.2 Fourier Transform Infrared Spectroscopy (FTIR)

FTIR was used to confirm the transformation from carboxylic acid to a carboxylate salt.

The salt formation was confirmed by the presence of the signal at 1700 cm^{-1}, attributed to a stretching of the C=O group in the carboxylic acid in the case of diclofenac (Fig 5.2). This method has previously been used by O'Connor and Corrigan (2001b) to confirm salt formation in a range of diclofenac salts.

With diclofenac salts, the presence of a band at 3350-3150 cm^{-1} was not confirmatory of ammonium salts, as diclofenac itself has a secondary amine group in its molecule. However, a peak is observed at 2100 cm^{-1} which is not seen in diclofenac and is only seen in $(R\text{-}NH_3^+)\bullet(R'\text{-}CO_2^-)$ salts with primary amines. There is no peak at 2100 cm^{-1} in DTEA (see Fig 5.4) or DDEA.

The infrared spectra for diclofenac and DAdam salt are included here as typical examples and the spectra for other salts are included in Appendix A.

Fig 5.2 FTIR scan for diclofenac

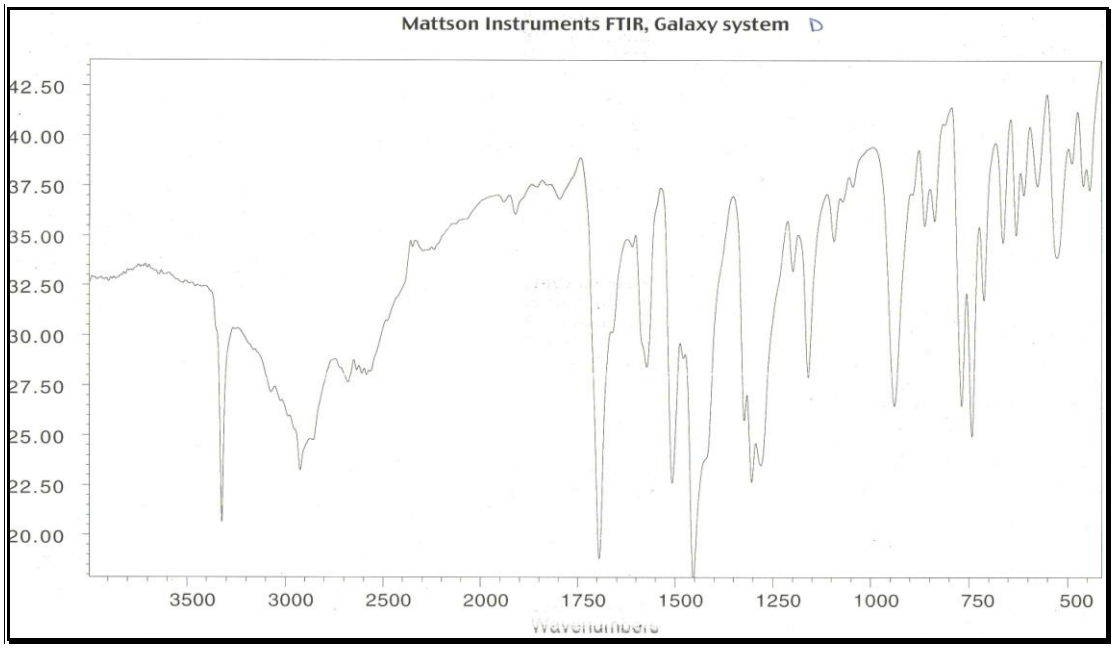

Fig 5.3 FTIR scan for DAdam salt

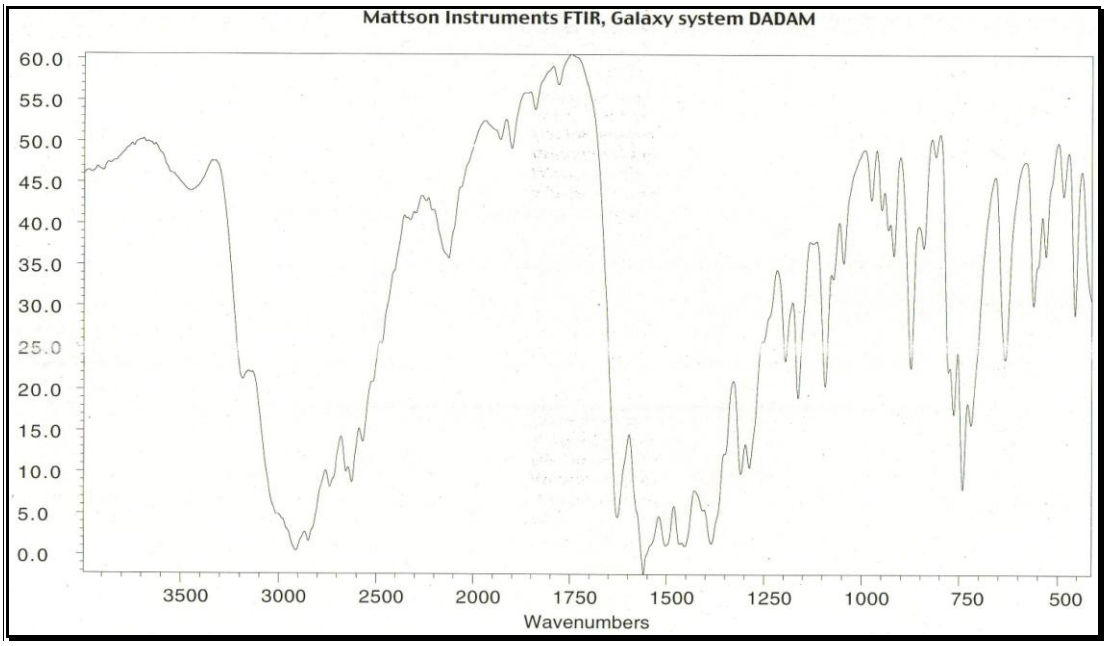

Fig 5.4 FTIR scan for DTEA salt

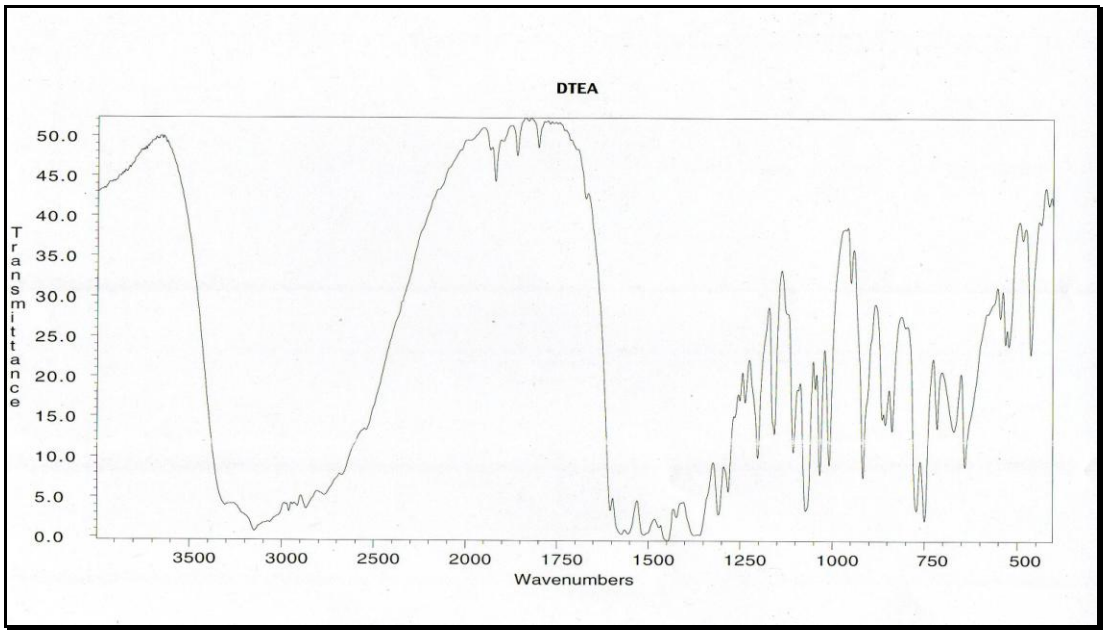

5.1.3 Nuclear Magnetic Resonance

The spectra accounted for every hydrogen in a 1:1 salt. Salt formation was confirmed by the appearance of the hydrogen associated with the carbon next to the carbonyl group at a lower chemical shift in salts compared to the acid. NMR spectra for diclofenac and DMEA and included here. The hydrogen on the carbon next to the carbonyl group appears at 3.69 ppm in diclofenac and at 3.44 ppm in the monoethanolamine salt. Spectra for the rest of the salts are in Appendix B.

5.2 Thermal studies

5.2.1 Material

All salts were obtained as described in section 5.1.

5.2.2 Methods

DSC and TGA methods were used as described in sections 2.2.1.2 and 2.2.2.2 respectively.

Fig 5.5 NMR scan for diclofenac

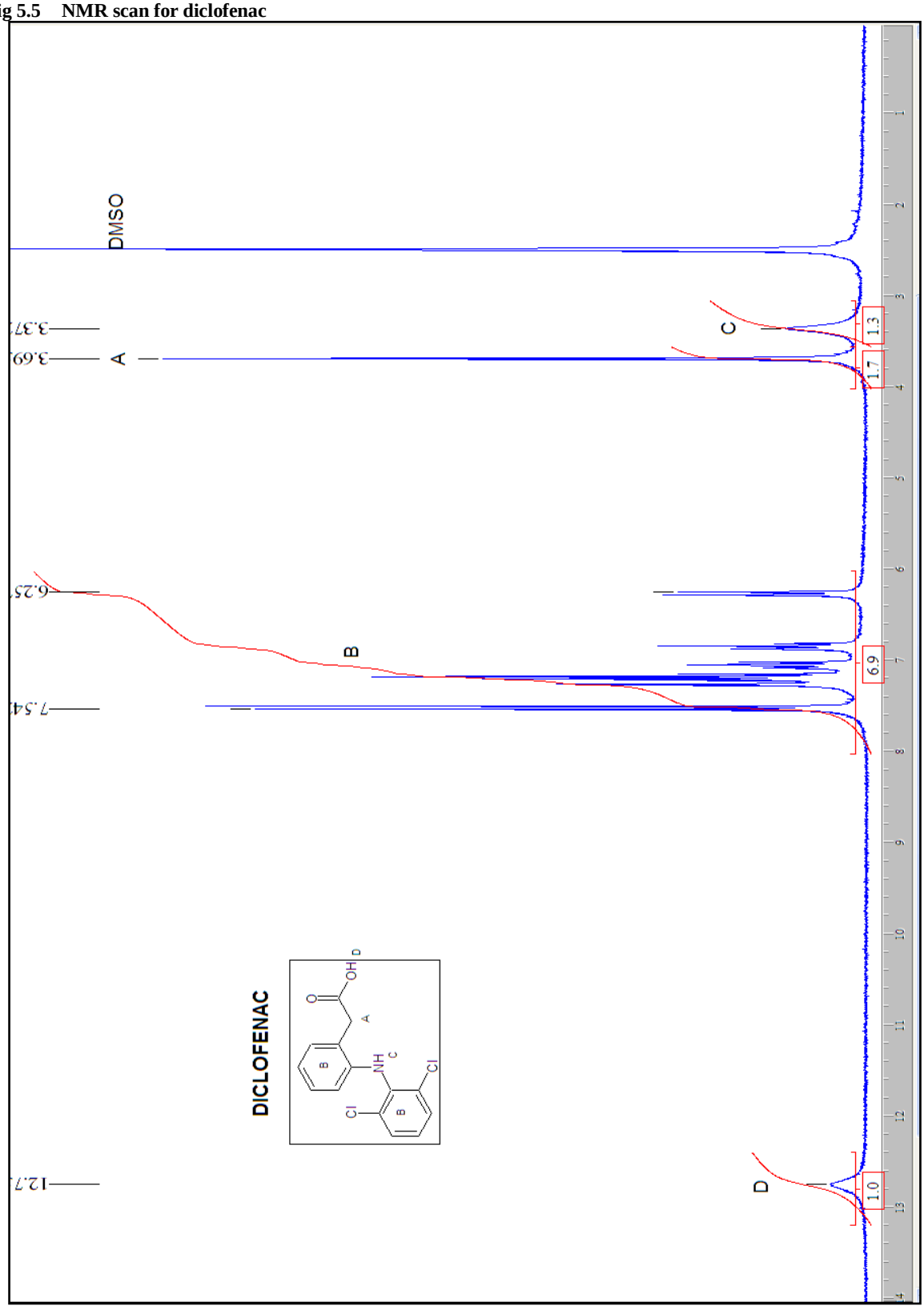

Fig 5.6 NMR scan for DMEA

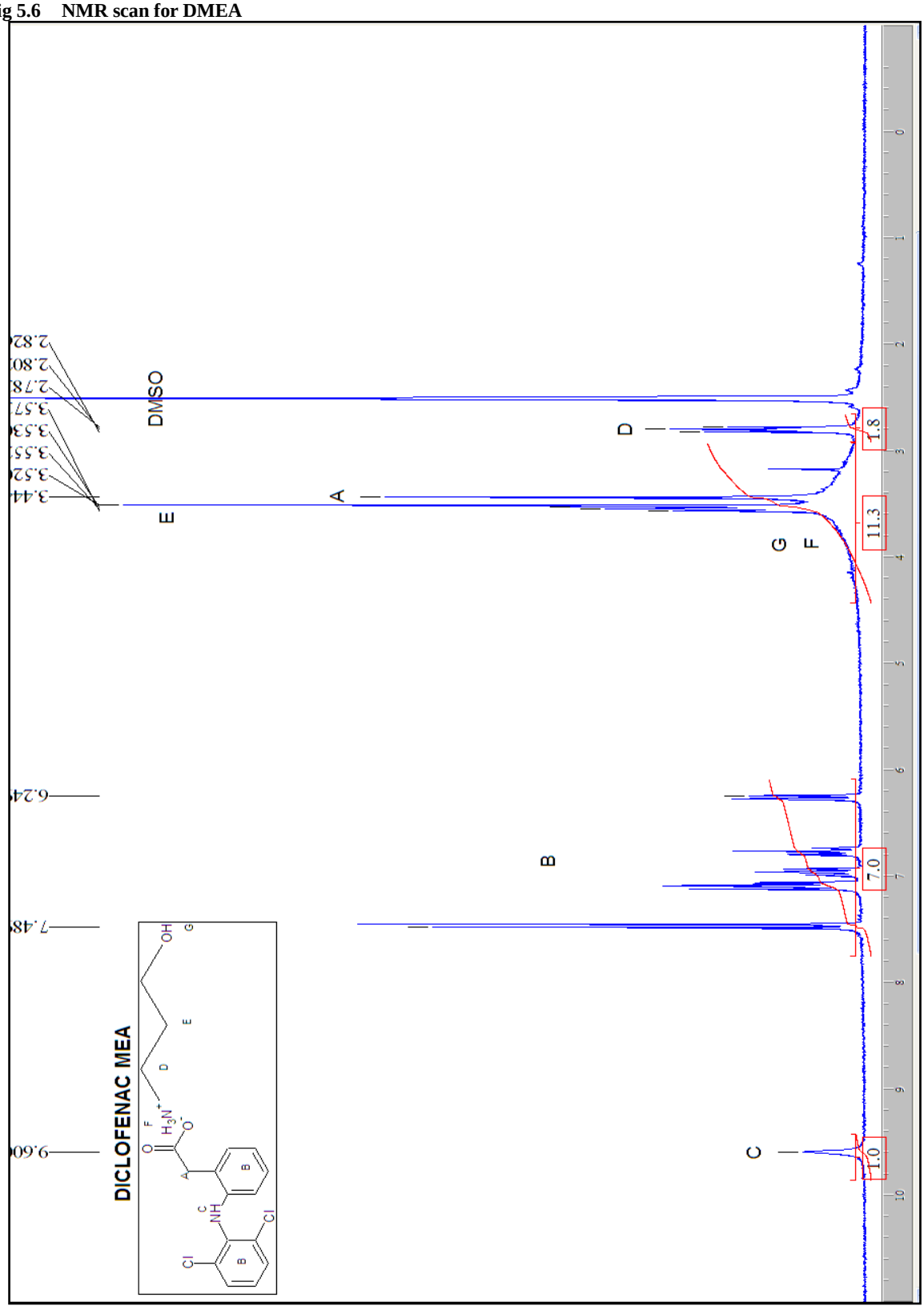

5.2.3 Results and discussion

Melting points are summarised in Table 5.2. An example of a DSC scan of diclofenac is shown in Fig 5.7. The rest are attached in Annex C. The absence of endothermal peaks at around 100°C was interpreted as the absence of hydrate-polymorphs. This was also confirmed by the lack of weight loss observed in TGA around 100 degrees and the gradual weight loss for all salts. Desolvation of bound solvent would have been observed as a multistage process, at a series of discrete temperatures.

Diclofenac thermogram (see Fig 5.7) is complicated. A melting point around 160°C has reported for diclofenac in the literature (Lund 1994; Merck 2010). DSC measurements in a controlled inert atmosphere showed that the fusion endotherm occurs approximately at 180°C. Both thermal data and HPLC mass spectrometry experiments demonstrated that, on heating, diclofenac undergoes a decomposition process when a potentially oxidative atmosphere is present and, therefore, the low value of fusion temperature reported (160°C) is due to the formation of decomposition products at high temperatures (Giordano et al. 2003).

Table 5.2Melting points for diclofenac and salt series (n=3, SD)

Drug	Melting point (°C)
Diclofenac	155.36 ± 0.10
DAdam	242.05 ± 2.04
DBenz	108.11 ± 2.36
DCHex	190.82 ± 1.59
DTBut	165.52 ± 2.12
DAMP1	143.72 ± 0.56
DAMP2	178.87 ± 1.59
DTris	207.24 ± 0.34
DMEA	140.30 ± 0.20
DDEA	131.24 ± 0.28
DTEA	135.47 ± 1.98

Thermograms of most salts are also complicated preventing reliable determination of the melting points. Two endotherms are often found: one associated with the melting and the second one with decomposition (see thermogram of DCHex in Fig 5.8) and often accompanied by weight loss.

Fig 5.7 DSC thermogram for diclofenac

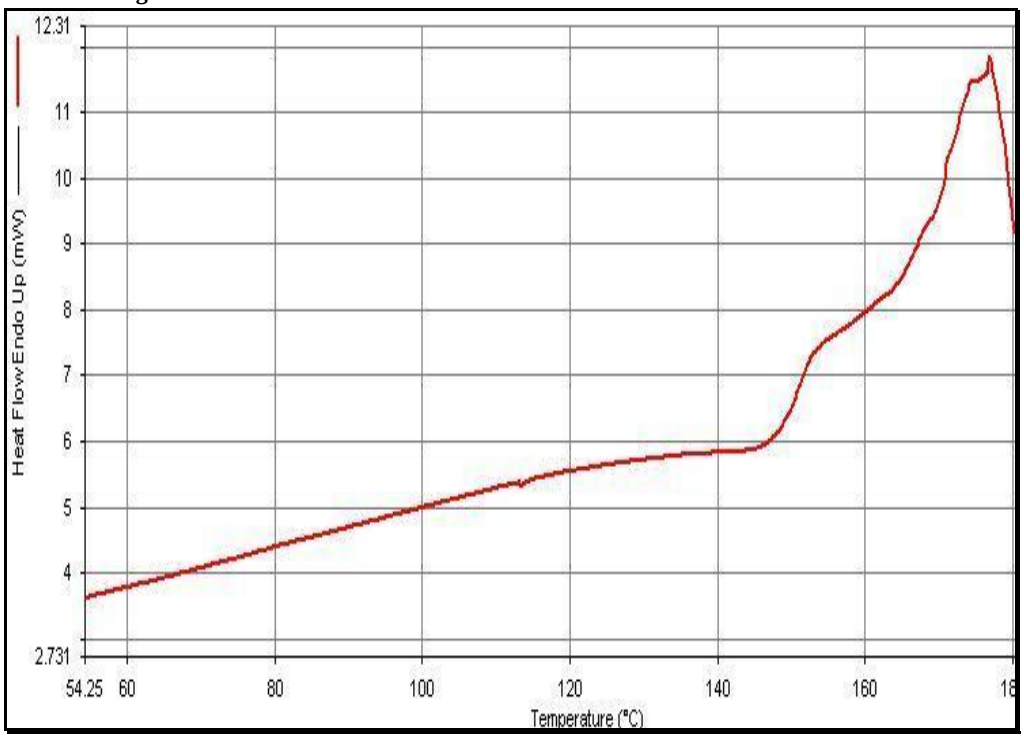

Fig 5.8 Thermogram of DCHex

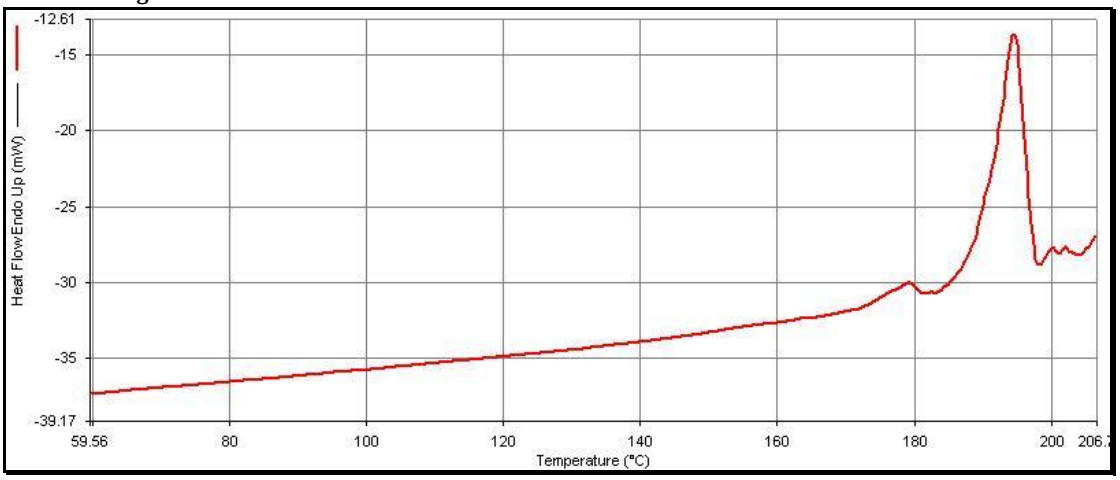

Fini et al. (2010) confirmed that the simplest thermogram of a diclofenac salt with aliphatic amines always shows two endotherms.

Fig 5.9 Melting point of DDEA

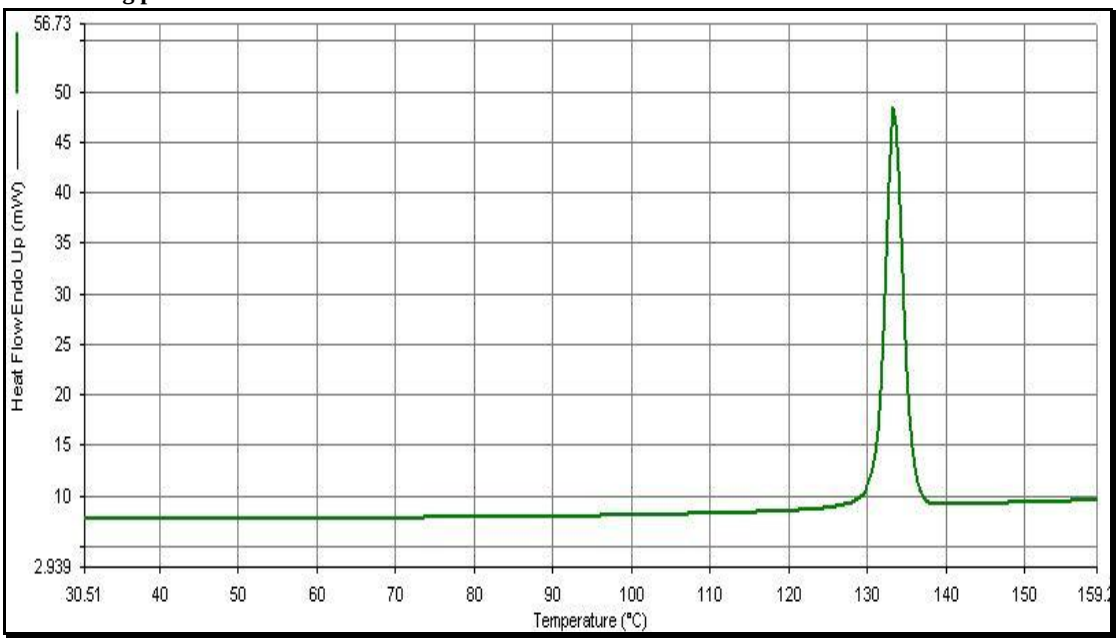

An increase in hydroxyl group number allows the formation of a close network of hydrogen bonds between anion and cation in the salts. DDEA, which has two hydroxyl groups and was obtained from acetone, showed a melting point of 131 °C (see Fig 5.9).

Fini et al. (2007) found two forms of DDEA salt which were very similar, having melting points very close together; crystallised from acetone (139 °C) or from water (122 °C)

In the case of DAMP2 (see Fig 5.10), which also contains two hydroxyl groups. The thermogram is less clear with melting point of the salt (180 ºC) accompanied by decomposition.

Fig 5.10 Fusion of endotherms in DAMP2 followed by decomposition

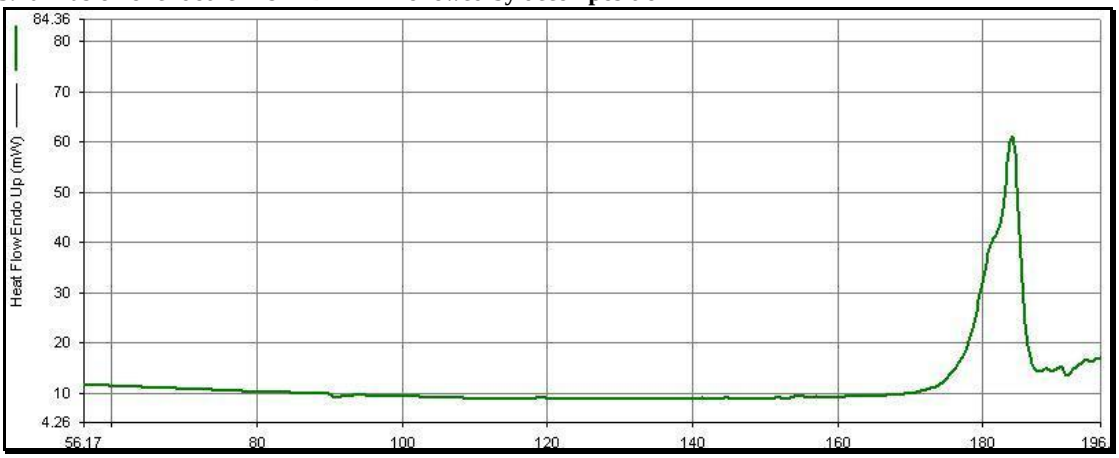

Fig 5.11 DSC thermogram for DTris

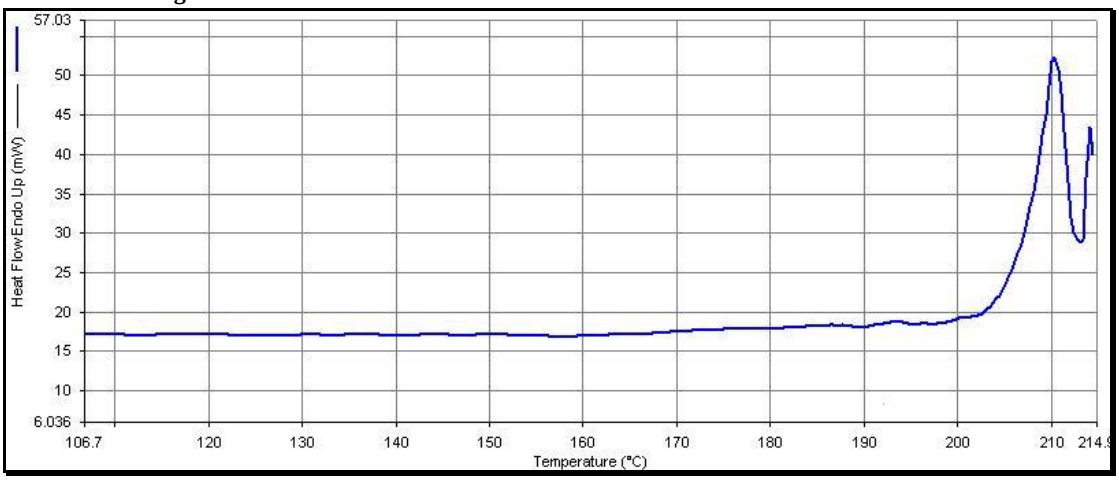

In the case of salts with three hydroxyl groups, only one form was isolated for Tris and TEA salts, with melting points of 207 °C and 135 °C (see Figs 5.11 and 5.12). In the case of DTEA, melting of the salt was followed by recrystallisation and melting of the new form, which was not be isolated, at 143 °C. The diclofenac salts formed with TEA or Tris bases did not offer evidence by thermal analysis of hydrates or polymorphs Fini et al. (2007). According to Fini et al. (2007) the presence of three hydroxyl groups further eliminates every complexity. It is the presence of water which accounts for the formation of the metastable form in many diclofenac salts. It is therefore probably important to pay attention to the drying or dehydration conditions in order not to dissociate the salt form.

Fig 5.12 DSC thermogram for DTEA

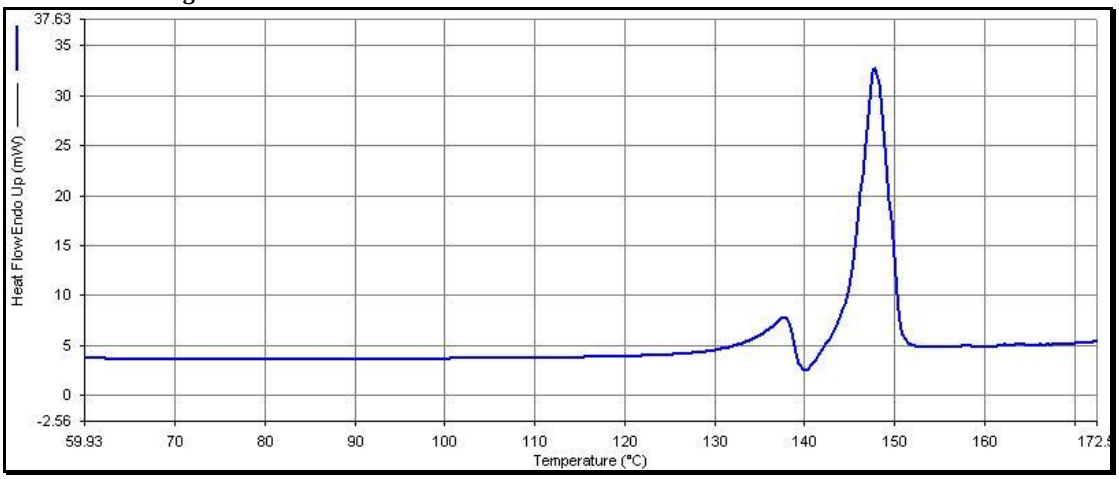

TGA analysis did not provide evidence of hydrates/solvates for any of the salts. It was probably related to the fact that none of the salts were recrystallised from water and that after drying in a

vacuum oven they were kept in sealed containers. Fini,et al. (2010) in a thermal and thermogravimetry study showed that in diclofenac salts, hydration occurs to different extents, as a function of the counterion and solvent and also that polymorphs are formed.

Both tri-hydroxy counterions are very different: the Tris base being a primary and the TEA a tertiary amine, but with almost similar pK_as (7.76 and 8.06, respectively). The difference in melting points (207 ºC and 135 ºC, respectively) clearly demonstrates how these H-bonded structures operate differently with the diclofenac Tris salt resulting in a more compact crystal lattice.

DAMP1 crystals were obtained from methanol and a melting point of 143.72 ºC was documented. O'Connor et al.(2001) found two forms of DAMP1, obtained from 35 and 7.5% of drug in acetone and melting points of 188 ºC and 161 ºC respectively. At his stage is not clear whether the former corresponds to one of the two forms described by O'Connor et al. (2001) or if it constitutes a third polymorph.

Fig 5.13 Correlation between counterion and diclofenac salt melting points

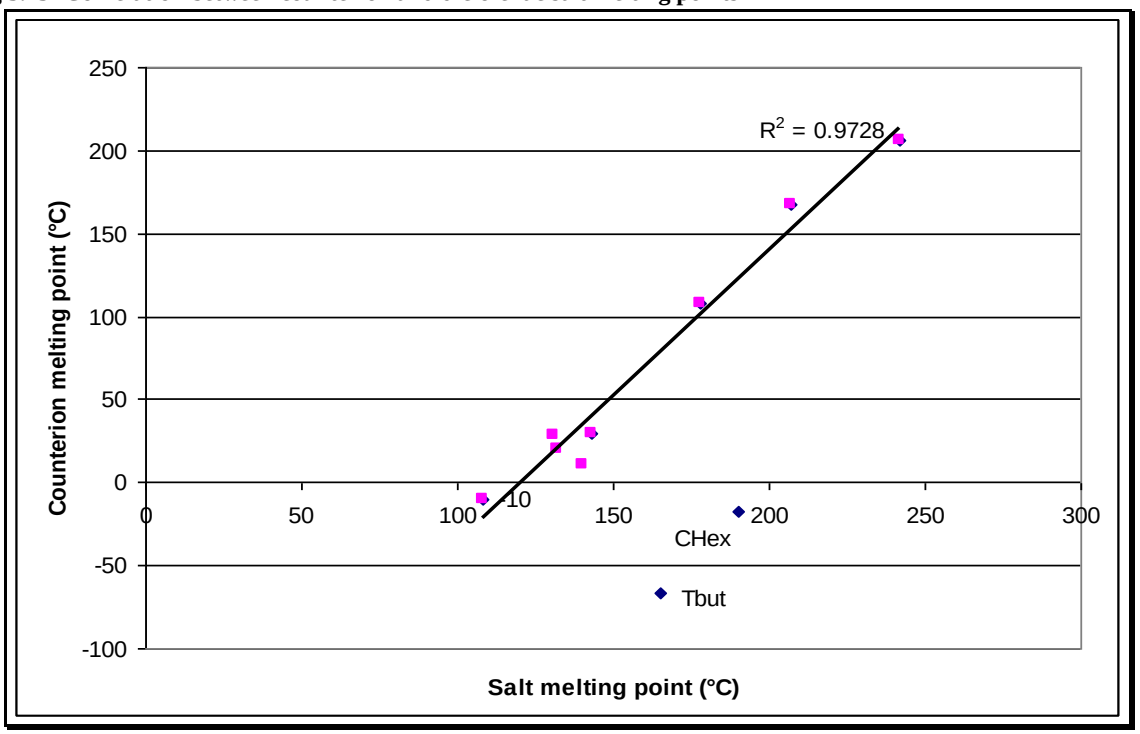

There was poor correlation between counterions and gemfibrozil melting points (R^2=0.3218, n=8) and even poorer with flurbiprofen melting points (R^2=0.0363, n=8). The correlation for the diclofenac salts is also quite poor (R^2=0.5066, n=10). If CHex and TBut salts are excluded, which happen to be

the counterions of lowest melting point, the correlation improves considerably (R^2=0.9728, n=8). Unfortunately, crystal structure for DCHex and DTBut could not be obtained and it is not possible to relate this fact to differences in crystal lattice. O'Connor et al. (2001b) characterized a range of diclofenac salts and examination of the data revealed reasonable correlation (R^2=0.7518, n=7) between the base and salt melting points.

A trend in melting points is observed for salts of the same counterions, particularly for counterions without hydroxyl groups.

Fig 5.14 Melting points of flurbiprofen, gemfibrozil and diclofenac salts

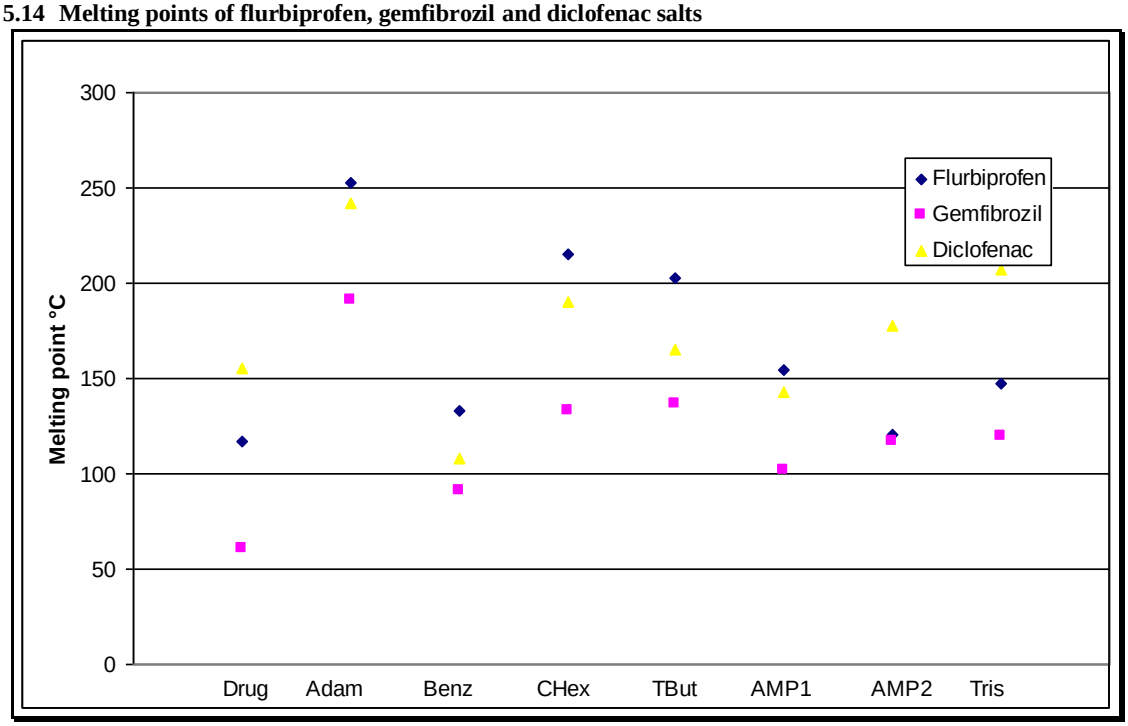

5.3 Solubility studies

5.3.1 Saturated solubility

Saturated solubility in water was measured for all the diclofenac series.

5.3.1.1 Materials

All materials were prepared as described in section 5.1.

5.3.1.2 Method

Saturated solubility was determined following the method described in section 2.3.2.2.2.

5.3.1.3 Results and discussion

Solubility of diclofenac was below the detection limit (0.021 mg/ml) of the calibration curve. Aqueous solubility of 0.071 mg/ml has been reported for diclofenac in the literature (Ledwidge and Corrigan 1998).

As expected, saturated solubility was improved in all cases by salt formation (Table 5.3). Counterions increased the diclofenac aqueous solubility up to over 200-fold with the highest increase corresponding to DTEA. All salts provided lower solubilities compared to the 19.54 mg/ml (65.84 mM) of diclofenac sodium, the typical commercially available salt for oral administration (Ledwidge and Corrigan 1998). This shows that the inherent hydrophobicity of the parent molecule is partly maintained even when the drug is in salt form with amines. Solubilities of diclofenac salts are in general lower than flurbiprofen or gemfibrozil salts. The presence of a secondary amine group and the chlorine atoms in one of the aromatic rings represent the source of intramolecular H-bonds (see crystal structure in section 5.4). All the H-bonds involve the hydrophilic groups and therefore make the diclofenac molecule less available for intermolecular interaction with the environment, such as water molecules (Fini et al. 2010).

Table 5.3 Saturated solubility and pH of final solution of diclofenac salts at 21 °C (n=3, SD)

	Solubility (mg/ml)	Solubility (mM)	pH
Diclofenac	< 0.021	-	5.68 ± 0.01
DAdam	0.038 ± 0.001	0.12	6.43 ± 0.01
DBenz	1.15 ± 0.35	3.88	7.30 ± 0.01
DCHex	1.32 ± 0.15	4.45	7.35 ± 0.01
DTBut	1.82 ± 0.20	6.14	7.32 ± 0.03
DAMP1	6.38 ± 0.65	21.54	7.71 ± 0.01
DAMP2	4.64 ± 1.81	15.66	6.98 ± 0.02
DTris	3.18 ± 0.60	10.73	6.87 ± 0.01
DMEA	6.34 ±0.05	21.40	7.36 ± 0.01
DDEA	5.91 ± 0.02	19.95	7.47 ± 0.01
DTEA	15.74 ± 0.19	53.14	7.66 ± 0.01

There is considerable variability in the solubilities quoted for diclofenac salts in the literature.

Table 5.4Solubility values obtained compared to literature (all solubilites in mM)

		Fini, Cavallari et al. (2010)	Fini, Fazio et al. (2007)
DMEA	21.4	26.5	12
DDEA	19.9	45.7	16
DTEA	53.1	7.6	17
DTris	10.7	3.5	4

These differences are probably related to formation of hydrates or other solvates with different solubility values.

DTEA does not form a salt of the carboxylate-ammonium type. Despite the ionic nature of the triethanolamine salt, apparently no direct electrostatic interaction between the positively charged cation and the negatively charged diclofenac anion is observed. This fact can be attributed to the shielding of the positive centre by the hydroxyethyl arms of the cation from any intermolecular interaction in a *gauche* conformation. The hydrogen bonded ion-pair occurs between the three hydroxyl groups of the TEA molecule and carboxylate oxygens. The proton transfer does not occur to the same extent and is probably responsible for the higher solubility of this salt. In view of the much higher DTEA solubility value obtained in this study (53.1 mM) compared to values obtained by other authors (17mM and 7.6 mM), it is possible that the latter correspond to a different polymorph with the usual $(R\text{-}NH_3^+)\bullet(R'\text{-}CO_2^-)$ salt formation, rather than the carboxylate hydroxyl groups interaction observed here (see section 5.4.3.8).

When comparing the solubilities the all three flurbiprofen, gemfibrozil and diclofenac series, similar trends are observed for the same counterions, with the exception of the AMP2 salts (see Fig 5.15). For both flurbiprofen and gemfibrozil, the AMP2 salt is the one with the highest solubility in the TBut-AMP1-AMP2-Tris series; for diclofenac, DAMP1 has the highest solubility. O'Connor et al. (2001b) determined that the equilibrium saturated solubility of DAMP2 was limited to that of the monohydrate form of the salt. Rubino (1989) had already reported instantaneous hydration of the solid on the surface of discs upon hydration. In the majority of cases, anhydrate forms exhibit higher solubilities than the equivalent hydrates with solubility ratios of between 1-2 and exceptionally higher (Pudipeddi and Serajuddin 2005).

Fig 5.15 Solubilities of flurbiprofen, gemfibrozil and diclofenac salts (mM) with the same counterions

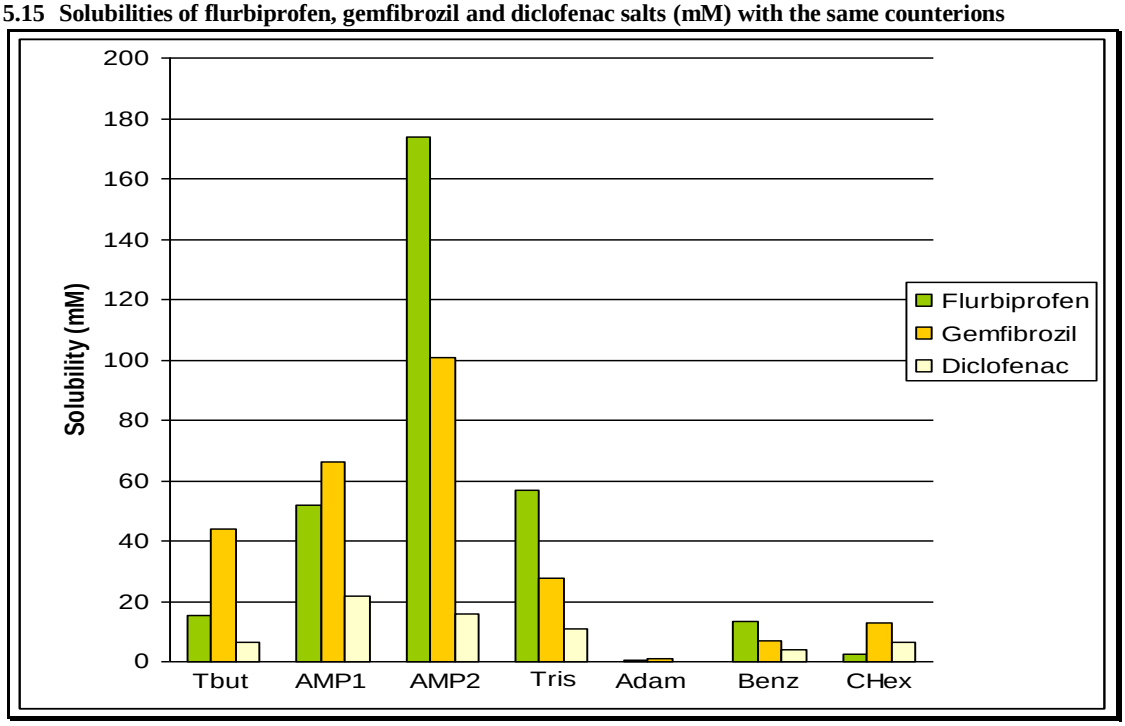

Saturated solubilities and resulting pHs correspond very well with theoretical pH-solubility profile for diclofenac. The higher the pH of the obtained saturated solution the higher the solubility (see Fig 5.16). An intrinsic solubility value of 0.011 mg/ml and a pK_a of 5.02 (Ledwidge and Corrigan 1998) was used to calculate the theoretical pH solubility profile according to the equation:

$$pK_a = pH - \log \frac{S - S_0}{S_0}$$

In conclusion, in line with the flurbiprofen and gemfibrozil series salt formation increases drug solubility, although in the case of diclofenac some hydrophobicity of the parent drug is maintained. None of the counterions result in salts more soluble than the sodium salt, commercially available for oral administration. The increased hydrogen bonding has been postulated as an explanation for the low solubility of diclofenac and its salts. The hydrogen bonding makes the diclofenac molecule less available to intermolecular interaction with the environment, such as the water molecules of the solvent (Fini et al. 2010).

Fig 5.16 Saturated solubility (mM) versus pH of diclofenac and its salts. Theoretical pH solubility profile for diclofenac shown in pink

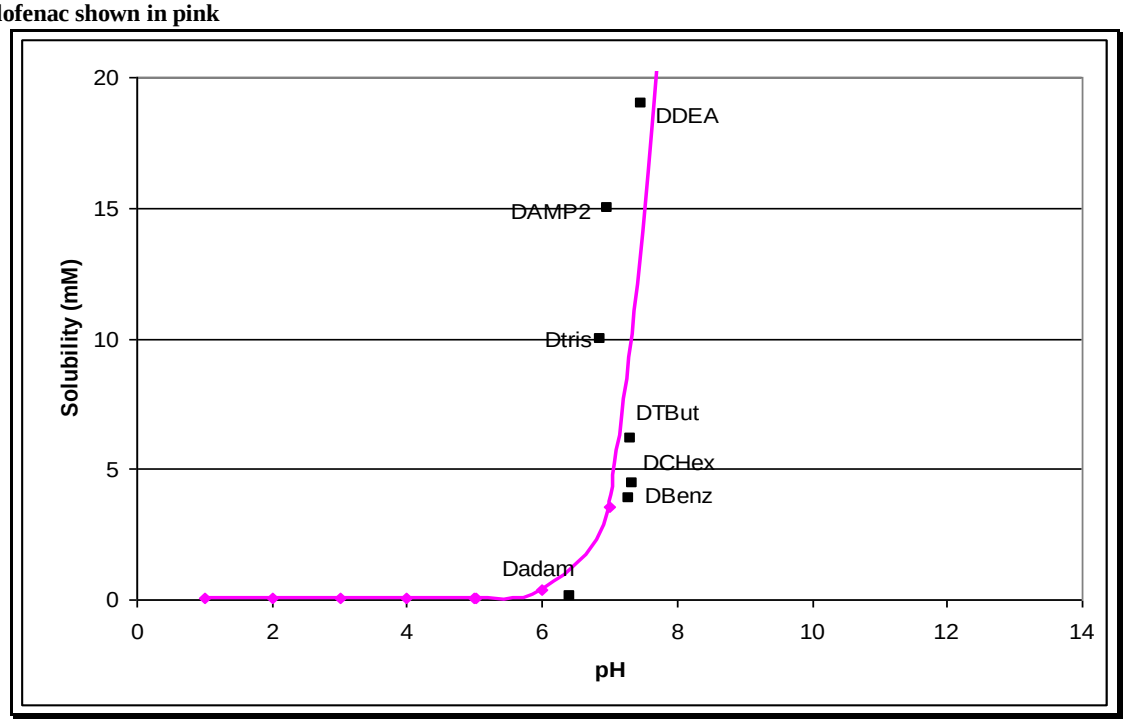

As observed with the flurbiprofen and gemfibrozil series, increasing the hydrophilicity of the counterions does not mean increasing solubility of the corresponding salts. However, in the TBut-AMP1-AMP2-Tris series, the highest solubility does not correspond to the AMP2 salt, as seen with flurbiprofen and gemfibrozil, as instant hydration occurs in contact with water and the saturated solubility is limited to that of the monohydrate form.

5.4 Crystal structure

5.4.1 Material

All salts were prepared as described in section 2.1.1.

5.4.2 Methods

5.4.2.1 Crystal growth

Most crystals were obtained by slow evaporation from methanol.

Single crystals of the following structures were already available in the Cambridge Structural Database (CSD): diclofenac, *SIKLIH02*, DDEA *ZIKPOY*, DTEA *TEKVAG* and DTris *TUDPIR*

(Castellari and Ottani 1995; Castellari and Ottani 1996; Castellari and Ottani 1997b; Castellari and Ottani 1997a).

5.4.2.2 Crystal structure determination

Crystal data were collected at the EPSRC National Crystallography Service. Structures were solved by direct methods and refined by full-matrix least squares. Mercury was the crystal structure visualizing program used to measure intermolecular contacts.

5.4.3 Results and discussion

Compared to flurbiprofen and gemfibrozil, diclofenac has an extra –NH group with potential for creating further hydrogen bonds. This should therefore influence the crystal lattice.

Table 5.5 Crystal parameters and particle size for diclofenac acid and its salts

D	***DAdam***	***DAMP1***	***DAMP2***
Monoclinic,	**Orthorrombic,**	**Orthorrombic,**	**Monoclinic,**
$P2_1/c$	**$Pna2_1$**	**$P2_12_12_1$**	**$P2_1/c$**
Z = 4	**Z = 4**	**Z = 4**	**Z = 4**
a = 8.384 Å	**a = 17.5428 Å**	**a = 6.394 Å**	**a = 19.514 Å**
b = 10.898 Å	**b = 19.2773 Å**	**b = 15.034 Å**	**b = 9.523 Å**
c = 14.822 Å	**c = 6.5278 Å**	**c = 19.777 Å**	**c = 9.875 Å**
α = 90	**α = 90**	**α = 90**	**α = 90**
β = 92.760	**β = 90**	**β = 90**	**β = 91.286**
γ = 90	**γ = 90**	**γ = 90**	**γ = 90**
R_{int} = 3.74	**R_{int} = 4.33**	**R_{int} = 5.85**	**R_{int} = 3.39**
PS = 44.77 µm	**PS =39.48 µm**	**PS = 65.46 µm**	**PS = 38.06 µm**

DTris	*DMEA*	*DDEA*	*DTEA*
Monoclinic,	**Monoclinic,**	**Monoclinic,**	**Monoclinic,**
$P2_1/a$	**$P2_1/c$**	**$P2_1/a$**	**$P2_1/a$**
Z = 4	**Z = 16**	**Z = 4**	**Z = 4**
a = 0.152 Å	**a = 9.6675 Å**	**a = 11.772 Å**	**a = 10.589 Å**
b = 9.407 Å	**b = 19.0889 Å**	**b = 9.346 Å**	**b = 9.396 Å**
c = 19.448 Å	**c = 35.6278 Å**	**c = 17.186 Å**	**c = 21.132 Å**
α = 90	**α = 90**	**α = 90**	**α = 90**
β = 90.12	**β = 91.38**	**β = 91.70**	**β = 93.24**
γ = 90	**γ = 90**	**γ = 90**	**γ = 90**
R_{int} = 4.14	**R_{int} = 6.68**	**R_{int} = 2.20**	**R_{int} = 10.50**
PS = 49.31 µm	**PS = 51.78 µm**	**PS = 64.93 µm**	**PS = 67.58 µm**

5.4.3.1 Diclofenac

Monocarboxylic acids, like diclofenac, which are non-chiral, almost invariably form hydrogen bonded pairs (Leiserowitz 1976). Three diclofenac forms have been reported, two monoclinic ($C2/_c$ and P21/c) (Castellari and Ottani 1997b) and one orthorhombic (Pcan) (Jaiboon et al. 2001). The latter does not form dimers and no intermolecular hydrogen bonds are observed. The diclofenac form used in this work corresponds to the monoclinic $C2/_c$ form (*SIKLIH02* in the CCDC) as it was prepared as described by their authors (Castellari and Ottani 1997b). The dimers are packed in such a way that neither any strong interactions, nor van der Waals forces, arise between them. The -NH group originates a bifurcate intramolecular hydrogen bond with the adjacent carboxylate O^-.

Fig 5.17a Crystal structure of diclofenac ($P2_1/c$)

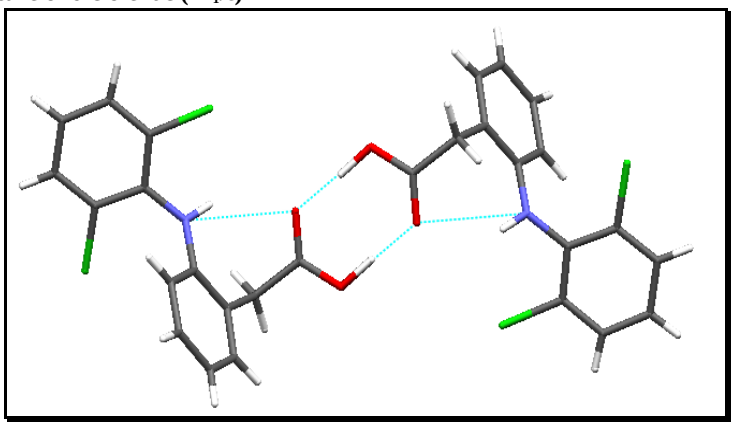

Fig 5.17bCrystal structure of diclofenac ($P2_1/c$)

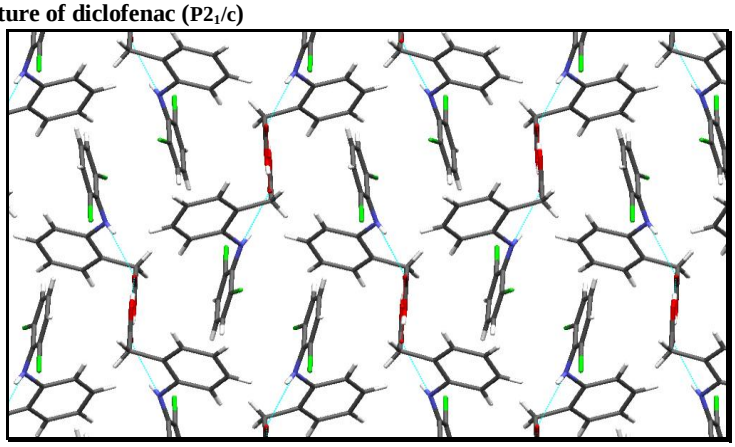

5.4.3.2 Diclofenac adamantamine (DAdam)

$R_4^3(10)$ columns are observed, held together with neighbouring columns by van der Waals forces. What is different from the flurbiprofen and gemfibrozil salts are the two additional hydrogen bonds; one donated by the diclofenac amine group to the carboxylate oxygen, a common feature with many diclofenac salts presented in this thesis, and another one donated by the carboxylate oxygen to the chlorine.

Fig 5.18aCrystal structure of diclofenac adamantamine ($Pna2_1$)

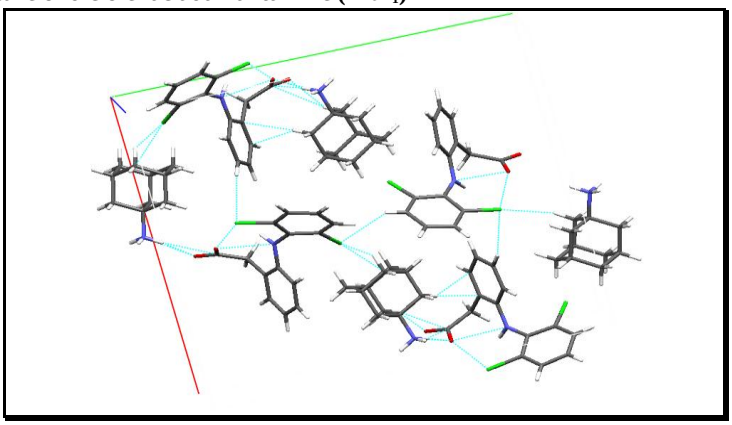

Fig 5.18bCrystal structure of diclofenac adamantamine ($Pna2_1$)

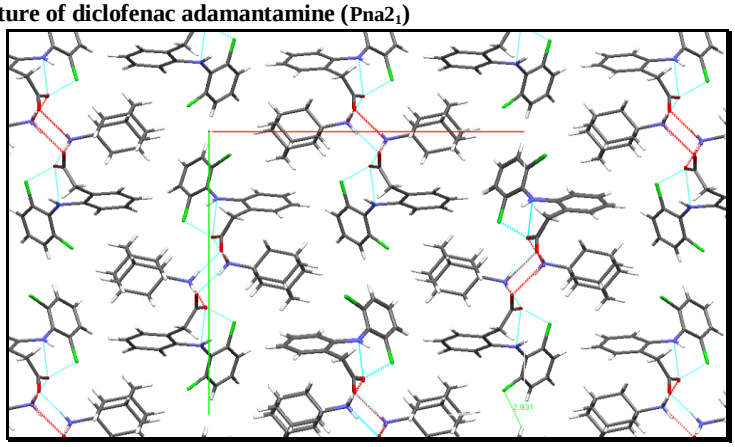

5.4.3.3 Diclofenac AMP1

In DAMP1, an interesting variation of the $R_4^3(10)$ columns can be observed. Instead of creating a hydrogen bond with a nearby column to give the two-dimensional type V structure, the hydroxyl group donates a hydrogen bond to the carboxylate in the same column. This means that this carboxylate oxygen is accepting three hydrogen bonds as there is an additional one provided intramolecularly by the diclofenac amine group. The columns are not cross-linked by van der Waals forces (Fig 5.18).

The additional hydrogen bonds make the $R_4^3(10)$ ladders adopt a less flat conformation than other $R_4^3(10)$ columns described in this work. In a study of hydrogen bonds of N-H···O=C bonds, in the Cambridge Structural Database in 1982, it appeared that when one carboxylate oxygen accepts three hydrogen bonds, steric repulsions tend to force one of the hydrogen bonds out of the O-C-O plane. However, the result may be due to statistical chance because only in 34 bonds out of 1509 N-H···O=C hydrogen bonds one carboxylate oxygen accepts three hydrogen bond (Taylor et al. 1983). In DAMP1, the angles formed by the hydrogen bonds donors and the O-C-O plane are nearly flat for the ammonium nitrogen and the intramolecular diclofenac –NH (6.63 and 7.17°, respectively) whereas steric repulsions force the hydroxyl group away from this plane (39.53°).

Fig 5.19a Crystal structure of diclofenac AMP1 ($P2_12_12_1$)

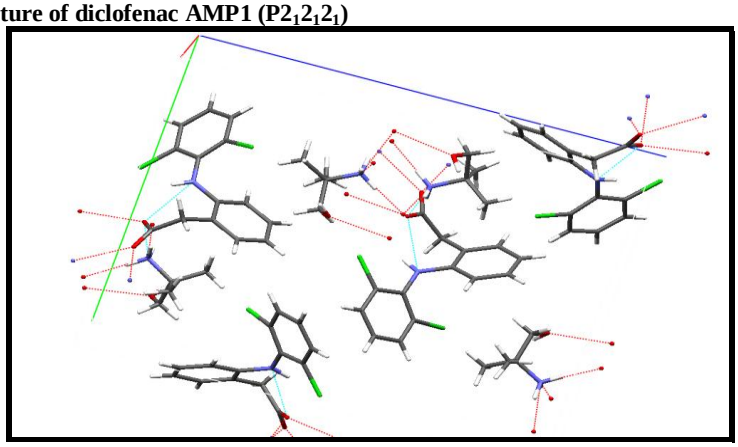

Fig 5.19b Crystal structure of diclofenac AMP1 ($P2_12_12_1$)

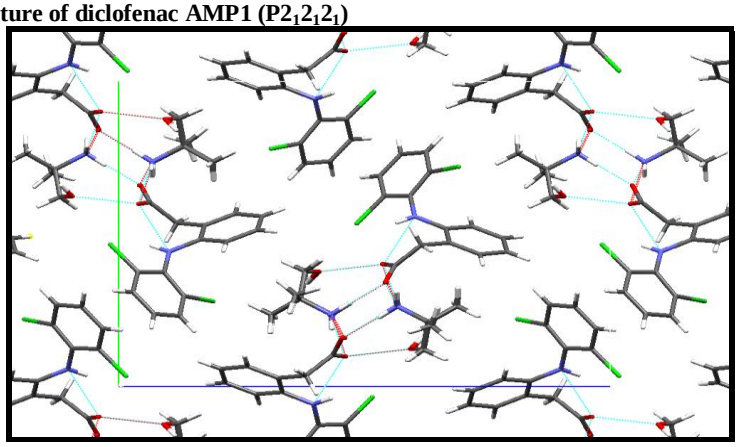

5.4.3.4 Diclofenac AMP2

DAMP2 consists of an inner portion containing a double layer of cations arranged in such way that two cations of AMP2 form a dimer around a symmetry centre of the crystal. The hydroxyl group of one AMP2 molecule and the ammonium group of the other AMP2 molecule donate a hydrogen bond to each carboxylate oxygen on each side. The additional hydroxy group (from the AMP2) donates another hydrogen bond to the neighbouring carboxylate and accepts a hydrogen bond from another neighbouring ammonium. The system adopts a two-dimensional network. There are van der Waals forces that hold adjacent layers together.

Fig 5.20a Crystal structure of diclofenac AMP2 ($P2_1/c$)

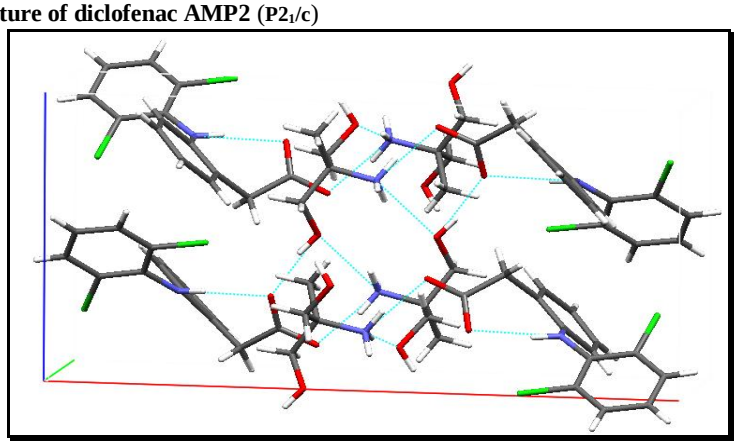

Fig 5.20b Crystal structure of diclofenac AMP2 ($P2_1/c$)

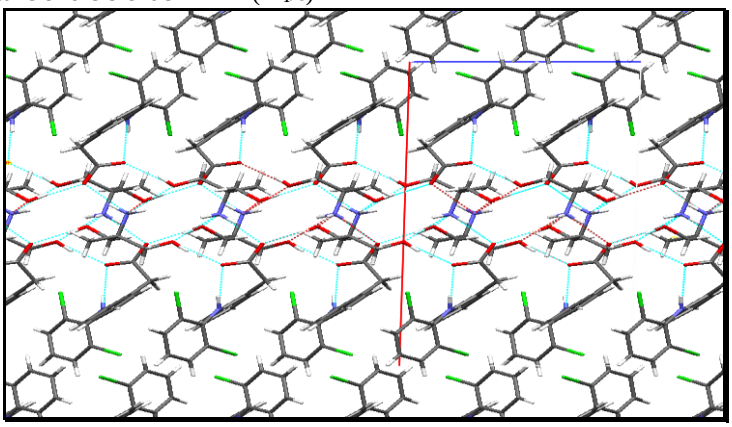

5.4.3.5 Diclofenac tris (DTris)

DTris has many similarities with DAMP2. Dimers are observed comprising tris molecules with one hydroxyl and one ammonium group donating hydrogen bonds to lateral carboxylates on each side.

Fig 5.21a Crystal structure of diclofenac Tris ($P2_1/a$)

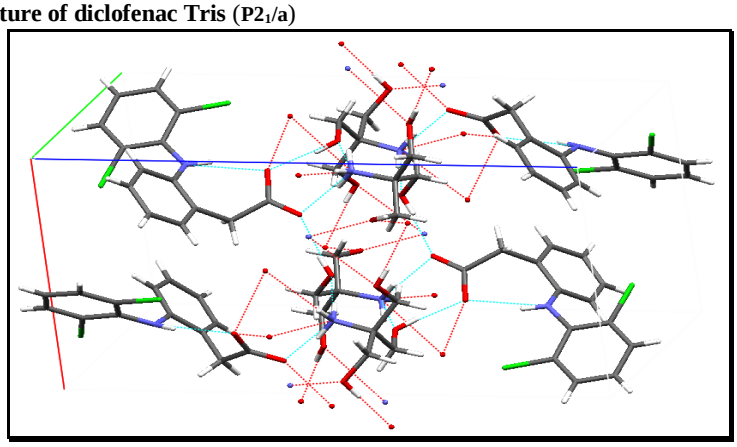

The second hydroxyl group donates another hydrogen bond to a neighbouring carboxylate and receives another one from a neighbouring ammonium group. The third hydroxyl group takes part in two additional hydrogen bonds of the type O–···O–H and H3N+···O–H providing extra stability to the whole structure. The resulting network resembles that of DAMP2 with extra hydrogen bonding; parallel layers are cross-linked by van der Waals forces.

Fig 5.21b Crystal structure of diclofenac Tris ($P2_1/a$)

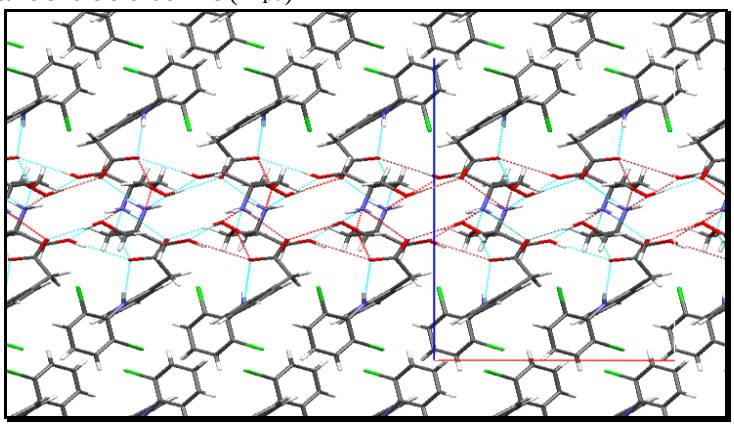

5.4.3.6 Diclofenac monoethanolamine (DMEA)

In DMEA, the unit cell is a large one, sufficient to contain 16 cation-anion pairs. The asymmetric unit contains 4 molecules that actually comprise 4 different conformers. The monoethanolamine molecules adopt a claw-shape, with each of the conformers displaying different torsion angles between N1-C12-C2-O1: 74.51°, 66.67°, 70.08° and 66.81°. Similarly, the twist angles between the phenyl groups of each diclofenac conformer are different: 55.10°, 35.12°, 56.19° and 56.08°. In every case, hydrogen bonded dimers are situated between the carboxylate oxygens and the ammonium and hydroxyl groups of a monoethanolamine molecule. Also, in two conformers, the

carboxylate oxygens receive additional hydrogen bonds from adjacent ammonium and hydroxyl groups and in the two other conformers, one oxygen receives an internal hydrogen bond from the amine group and the other one receives a hydrogen bond from a nearby ammonium group. In the latter dimers, the ammonium group of the monoethanolamine molecule only donates one hydrogen bond. The overall structure results in a densely bonded layer with the diclofenac molecules projected towards the interplanar space, which is cross linked by van der Waals forces (see Fig 5.22).

Fig 5.22a Crystal structure of diclofenac monoethanolamine (P21/c)

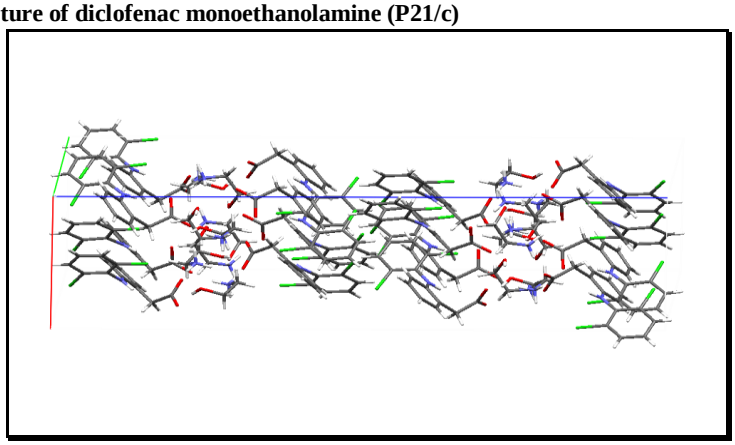

Fig 5.22b Crystal structure of diclofenac monoethanolamine (P21/c)

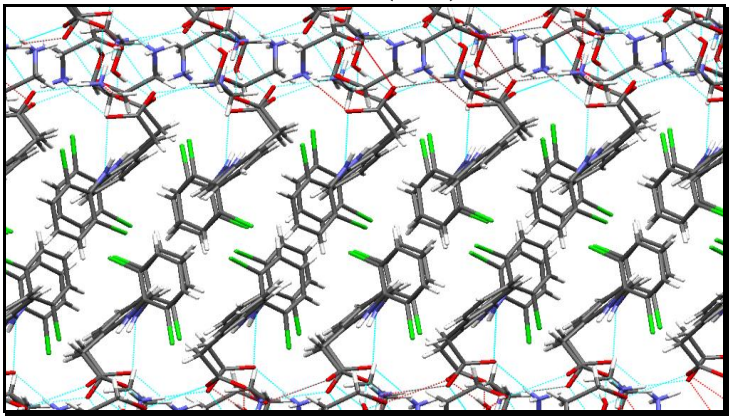

5.4.3.7 Diclofenac diethanolamine (DDEA)

The DEA cation adopts a claw-shaped conformation similar to that observed in FDEA (see section 3.4.3.12). Hydrogen bonds are seen between the hydroxyl groups of two neighbouring cations, by means of a head-to-tail link (see Fig 5.23). Two anions and two cations form 2:2 ion pairs forming $R_4^2(8)$ rings. In contrast to FDEA, in DDEA, the 2:2 ion pairs are stabilized by the presence of 4 hydrogen bonds (2 accepted by the remaining carboxylate O- and two donated by the DEA hydroxyl

groups) to neighbouring 2:2 pairs. The final network is a two-dimensional layer. Adjacent layers are free of van der Waals interactions.

Fig 5.23a Crystal structure of diclofenac DEA ($P2_1/a$)

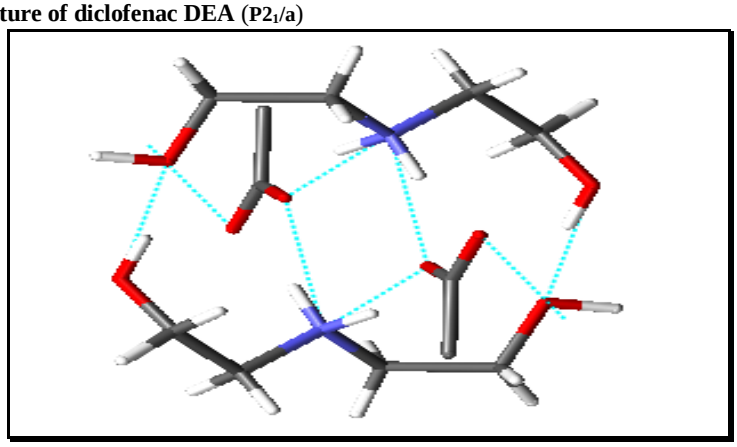

Fig 5.23b Crystal structure of diclofenac DEA ($P2_1/a$)

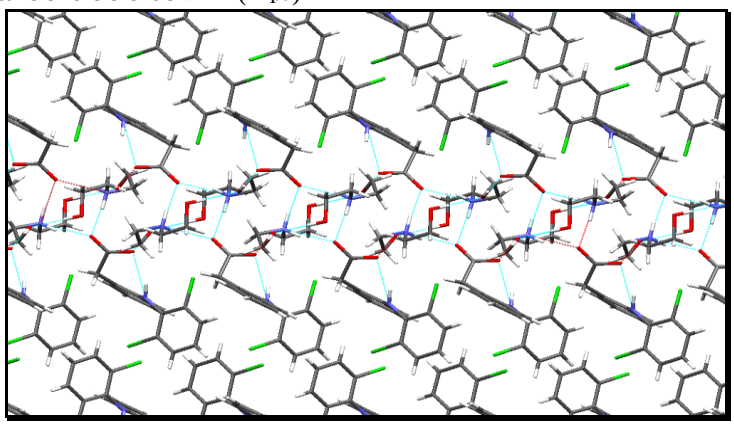

5.4.3.8 Diclofenac triethanolamine (DTEA)

Although DTEA is a salt-like adduct, apparently no electrostatic interaction, $NH^+\cdots O^-$, between the positively charged ammonium ions and the negatively charged acetate groups is observed. This breaks Etter's first rule which states that all good proton donors and acceptors are used in hydrogen bonding (Etter 1990). This is likely due to steric hindrance as the three hydroxyethyl arms with a *gauche* conformation surround the ammonium group, shielding its proton from intermolecular interactions. This type of bonding has been seen before with hydroxyethyl fragments and carboxylic acids (Dhanaraj and Vijayan 1987). The hydroxyl group also interacts via a hydrogen bond with the carboxylate group in GTEA, but in this case the ammonium group is not completely shielded and manages to donate a hydrogen bond to a neighbouring hydroxyl group (see section 4.4.3.9). There are 3 examples of salts between carboxylic acids and triethanolamine observed in the CCSD (*BEVMIY*,

BUZSUK and GAHJOO) they all form carboxylate-hydroxyl interaction type salts and in all of them the ammonium groups are shielded by the hydroxyethyl arms that they do not take part in intermolecular interactions. The hydroxyl group also interacts via a hydrogen bond with the carboxylate group in GTEA, but in this case the ammonium group is not completely shielded and manages to donate a hydrogen bond to a neighbouring hydroxyl group.

Each carboxylate oxygen receives a hydrogen bond from hydroxyl groups of different triethanolamine molecules. Of the remaining hydroxyl groups in each TEA molecule, one donates a hydrogen bond to a third TEA molecule and the remaining hydroxyl group donates a hydrogen bond to a different carboxyl oxygen while receiving one from a fourth TEA molecule. An infinite two-dimensional network is formed. Layers are cross-linked by van der Waals forces.

Fig 5.24a Crystal structure of diclofenac TEA ($P2_1/a$)

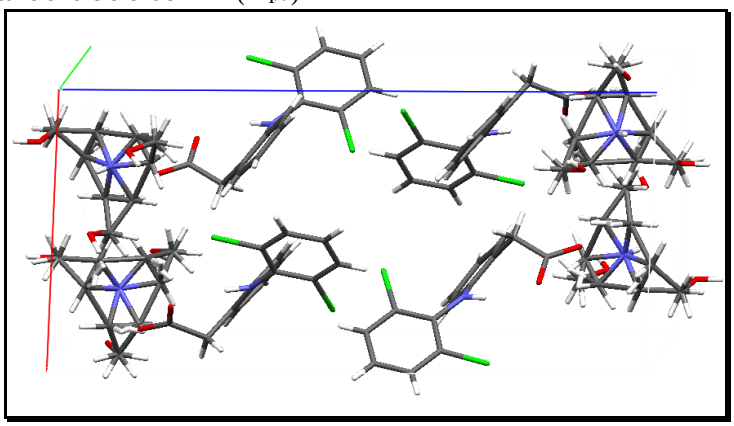

Fig 5.24b Crystal structure of diclofenac TEA ($P2_1/a$)

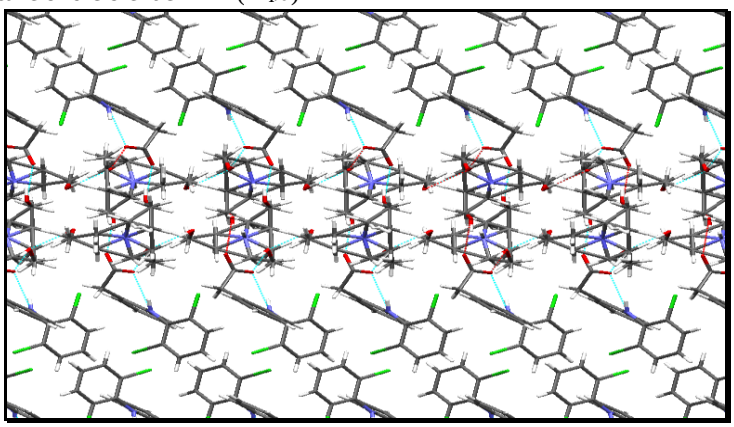

All crystal parameters for diclofenac salts are summarized in Table 5.5.

5.5 Mechanical properties

5.5.1 Compaction replicator

5.5.1.1 Materials

All diclofenac salts were obtained as described in section 2.1.1. A sieved fraction between 96 – 250 μm was selected for use in mechanical testing.

5.5.1.2 Method

A Stylcam 100R compaction replicator (Medelpharm, Bourge-en Bresse, France) with acquisition software (Analis version 2.01.27, Medelpharm) was used as detailed in section 2.5.2.1.

5.5.1.3 Results and discussion

Table 5.6True density values for diclofenac and its salts (n = 5, SD)

	True Density (g/cm^3)
D	1.4735 ± 0.005
DAdam	1.3173 ± 0.002
DAMP1	1.3223 ± 0.001
DAMP2	1.4919 ± 0.002
DTris	1.4812 ± 0.004
DDEA	1.4222 ± 0.007
DMEA	1.4394 ± 0.002
DTEA	1.3675 ± 0.002

Table 5.6 contains the true density values calculated using the helium pycnometer and the salts in this group have higher densities than the equivalent salts of gemfibrozil and flurbiprofen (see sections 3.7 and 4.6). It is possible that the amine group in the diclofenac molecule provides an additional site for hydrogen bonding (even if it is intramolecular) and is associated with better packing.

Except for DTris all salts correspond to pharmaceutical materials that consolidate by a combination of plastic and elastic deformation (see Table 3.36). DTris, with a yield pressure value of 279.23 MPa, is a brittle material that consolidates mainly by fragmentation. Indeed, it was observed that DTris tablets were very prone to laminate and breakage upon ejection and were very brittle to handle. These characteristics are reflected in their low tensile strength (0.1 MPa) and high elastic recovery (14.53%).

Table 5.7 Yield Pressure (MPa) and elastic recovery (%) for diclofenac salts

	Yield Pressure, (MPa)	Elastic Recovery, (%)
Diclofenac	48.46	6.44
DAdam	53.35	5.53
DAMP1	41.95	2.96
DAMP2	99.20	6.75
DTris	279.23	14.53
DMEA	65.71	4.82
DDEA	54.26	4.32
DTEA	80.4	5.64

Tensile strengths are summarized in Table 5.8 and Fig 5.25. None of the diclofenac salts reaches acceptable tensile strength values (nominally 1 MPa). Although the DTEA is not a typical (R-NH_3^+)•(R'-CO_2^-) salt, the tensile strength is among the highest in the group. However, at these low values of tensile strength, comparison is hard, but tendencies can be found if molecules with similar features are explored.

Fig 5.25 Tensile strength for diclofenac salt series (n=6; mean±s.d.)

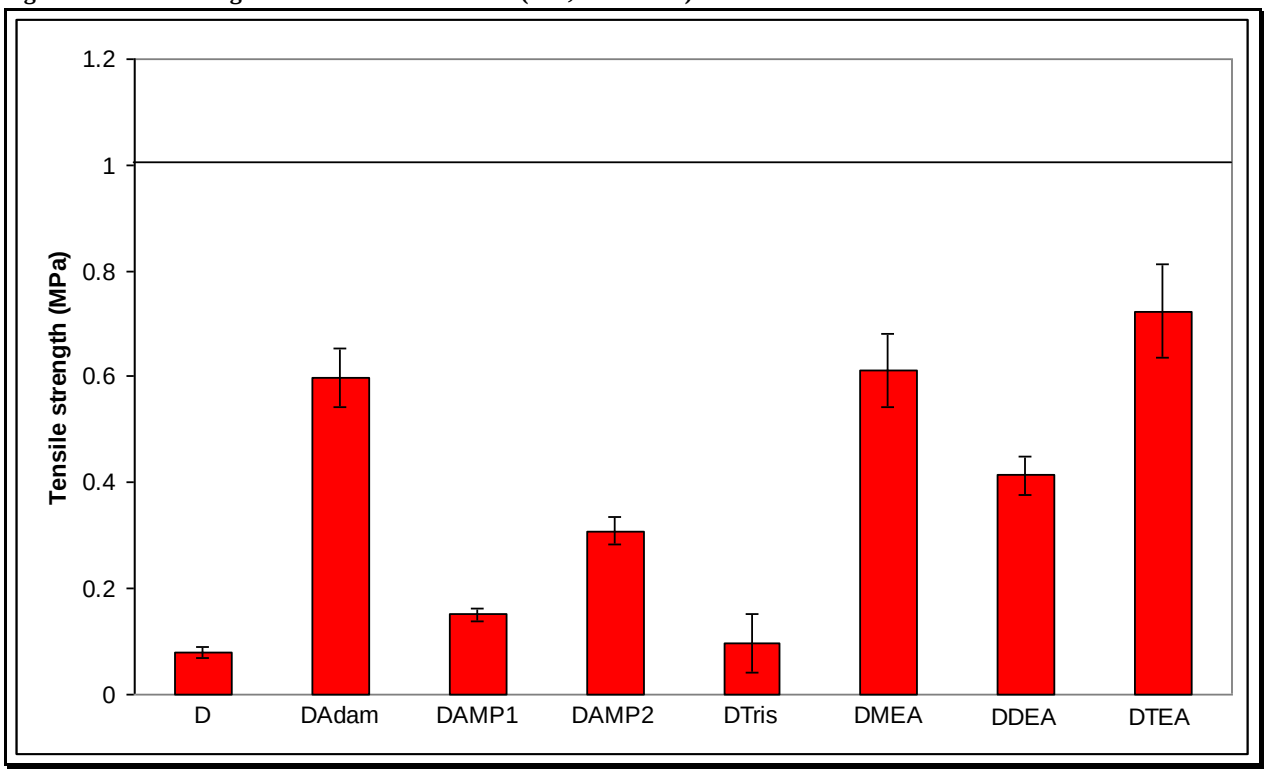

Table 5.8 Tensile strength values for diclofenac salts (MPa) (n=6; mean±s.d.)

	D	DAdam	DAMP1	DAMP2	DTris	DMEA	DDEA	DTEA
TS (MPa)	**0.08**	**0.59**	**0.15**	**0.30**	**0.10**	**0.60**	**0.41**	**0.72**
SD	0.011	0.055	0.011	0.025	0.05	0.06	0.030	0.08

5.5.1.3.1 DAdam

DAdam is one of the salts with highest tensile strength of the compacts in this series (0.59 MPa) characterised by an overall poor mechanical strength. Tensile strength values of DAdam compacts show values similar to other salts in the previous series displaying $R_4^3(10)$ columns cross-linked by van der Waals forces i.e. FBenz, FCBut, GCBut. On the other hand, tensile strength of DAdam compacts is higher than other salts with hydroxyl groups, which was seen as a contributing factor in producing stronger compacts for the other drug series (see section 3.5.2.3.4). One possible explanation could be that, as was also observed in the flurbiprofen and gemfibrozil series, $R_4^3(10)$ configurations are associated with higher tensile strength values, even compared to conformations adopted with salts containing counterions with hydroxyl groups.

5.5.1.3.2 DTEA

DTEA, which exhibits a different salt adduct to the typical (R-NH_3^+)•(R'-CO_2^-) has the highest tensile strength values (0.72 MPa) despite the fact that the layers are also joined by van der Waals forces. It is possible that that salts between hydroxyl and carboxylic acids are associated with improved mechanical properties. Two different explanations can be hypothesized to account for the improved tabletability of DTEA. First, highly hydrogen bonded layers are formed as a result of a higher number of hydroxyl groups. As was hypothesised before, densely bonded layers can help to reduce the attachment energy between layers. Second, the relatively low density of DTEA (1.3675 g/cm^3). DTEA has a lower density than other diclofenac salts with two or three hydroxyl group i.e. DDEA, DAMP2, DTris, which could results in it being more easily deformed due to a more stable conformation free of strain whithin its functional groups.

5.5.1.3.3 DAMP1and DAdam

DAMP1 and DAdam are the two only examples of $R_4^3(10)$ columns in this group. Surprisingly, DAMP1, despite the hydrogen bonding network and that the columns in the zigzagging plane are not joined by van der Waals forces, has very poor mechanical properties. Although there is no immediate obvious explanation, there is the chance that the extra intramolecular hydrogen bond (–COO^- ⋯ HO–) forces the $R_4^3(10)$ into a more twisted conformation (see Fig 5.26) that those observed in DAdam or other $R_4^3(10)$ examples in flurbiprofen and gemfibrozil salts. DAMP1 could constitute another example of strained conformation.

Figure 5.26 Strained $R_4^3(10)$ column due to additional intramolecular H-bonds

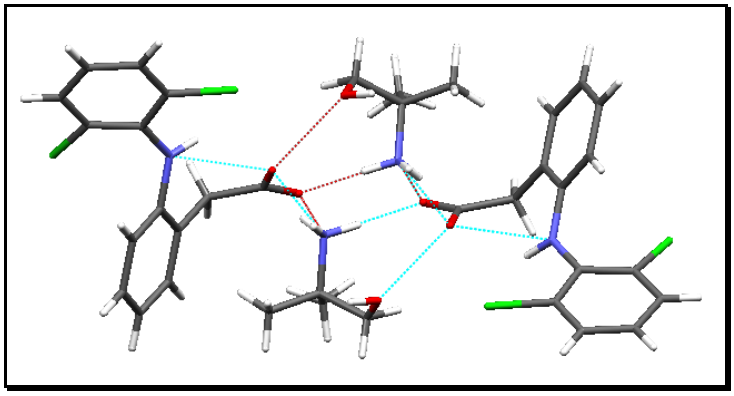

5.5.1.3.4 DTris and DAMP2

These two systems crystallise in the monoclinic P21/c and P21/a space groups and adopt a similar arrangement with cationic dimers and the overall network in arranged in layers with the hydrogen bonding towards the inside and projecting the diclofenac moieties to the interlayer space. In both cases, there are van der Waals attractions between adjacent layers.

The additional $O^{-}\cdots O–H$ and $H_3N^{+}\cdots O–H$ bonding provided by the extra hydroxyl group in DTris would be expected to provide stability to the network and ultimately increase plasticity by decreasing attachment energy between layers. In reality, though still poor, tensile strength of DAMP2 compacts is higher that that of DTris (0.30 vs. 0.10 MPa).

Fig 5.27 DAMP2 network

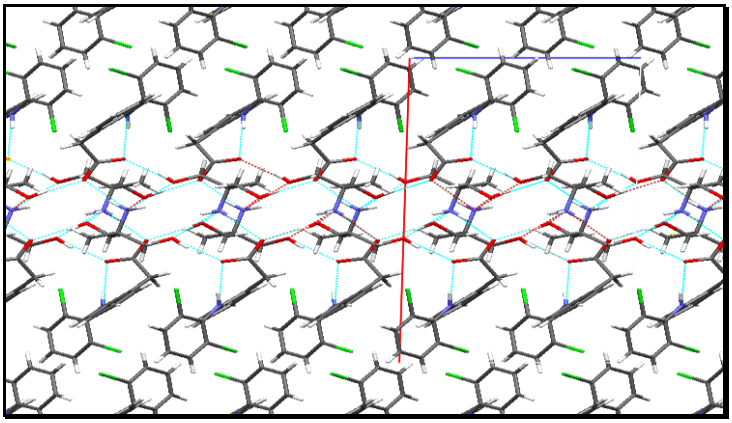

Fig 5.28 DTris network

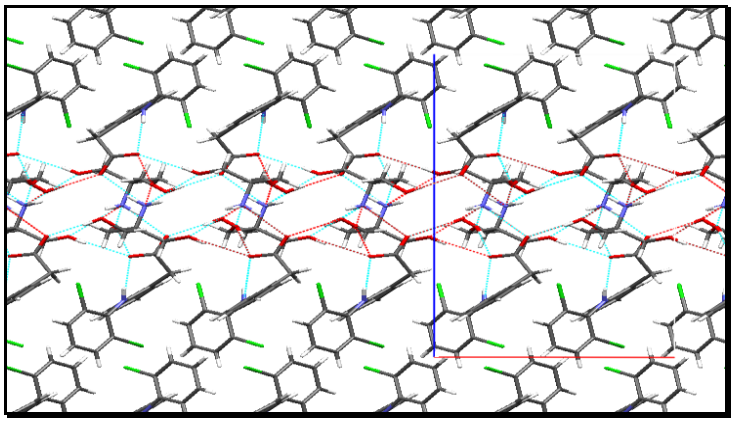

It is not certain whether other parameters such as differences in particle size between DAMP2 and DTris (38 vs. 49 μm) are responsible for these differences or comparisons are not possible in the lower end of the tensile strength values.

5.5.1.4 Conclusions

The conclusions from the diclofenac series are not in line with the ones from the other two series. On one hand, it is probably not possible to relate mechanical properties to crystal structure when the mechanical properties are so poor. On the other hand, these poor mechanical properties are probably related to the known thermal instability of diclofenac and propensity to form polymorphs and hydrates of the diclofenac salts.

As the number of hydroxyl groups in the counterion increases, this allows the formation of a close network of hydrogen bonds between anion and cation in the salts. Two hydroxyl groups, as in the cation of DDEA salt, have been reported to be sufficient to prevent the formation of hydrates (Fini et al. 2010) and the presence of three hydroxyl groups eliminates all complexity: only one form could be found for TEA and TRIS salts (Fini et al. 2007). In this work, neither hydrates nor polymorphs were found, probably helped due to one method of salt formation being used throughout and avoiding water as solvent. Similarly, DSC thermograms were clearer with increasing number of hydroxyl groups, confirming the relationship between the crystal stability provided by hydrogen bonds and thermal stability.

The increased hydrogen bonding has been postulated as an explanation for the low solubility of diclofenac and its salts. The intramolecular hydrogen bonding makes the diclofenac molecule less

available to intermolecular interaction with the environment, such as the water molecules of the solvent (Fini et al. 2010).

With regards to mechanical properties, more hydroxyl groups do not necessarily mean improved mechanical properties. In flurbiprofen and gemfibrozil salts a trend towards improved tensile strength in salts exhibiting hydroxyl groups was observed and in those salts with densely bonded layers. For diclofenac salts, the amine group in the molecule and in some occasions the chlorine atom, provided additional capacity for hydrogen bonding. It is likely that the intramolecular nature of the bonds, rather than intermolecular, as in gemfibrozil and flurbiprofen, forces strained conformations and reduced the flexibility of diclofenac, resulting in reduced plasticity and reduced tensile strength of the compacts.

6 Conclusions and further work

In contrast to the traditional regulatory system of quality by testing (QbT), the concept of pharmaceutical Quality by Design (QbD) (FDA 2006) is a systemic approach to pharmaceutical development that begins with predefined objectives and emphases product and process understanding and process control. It means designing and developing formulations and manufacturing processes to ensure predefined product quality. In order to do this the relationships between formulation and manufacturing process variables (including drug substance and excipient attributes and process parameters) and product characteristics are established and sources of variability identified.

Salt formation has extensively been used in drug manufacturing mainly to improve drug solubility and salt-forming agents are often chosen empirically. The preferred salt form is selected after considering the practical issues such as cost of raw materials, ease of crystallisation and percent yield and other basic considerations such as stability, hygroscopicity and flowability of the resulting salt form (Berge et al. 1977). Ideally, it would be useful to be able to predict the salt properties from the properties of the counterion used. Salt-forming agents are rarely chosen based on mechanical properties of the resulting salt.

Several studies have described the dependence of salt properties on the nature of the counterion used (Anderson and Conradi 1985; Gould 1986; Rubino 1989; Thomas and Rubino 1996). Unfortunately, no reliable way of predicting the influence of a salt-forming agent on the behaviour of the parent compound has been reported. Only qualitative 'rules of thumb' are generally found. Increasing the hydrophilicity of the counterion has been proposed as a means of increasing the water solubility of the resultant salt, as reported for a series of erythromycin salts (Jones et al. 1969). Subsequent research has shown that is too simplistic a concept as in the case of the diclofenac salts with hydroxyl amines. Anderson and Conradi (1985) previously reported a lack of relationship between solubility and increasing number of hydroxyl groups in the flurbiprofen TBut-AMP1-AMP2-Tris series. Their solubility ranking was FAMP2 > FTris > FAMP1 > FTBut. The same solubility ranking has been observed here with flurbiprofen and gemfibrozil salts. In the case of diclofenac, the highest salt solubility in this series corresponds to DAMP1. O'Connor et al. (2001b) determined that the equilibrium saturated solubility of DAMP2 was limited to that of the monohydrate form of the salt. Rubino (1989) had already reported instantaneous hydration of DAMP2 on the surface of discs upon hydration. Therefore, selection of an appropriate counterion to produce a salt with the desired

combination of properties is still being carried out on an empirical basis. O'Connor and Corrigan (2001b) concluded that the solubility of the salts of diclofenac and the four-carbon primary amines was not dependent on any one parameter, but on a combination of factors such as salt crystal lattice strength and the pH of the saturated salt solution.

Mechanical properties, though not reported as frequently as solubility considerations, can have a profound impact on solid dosage form development and processing. A sound understanding of mechanical properties of the drug and excipients can be useful in developing a processing method, rationally selecting excipients whose properties can compensate for the properties of the drug substance, and helping assess critical material attributes and root cause analysis during process scale-up or failure. The knowledge of mechanical properties of the drug and excipients are expected to play a more significant role in product design and development in the future.

Relationship between crystal structure and mechanical properties was investigated by measuring the tensile strength, which is the relection of many parameters which we tried to standardized throughout the studies.

Conclusions obtained from both flurbiprofen and gemfibrozil series are consistent, and prove a relationship between solid state and mechanical properties. In both salt series the presence of slip planes accounted for improved mechanical properties. Slip planes correspond to the regions of weakest interaction between adjacent planes and have been used to explain differences in mechanical properties between polymorphs (Roberts and Rowe 1996; Sun and Grant 2001c), hydrate/anhydrates (Sun and Grant 2004; Joiris et al. 2008) and structurally related molecules (Feng and Sun 2007). Slip planes allow movement within the crystal of one layer over the adjacent one, enabling greater plastic deformation to produce stronger tablets. It was observed that, despite the absence of hydrogen bonds, profuse van der Waals forces can result in ineffective slip planes where slippage of one layer over the adjacent one is more difficult: such was the case of the flurbiprofen benzylamine salt. Wide and straight slip planes are preferred to zigzagging spaces, as slippage occurs with more difficulty in one dimension as opposed to the two dimensional movement in a straight plane. In this respect, flurbiprofen cyclohexylamine formed compacts with higher tensile strength compared to flurbiprofen tert-butylamine, despite the fact that the nearest interlayer distance was shorter for FCHex salt.

In general terms, the presence of hydroxyl groups on the counterion was associated with the formation of stronger compacts. Without hydroxyl groups, only one-dimensional type II or type III columns were obtained, with type II columns being the most common motif as per the Cambridge Crystallographic Database analysis (Bernstein et al. 1995). Hydroxyl groups favoured the formation of two-dimensional networks and the latter were even more likely with an increasing number of hydroxyl groups. Taking into account the presence/absence and morphology of slip planes, as defined above, two dimensional networks resulted in compacts of higher tensile strength and with tensile strength being even higher for compounds with more densely bonded layers. Such is the explanation for the higher tensile strength of the compacts of FAMP1, which displays a two-dimensional network, compared to compacts of FCBut, FTBut and FCHex, which consist of columns arranged parallel to each other, and FTris II, which shares hydrogen bonding network with FAMP2, but the additional third hydroxyl groups allows a two-dimensional bonded layer. The proposed mechanism for this is a possible decrease in attachment energy between the stacked layers.

It was observed that certain molecules and fragments adopt preferred conformations that usually lie close to energy minima. In some cases, such as with FTris polymorph I and FCBut, strained conformations were observed and this was associated with reduced tensile strength of the obtained compacts. A biphenyl twist angle of 44.46 ± 2.71 º was measured for anionic flurbiprofen moieties. Twist angles outside this range were associated with compromised mechanical properties probably due to troublesome elastic recovery. For diclofenac, however, there was no obvious link between the mechanical properties and the angle between the phenyl rings.

The hydrogen bonding motif also seems to influence mechanical properties with a trend towards higher tensile strength in those compacts with type II columns compared to type III columns although unfortunately, only FAdam and FCProp displayed the less common type III motif. It is already believed that type II columns are more stable than type III, with melting points of structures comprising type II columns being higher than those of type III (Simperler et al. 2006; Lemmerer et al. 2008a). While limited to only a single example, it was shown that DTEA exhibits the highest tensile strength of the diclofenac series (though still comparatively low) and is the only compound in this series where the typical ammonium-carboxylate salt is not observed. A salt is formed with full proton transfer, as confirmed by the similar lengths of both C-O bonds which indicate delocalization typical of carboxylate salt species, but it involves carboxylate and hydroxyl groups and this type of salt formation may be linked to higher tensile strength compacts. If carboxylate-hydroxyl salts are related

to better tensile strength, this would be a new challenge, since the formation of this type of salt would potentially be in contradiction with Etter's rule which states that the strongest hydrogen bond donor interacts with the strongest hydrogen bond acceptor (Etter 1991). Its occurrence in DTEA is most likely due to steric hindrance as the three hydroxyethyl arms, with a *gauche* conformation, surround the ammonium group, shielding its proton from intermolecular interactions.

When studying diclofenac salts, the situation is somewhat changed. Slip planes, more hydroxyl groups or densely bonded two dimensional layers do not translate to improved mechanical properties. Possible explanations are probably related to the already known thermal instability of diclofenac salts (Fini et al. 2007; Fini et al. 2010) or the difficulty in carrying out a qualitative comparison in a series of salts with very poor mechanical properties. As a new feature, diclofenac contains an amine group and chlorine atoms that are often source of intra-, not intermolecular, hydrogen bonds that may force the molecules into a strained conformation as well as preventing a more extensive two-dimensional hydrogen bonding network from developing.

This work clearly demonstrates the potential of investigating crystal structure-mechanical property relationships in pharmaceutical materials. By strengthening our understanding of the impact of crystal properties (and other critical drug/excipient attributes) on bulk material properties, synthesis may be directed towards predefined candidates containing the mechanically favourable parameters described in this work.

6.1 Further work

Some interesting trends have been observed which should be studied in more depth.

Wide and straight slip planes, which are also free of van der Waals attractive forces, are related to improved mechanical properties. Formation of a series of flurbiprofen salts resulting in type II columns, arranged in layers and allowing straight slip planes free of attractive forces would enable a study to determine whether the tensile strength is related to the width of the interlayer space.

In relation to preferred conformations, it was observed for flurbiprofen salts, that biphenyl twist angles larger than average resulted in compromised mechanical properties, suggesting that coplanar conformations could be associated with better slippage and subsequent plasticity. It would be interesting to prove this point by correlating different angle values with tensile strength, normalised

for other parameters. Identification of the conformation of which fragments are crucial to the mechanical properties of a compound would enable the targeted development of candidates which favour the presence of required characteristics and determine their preferred one.

The intramolecular hydrogen bonding in diclofenac could be studied as a source of instability (thermal as well as mechanical) by studying structurally related molecules.
Type II columns are associated with thermal stability and possibly higher tensile strength. On one hand FAdam, produces type III columns whereas GAdam and DAdam produce Type II columns. At the moment it is unclear whether this depends on the parent drug (steric hindrance?) characteristics or counterion characteristics or a combination of both. Similarly it would be interesting to find other hydrogen bond arrangements linked desirable mechanical properties.

TEA salts seem to have very different thermal, solubility and mechanical properties to those of Tris salts despite both having the same number of hydroxyl groups and similar pK_a. From this study and the examples available in the Cambridge Structural Database, it seems that there is a tendency for TEA to form salts between carboxylate and hydroxyl groups, resulting in many cases in the ammonium hydrogens not taking part in hydrogen bonds at all. It is likely that the differences in hydrogen bonding are responsible for these differences in physicochemical and mechanical properties and it is a field worth exploring.

REFERENCES

Adeyeye, M. and H. Brittain (2008). Preformulation in solid dosage form development. New York.

Agharkar, S., S. Lindenbaum and T. Higuchi (1976). "Enhancement of solubility of drug salts by hydrophilic counterions: properties of organic salts of an antimalarial drug." J Pharm Sci **65**(5): 747-9.

Aigner, Z. (2005). "Thermoanalytical, FTIR and X-ray studies of gemfibrozil-cyclodextrin complexes." Journal of Thermal Analysis and Calorimetry **81 **(2): 267-272.

Alderborn, G. and C. Nystroem (1982). "Studies on direct compression of tablets. IV. The effect of particle size on the mechanical strength of tablets." Acta Pharm Suec **19**: 381-90.

Alderborn, G. and C. Nystroem (1984). "Radial and axial tensile strength and strength variability of paracetamol tablets." Acta Pharm Suec **21**: 1-8.

Alderborn, G. and C. Nystroem (1996). Pharmaceutical powder compactation technology.

Allen, F. and W. Motherwell (2002). "Applications of the Cambridge Structural Database in organic chemistry and crystal chemistry." Acta Cryst **B58**: 407-22.

Allen, F. H., S. E. Harris and R. Taylor (1996). "Comparison of conformer distributions in the crystalline state with conformational energies calculated by ab initio techniques." J Comput Aided Mol Des **10**(3): 247-54.

Almenningen, A., O. Bastiansen and L. Fernholt (1985). "Structure and barrier of internal rotation of biphenyl derivatives in the gaseous state : Part 1. The molecular structure and normal coordinate analysis of normal biphenyl and pedeuterated biphenyl." J Mol Struct **128**: 59-76.

Amidon, G. L., H. Lennernas, V. P. Shah and J. R. Crison (1995). "A theoretical basis for a biopharmaceutic drug classification: the correlation of in vitro drug product dissolution and in vivo bioavailability." Pharm Res **12**(3): 413-20.

Anderson, B. D. and R. A. Conradi (1985). "Predictive relationships in the water solubility of salts os a nonsteroidal antiinflammatory drug." Journal of pharmaceutical sciences **74**(8): 815-20.

Anonimous (1991). Trolamine: concerns regarding potential carcinogenicity. . W. D. Inf, WHO Drug Inf. **5**.

Armstrong, N. and I. Govan (1988). "The effect of granulation on speed dependent compression properties of lactose." J Pharm Pharmacol **40**( ): 70.

Arulmozhiraja, S., C. P. Selvin and T. Fujii (2002). "Structures, potential energy curves and torsional barrier heights for selected polychlorinated biphenyls: A density functional theory study." J Phys Chem A **106**: 1765-9.

Bakatselou, V., R. C. Oppenheim and J. B. Dressman (1991). "Solubilization and wetting effects of bile salts on the dissolution of steroids." Pharm Res **8**(12): 1461-9.

Banakar, U. V. (1991). Pharmaceutical dissolution testing. New York, Marcel Dekker Inc.

Banerjee, R., B. K. Saha and G. R. Desiraju (2006). "Solid-state architecture of saccharin salts of some diamines." Acta Crystallogr C **62**(Pt 6): o346-9.

Bassam, F., P. York, R. C. Rowe and R. J. Roberts (1990). "Young's modulus of powders used as pharmaceutical excipients." International Journal of Pharmaceutics **64**(1): 55-60.

Bateman, S. (1987). "The effect of compression speed on the properties of ibuprofen tablets." J Pharm Pharmacol **39**: 66.

Bateman, S. D., M. H. Rubinstein, R. C. Rowe, R. J. Roberts, P. Drew and A. Y. K. Ho (1989). "A comparative investigation of compression simulators." International Journal of Pharmaceutics **49**(3): 209-212.

Bauer, J., S. Spanton, R. Henry, J. Quick, W. Dziki, W. Porter and J. Morris (2001). "Ritonavir: An Extraordinary Example of Conformational Polymorphism." Pharmaceutical Research **18**(6): 859-866.

Berge, S., L. Bighley and D. Monkhouse (1977). "Pharmaceutical salts." J Pharm Sci **66**(1): 1-19.

Bernstein, J. (1987). Conformational Polymorphism. In Organic Solid State Chemistry. G. R. Desiraju. Amsterdam, Ed. Elsevier.

Bernstein, J., R. Davis, L. Shimoni and N.-L. Chang (1995). "Patterns in Hydrogen Bonding: Functionality and Graph Set Analysis in Crystals." Angewandte Chemie International Edition in English **34**(15): 1555-1573.

Bighley, L., S. Berge and D. Monkhouse (1996). Salt forms of drugs and absorption. New York, Marcel Dekker.

Brittain, H. (1999). Methods for the characterization of polymorphs and solvates. Polymorphism in Pharmaceutical Solids. New York, Marcel Dekker, Inc.**:** 227-278.

Brittain, H. and E. Fiese (1999). Effect of pharmaceutical processing on drug polymorphs and solvates. Polymorphism in Pharmaceutical Solids. New York, Marcel Dekker, Inc**:** 331-362.

Brock, C. and R. Minton (1989). "Systematic effects of crystal-packing forces: biphenyl fragments with H atoms in all four ortho positions." J Am Chem Soc **111**: 4586-93.

Burger, A. and R. Ramberger (1979). "Polymorphism of pharmaceuticals and other molecular crystals. I. Theory of thermodynamic rules. ." Mikrochim. Acta **2**: 259-71.

Burt, H. M. and A. G. Mitchell (1981). "Crystal defects and dissolution." International Journal of Pharmaceutics **9**(2): 137-152.

Busignies, V., F. Michaut, C. Fouquereau, B. Huet de Barochez, B. Leclerc and P. Tchoreloff (2010). Potentialities of a tablet press simulator for the characterization of compaction properties of pharmaceutical excipients. 7th world meeting on pharmaceutis, biopharmaceutics and pharmaceutical technology, Malta.

Byrn, S. R. (1982). Solid State Chemistry of Drugs. New York

Carstensen, J. T. (1980). Solid Pharmaceutics: mechanical properties and rate phenomena. New York, Academic Press.

Carvajal, M. T. and J. N. Staniforth (2006). "Interactions of water with the surfaces of crystal polymorphs." International Journal of Pharmaceutics **307**(2): 216-224.

Castellari, C. and S. Ottani (1995). "Anti-Inflammatory Drugs. II. Salt of 2-(2,6-Dichlorophenylamino)phenylacetic Acid with Diethanolamine." Acta Cryst **C51**: 2612-15.

Castellari, C. and S. Ottani (1996). "Diclofenac Salts. IV. Tris(2-hydroxyethyl)ammonium 2-(2,6-Dichlorophenylamino)phenylacetate." Acta Cryst **C52**: 2619-22.

Castellari, C. and S. Ottani (1997a). "Anti-Inflammatory Drugs. V. [Tris-(2-hydroxymethyl)methyl]ammonium 2-[(2,6-Dichlorophenyl)amino]phenylacetate (TRISH. D)." Acta Cryst **C53**: 482-6.

Castellari, C. and S. Ottani (1997b). "Two monoclinic forms of diclofenac acid." Acta Cryst **C53**: 794-7.

Charman, W. N., C. J. Porter, S. Mithani and J. B. Dressman (1997). "Physiochemical and physiological mechanisms for the effects of food on drug absorption: the role of lipids and pH." J Pharm Sci **86**(3): 269-82.

Chen, Y.-M., P.-C. Lin, M. Tang and Y.-P. Chen (2010). "Solid solubility of antilipemic agents and micronization of gemfibrozil in supercritical carbon dioxide." The Journal of Supercritical Fluids **52**(2): 175-182.

Cheung, E. Y., S. E. David, K. D. M. Harris, B. R. Conway and P. Timmins (2007). "Structural properties of a family of hydrogen-bonded co-crystals formed between gemfibrozil and hydroxy derivatives of t-butylamine, determined directly from powder X-ray diffraction data." Journal of Solid State Chemistry **180**(3): 1068-1075.

Childs, S. L., L. J. Chyall, J. T. Dunlap, V. N. Smolenskaya, B. C. Stahly and G. P. Stahly (2004). "Crystal Engineering Approach To Forming Cocrystals of Amine Hydrochlorides with Organic Acids. Molecular Complexes of Fluoxetine Hydrochloride with Benzoic, Succinic, and Fumaric Acids." Journal of the American Chemical Society **126**(41): 13335-13342.

Cuine, J. F., C. W. Charman, C. W. Pouton, G. A. Edwards and C. J. H. Porter (2007). "Increasing the proprotional content of surfactant (Cremophor EL) relative to lipid in self-emulsifying lipid-based formulations of danazol reduces oral bioavailability in beagle dogs." Pharm Res **24**: 148-57.

Desiraju, G. R. (2002). "Hydrogen bridges in crystal engineering: interactions without borders." Acc Chem Res **35**(7): 565-73.

Desiraju, G. R. (2005). "C-H...O and other weak hydrogen bonds. From crystal engineering to virtual screening." Chem Commun (Camb)(24): 2995-3001.

Desiraju, G. R. (2007). "Crystal Engineering: A Holistic View." Angewandte Chemie International Edition **46**(44): 8342-8356.

Dhanaraj, V. and M. Vijayan (1987). "Crystal structures of 1 : 1 complexes of meclofenamic acid with choline and ethanolamine." Biochim Biophys Acta **924**(1): 135-46.

DiMasi, J. A., R. W. Hansen and H. G. Grabowski (2003). "The price of innovation: new estimates of drug development costs." J Health Econ **22**(2): 151-85.

Dressman, J. B., G. L. Amidon, C. Reppas and V. P. Shah (1998). "Dissolution testing as a prognostic tool for oral drug absorption: immediate release dosage forms." Pharm Res **15**(1): 11-22.

Dressman, J. B. and C. Reppas (2000). "In vitro-in vivo correlations for lipophilic, poorly water-soluble drugs." Eur J Pharm Sci **11 Suppl 2**: S73-80.

Duddu, S. P. and D. J. W. Grant (1995). "The use of thermal analysis in the assessment of crystal disruption." Thermochimica Acta **248**: 131-145.

Dunitz, J. (1995). "Phase changes and chemical reactions in molecular crystals." Acta Crystallographica Section B **51**(4): 619-631.

Eichler, H., B. Aronsson, E. Abadie and T. Salmonson (2010). "New drug approval success rate in Europe in 2009." Nat Rev Drug Discov **9**(5): 355-356.

EMA (2010) European Medicines Agency. Human medicines (website) **Volume**, DOI:

Emara, L., N. Taha and M. NM (2009). "Investigation of the Effect of Different Flow-Through Cell Designs on the Release of Diclofenac Sodium SR Tablets " Dissolution technologies **16**(2): 23-32.

EMEA (2001). Guidance on the investigation of bioavailability and bioequivalence. . C. f. P. M. P. European Agency for Evaluation of Medicinal Products.

Etter, M. (1990). "Encoding and decoding hydrogen-bond patterns of organic compounds." Acc Chem Res **23**(4): 122-6.

Etter, M. (1991). "Hydrogen bonds as design elements in organic chemistry." Phys Chem **95**: 4601-10.

Faucci, M. T. and P. Mura (2001). "Effect of water soluble polymers on naproxen complextaion with natural and chemically modified B-cyclodextrins." Drug Dev Ind Pharm **27**: 909-27.

FDA (2006). Guidance for industry, Q8 pharmaceutical development. CDER.

Feng, Y. and C. Sun (2007). "Influence of crystal structure on the tableting properties of n-alkyl 4-hydroxybenzoate esters (Parabens)." J Pharm Sci **96**(12): 3324-33.

Fernández, L., M. C. Martínez-Ohárriz, C. Martín, I. Vélaz, M. Sánchez and A. Zornoza (2008). "Analysis of the complexation of gemfibrozil with [gamma]- and hydroxypropyl-[gamma]-cyclodextrins." Journal of Pharmaceutical and Biomedical Analysis **47**(4-5): 943-948.

Fichtner, F., A. Rasmuson and G. Alderborn (2005). "Particle size distribution and evolution in tablet structure during and after compaction." Int J Pharm **292**(1-2): 211-25.

Fini, A., C. Cavallari and F. Ospitali (2010). "Diclofenac Salts. V. Examples of Polymorphism among Diclofenac Salts with Alkyl-hydroxy Amines Studied by DSC and HSM." Pharmaceutics **2**: 156-8.

Fini, A., G. Fazio, L. Benetti and V. Ghedini (2007). "Thermal analysis of some diclofenac salts with alkyl and alkylhydroxy amines." Thermochimica Acta **464**(2007): 65-74.

Flippen, J. and R. Gilardi (1975). "(±)-2-(2-Fluoro-4-biphenyl)propionic acid (flurbiprofen)." Acta Crystallogr B **31**: 926-8.

Florence, A. and D. Attwood (1998). Physicochemical principles of pharmacy. London, Macmillan Press Ltd.

Frechette, V. (1990). Failure analysis of brittel materials. Westerville, Ohio, American ceramic society, Inc.

Garekani, H., J. Ford, M. Rubinstein and A. RajabiSiahboomi (1999a). "Crystal habit modifications of ibuprofen and their physicomechanical characteristics." Int J Pharm **187**: 77.

Garekani, H. A., J. L. Ford, M. H. Rubinstein and A. R. Rajabi-Siahboomi (1999b). "Formation and compression characteristics of prismatic polyhedral and thin plate-like crystals of paracetamol." International Journal of Pharmaceutics **187**(1): 77-89.

Giordano, F., A. Rossi, I. Pasquali, R. Bettini, E. Frigo, A. Gazzaniga, M. Sangalli, V. Mileo and S. Catinella (2003). "Thermal degradation and melting point determination of diclofenac " Journal of thermal analysis and calorimetry **73**(2): 509-18.

Gould, P. L. (1986). "Salt selection for basic drugs." International Journal of Pharmaceutics **33**(1-3): 201-217.

Grant, D. J. (1999). Theory and origin of polymorphism. Polymorphism in pharmaceutical solids. New York, Marcel Dekker, Inc.**:** 1-34.

Grant, D. j. w. and T. Higuchi (1990). Solubility behavior of organic compounds. New York, John Wiley & Sons.

Grein, F. (2002). "Twist andles and rotational energy barriers of biphenyl and substituted biphenyls." J Phys Chem A **106**: 3823-7.

Grzesiak, A. L. and A. J. Matzger (2007). "New form discovery for the analgesics flurbiprofen and sulindac facilitated by polymer-induced heteronucleation." J Pharm Sci **96**(11): 2978-86.

Gu, L. and R. Strickley (1987). "Preformulation salt selection. Physical property comparisons of the tris(hydroxymethyl)aminomethane (THAM) salts of four analgesic/anti-inflammatory agents with the sodium salts and the free acids." Pharm Res **4**(3): 255-7.

Hancock, B., J. Colvin, P. Mullarney and A. Zinchuk (2003). "The relative densities of pharmaceutical powders, blends, dry granulations, and immediate-release tablets." Pharm. Technol. **27**: 64-80.

Hancock, B. C., G. T. Carlson, D. D. Ladipo, B. A. Langdon and M. P. Mullarney (2002). "Comparison of the mechanical properties of the crystalline and amorphous forms of a drug substance." International Journal of Pharmaceutics **241**(1): 73-85.

Hancock, B. C. and G. Zografi (1997). "Characteristics and significance of the amorphous state in pharmaceutical systems." J Pharm Sci **86**(1): 1-12.

Hassan, H. (2004). "Preparation and Investigation of Inclusion Complexes Containing Gemfibrozil and DIMEB." Journal of Inclusion Phenomena and Macrocyclic Chemistry **50**(s): 219-225.

Henck, J. O. and M. Kuhnert-Brandstatter (1999). "Demonstration of the terms enantiotropy and monotropy in polymorphism research exemplified by flurbiprofen." J Pharm Sci **88**(1): 103-8.

Humbert-Droz, P., R. Gurny, D. Mordier and E. Doelker (1983). "Densification behaviour of drugs presenting availability problems." int J Pharm Technol Prod Manuf **4**: 29-35.

Hüttenrauch, R. (1983). "Modification of starting materials to improve tableting properties." Pharm Ind **45**: 435-40.

Jaiboon, N., K. Yos-In, S. Ruangchaithaweesuk, N. Chaichit, R. Thutivoranath, K. Siritaedmukul and S. Hannongbua (2001). "New orthorhombic form of 2-[(2,6-dichlorophenyl)amino]benzeneacetic acid (diclofenac acid)." Anal Sci **17**(12): 1465-6.

Joiris, E., P. Di Martino, C. Berneron, A. Guyot-Hermann and J. Guyot (1998). "Compression behavior of orthorhombic paracetamol." Pharm Res **15**(7): 1122-30.

Joiris, E., P. Di Martino, L. Malaj, R. Censi, C. Barthelemy and P. Odou (2008). "Influence of crystal hydration on the mechanical properties of sodium naproxen." Eur J Pharmaceutics and Biopharmaceutics **70**: 345-56.

Jones, P., E. Rowley, A. Weiss, D. Bishop and A. Chun (1969). "Insoluble erythromycin salts." Journal of Pharmaceutical Sciences **58**(3): 337-339.

Kachrimanis, K. and S. Malamataris (2004). ""Apparent" Young's elastic modulus and radial recovery for some tableted pharmaceutical excipients." Eur J Pharm Sci **21**(2-3): 197-207.

Kawakami, K., K. Miyoshi, T. Funaki and Y. Ida (2006a). "Solubilization behaviour of poorly soluble drug under combined use of surfactans and cosolvents." Eur J Pharm Sci **28**: 7-14.

Kawakami, K., K. Miyoshi and Y. Ida (2004). "Solubilization behaviour of poorly soluble drugs with combined use of gelucire 44/14 and cosolvents." j Pharm Sci **93**: 1471-1479.

Kawakami, K., K. Miyoshi, N. Tamura, T. Yamaguchi and Y. Ida (2006b). "Crystallization of sucrose glass under ambient conditions: Evaluation of crystallization rate and unusual melting behavior of resultant crystals." Journal of Pharmaceutical Sciences **95**(6): 1354-1363.

Kinbara, K., Y. Hashimoto, M. Sukegawa, H. Nohira and K. Saigo (1996). "Crystal Structures of the Salts of Chiral Primary Amines with Achiral Carboxylic Acids: Recognition of the Commonly-Occuring Supramolecular Assemblies of Hydrogen-Bond Networks and Their Role in the Formation of Conglomerate
" J Am Chem Soc **118**: 3441–3449.

Konkel, P. and J. B. Mielck (1997). "Associations of parameters characterizing the time course of the tabletting process on a reciprocating and on a rotary tabletting machine for high-speed production." European Journal of Pharmaceutics and Biopharmaceutics **44**(3): 289-301.

Ledwidge, M. T. and O. I. Corrigan (1998). "Effects of surface active characteristics and solid state forms on the pH solubility profiles of drug-salt systems." International Journal of Pharmaceutics **174**(1-2): 187-200.

Leeson, L. J. and J. T. Carstensen (1974). Dissolution Technology. Washington D.C., American Pharmaceutical Association

Leiserowitz, L. (1976). "Molecular packing modes. Carboxylic acids." Acta Cryst Sect B **32**: 775-802.

Leiserowitz, L. and F. Nader (1977). "The molecular packing modes and the hydrogen-bonding properties of amide:dicarboxylic acid complexes." Acta Cryst Sect B **33**.

Lemmerer, A. (2008). "The hydrogen-bonding patterns of 3-phenylpropylammonium benzoate and 3-phenylpropylammonium 3-iodobenzoate: generation of chiral crystals from achiral molecules." Acta Crystallogr C **64**(Pt 12): 626-9.

Lemmerer, A., S. Bourne and M. Fernandes (2008a). "Disruption of a robust supramolecular heterosynthon in achiral benzylammonium and (pyridylmethyl)ammonium m-iodobenzoate salts." CrystEngComm **10**: 1750-7.

Lemmerer, A., S. Bourne and M. Fernandes (2008b). "Structural and melting point characterisation of six chiral ammonium napthalene carboxylate salts." CrystEngComm **10**: 1605-12.

Li, S., P. Doyle, S. Metz, A. E. Royce and A. T. Serajuddin (2005). "Effect of chloride ion on dissolution of different salt forms of haloperidol, a model basic drug." J Pharm Sci **94**(10): 2224-31.

Lipinski, C. A. (2000). "Drug-like properties and the causes of poor permeability and poor solubility
" J of Pharmacol and Toxicol Methods **44**(1): 235-49.

Liversidge, G. G. and K. C. Cundy (1995). "Particle size reduction for improvement in oral bioavailability of hydrophobic drugs: I. Absolute bioavailability of nanocrystalline danazol in beagle dgos." Int J Pharm **125**: 91-7.

Longuemard, P., M. Jbilou, A. M. Guyot-Hermann and J. C. Guyot (1998). "Ground and native crystals: comparison of compression capacity and dissolution rate." International Journal of Pharmaceutics **170**(1): 51-61.

Lund, W. (1994). The Pharmaceutical Codex: Principles and Practise of Pharmaceutics. London, The Pharmaceutical Press.

Maitre, M. M., M. R. Longhi and G. G. Granero (2007). "Ternary complexes of flurbiprofen with HP-beta-CD and ethanolamines characterization and transdermal delivery." Drug Dev Ind Pharm **33**(3): 311-26.

Marra-Feil, M. and B. D. Anderson (1998). "Investigation of Ksp Relationships for Salts of Vicenistatin in a Multiple Counterion 'Cocktail' using Capillary Electrophoresis." Pharm Sci **1(suppl)**: s400.

Martindale (2007). The complete drug reference. London, Pharmaceutical Press.

Mateos-Timoneda, M., M. Crego-Calama and D. Reinhoudt (2004). "Supramolecular chirality of self-assembled systems in solution." Chem Soc Rev **33**: 363-72.

Matsuura, T. and H. Koshima (2005). "Introduction to chiral crystallization of achiral organic compounds: Spontaneous generation of chirality." Journal of Photochemistry and Photobiology C: Photochemistry Reviews **6**(1): 7-24.

McKenna, A. and D. F. McCafferty (1982). "Effect on particle size on the compaction mechanism and tensile strength of tablets." J Pharm Pharmacol **34**(6): 347-51.

McNamara, D., S. Childs, J. Giordano, A. Iarriccio, J. Cassidy, M. Shet, R. Mannion, E. O'Donnell and A. Park (2006). "Use of a Glutaric Acid Cocrystal to Improve Oral Bioavailability of a Low Solubility API." Pharmaceutical Research **23**(8): 1888-1897.

Merck (2010). The Merck Index. NJ, Merck & Co. Inc.

Michaut, F., V. Busignies, C. Fouquereau, B. H. d. Barochez, B. Leclerc and P. Tchoreloff (2009). "Evaluation of a rotary tablet press simulator as a tool for the characterization of compaction properties of pharmaceutical products." Journal of Pharmaceutical Sciences **99**(6): 2874-2885.

Miller, L. A., R. L. Carrier and I. Ahmed (2006). "Practical considerations in development of solid dosage forms that contain cyclodextrin." J Pharm Sci **96**: 1691-1701.

Mullin, R. (2003). "Drug development costs about $1.7 billion." Chem Eng **81**(8).

Nagahama, S., K. Inoue, K. Sada, M. Miyata and A. Matsumoto (2003). "Two-Dimensional Hydrogen Bond Networks Supported by CH/Phi Interaction Leading to a Molecular Packing Appropriate for Topochemical Polymerization of 1,3-Diene Monomers." Crystal Growth & Design **3**(2): 247-256.

O'Connor, K. M. and O. I. Corrigan (2001a). "Comparison of the physicochemical properties of the N-(2-hydroxyethyl) pyrrolidine, diethylamine and sodium salt forms of diclofenac." International Journal of Pharmaceutics **222**(2): 281-293.

O'Connor, K. M. and O. I. Corrigan (2001b). "Preparation and characterisation of a range of diclofenac salts." International Journal of Pharmaceutics **226**(1-2): 163-179.

Palomo, M. E., M. P. Ballesteros and P. Frutos (1999). "Analysis of diclofenac sodium and derivatives." J Pharm Biomed Anal **21**(1): 83-94.

Parke-Davis (1982). Lopid® (gemfibrozil) compendium of pharmacological and clinical studies. NJ.

Paronen, P. (1986). Using the Heckel equation in the compression studies of pharmaceuticals. Proceedings of the 4th International Conference on Pharmaceutical Technology, Paris.

Peagram, R., R. Gibb and K. Sooben (2005). "The rational selection of formulations for preclinical studies- an industrial perspective." Bull. Tech. Gatefosse **98**: 53-64.

PhRMA (2006). Pharmaceutical Research and Manufacturers of America Pharmaceutical. Industry Profile 2006. Washington D.C.

Pickering, S., D. Lampard and J. Mugglestone (2000). "The Use of Computational Fluid Dynamics in the Thermal Design of Rotating Electrical Machines." Journal of Advanced Engineering **4**.

Pidcock, E. (2005). "Achiral molecules in non-centrosymmetric space groups
" EChem. Commun: 3457-9.

Podczeck, F. (2001). "Investigations into the fracture mechanics of acetylsalicylic acid and lactose monohydrate." Journal of Material Science **36**: 4687-93.

Podczeck, F. and U. Wenzel (1989). "Untersuchungen zur Direkttablettierung von Arnzneistoffen." Pharm Ind **517**: 524-7.

Polli, J., L. Yu, J. Cook, G. L. Amidon, R. Borchardt, B. Burnside, P. Burton, M. Chen, D. Conner, P. Faustino, A. Hawi, A. Hussain, H. Joshi, G. Kwei, V. Lee, L. Lesko, R. Lipper, A. Loper, S. Nerurkar, J. Polli, D. Sanvordeker, R. Taneja, R. Uppoor, C. Vattikonda, I. Wilding and G. Zhang (2004). Summary workshop report: biopharmaceutics classification system--implementation challenges and extension opportunities. . J Pharm Sci. **93:** 1375-81.

Pudipeddi, M. and A. Serajuddin (2005). "Trends in solubility of polymorphs." Journal of Pharmaceutical Sciences **94**(5): 929-939.

Rao, V. and V. J. Stella (2003). "When can cydlodextrins be considered for solubilization purposes?" J Pharm Sci **92**(927-32).

Rees, J. and K. Tsardaka (1994). "Some effects of moisture on the viscoelastic behaviour of modified starch during powder compaction." Eur. J. Pharm. Biopharm. **40**: 193-7.

Remenar, J. F., S. L. Morissette, M. L. Peterson, B. Moulton, J. M. MacPhee, H. c. R. GuzmÃ¡n and Ã. r. Almarsson (2003). "Crystal Engineering of Novel Cocrystals of a Triazole Drug with 1,4-Dicarboxylic Acids." Journal of the American Chemical Society **125**(28): 8456-8457.

Reutzel, S. and M. Etter (1992). "Evaluation of the conformational, hydrogen bonding and crystal packing preferences of acyclic imides." Journal of Physical Organic Chemistry **5**(1): 44-54.

Rhodes (1986). Parke-Davis and M. Plains. NJ.

Roberts, R. and R. Rowe (1985). "The effect of punch velocity on the compaction of a variety of materials." J Pharm Pharmacol **37**: 377-84.

Roberts, R. and R. Rowe (1996). "Influence of polymorphism on the Young's modulus and yield stress of carbamazepine, sulfathiazole and sulfanilamide." Int J Pharm **129**: 79-94.

Roberts, R., R. Rowe and P. York (1991). "The relationship between Young's modulus of elasticity of organic solids and their molecular structure." Powder technology **65**: 139-46.

Roberts, R. J. and R. C. Rowe (1987). "Brittle/ductile behaviour in pharmaceutical materials used in tabletting." International Journal of Pharmaceutics **36**(2-3): 205-209.

Rowe, R. C., R. J. Roberts, G. Alderborn and C. Nystroem (1996). Mechanical properties. New York, Marcel Dekker Inc.

Rubino, J. T. (1989). "Solubilities and solid state properties of the sodium salts of drugs." J Pharm Sci **78**(6): 485-9.

Sebhatu, T. and G. Alderborn (1999). "Relationships between the effective interparticulate contact area and the tensile strength of tablets of amorphous and crystalline lactose of varying particle size." European Journal of Pharmaceutical Sciences **8**(4): 235-242.

Serajuddin, A. T. (2002). A systematic approach to the identification of chemical and physical forms. AAPS workshop on chemical and physical selection of drug candidates. Arlington, VA, AAPS workshop on chemical and physical selection of drug candidates. American Association of Pharmaceutical Scientists.

Serajuddin, A. T., P. C. Sheen and M. A. Augustine (1987). "Common ion effect on solubility and dissolution rate of the sodium salt of an organic acid." J Pharm Pharmacol **39**(8): 587-91.

Serajuddin, A. T. M. (2007). "Salt formation to improve drug solubility." Advanced Drug Delivery Reviews **59**(7): 603-616.

Shalaev, E. Y., M. Shalaeva, S. R. Byrn and G. Zografi (1997). "Effects of processing on the solid-state methyl transfer of tetraglycine methyl ester." International Journal of Pharmaceutics **152**(1): 75-88.

Shaw, L. (2001). The development of a novel in vitro model suitable for prediction of bioavailability. Life and Helath Sciences. Birmingham, Aston University.

Sheikh-Salem, M. and J. Fell (1982). "The tensile strength of tablets of lactose, sodium chloride, and their mixtures." Acta Pharm. Suec. **19**: 391-6.

Silverstein, R., G. Basle and B. Morris (1991). Spectometric identification of organic compounds
New York, John Wiley & Sons.

Simperler, A., S. Watt, P. Bonnet, W. Jones and W. Motherwell (2006). "Correlation of melting points of inositols with hydrogen bonding patterns." CrystEngComm **9**: 589-600.

Socrates, G. (1994). Infrared Characteristic Group Frequencies. New York, Wiley.

Sonnergaard, J. M. (1999). "A critical evaluation of the Heckel equation." International Journal of Pharmaceutics **193**(1): 63-71.

Staggers, J. E., O. Hernell, R. J. Stafford and M. C. Carey (1990). "Physical-chemical behavior of dietary and biliary lipids during intestinal digestion and absorption. 1. Phase behavior and aggregation states of model lipid systems patterned after aqueous duodenal contents of healthy adult human beings." Biochemistry **29**(8): 2028-40.

Stahl, P. and C. Wermuth (2002). Handbook of pharmaceutical salts: properties, selection and use. Weinheim, Wyley - VCH.

Steiner, T. and W. Saenger (1995). "Reliability of assigning O---H ⋯ O hydrogen bonds to short intermolecular O ⋯ O separations in cyclodextrin and oligosaccharide crystal structures: Addendum." Carbohydrate Research **266**(1): 1-3.

Strickley, R. G. (2004). "Solubilizing excipients in oral and injectable formulations." Pharm Res **21**(2): 201-30.

Sun, C. and D. Grant (2004). "Improved tableting properties of p-hydroxy-benzoic acid by water crystallization: a molecular insight." Pharm Res **21**: 382-6.

Sun, C. and D. J. Grant (2001a). "Effects of initial particle size on the tableting properties of L-lysine monohydrochloride dihydrate powder." Int J Pharm **215**(1-2): 221-8.

Sun, C. and D. J. Grant (2001b). "Influence of crystal shape on the tableting performance of L-lysine monohydrochloride dihydrate." Journal of Pharmaceutical Sciences **90**(5): 569-579.

Sun, C. and D. J. Grant (2001c). "Influence of Crystal Structure on the Tableting Properties of Sulfamerazine Polymorphs " Pharm Res **18**(3): 274-280.

Sun, C. and H. Hou (2008). "Improving mechanical properties of caffeine and methyl gallate crystals by cocrystallization." Crystal growth and design **8**(5): 1575-9.

Szente, L. and J. Szejtli (1999). "Highly soluble cyclodextrin derivatives: chemistry, properties and trends in development." Adv Drug Deliv. Rev. **36**(17-28).

Tavornvipas, S., F. Hirayama, H. Arima, K. Uekama, T. Ishiguro, M. Oka, K. Hamayasu and H. Hashimoto (2002). "6-O-alpha-(4-O-alpha-D-glucuronyl)-D-glucosyl-beta-cyclodextrin: solubilizing ability and some cellular effects." Int J Pharm **249**(1-2): 199-209.

Taylor, R., O. Kennard and W. Versichel (1983). "Geometry of the imino-carbonyl (N-H...O:C) hydrogen bond. 1. Lone-pair directionality." Journal of the American Chemical Society **105**(18): 5761-5766.

The United States Pharmacopeia and the National Formulary (2003). Intrinsic dissolution. Toronto.

Thomas, E. and J. Rubino (1996). "Solubility, melting point and salting-out relationships in a group of secondary amine hydrochloride salts." International Journal of Pharmaceutics **130**(2): 179-185.

Tye, C., C. Sun and G. L. Amidon (2005). "Evaluation of the effects of tableting speed on the relationships between compaction pressure, tablet tensile strength, and tablet solid fraction." Journal of Pharmaceutical Sciences **94**(3): 465-472.

USP (2006). USP 29–NF 24. . US Pharmacopeial Convention, Rockville, MD.

Yamamoto, Y., Y. Nagasaki, Y. Kato, Y. Sugiyama and K. Kataoka (2001). "Long-circulating poly(ethylene glycol)-poly(D,L-lactide) block copolymer micelles with modulated surface charge." J Control Release **77**(1-2): 27-38.

Yu, H. C. M., M. H. Rubinstein, I. M. Jackson and H. M. Elsabbagh (1989). "Compaction Characterisation of Paracetamol and Avicel Mixtures." Drug Development and Industrial Pharmacy **15**(5): 801-823.

Yu, L. X., G. L. Amidon, J. E. Polli, H. Zhao, M. U. Mehta, D. P. Conner, V. P. Shah, L. J. Lesko, M. L. Chen, V. H. Lee and A. S. Hussain (2002). "Biopharmaceutics classification system: the scientific basis for biowaiver extensions." Pharm Res **19**(7): 921-5.

Yu, L. X., A. S. Carlin, G. L. Amidon and A. S. Hussain (2004). "Feasibility studies of utilizing disk intrinsic dissolution rate to classify drugs." Int J Pharm **270**(1-2): 221-7.

APPENDIX A

FTIR

FLURBIPROFEN

FTIR spectrum for FAdam

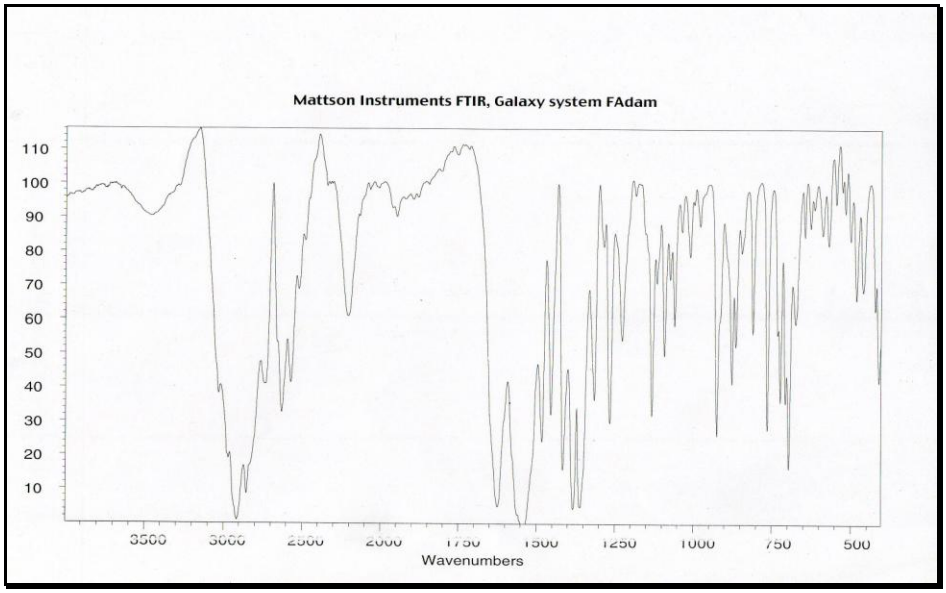

FTIR spectrum for FBenz

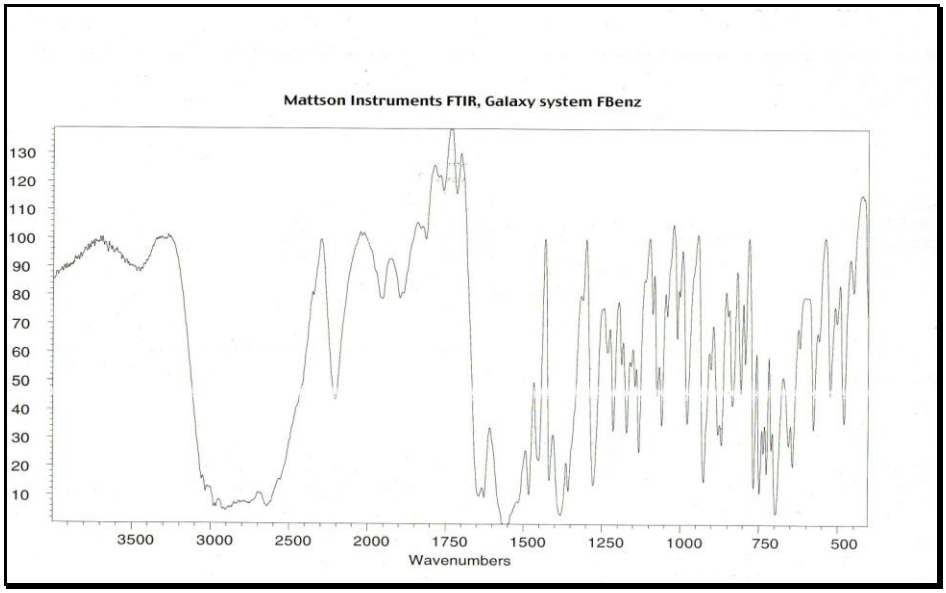

FTIR spectra for FCProp

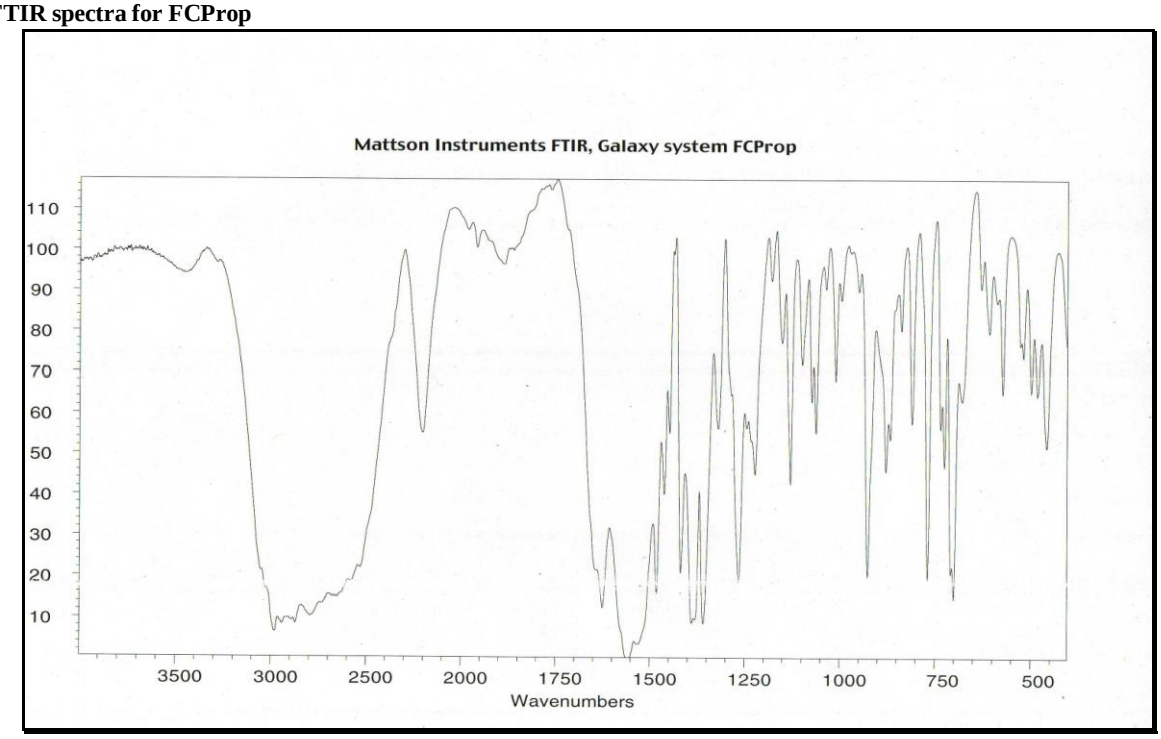

FTIR spectrum for FCHex

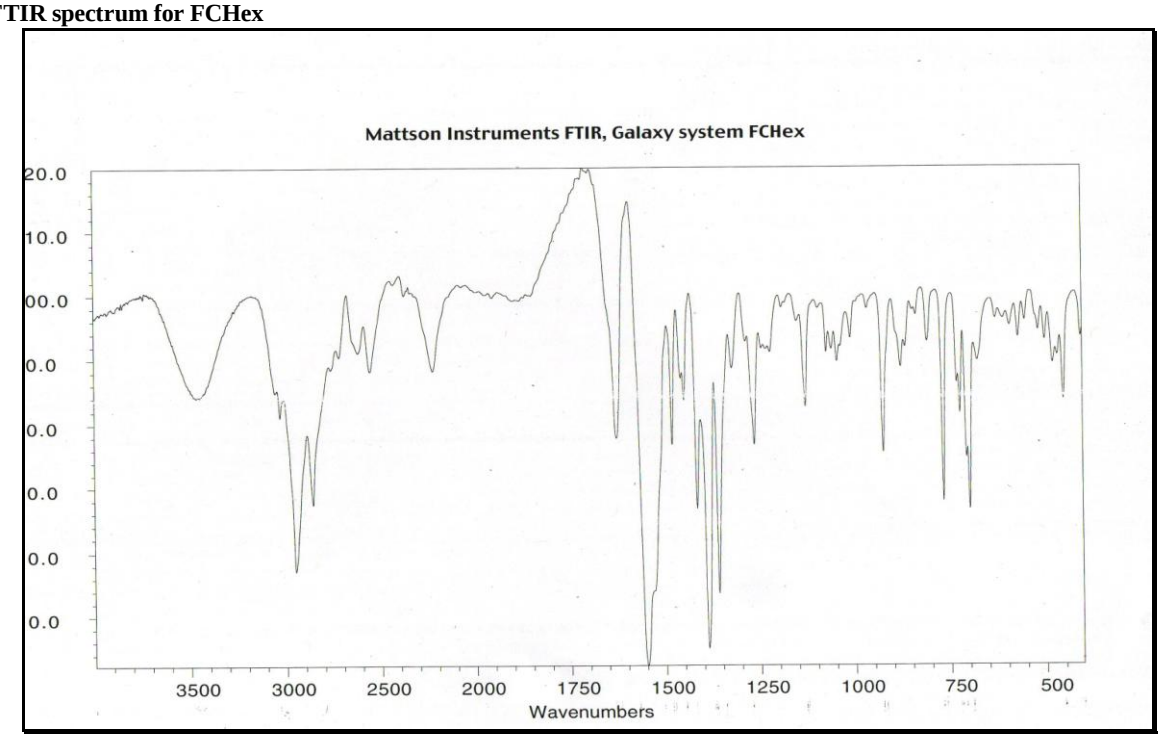

FTIR spectrum FTBut

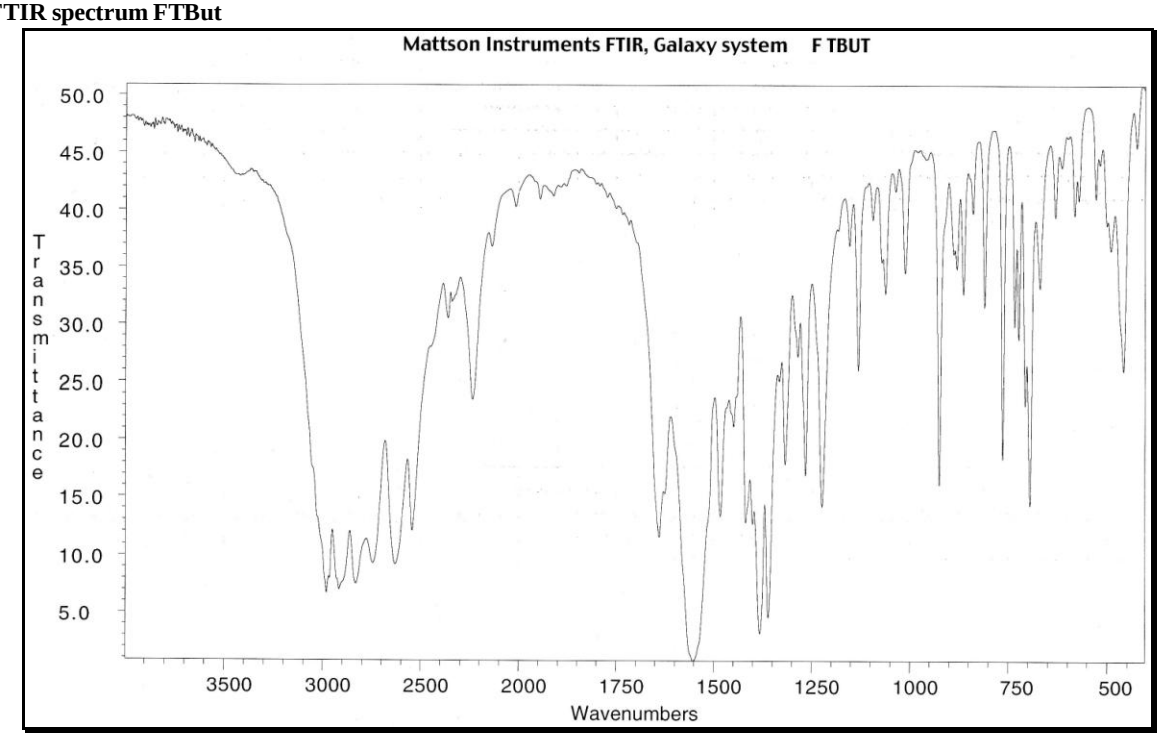

FTIR spectrum for FAMP1

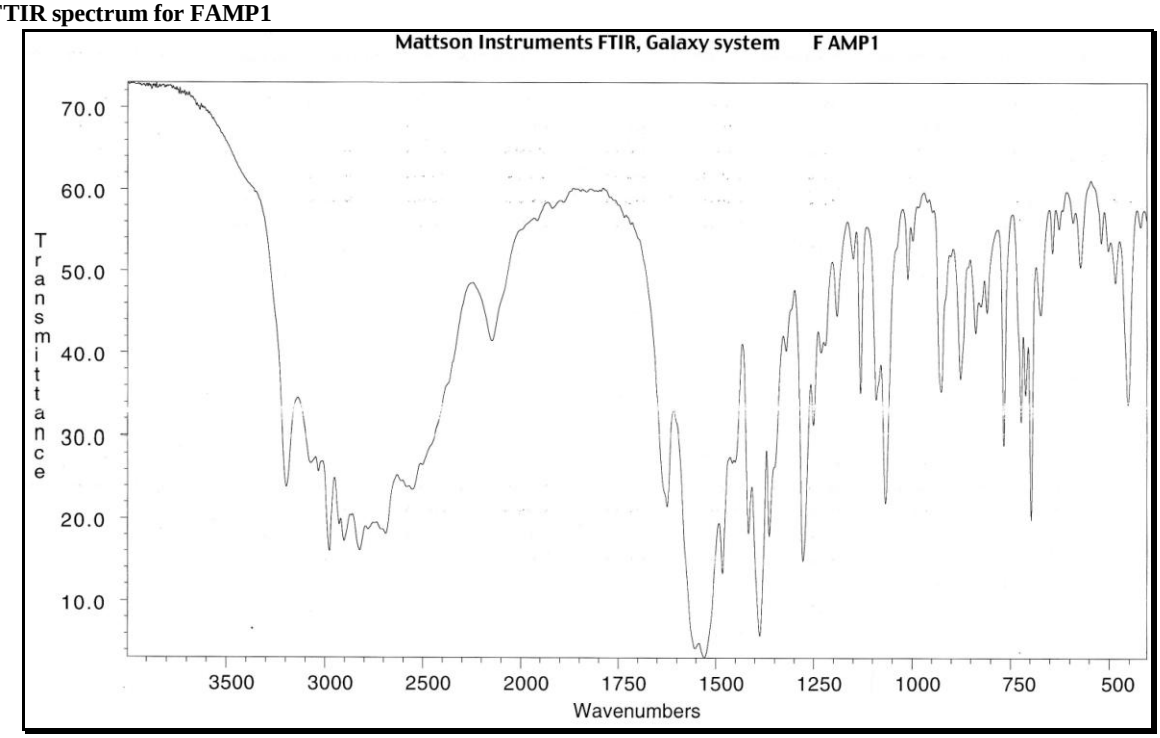

FTIR spectrum for FAMP2

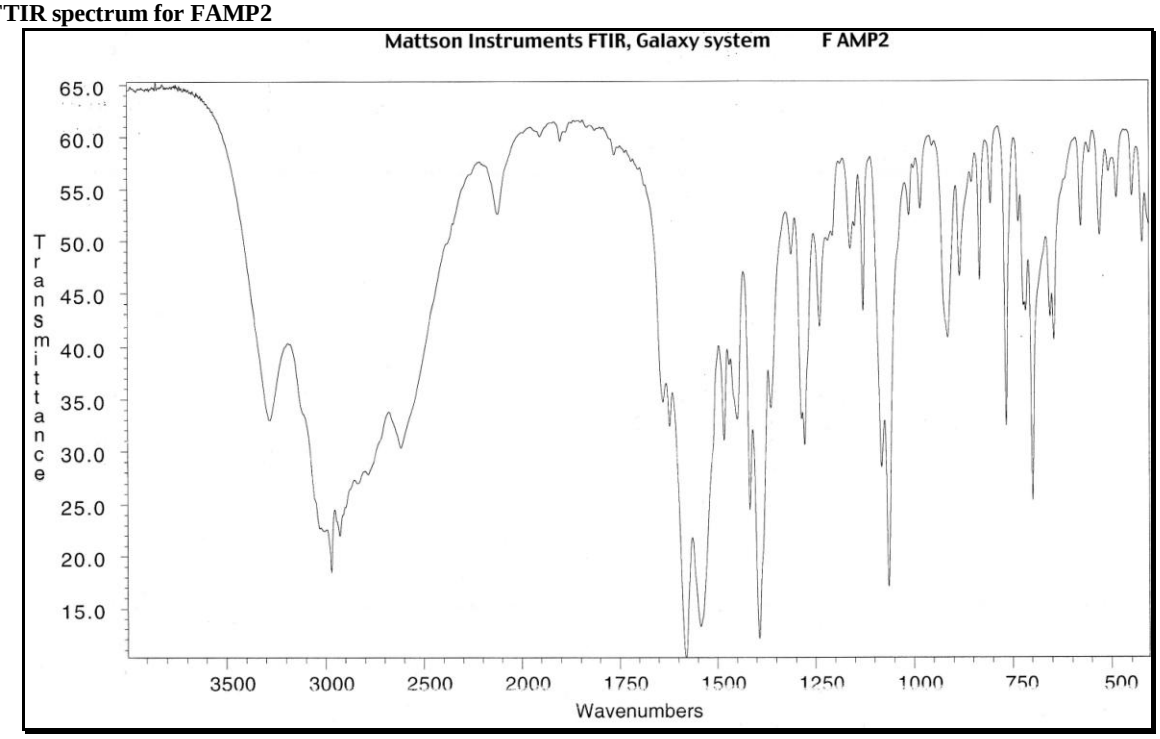

FTIR spectrum for FTris I

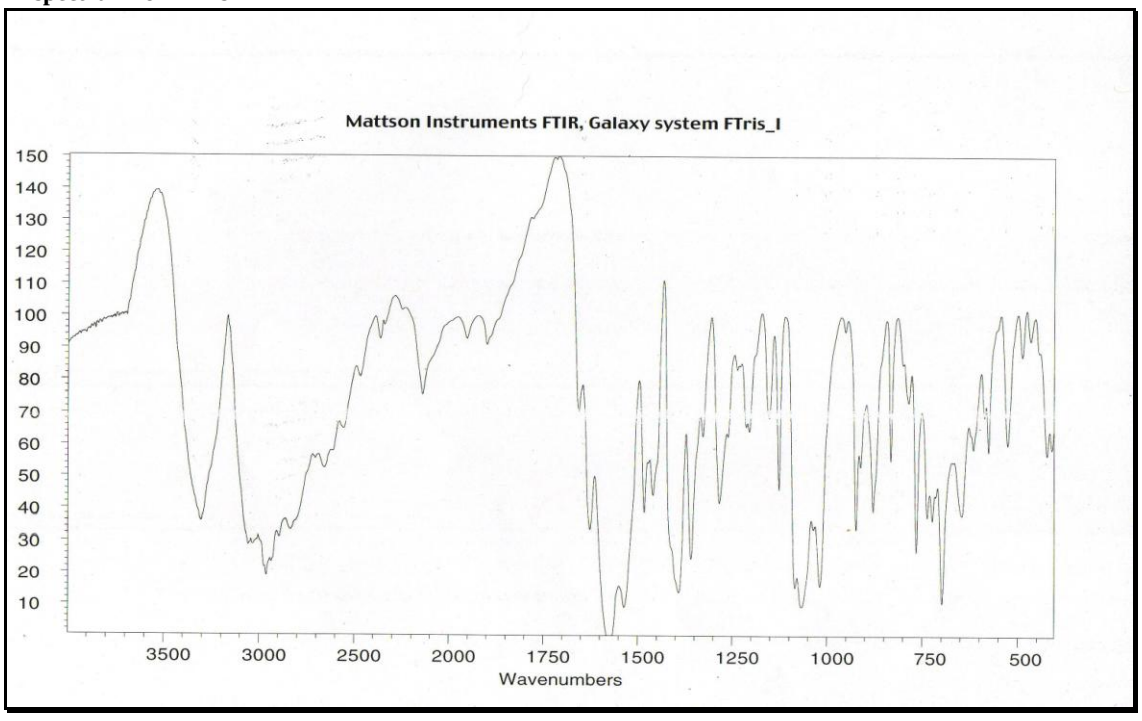

FTIR spectrum for FTris II

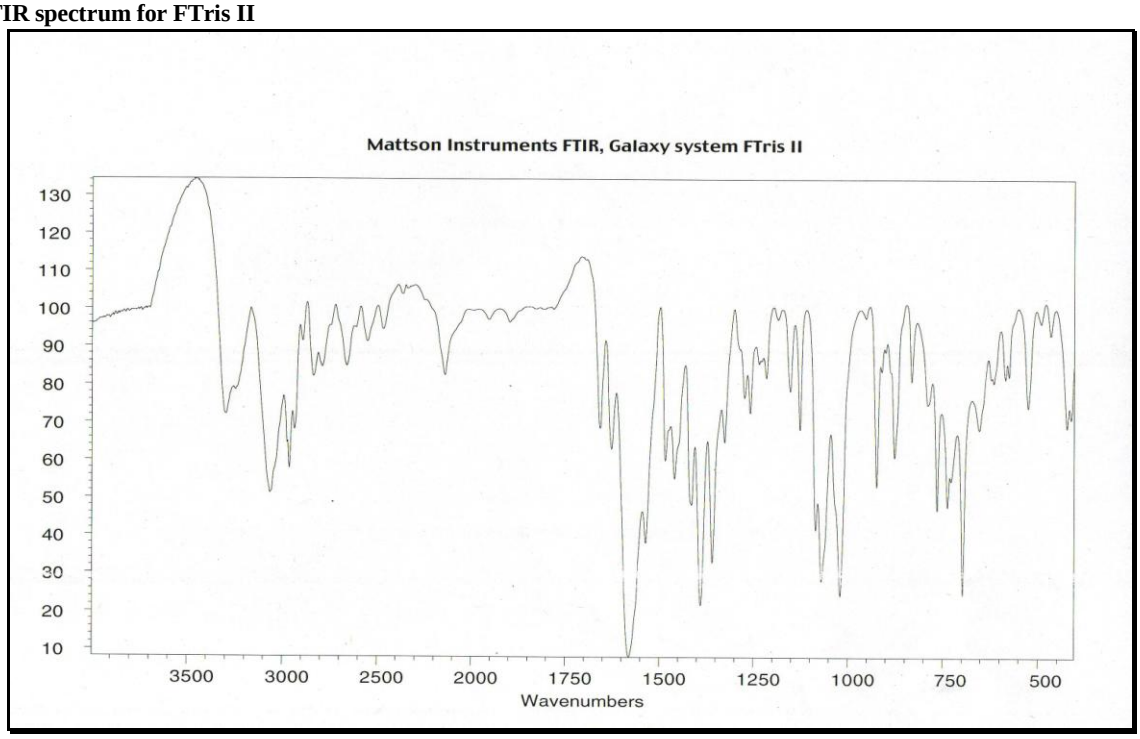

FTIR spectrum for FMEA

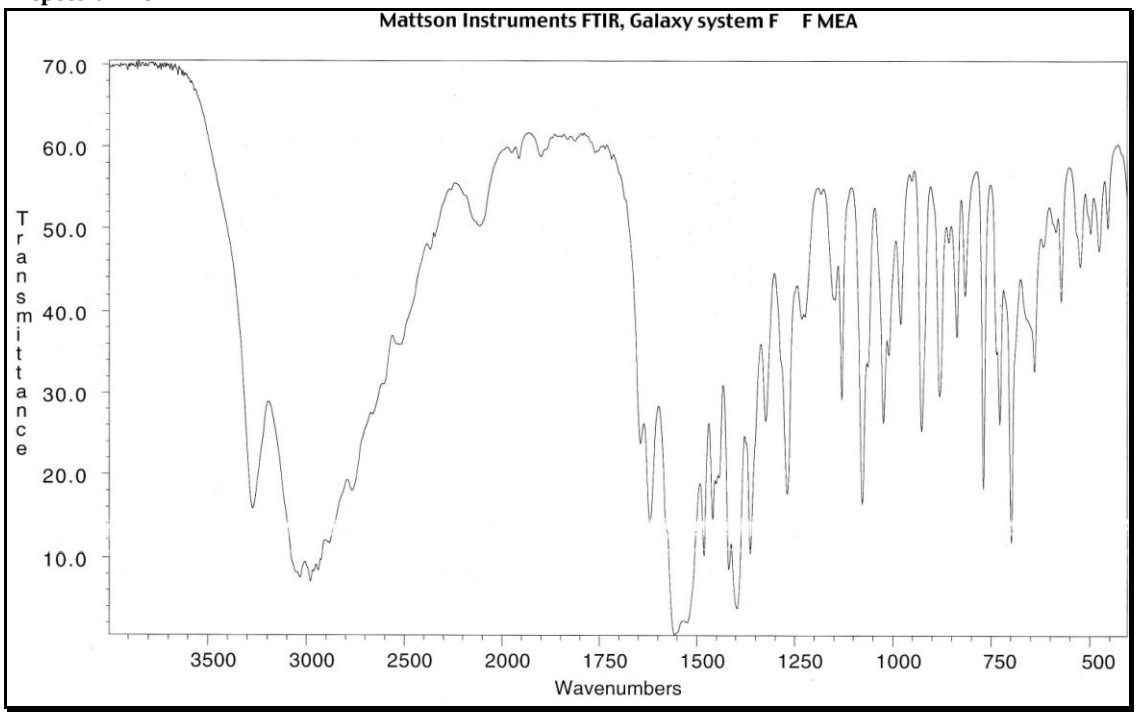

APPENDIX A

FTIR spectrum for FDEA

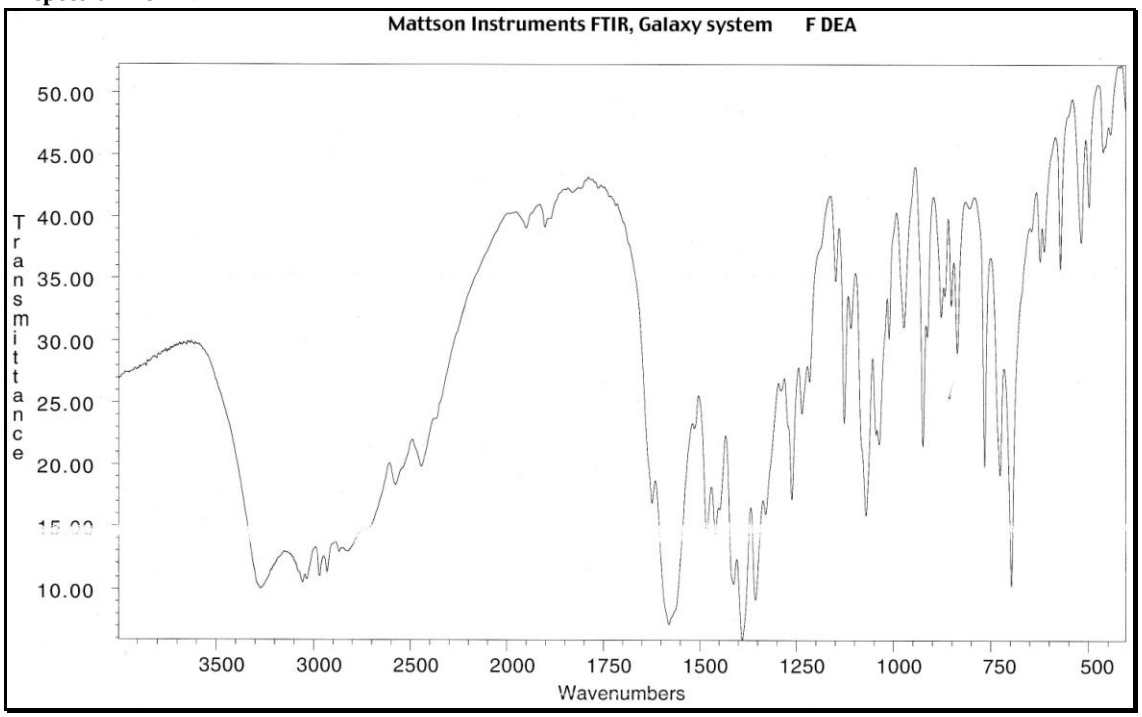

FTIR spectrum for FTEA

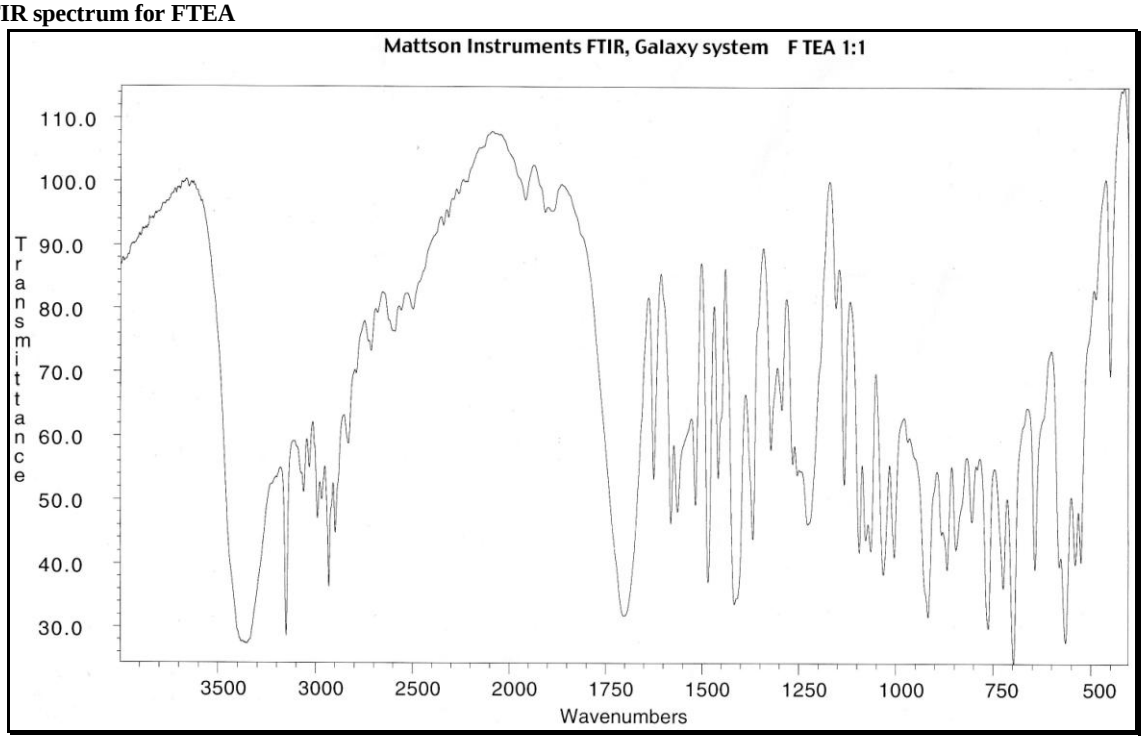

GEMFIBROZIL

FTIR spectrum GBenz

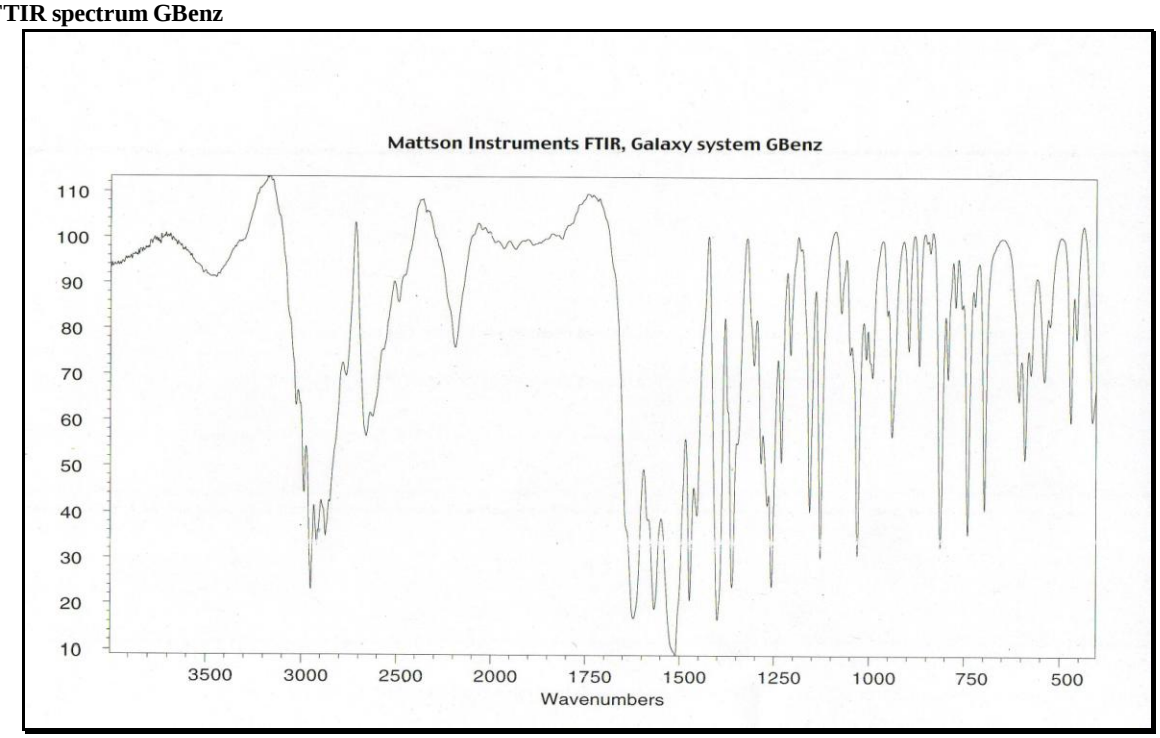

FTIR spectrum for GCProp

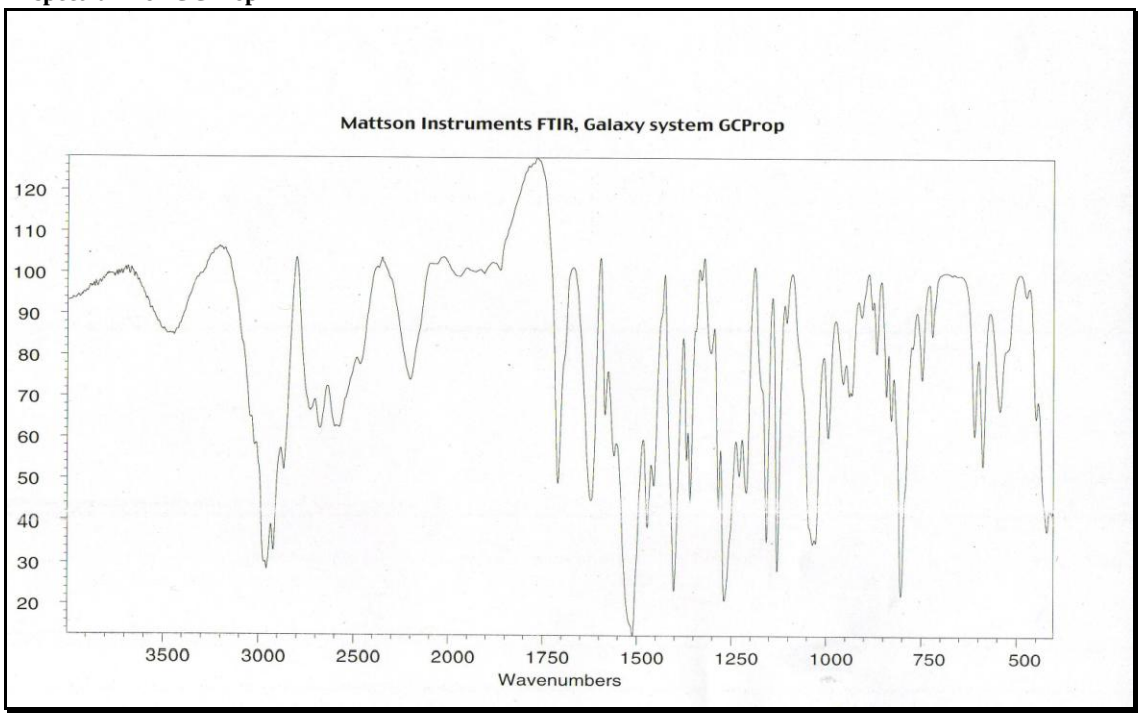

FTIR spectrum for FCHex

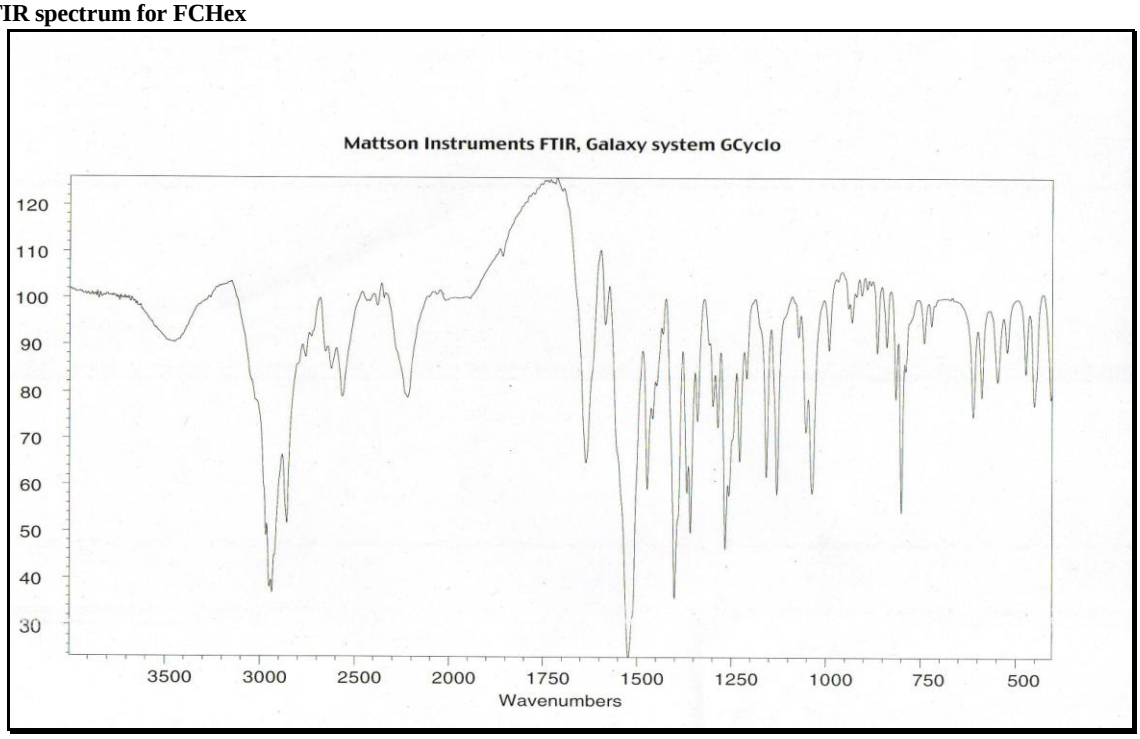

FTIR spectrum GTBut

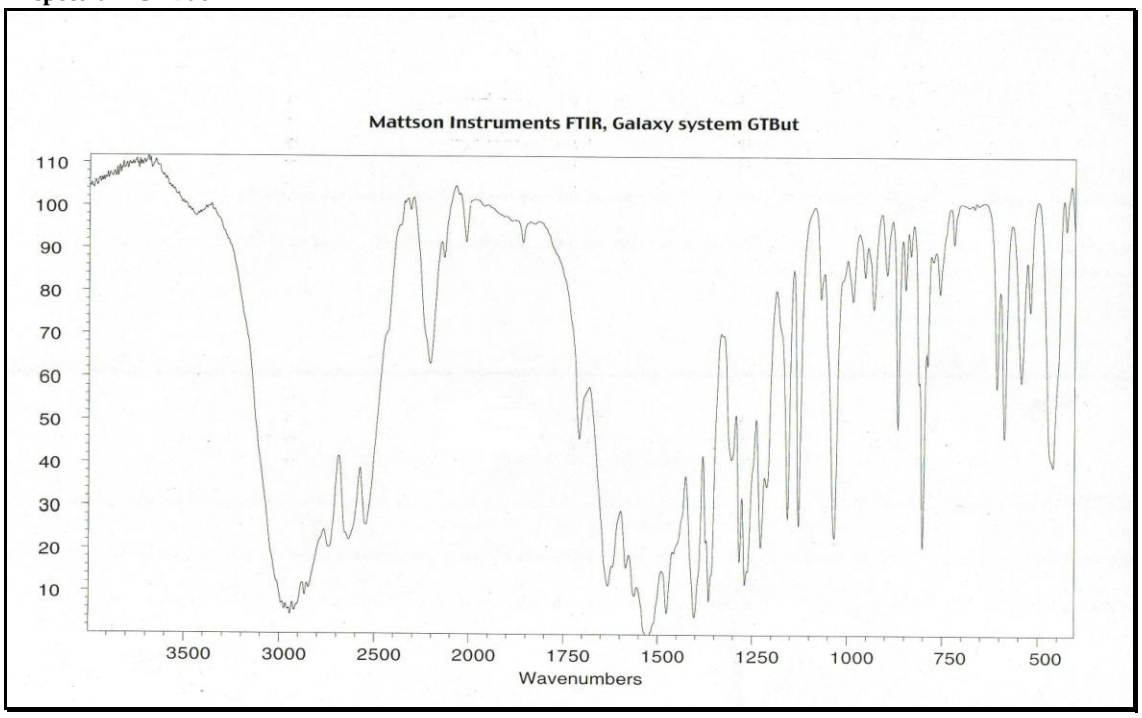

FTIR spectrum GAMP1

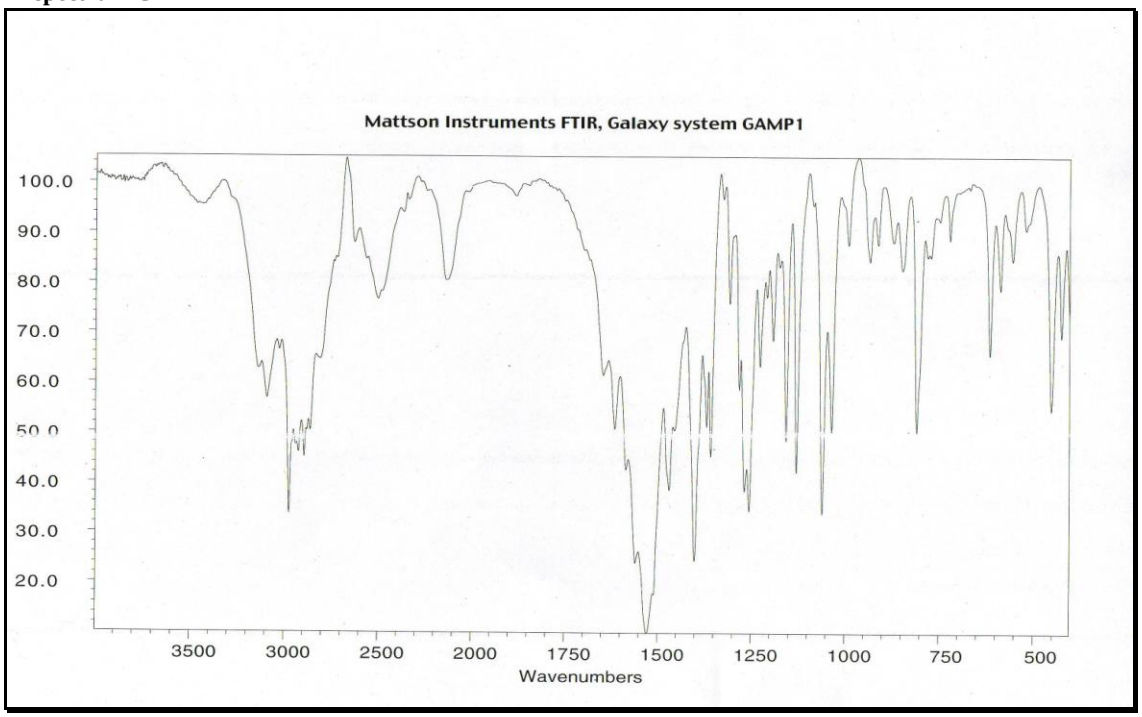

FTIR spectrum GAMP2

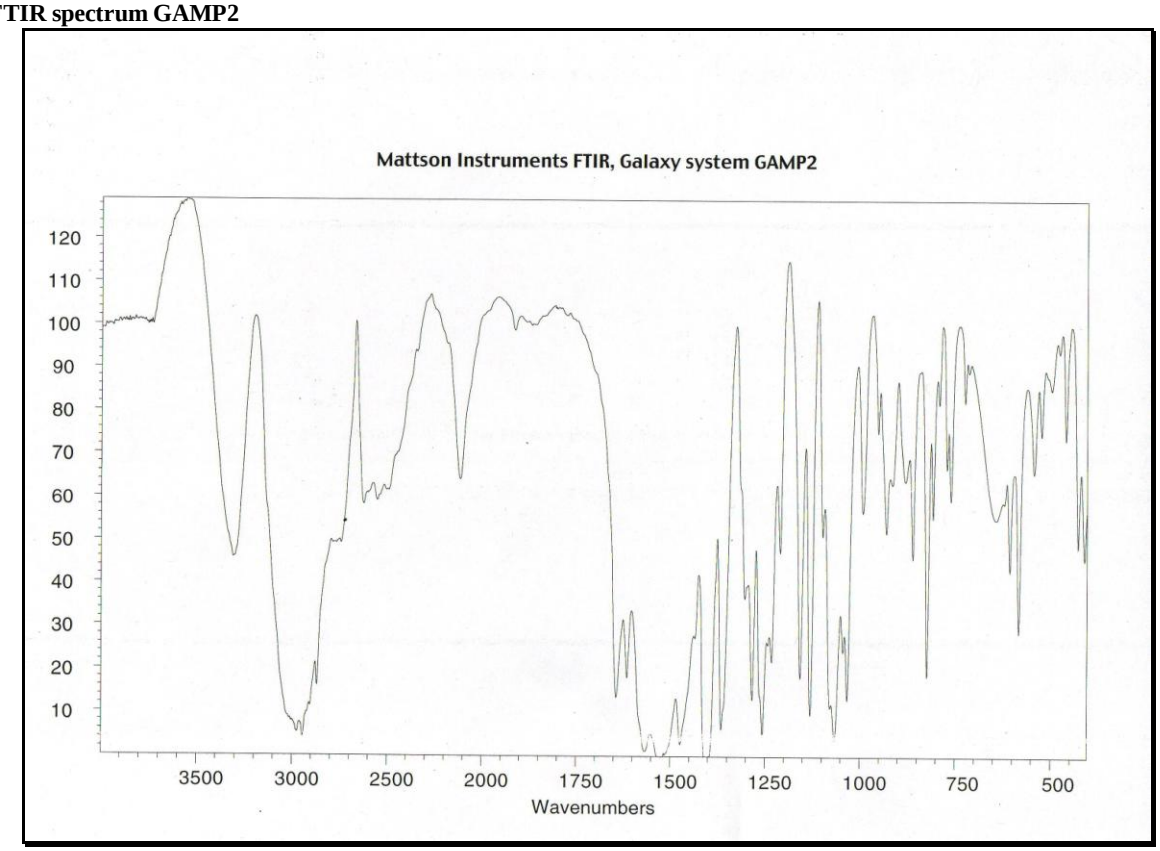

FTIR spectrum GTris

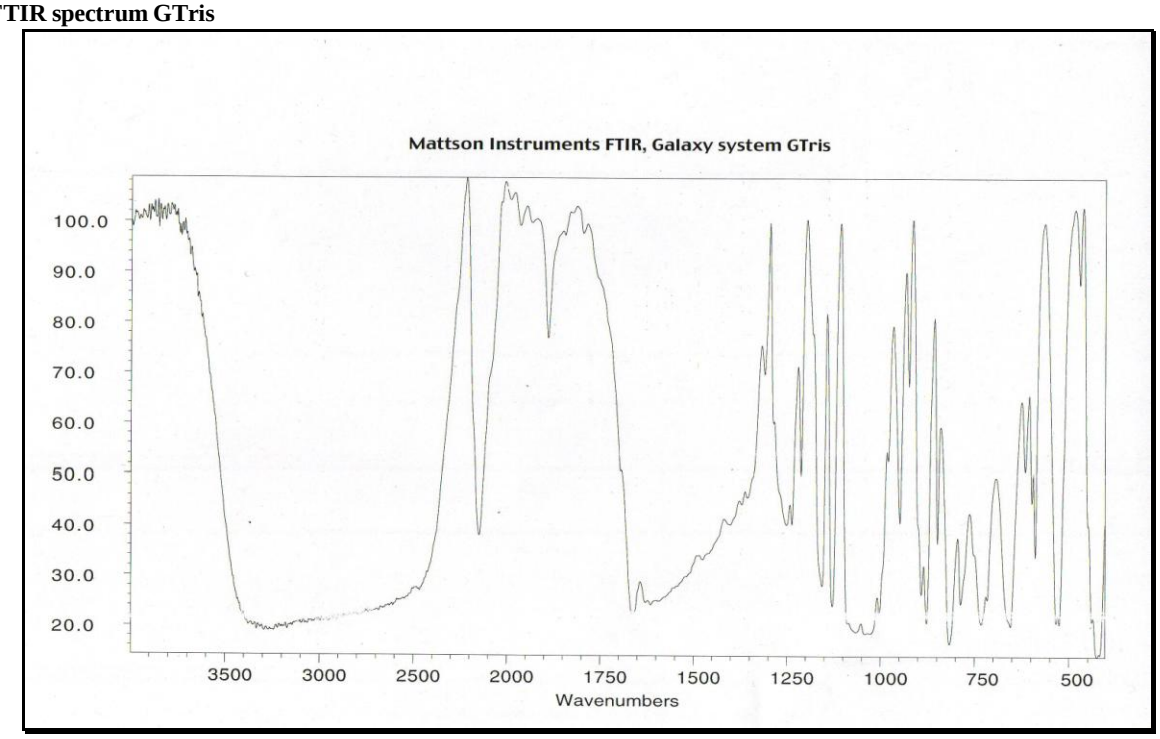

DICLOFENAC

FTIR spectrum DBenz

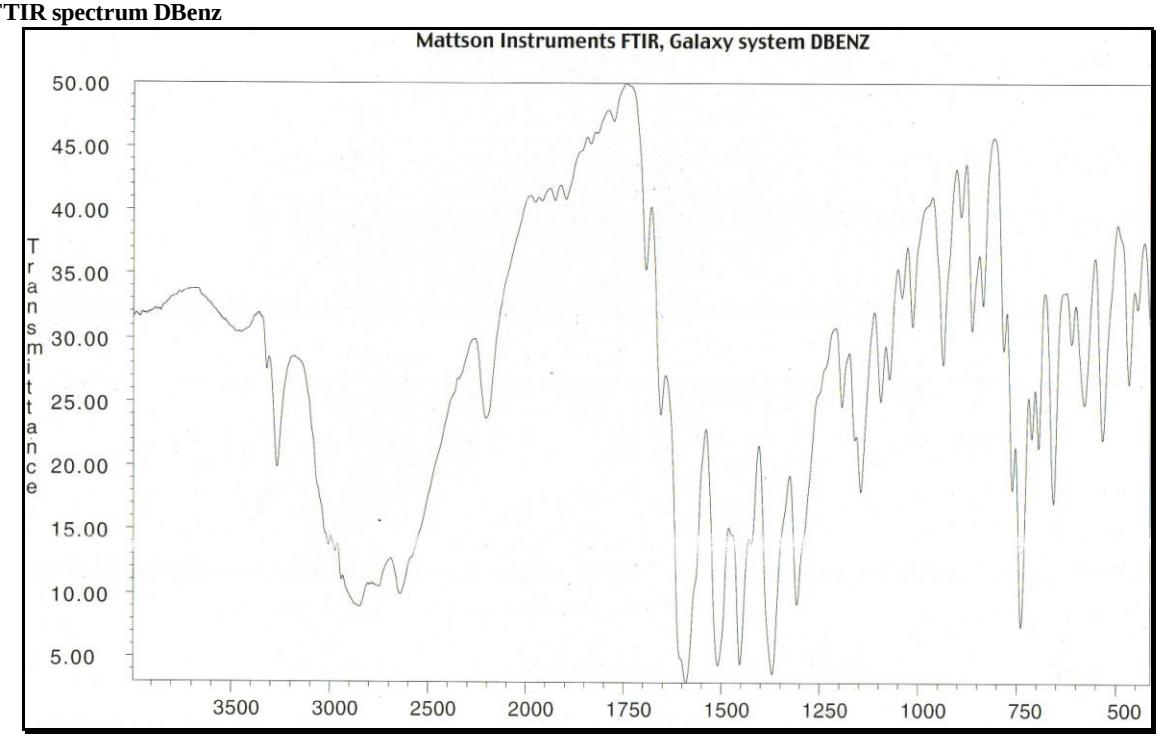

FTIR spectrum DCHex

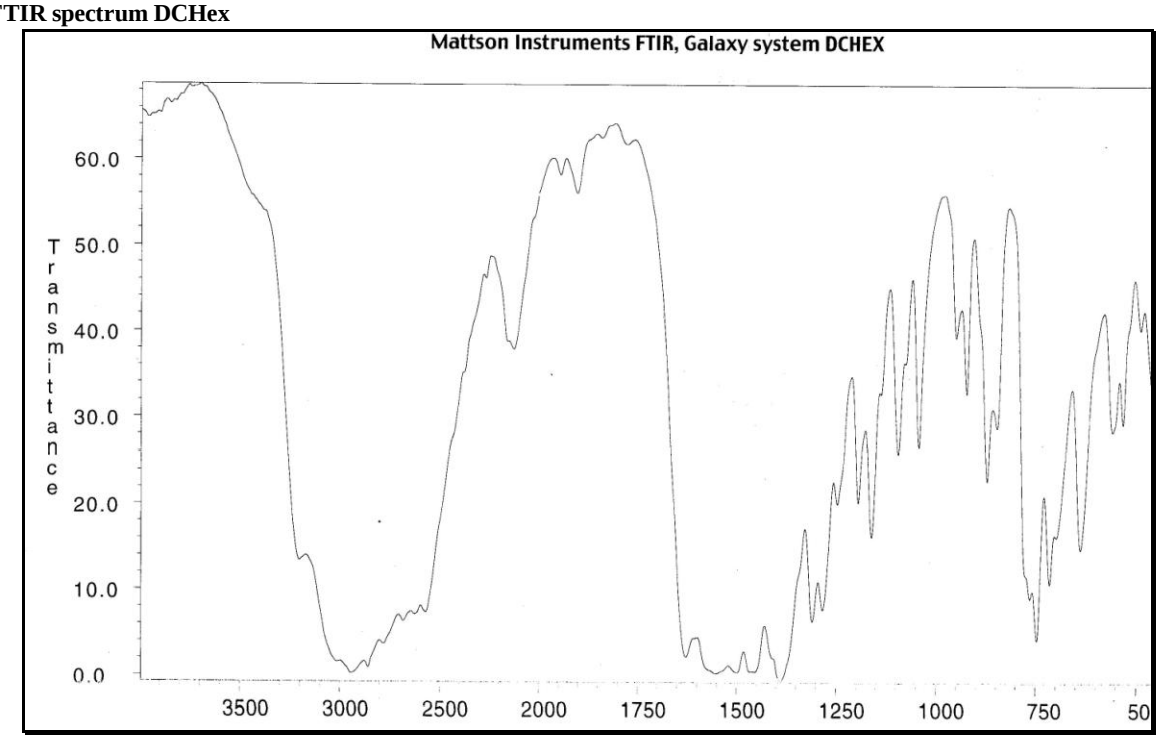

FTIR spectrum DTBut

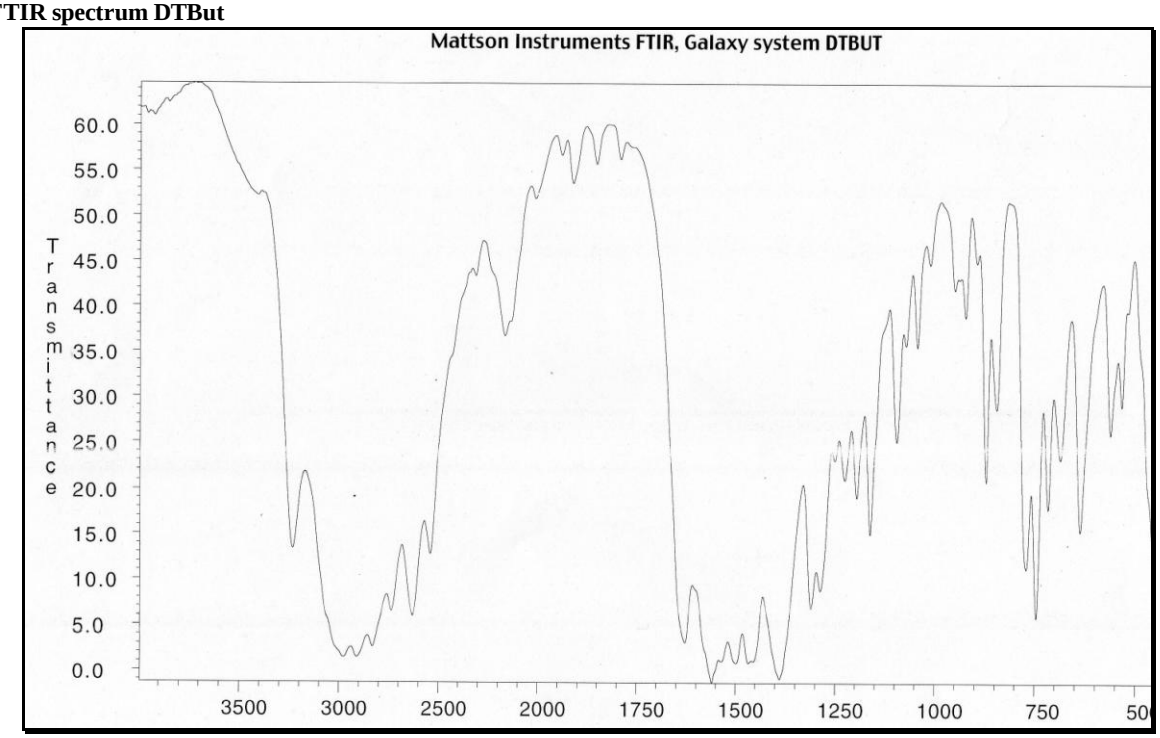

FTIR spectrum DAMP1

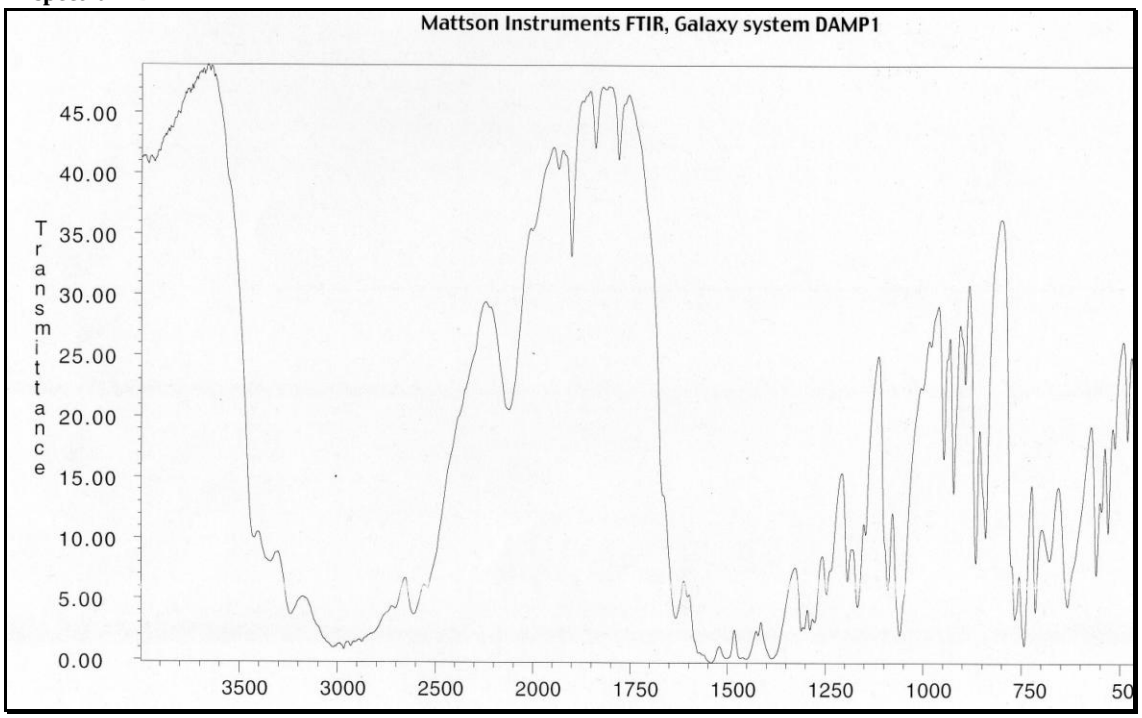

FTIR spectrum DAMP2

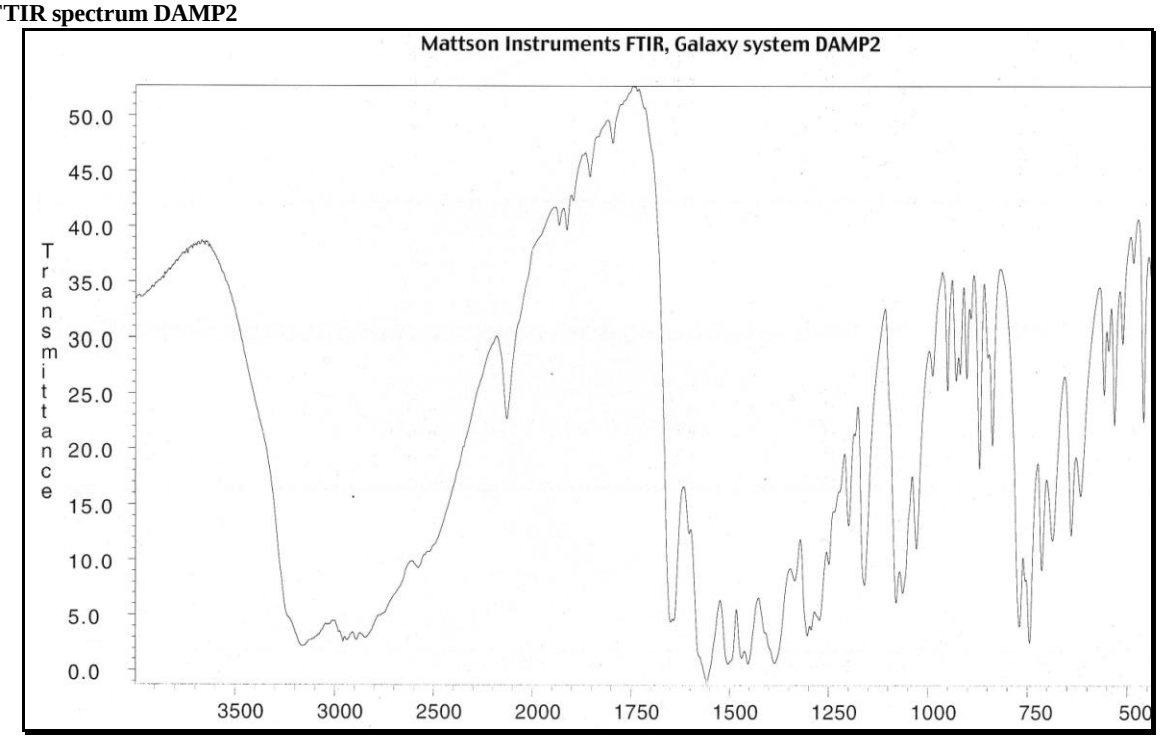

FTIR spectrum DTris

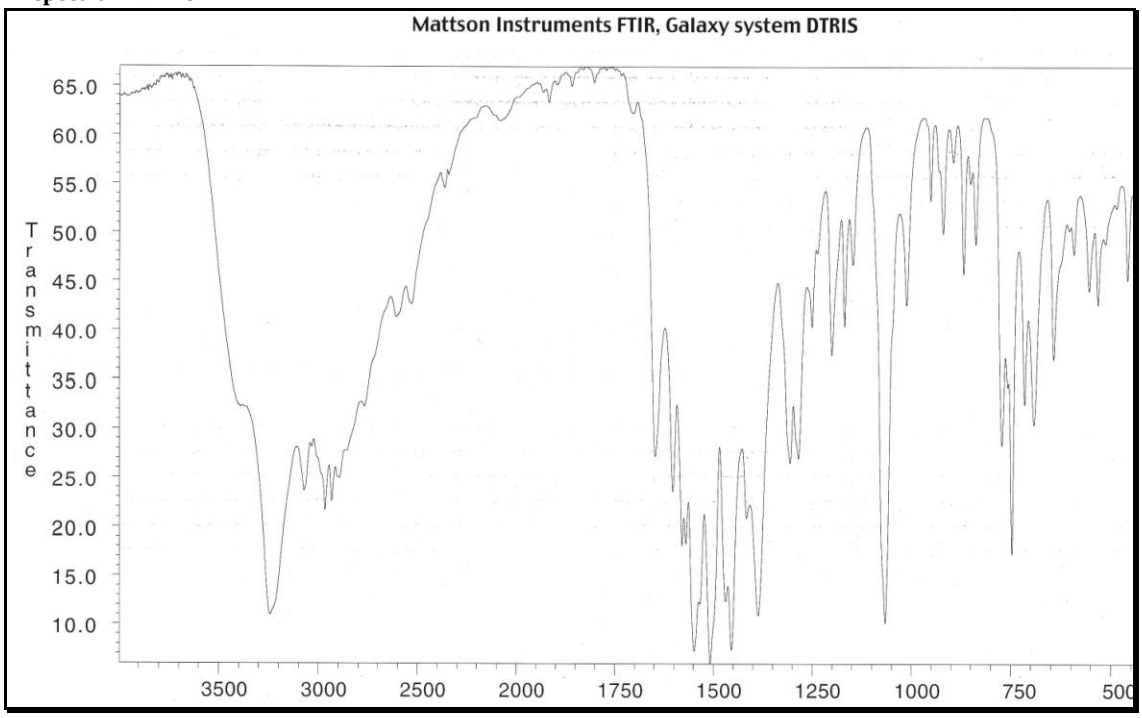

FTIR spectrum DMEA

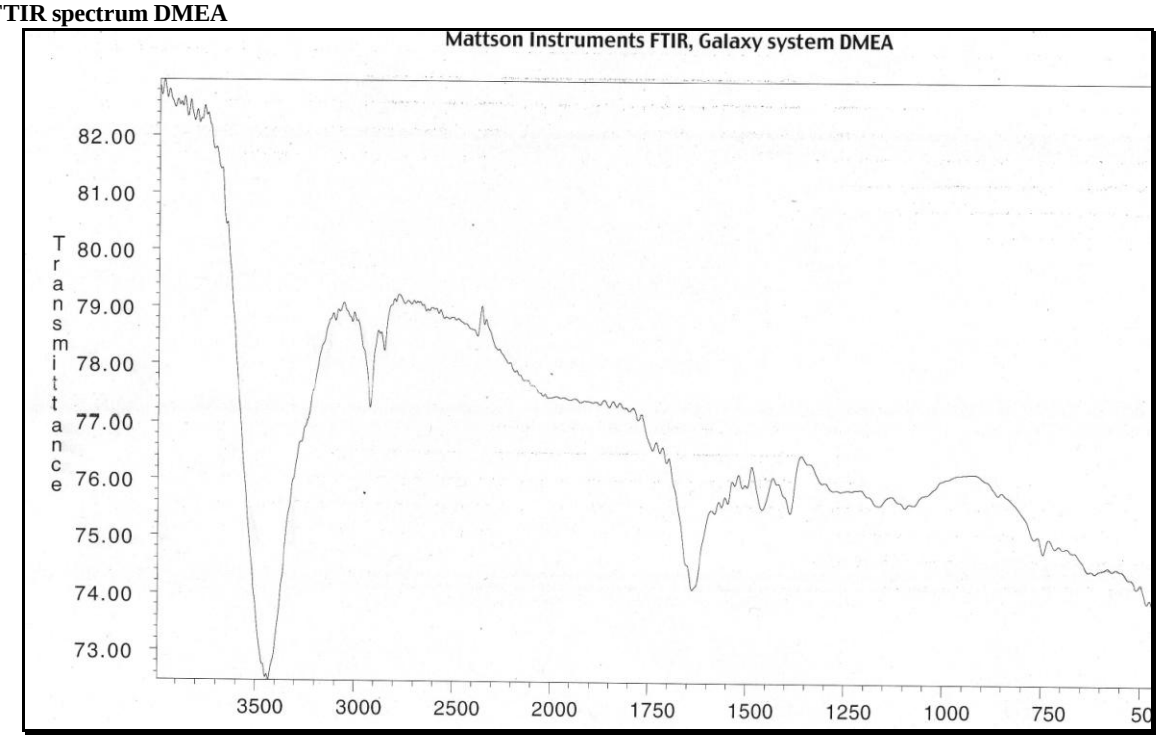

FTIR spectrum DDEA

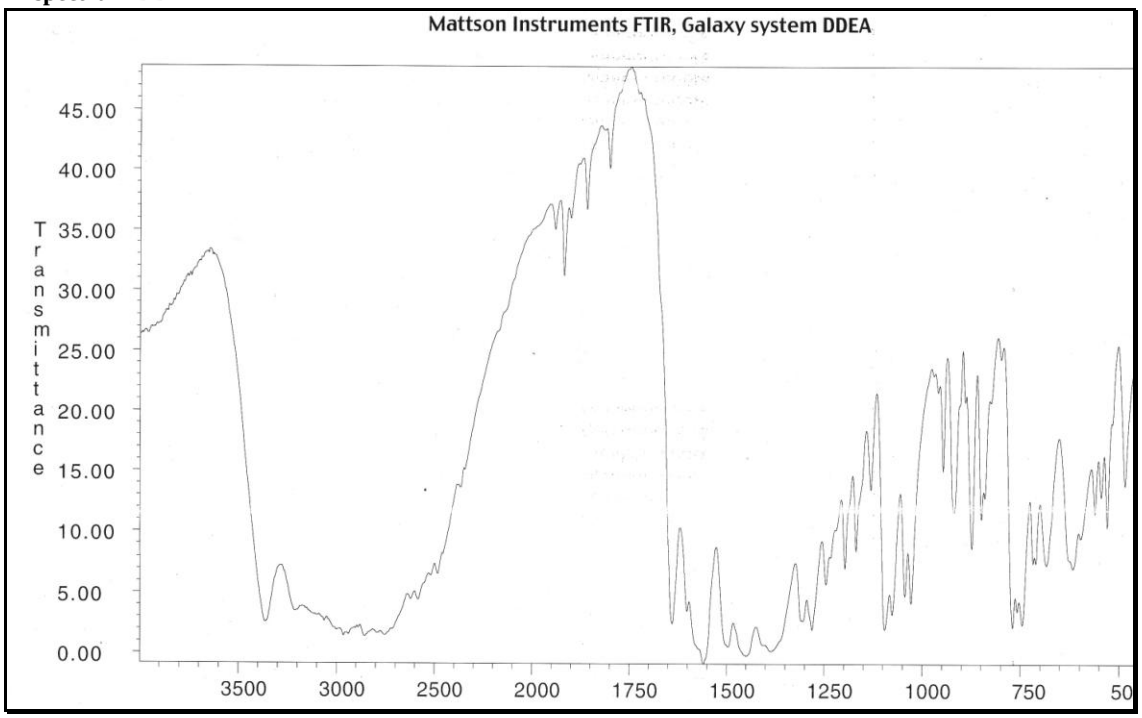

APPENDIX B

NMR spectra

FLURBIPROFEN

FLURBIPROFEN

δ 1.41 (d, 3H, J = 6.95 Hz, A)

δ 3.80 (q, 1H, J_1 = 7.58 Hz, J_2 = 6.95 Hz, B)

δ 7.22-7.57 (overlapping m, 8H, C)

δ 12.54 (s, 1H, D)

FTBut

δ 1.10 (s, 9H, E)

δ 3.61 (q, 1H, J_1 = 7.26 Hz, J_2 = 7.11, B)

δ 4.14 (bs, 3H, E)

δ 7.11-7.52 (overlapping m, 8H, C)

δ 7.11-7.52 (overlapping m, 8H, C)

FAMP1

δ 1.09 (s, 6H, E)

δ 1.31 n(d, 3H, J=6.95 Hz, A)

δ 3.27 (s, 2H, F)

δ 3.46 (q, 1H, J_1= 4.582 Jz, J_2 = 6.95 Hz, B)

δ7.16-7.53 (overlapping m, 13H, C/D/G)

FAMP2

δ 1.03 (s, 3H, E)

δ 1.33 (d, 3H, J_1 = 6.9 5Hz, A)

δ 3.35 (q, 4H, J_1 = 6.32 Hz, J_2 = 11.37 Hz, F)

δ 3.48 (q, 2H, J_1 = 6.95 Hz, J_2 = 6.95 Hz, B)

δ 6.71-7.55 (overlapped m, 13H, C/D/G)

FTris

δ 1.34 (d, 3H, J_1 = 6.95 Hz, A)

δ 3.37 (s, 6H, F)

δ 3.54 (q, 1H, J_1 = 6.95 Hz, J_2 = 6.95 Hz, B)

δ 6.10 (bs, 6H, D/G)

δ 7.18-7.55 (overlapping m, 8H, C)

FMEA

δ 1.32 (d, 3H, J=6.95 Hz, A)

δ 2.73 (t, 2H, J = 5.05 Hz, E)

δ 3.44-5.54 (overlapping m, 3H, B/F)

δ 7.05-7.54 (overlapping m, 12H, C/D/G)

FTEA

δ 1.40 (d,, 3H, J = 6095 Hz, A)

δ 2.58 (t, 6H, J = 6.32 Hz, E)

δ 3.00-4.21 (overlapping m, 6H, D/G)

δ 3.42 (t, 6H, J = 5.68 Hz, F)

δ 3.75 (q, 1H, J_1 = 6.95 Hz, J_2 = 6.95 Hz, B)

δ 7.21-7.56 (overlapping m, 8H, C)

FAdam

δ 1.32 (d, 3H, J = 6.95 Hz, A)

δ 1.50-4.63 (overlapping m, 12H, E/F)

δ 3.22 (bs, 3H, D)

δ 3.51 (overlaping, 1H, B)

δ 7.17-7.54 (overlapping m, 8H, C)

FBenz

δ 1.34 (d, 3H, J=7.58 Hz, A)

δ 3.57 (q, 1H, J_1= 6.95 Hz, J_2= 6.95 Hz, B)

δ 3.86 (s, 2H, E)

δ 5.48 (bs, 3H, D)

δ 7.17-7.54 (overlapping m, 13H, C/F)

FCProp

δ 1.51 (d, 3H, J=6.95 Hz, A)

δ 2.50 (m, 1H, J_1= 10.7 Hz, J_2= 3.79 Hz, F)

δ 3.76 (q, 1H, J_1= 6.95 Hz, J_2= 6.95 Hz, B)

δ 6.63 (overlapping m, 4H, E)

δ 7.10-7.69 (overlapping m, 11H, C/D)

FCBut

FCHex

δ 1.33 (d, 3H, J=6.95 Hz, A)

δ 1.55-1.70 (m, 2H, F)

δ 1.84-2.14 (overlapping m., 4H, E/G)

δ 3.41-3.54 (overlapping n, 2H, B/H)

δ 5.79 (bs, 3H, D)

δ 7.17-7.53 (overlapping m, 8H, C)

δ 1.11-1.83 (overlapping m, 10H, E)

δ 1.31 (d, 3H, J=6.95 Hz, A)

δ 3.51 (bs, 3H, D)

δ 3.45-3.50 (overlapping m, 2H, B/F)

δ 7.16-7.53) (overlapping m, 8H, C)

NMR spectrum for FTBut

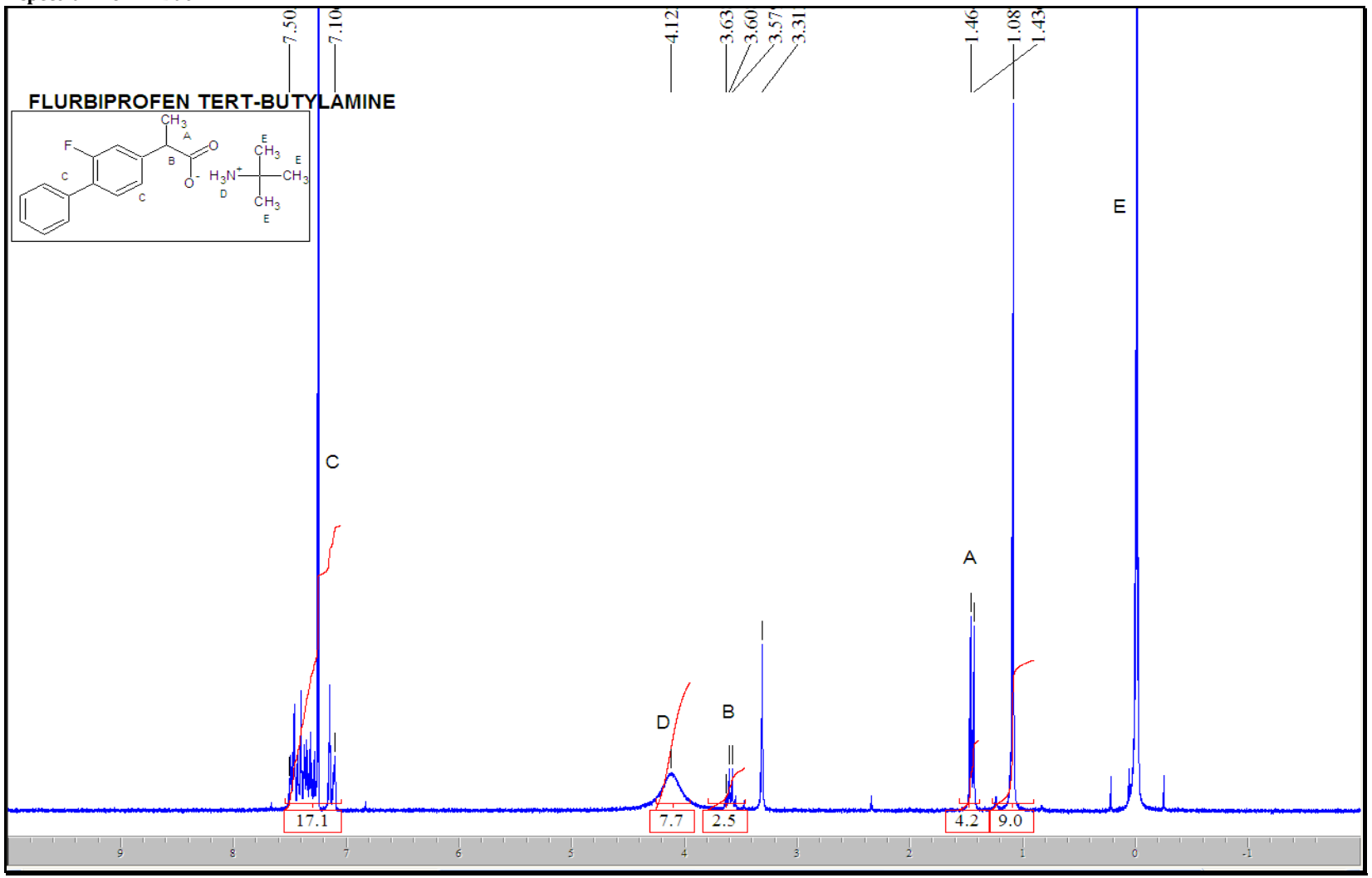

NMR spectrum for FAMP1

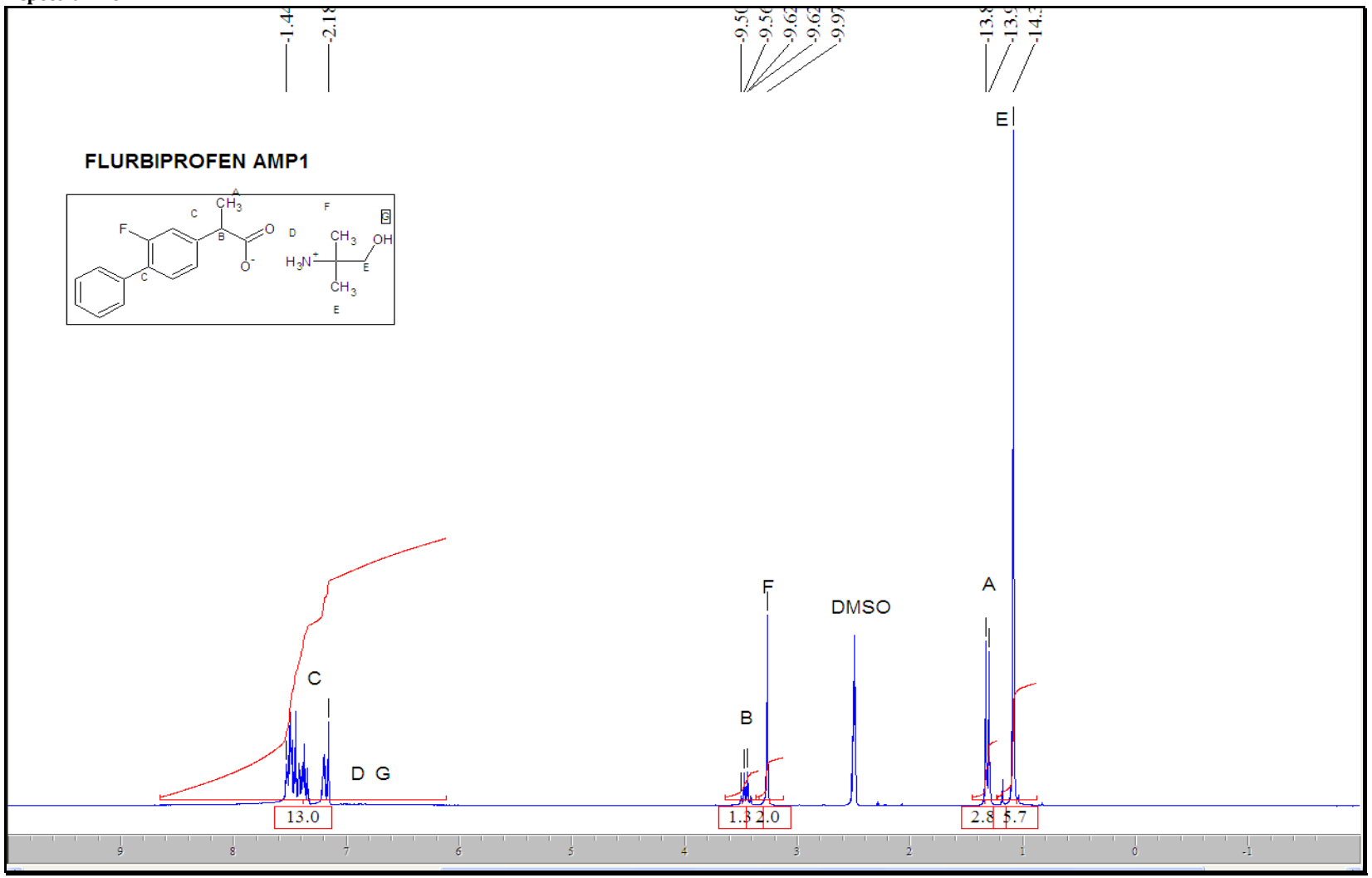

NMR spectrum for FAMP2

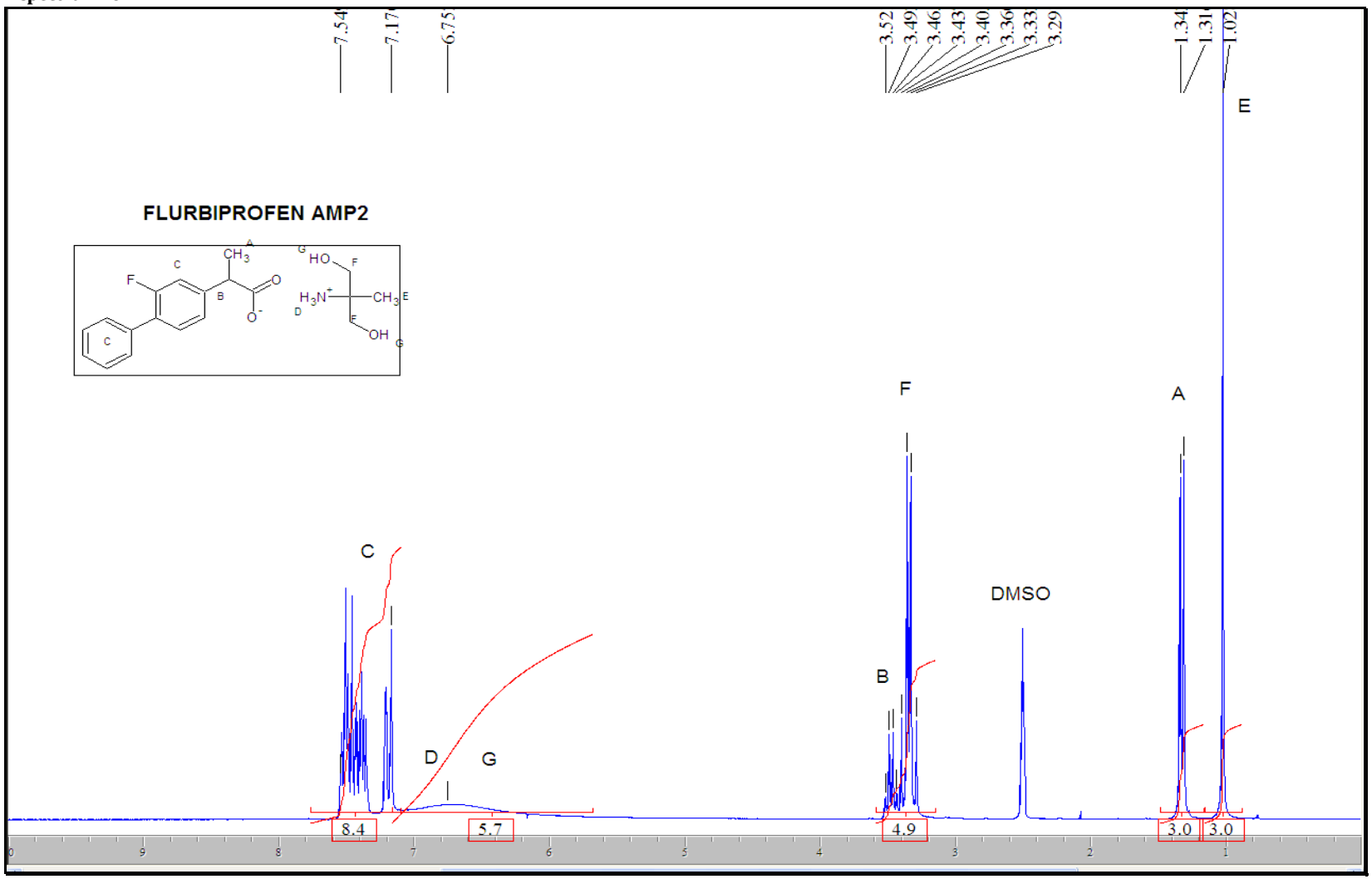

NMR spectrum for FTris

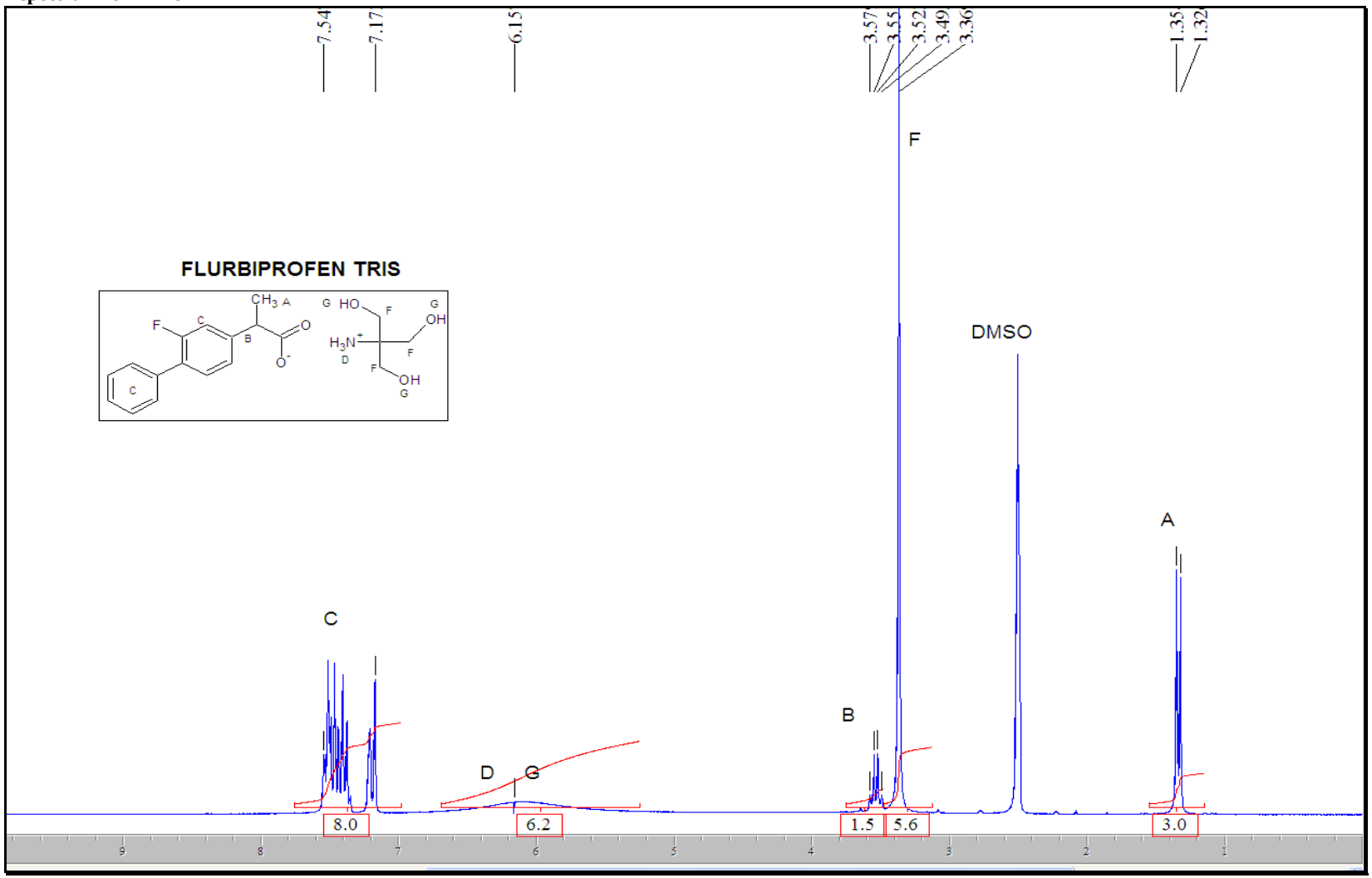

NMR spectrum for FAdam

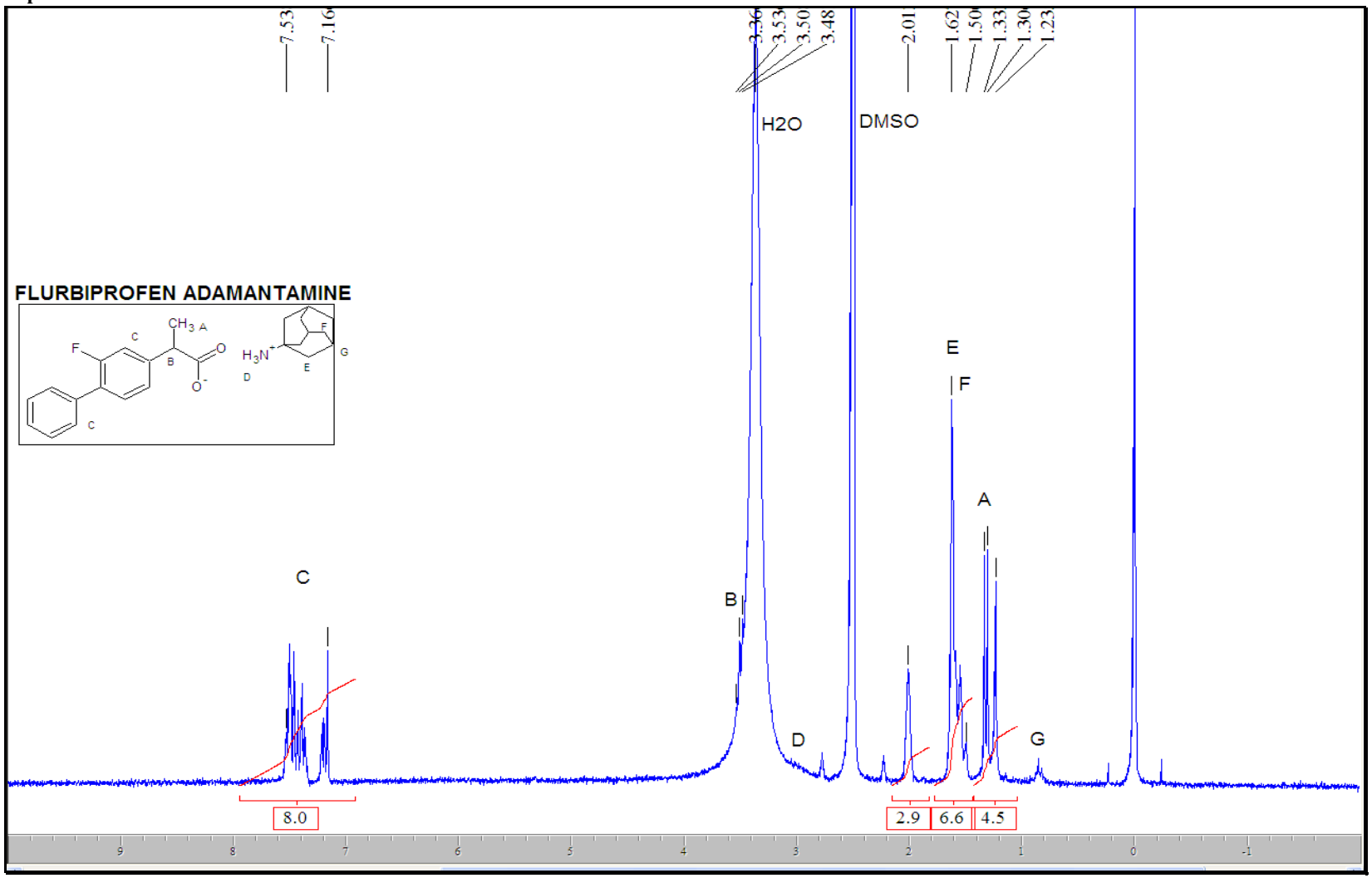

NMR spectrum for FBenz

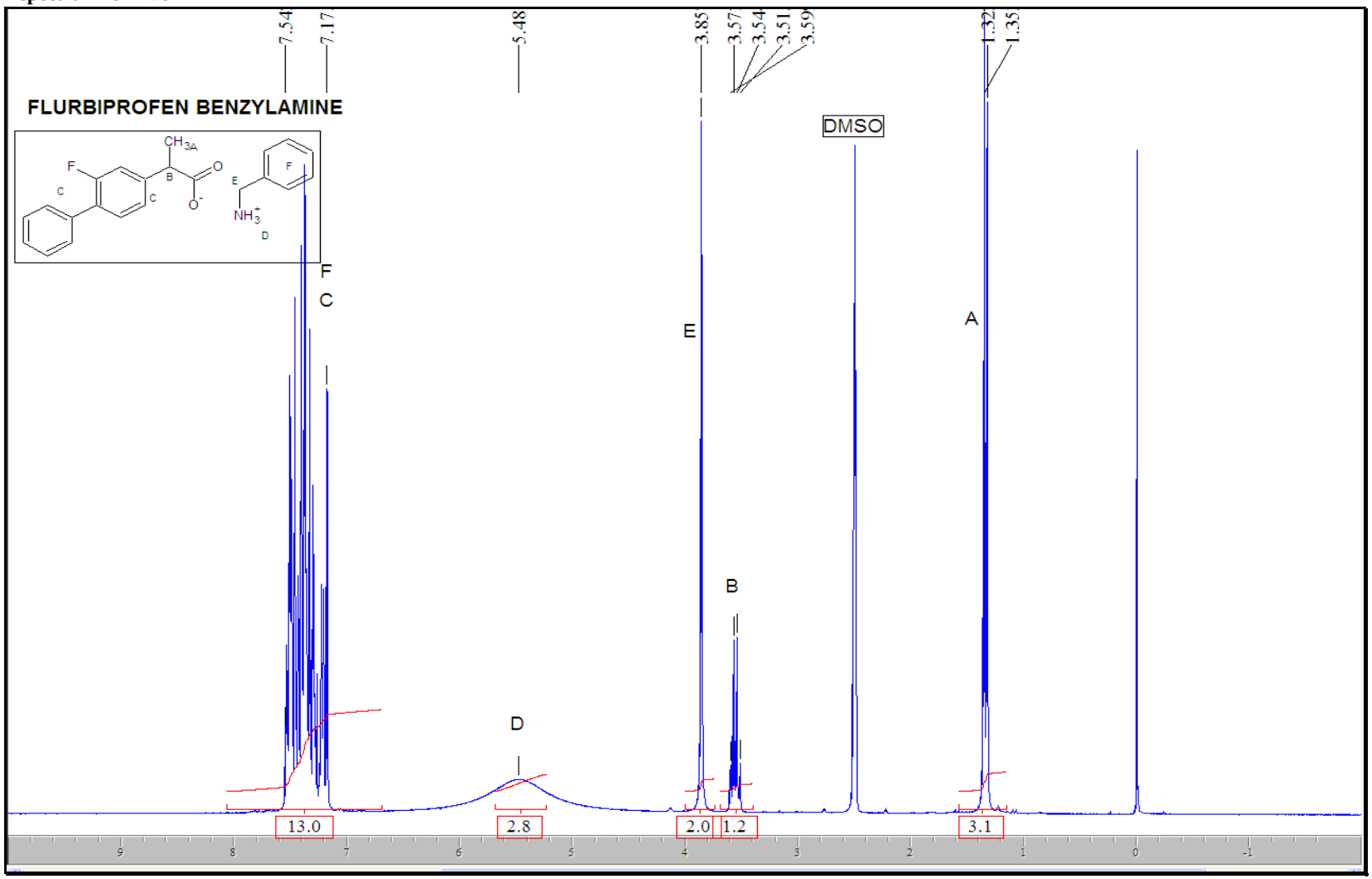

NMR spectrum for FCBut

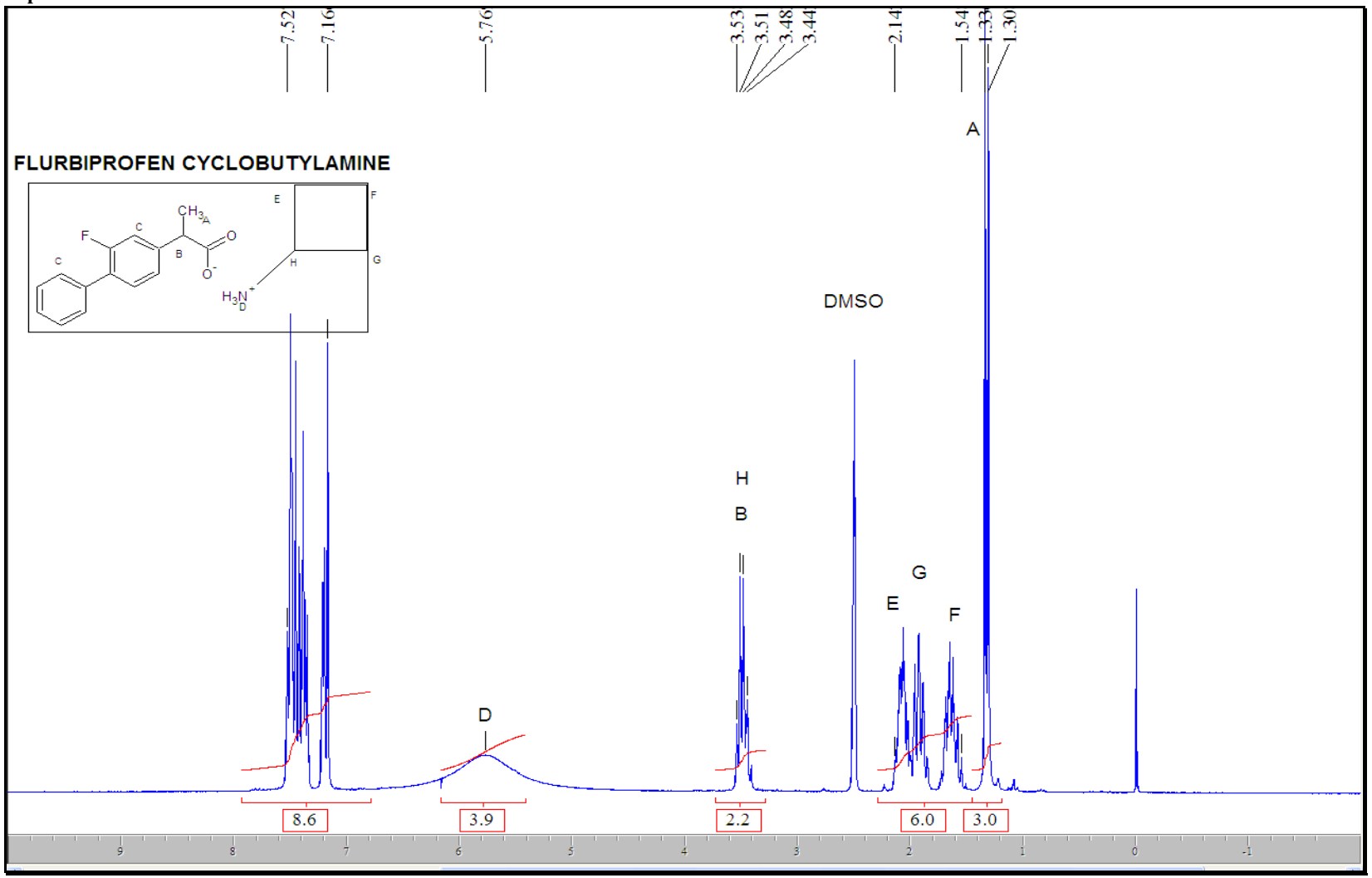

NMR spectrum for FCProp

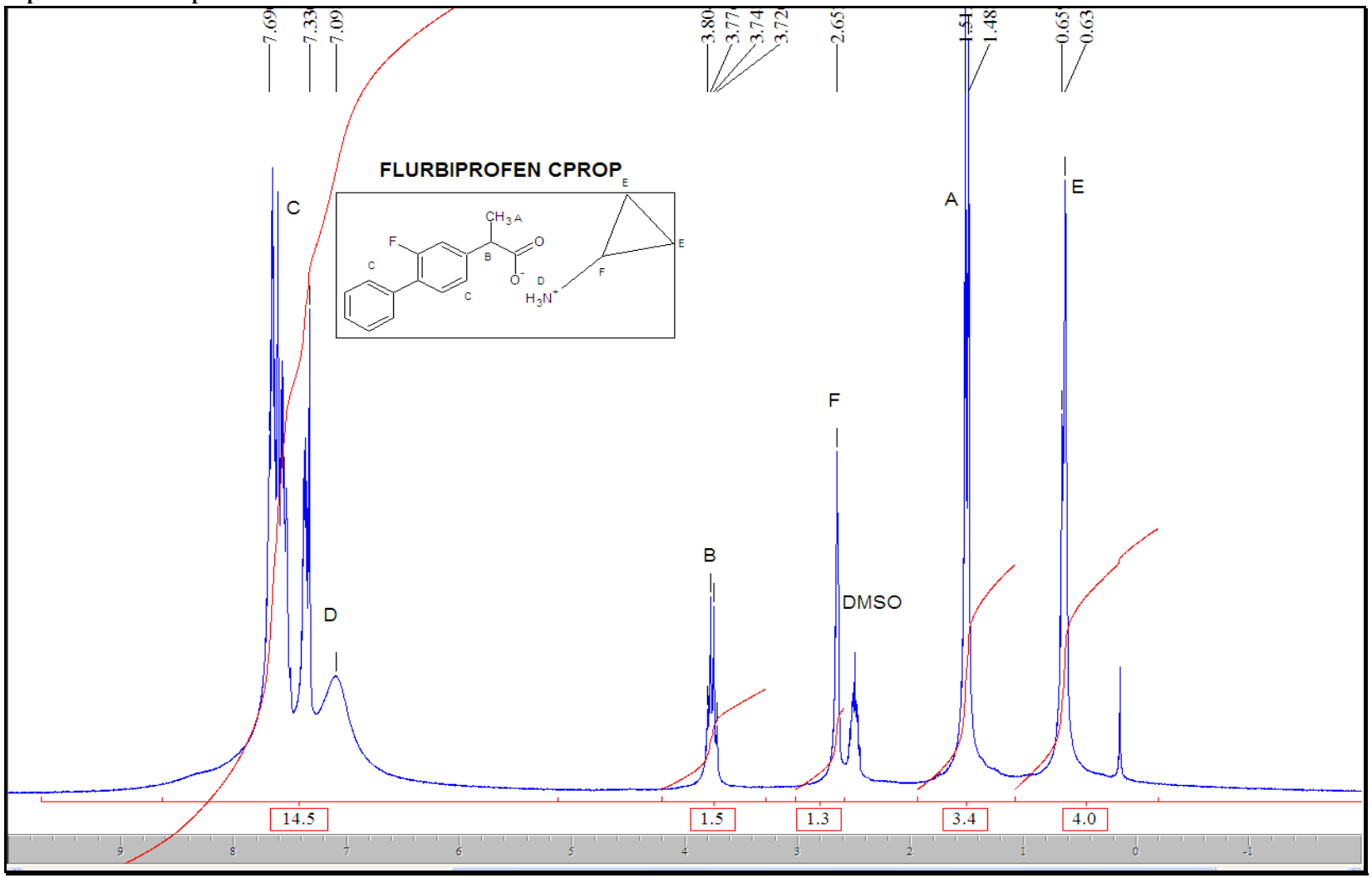

NMR spectrum for FCHex

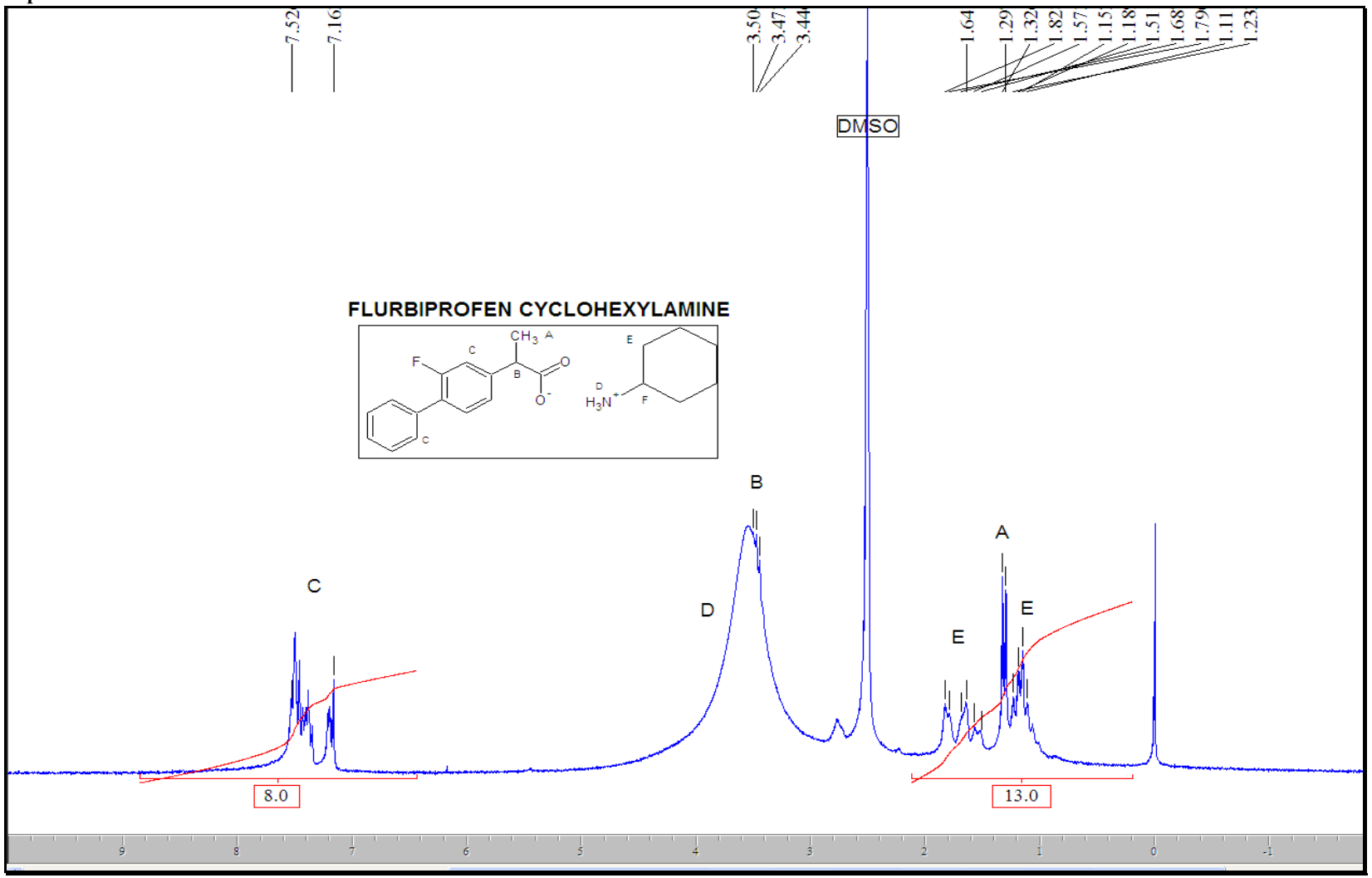

NMR spectrum for FTEA

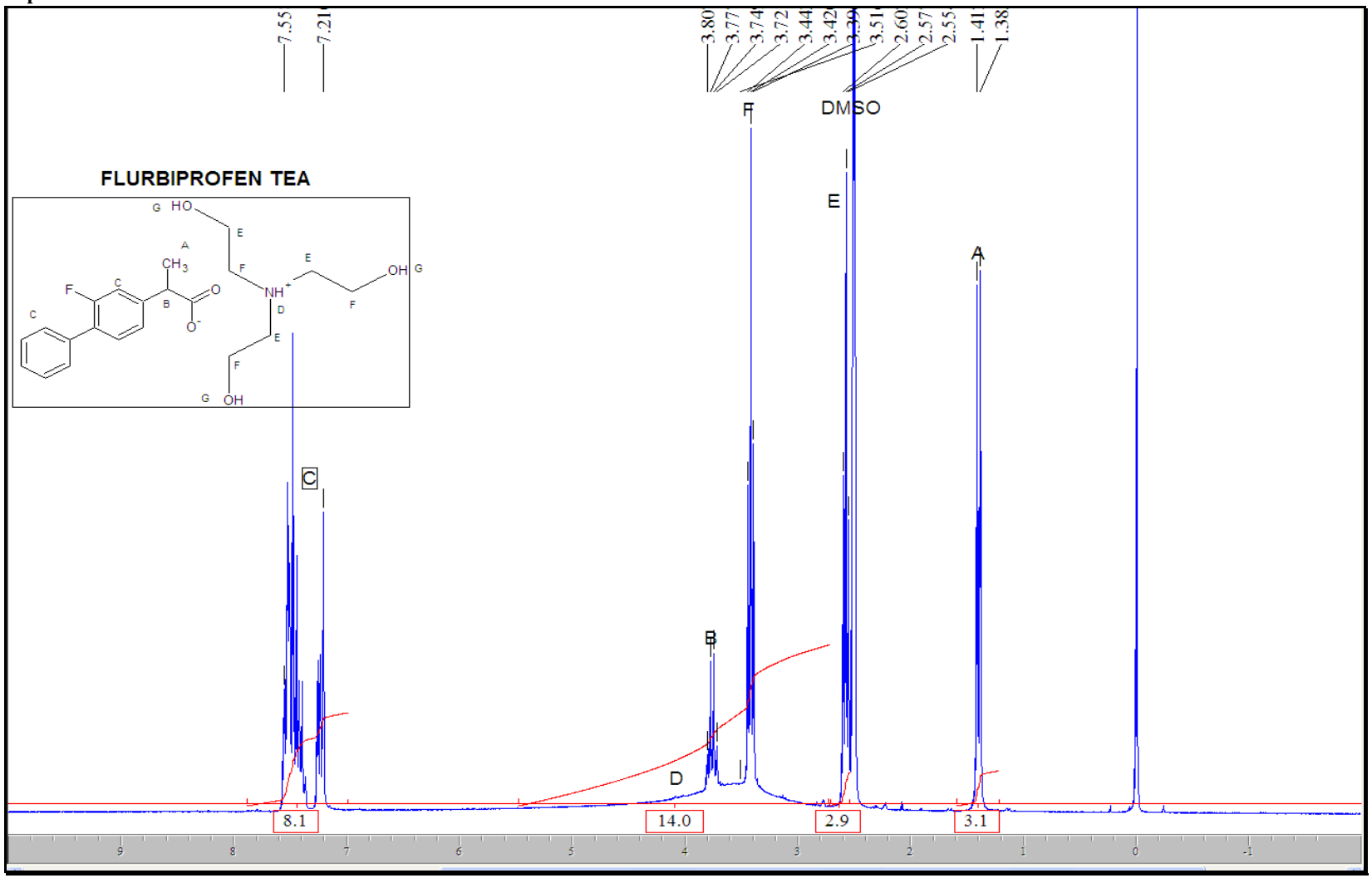

NMR spectra

GEMFIBROZIL

GTBut

δ 1.06 (s, 9H, I)

δ 1.17 (s, 6H, C)

δ 2.07 (s, 3H, B)

δ 2.23 (s, 3H, A)

δ 1.53-1.69 (overlapping m, 4H, E/F)

δ 3.88 (t, 2H, J1= 6.32 Hz, D)

δ 3.97 (bs, 3H, H)

GAMP1

δ 1.04 (s, 6H, I)

δ 1.07 (s, 6H, C)

δ 2.07 (s, 3H, B)

δ 2.24 (s, 3H, A)

δ 1.49-1.70 (overlapping m, 4H, E/F)

δ 3.24 (s, 2H, J)

δ 3.87 (t, 2H, J=6.95 Hz, D)

δ 4.03 (overlapping m, 4H, H/K)

δ 6.61 (d, 1H, J=7.58 Hz, G2)

δ 6.69 (s, 1H, G3)

δ 6.97 (d, 1H, J=7.58 Hz, G1)

GAMP2

δ 0.99 (s, 3H, I)

δ 1.04 (s, 6H, C)

δ 2.07 (s, 3H, A)

δ 2.23 (s, 3H, B)

δ 1.49-1.72 (overlapping m, 4H, E/F)

GTris

δ 1.05 (s, 6H, C)

δ 2.07 (s, 3H, A)

δ 1.49-1.72 (overlaping m, 4H, E/F)

δ 2.23 (s, 3H, B)

δ 3.35 (s, 6H, J)

δ 3.30 (q, 4H, J_1= 4.42 Hz, J_2= 10.74 Hz, J)

δ 3.87 (t, 2H, J= 6.69 Hz, D)

δ 4.82 (overlapping m, 5H, H/K)

δ 6.60 (d, 1H, J= 7.58 Hz, G2)

δ 6.69 (s, 1H, G3)

δ 6.96 (d, 1H, J=7.58 Hz, G1)

δ 3.87 (t, 2H, J= 6.00 Hz, D)

δ 5.23 (overlapping m, 6H, H/K)

δ 6.61 (d, 1H, J= 7.58 Hz, G2)

δ 6.69 (s, 1H, G3)

δ 6.96 (d, 1H, J=7.58 Hz, G1)

GBenz

δ 1.08 (s, 6H, C)

δ 2.08 (s, 3H, B)

δ 2.24 (s, 3H, A)

δ 1.53-1.70 (overlapping m, 4H, E/F)

δ 3.70 (s, 2H, I)

δ 3.88 (t, 2H, J=5.69 Hz, D)

δ 4.86 (bs, 3H, H)

δ 6.61 (d, 1H, J= 7.58 Hz, G2)

δ 6.69 (s, 1H, G3)

δ 6.97 (d, 1H, J=7.58 Hz, G1)

δ 7.18-7.37 (overlapping m, 5H, J)

GAdam

δ 1.08 (s, 6H, C)

δ 1.57 (overlapping m, 16H, I/E/F)

δ 1.99 (s, 3H, J)

δ 2.08 (s, 2H, B)

δ 2.24 (s, 2H, A)

δ 3.50 (m, 3H, H)

δ 3.89 (t, 2H, J=6.31 Hz, D)

δ 6.61 (d, 1H, J= 8.21 Hz, G2)

δ 6.70 (s, 1H, G3)

δ 6.97 (d, 1H, J=7.58 Hz, G1)

GCHex

δ 1.05 (s, 6H, C)

δ 1.13-1.22 (overlapping m, 2H, L)

δ 1.52-1.80 (overlapping m, 6H, E/F/K)

δ 2.07 (s, 3H, B)

δ 2.23(s, 3H, A)

δ 2.64 (overlapping m, 1H, I)

δ 3.76 (bs, 3H, H)

δ 3.87 (t, 2H, J= 6.32 Hz, D)

δ 6.61 (d, 1H, J= 7.58 Hz, G2)

δ 6.69 (s, 1H, G3)

δ 6.97 (d, 1H, J=7.58 Hz, G1)

NMR spectrum for GCHex

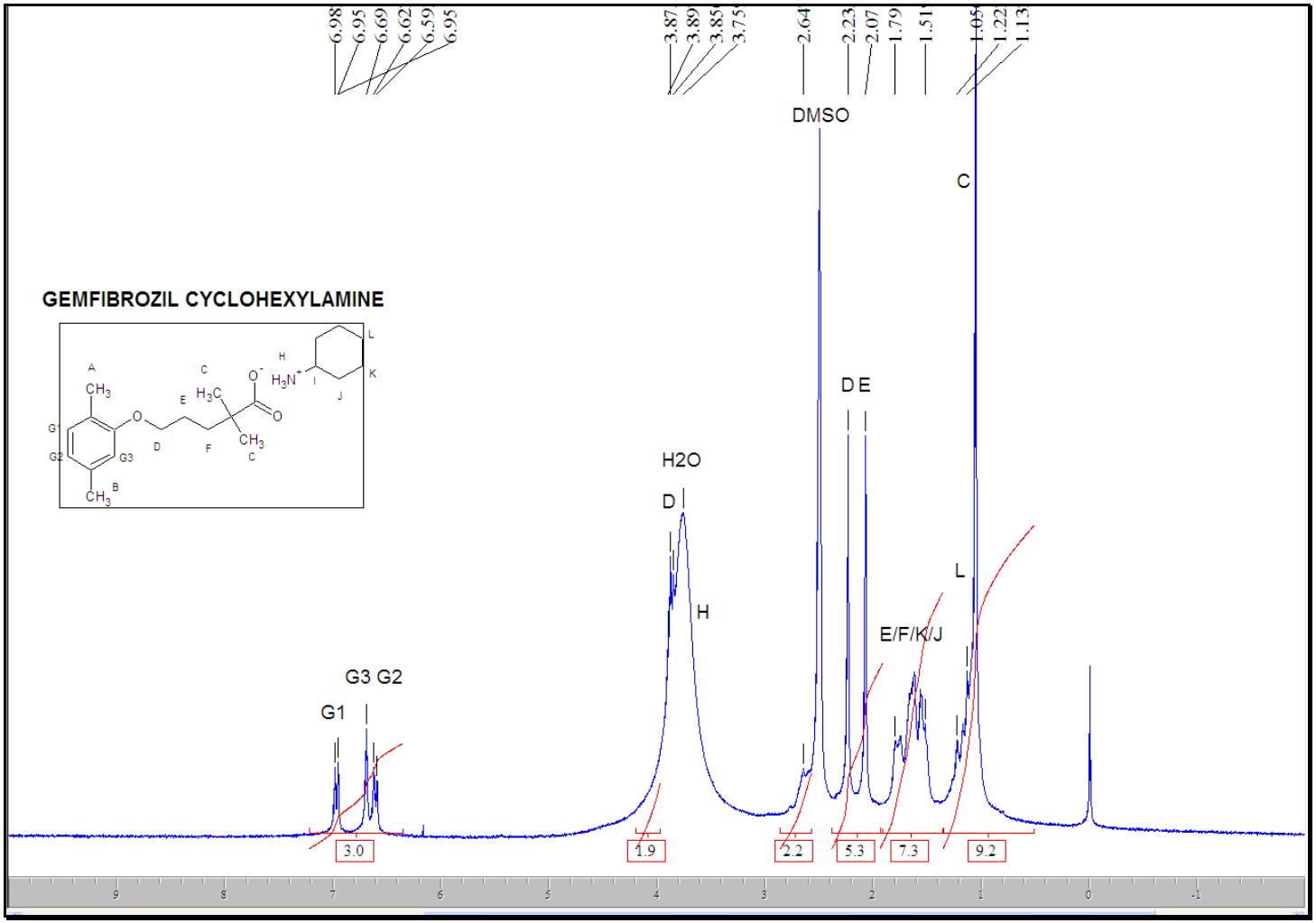

NMR spectrum for GTBut

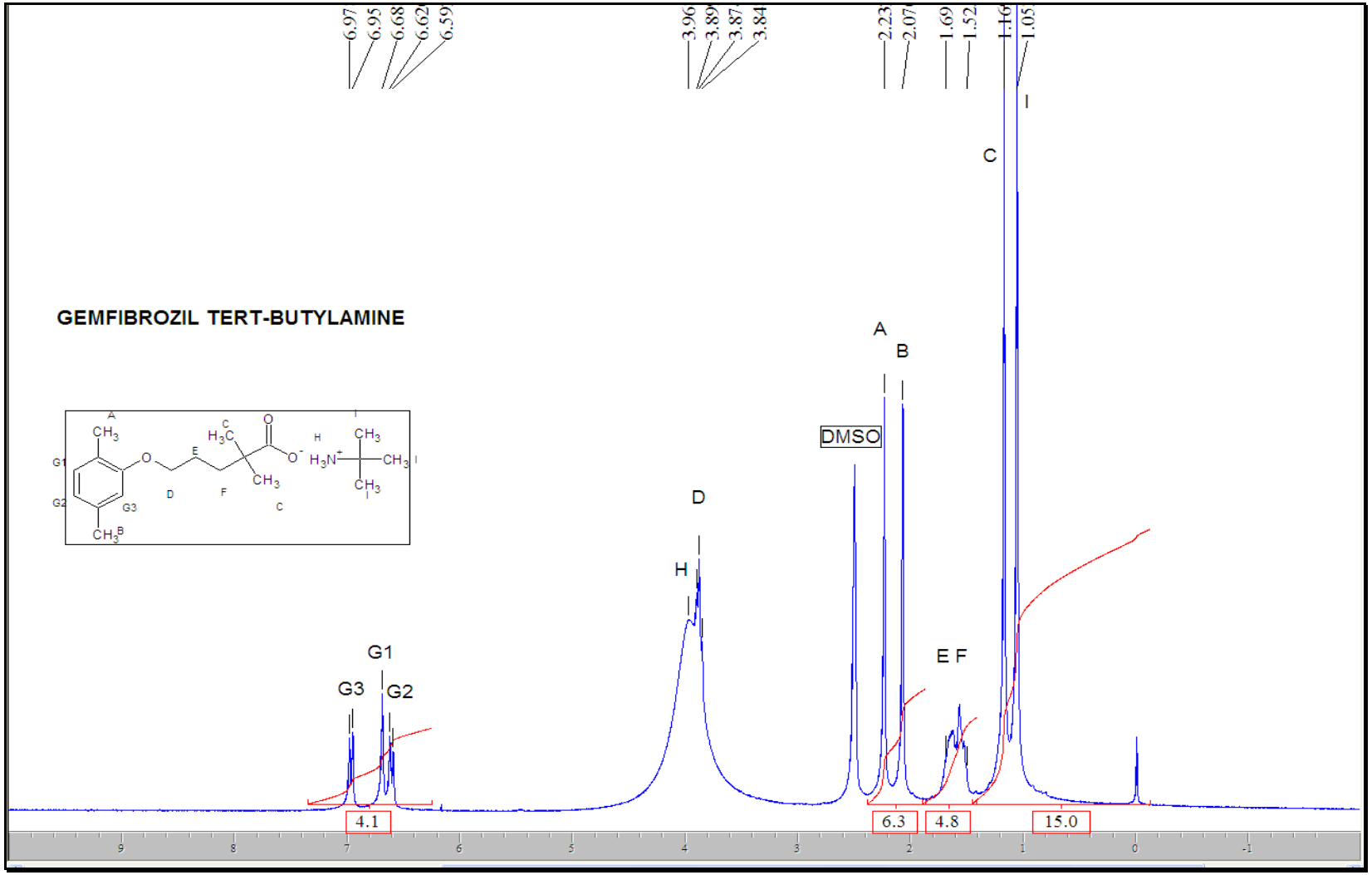

NMR spectrum for GAMP1

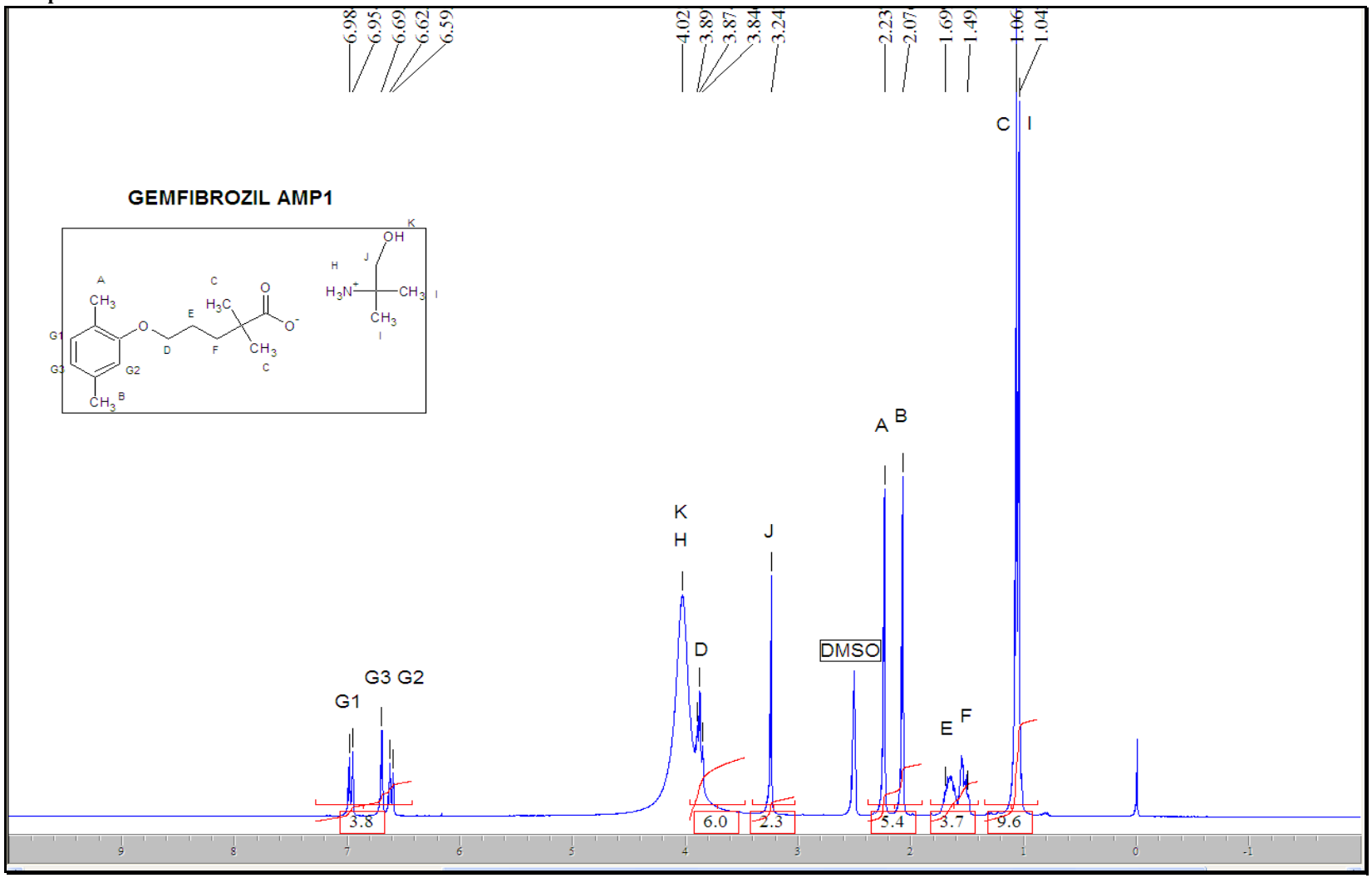

NMR spectrum for GAMP2

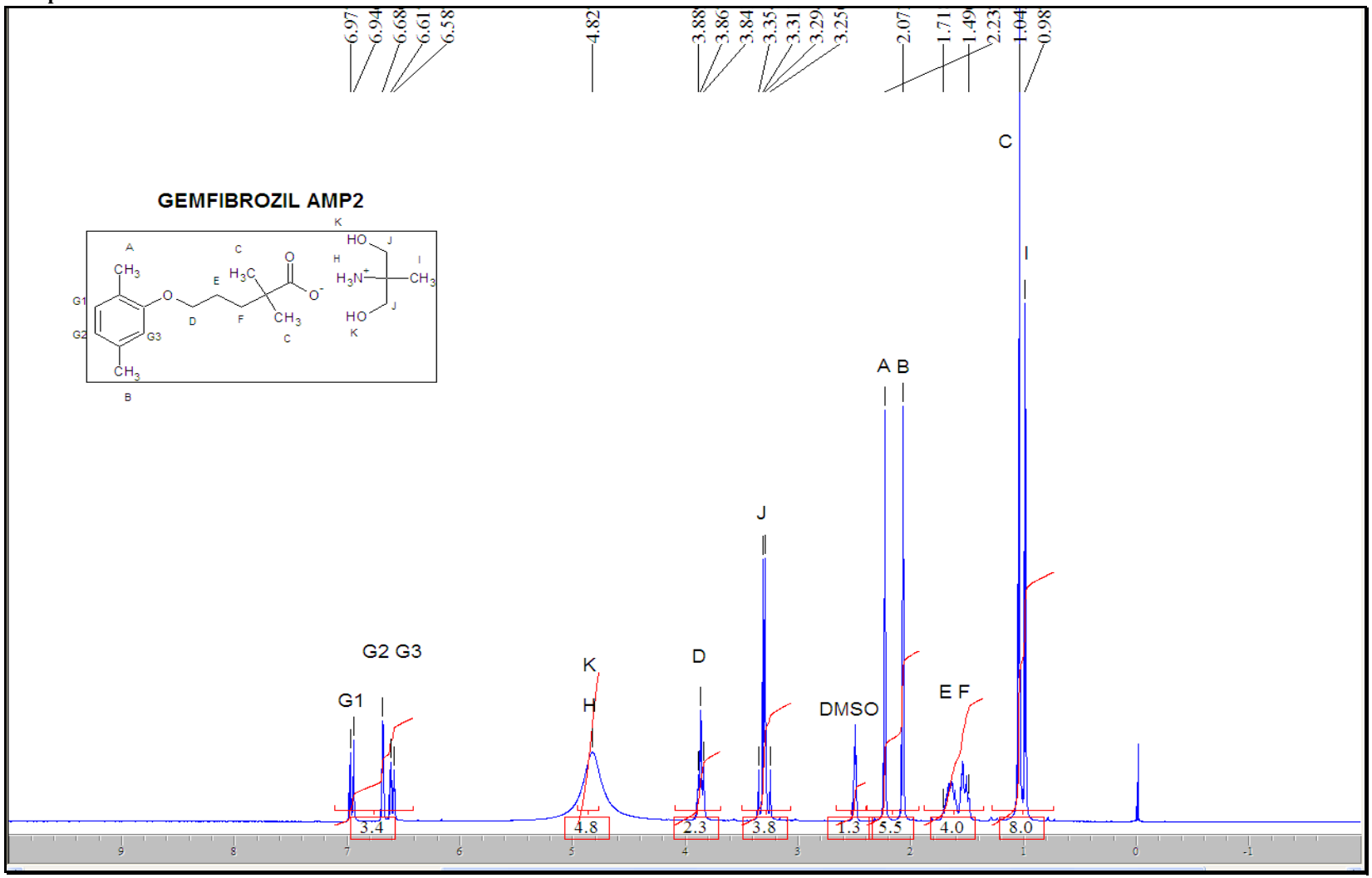

NMR spectrum for GTris

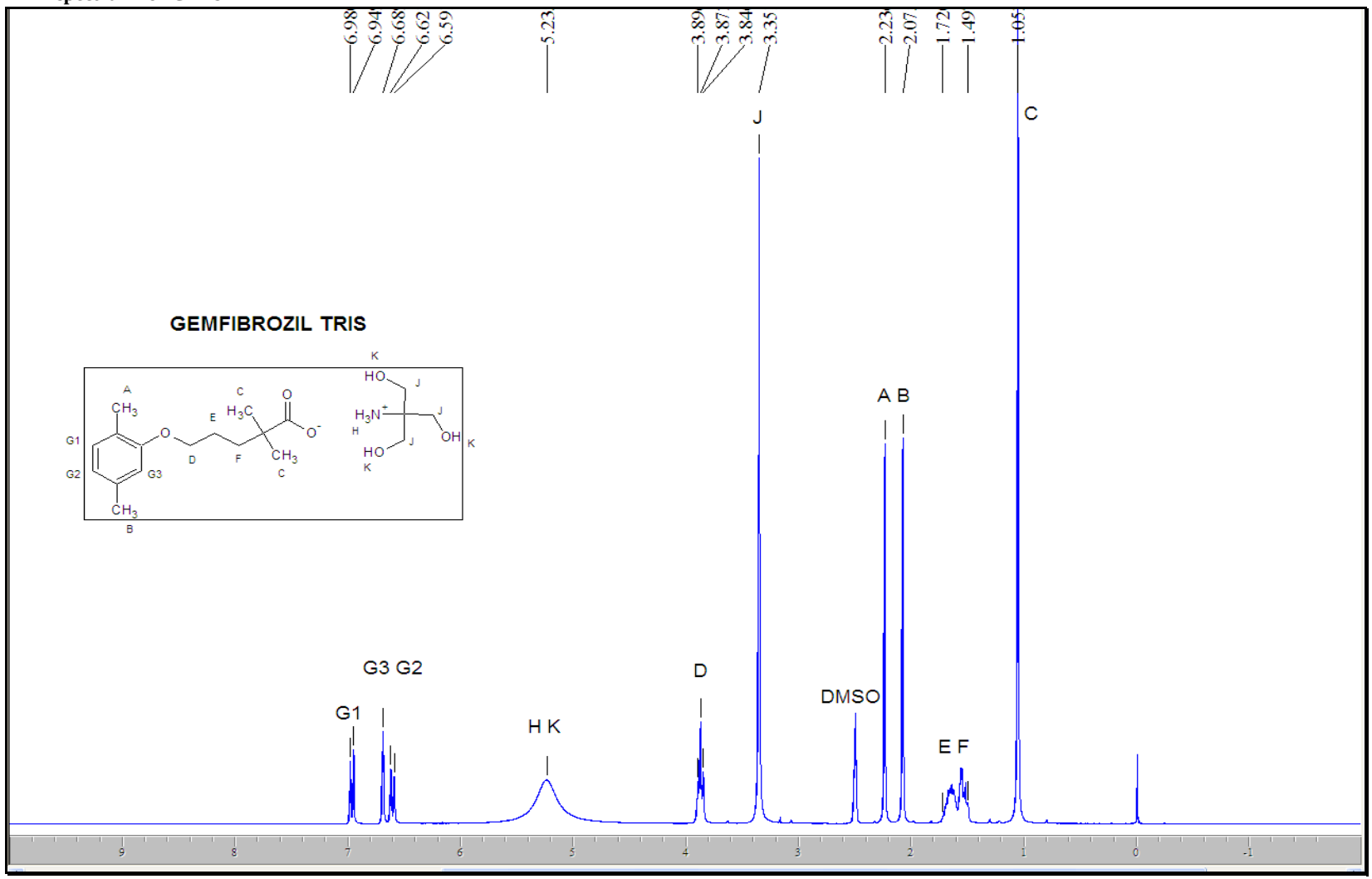

NMR spectra

DICLOFENAC

DICLOFENAC

δ 3.37 (bs, 2H, C)

δ 3.69 (s, 2H, A)

δ 6.26-7.54 (overlapping m, 7H, B)

δ 12.76 (s, 1H, D)

DMEA

δ 2.80 (t, 2H, J= 5.05 Hz, D)

δ 3.44 (s, 2H, A)

δ 3.52 (overlapping m, 4H, G/F)

δ 3.55 (t, 2H, J=5.05 Hz, E)

δ 6.25-7.49 (overlapping m, 7H, B)

δ 9.60 (bs, 1H, C)

DDEA

δ 2.85 (t, 4H, J= 5.05 Hz, D)

δ 3.50 (s, 2H, A)

δ 3.80 (overlapping m, 5H, G/F)

δ 3.58 (t, 4H, J=5.05 Hz, E)

δ 6.24-7.49 (overlapping m, 7H, B)

δ 8.96 (bs, 1H, C)

DTEA

δ 2.62 (t, 6H, J= 6.32 Hz, D)

δ 3.66 (s, 2H, A)

δ 3.52 (overlapping m, 6H, G/F)

δ 3.44 (t, 6H, J=6.32 Hz, E)

δ 6.25-7.49 (overlapping m, 7H, B)

δ 9.60 (bs, 1H, C)

DTBut

δ 1.21 (s, 9H, D)

δ 3.39 (s, 2H, A)

DAMP1

δ 1.13 (s, 6H, D)

δ 3.31 (s, 2H, E)

δ 7.22-7.47 (overlapping m, 7H, B)

δ 8.08 (bs, 3H, E)

δ 9.95 (s, 1H, C)

δ 3.34 (overlapping m, 3H, F)

δ 3.42 (s, 2H, A)

δ 6.25-7.44 (overlapping m, 7H, B)

δ 6.95 (overlapping m, 1H, G)

δ 9.71 (s, 1H, C)

DAMP2

δ 1.04 (s, 3H, D)

δ 3.36 (d, 4H, J=5.69 HZ, E)

δ 3.37 (overlapping m, 3H, F)

δ 3.44 (s, 2H, A)

δ 6.24-7.47 (overlapping m, 7H, B)

δ 6.12 (obs, 2H, G)

δ 9.45 (s, 1H, C)

DTris

δ 3.18 (s3H, F)

δ 3.41 (s, 6H, D)

δ 3.49 (s, 2H, A)

δ 5.31 (bs, 3H, E)

δ 6.25-7.50 (overlapping m, 7H, B)

δ 9.18 (s, 1H, C)

DBenz

δ 3.48 (s, 2H, A)

δ 3.49 (bs, 3H, F)

δ 3.94 (s, 2H, D)

δ 6.24-7.49 (overlapping m, 12H, B/E)

9.33 (s, 1H, C)

DCHex

δ 1.51-1.84 (overlapping m, 10H, D/E/F)

δ 2.85 (bs, 3H, H)

δ 3.16 (s, 1H, G)

δ 3.40 (s, 2H, A)

δ 6.32-7.47 (overlapping m, 7H, B)

δ 9.79 (s, IH, C)

DAdam

δ 1.50-1.73 (overlapping m, 7H, B)

δ 2.02 (s, 3H, E)

δ 3.39 (s, 2H, A)

δ 6.23-7.48 (overlapping m, 7H, B)

δ 7.86 (bs, 3H, F)

NMR spectrum for DAdam

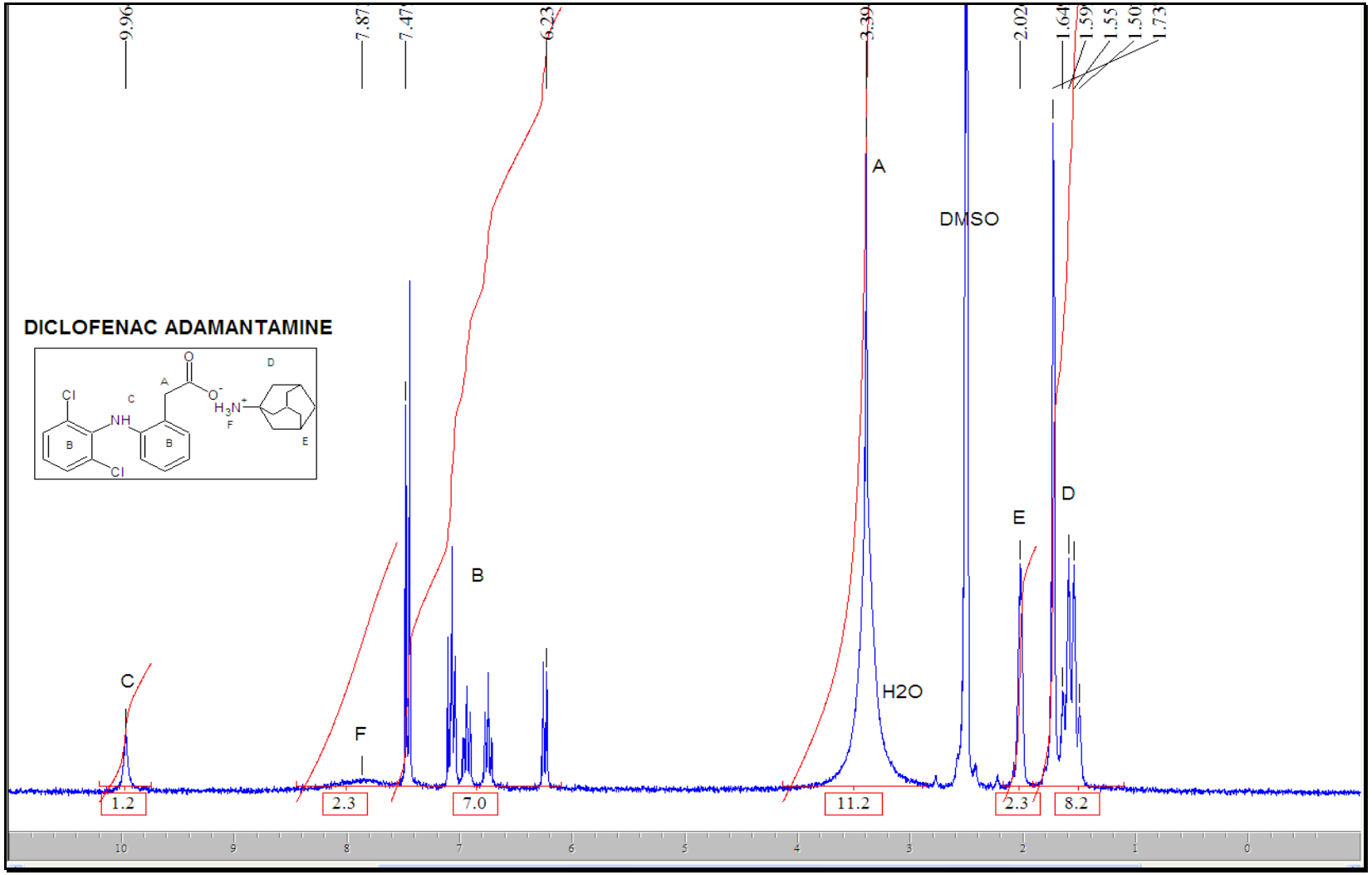

NMR spectrum for DBenz

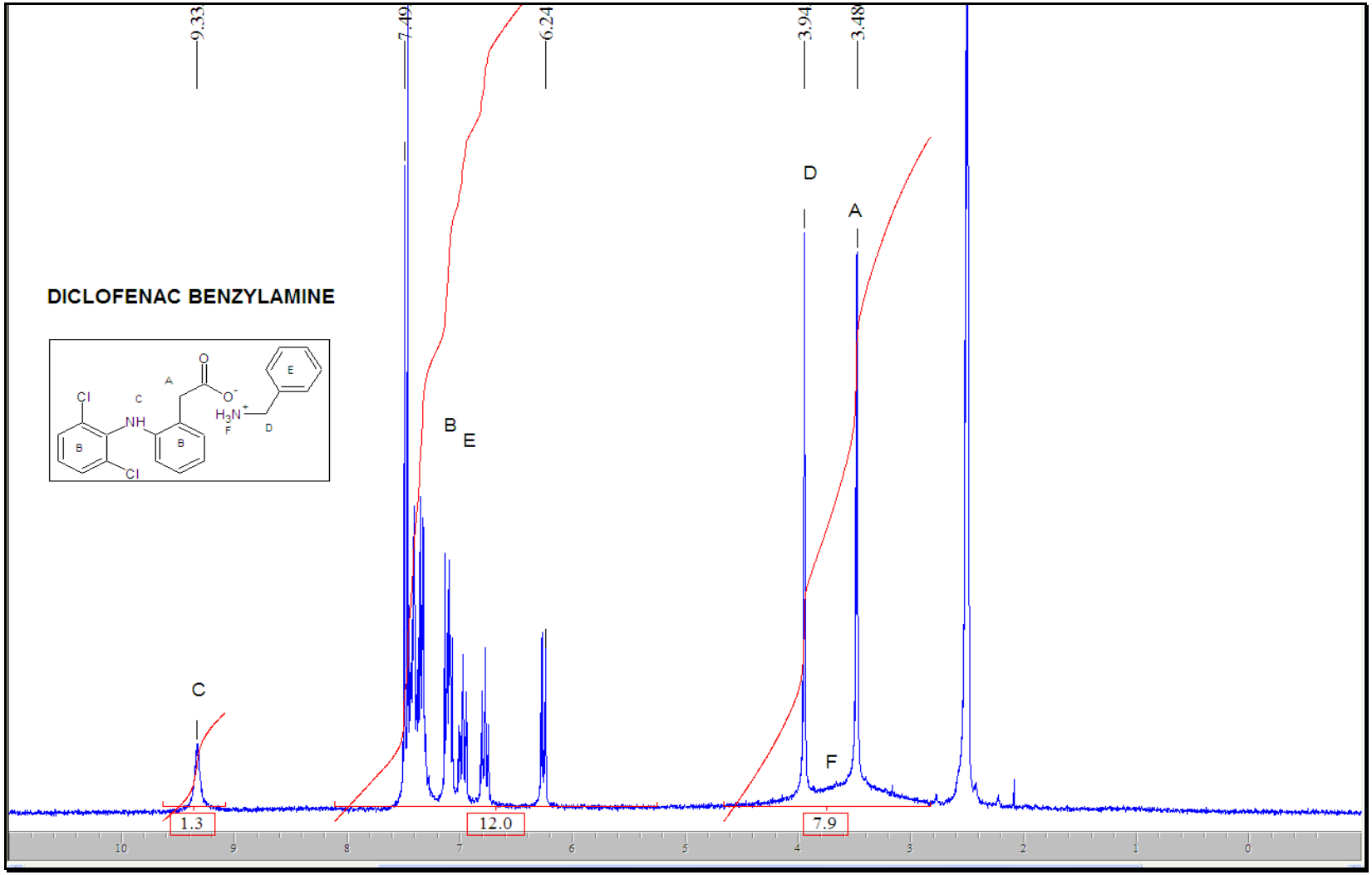

NMR spectrum for DCHex

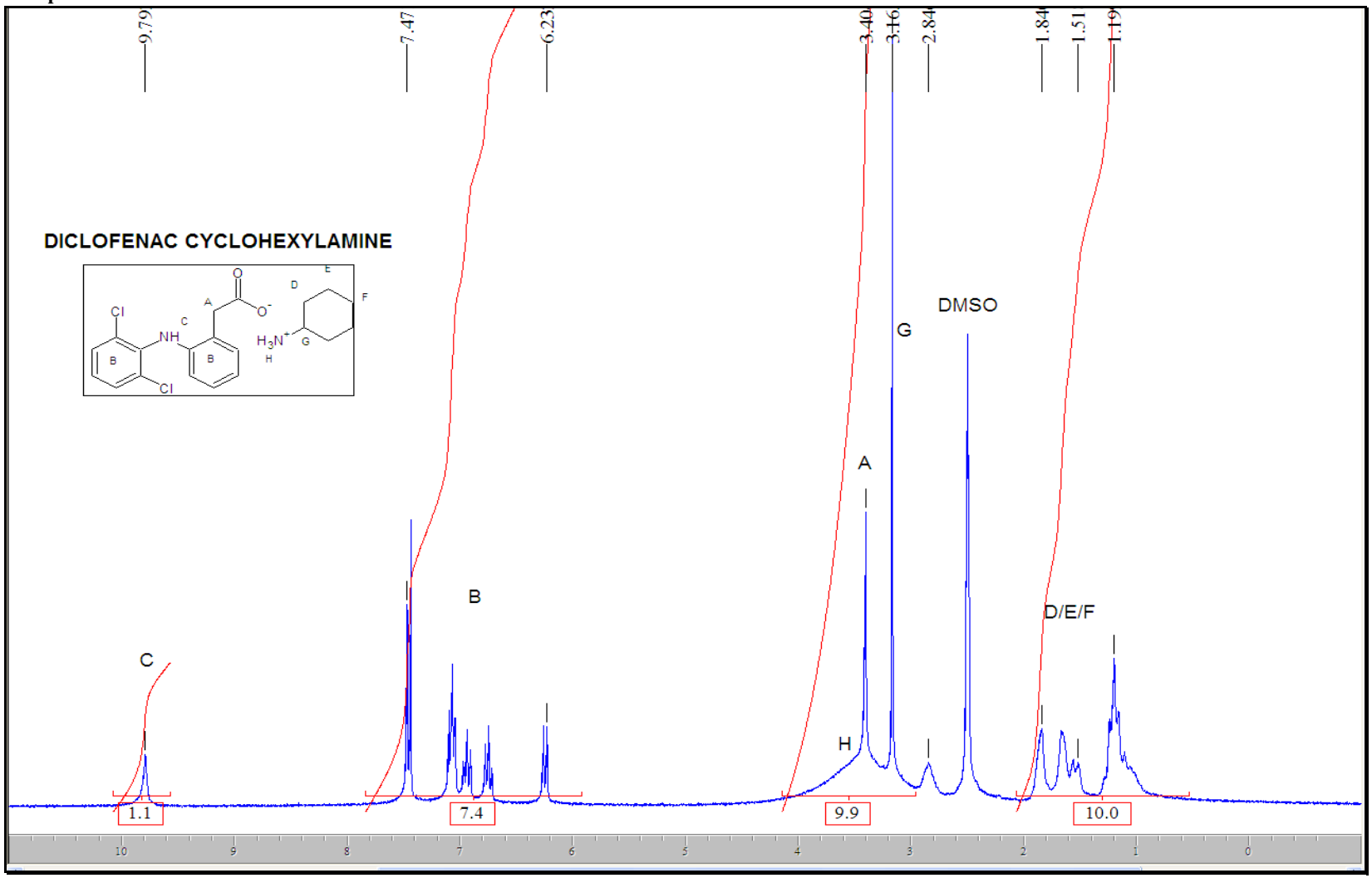

NMR spectrum for DTBut

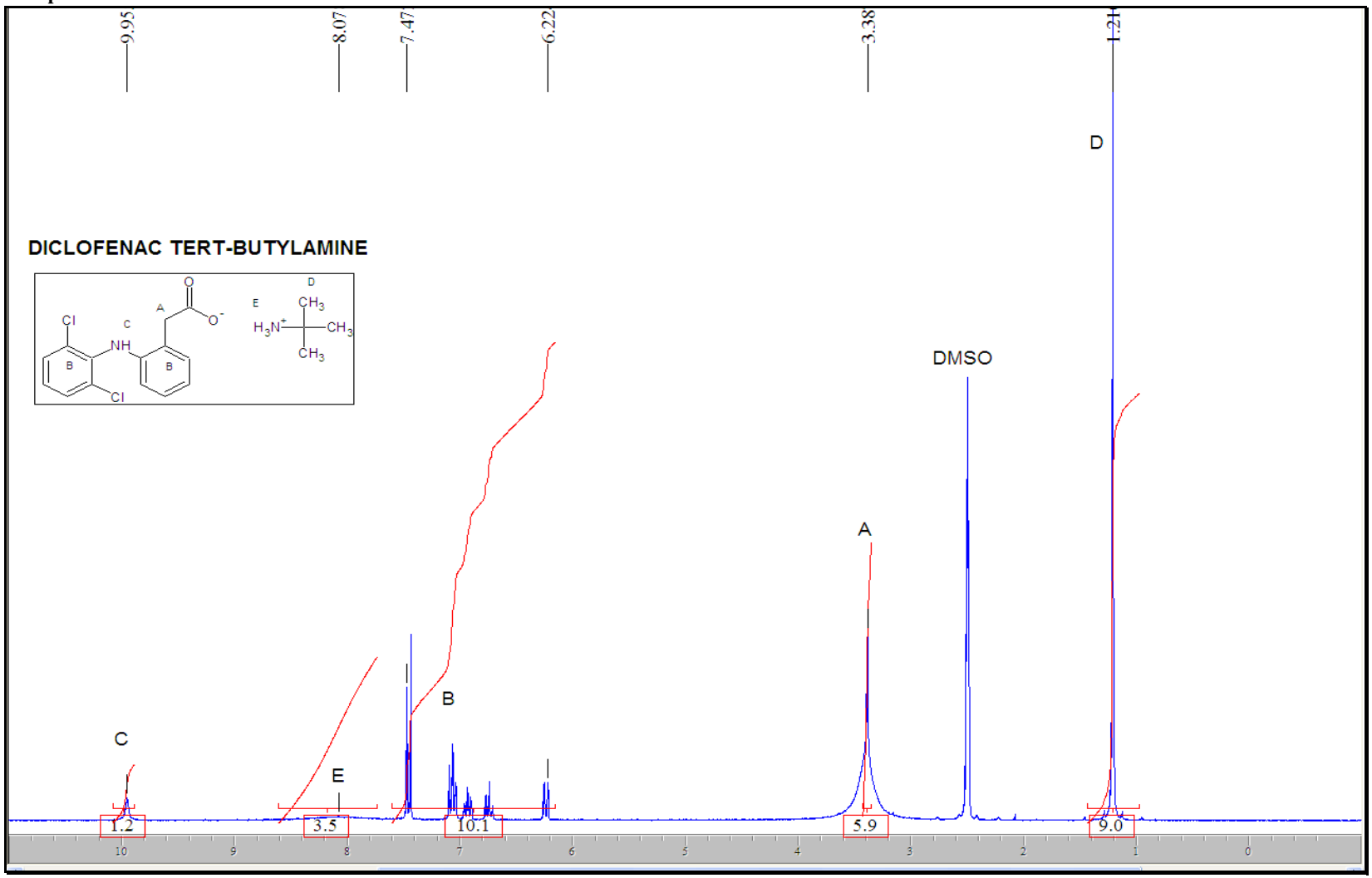

NMR spectrum for DAMP1

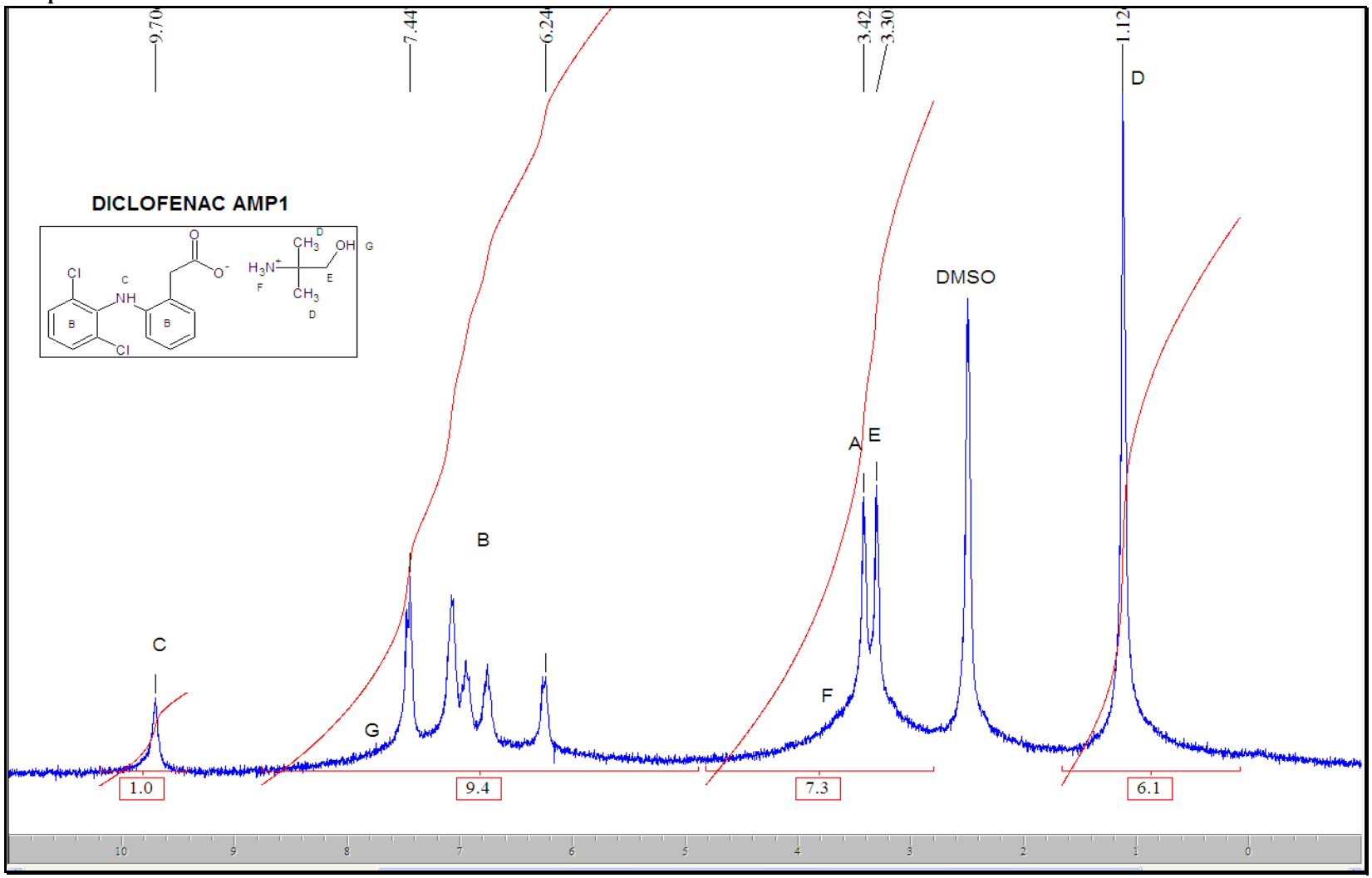

NMR spectrum for DAMP2

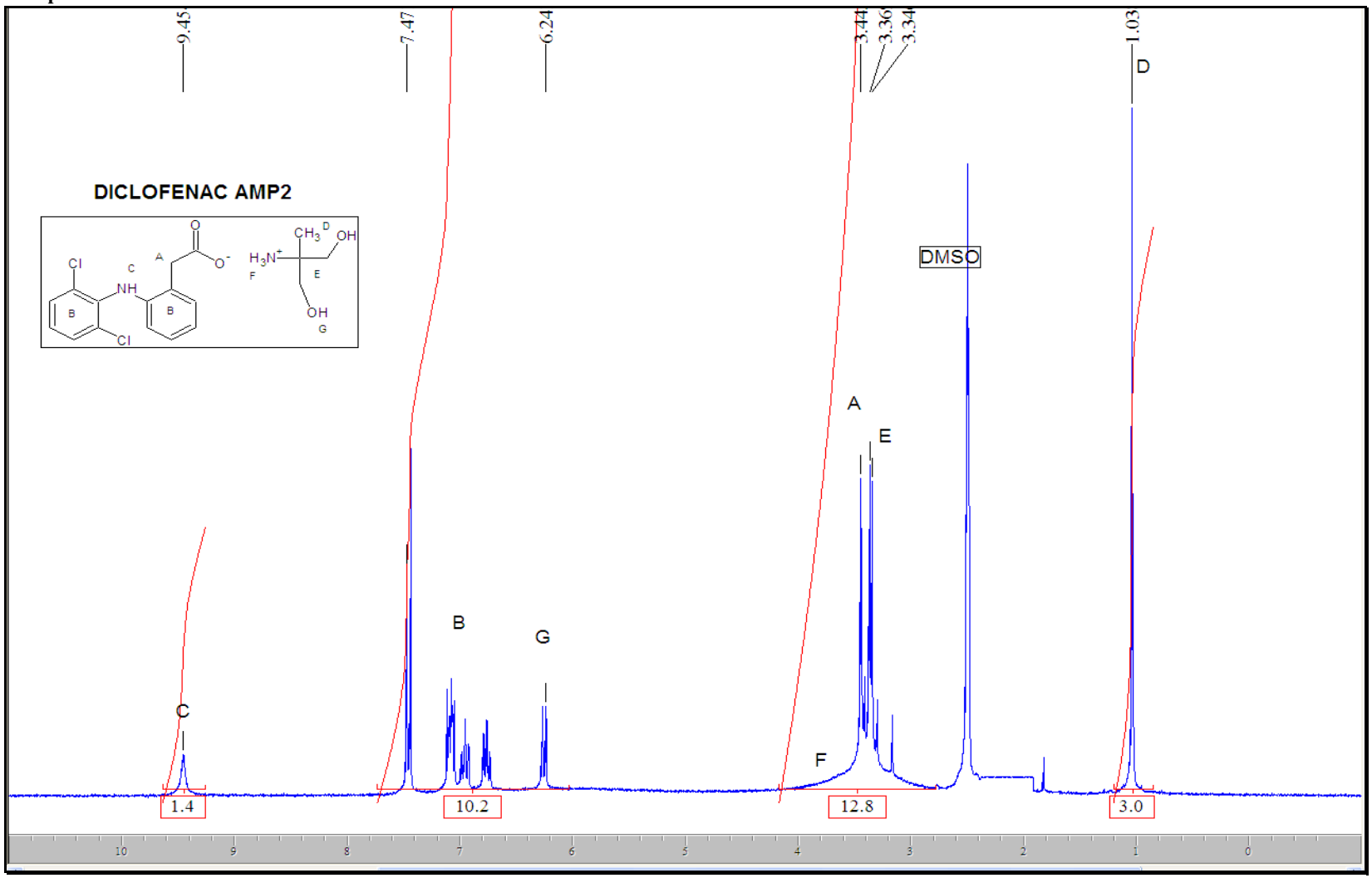

NMMR spectrum for DTris

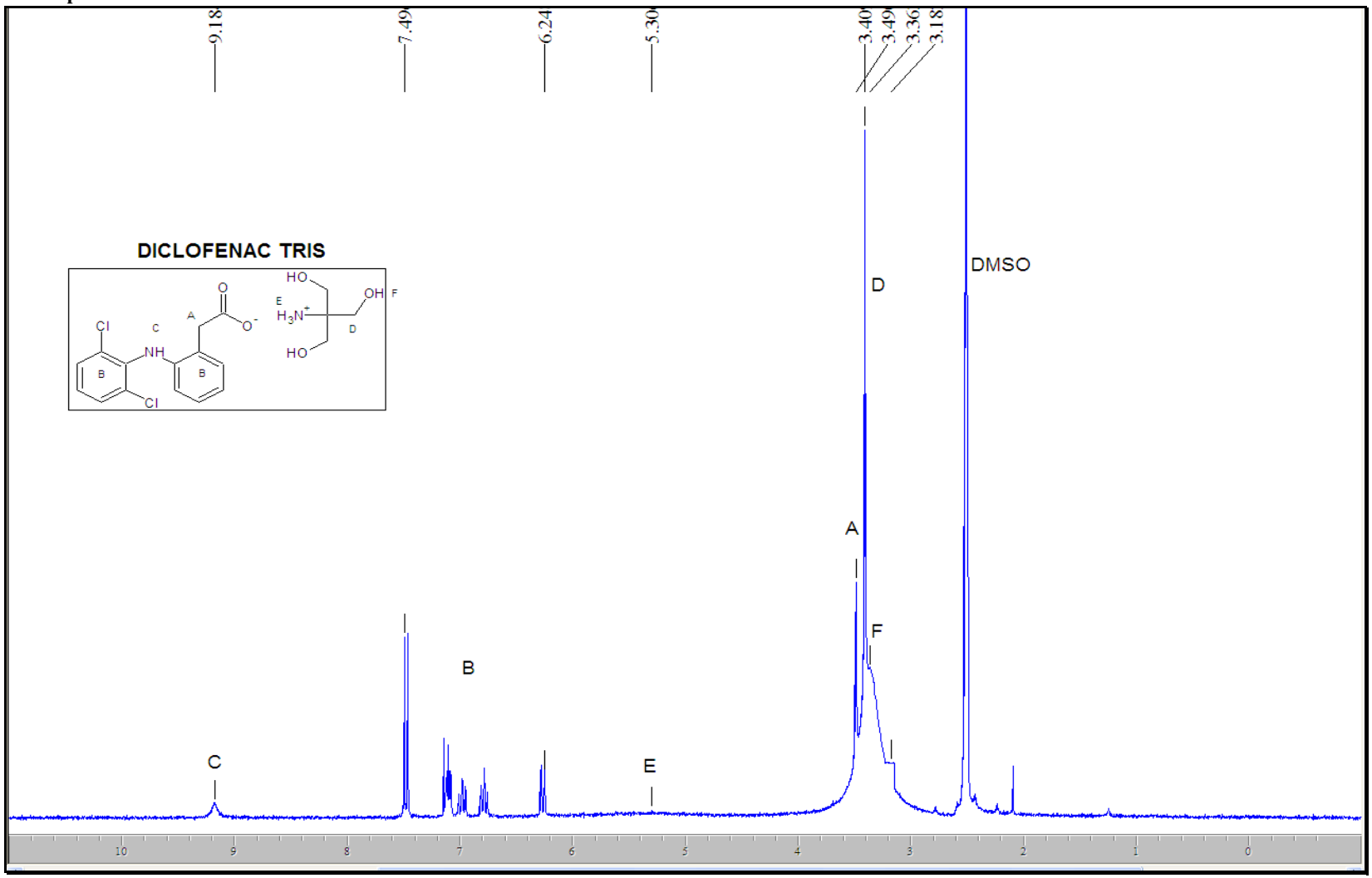

NMR spectrum for DDEA

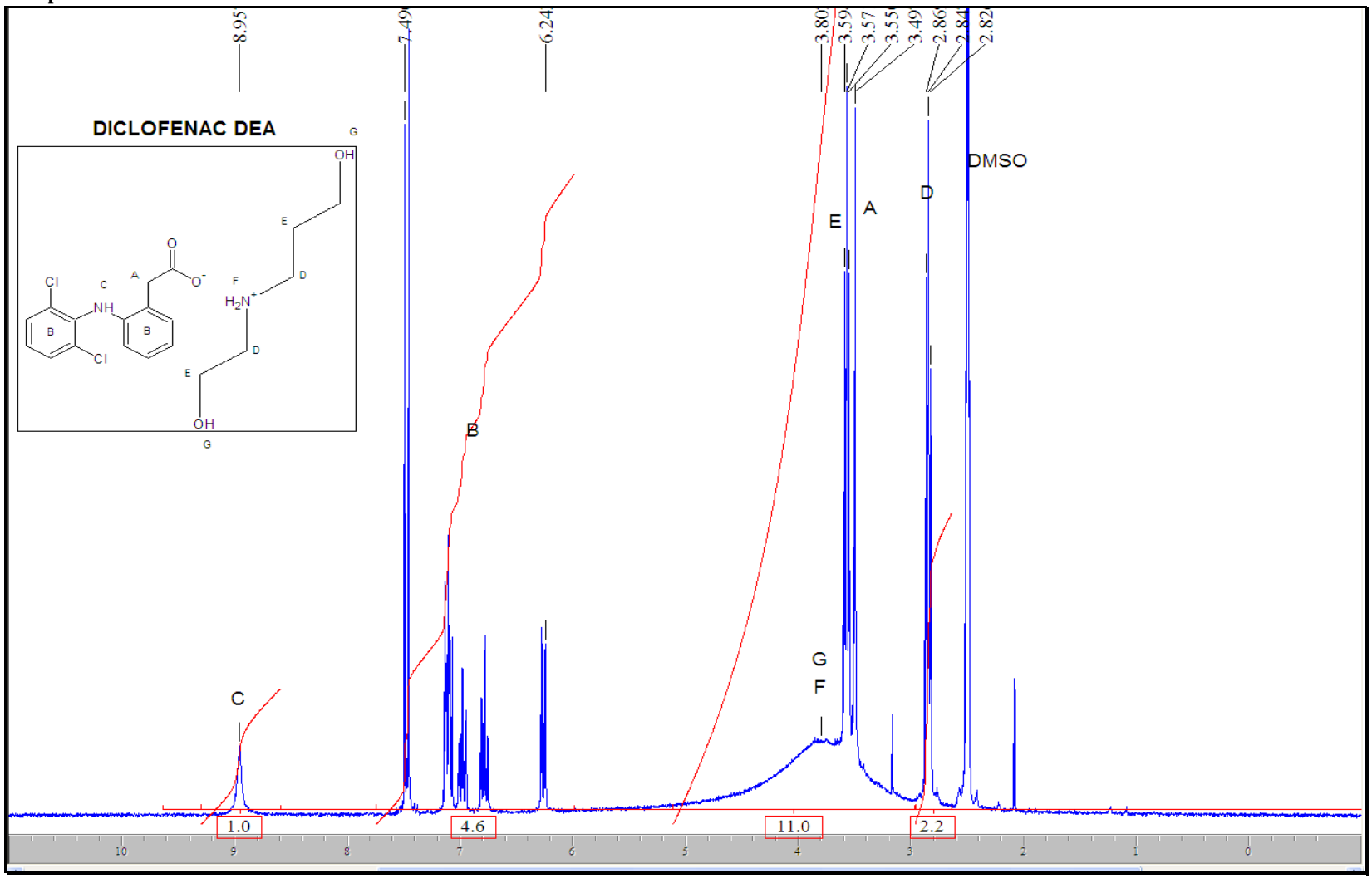

NMR spectrum for DTEA

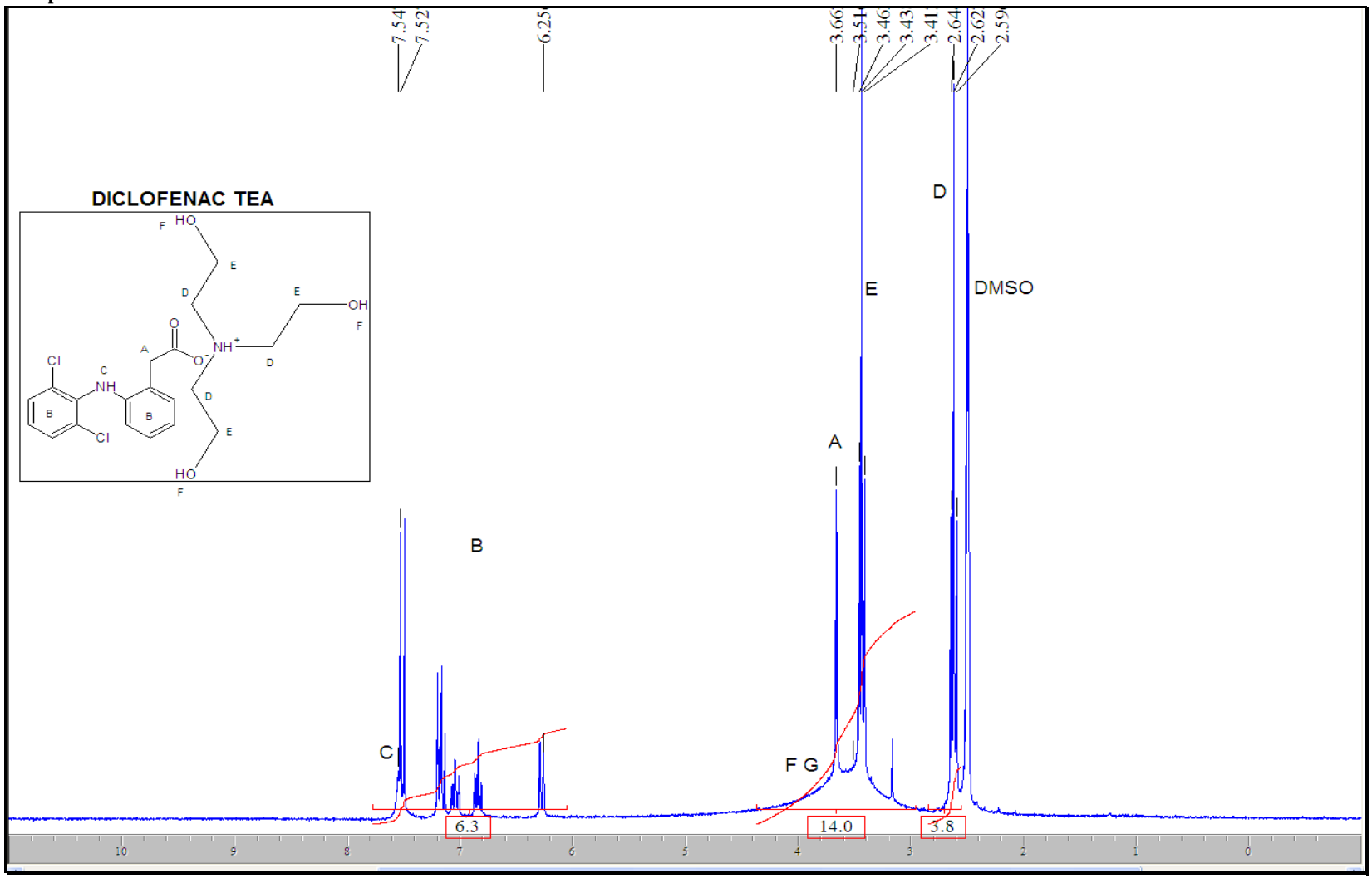

APPENDIX C

DSC Thermograms

FLURBIPROFEN

DSC thermogram for FAdam

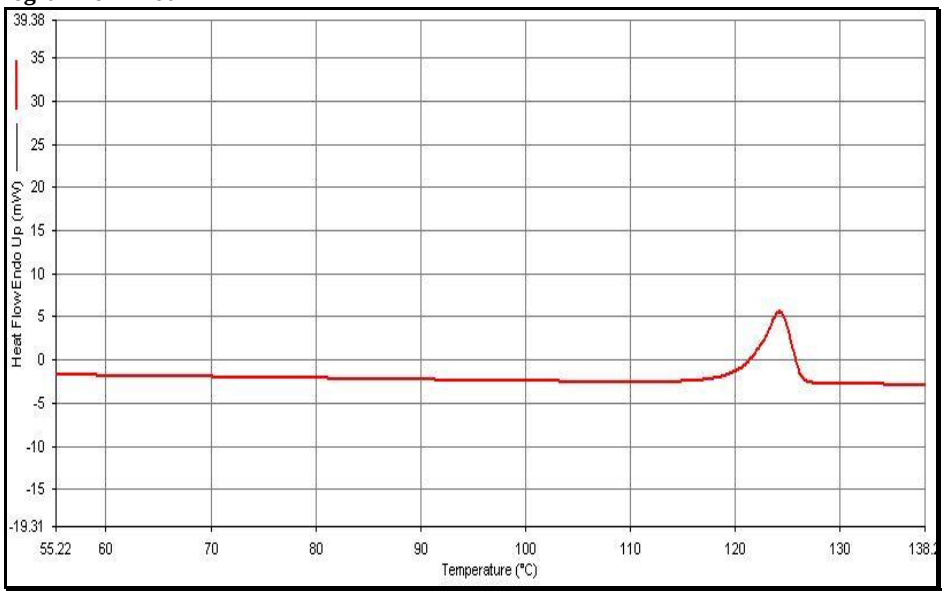

DSC thermogram for FBenz

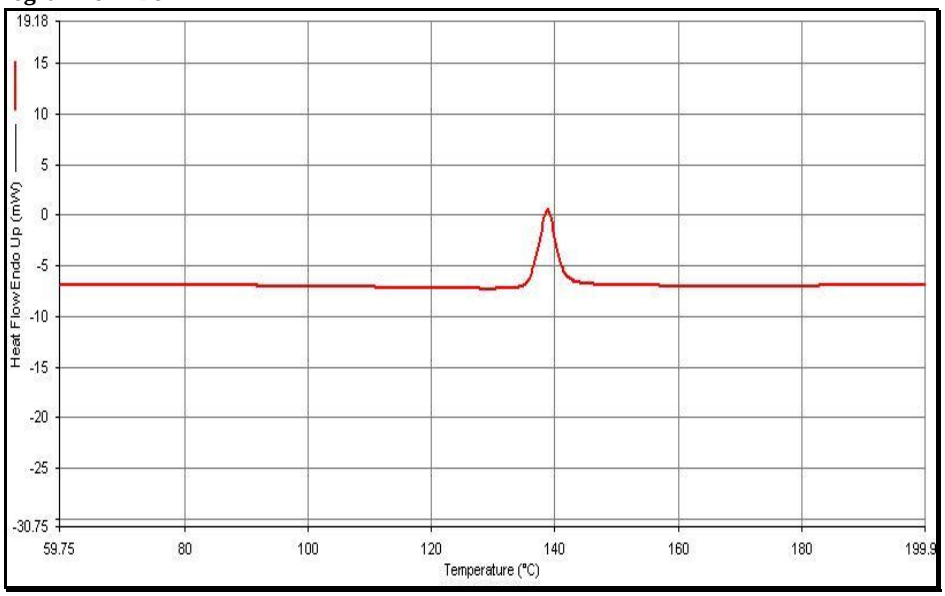

DSC thermogram for FCProp

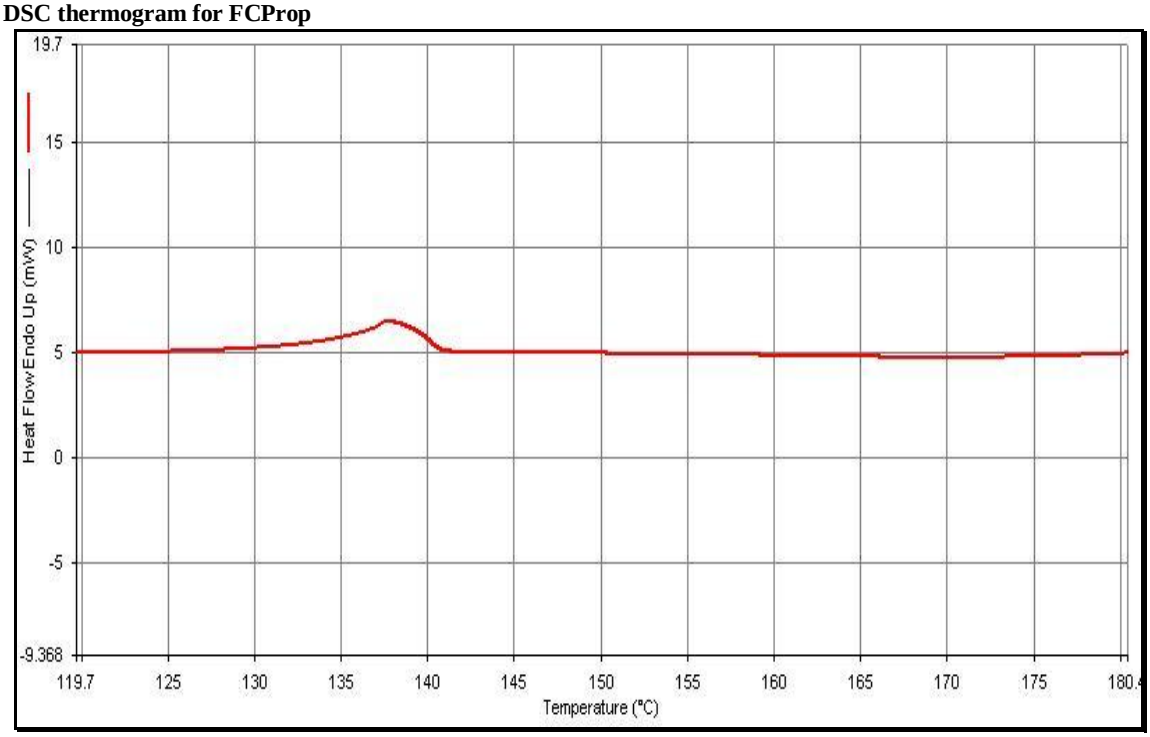

DSC thermogram for FCBut

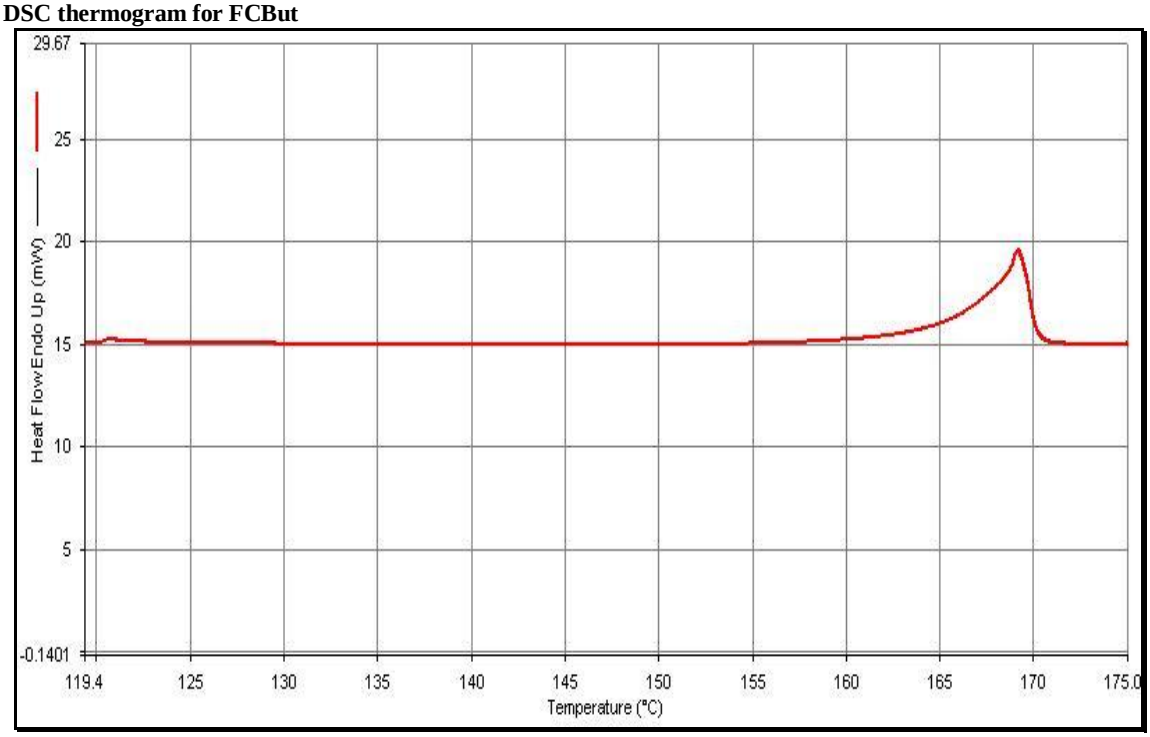

DSC thermogram for FCHex

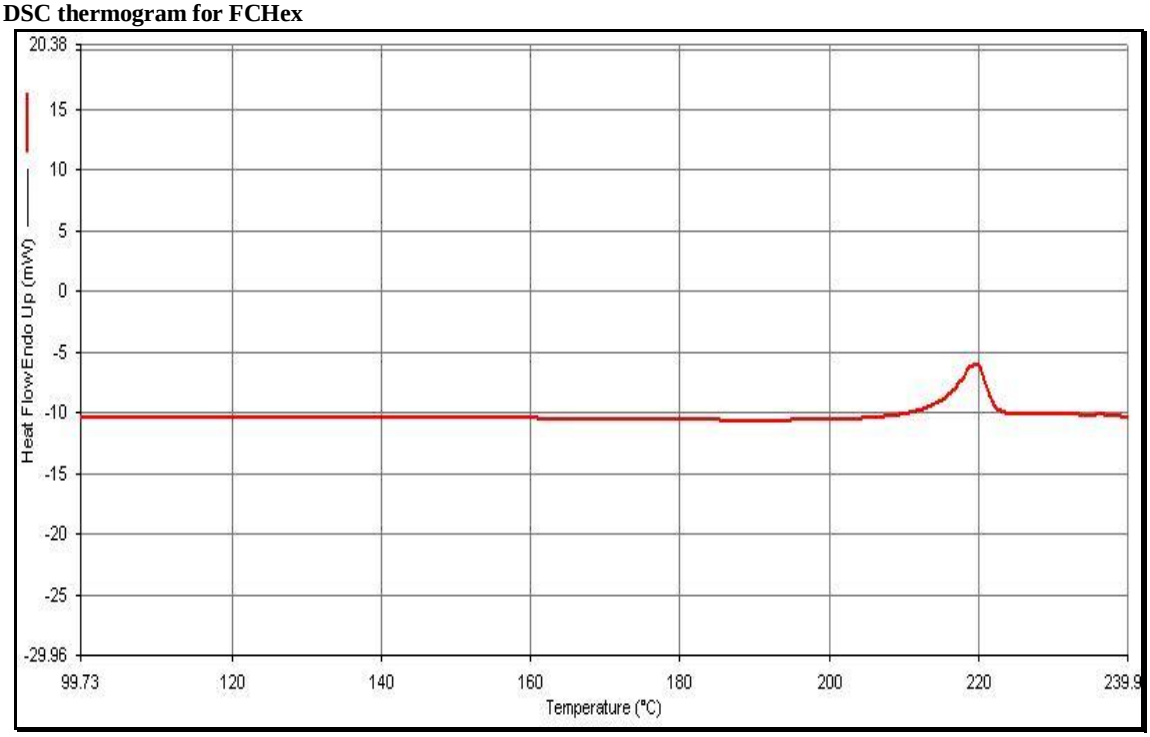

DSC thermogram for FTBut

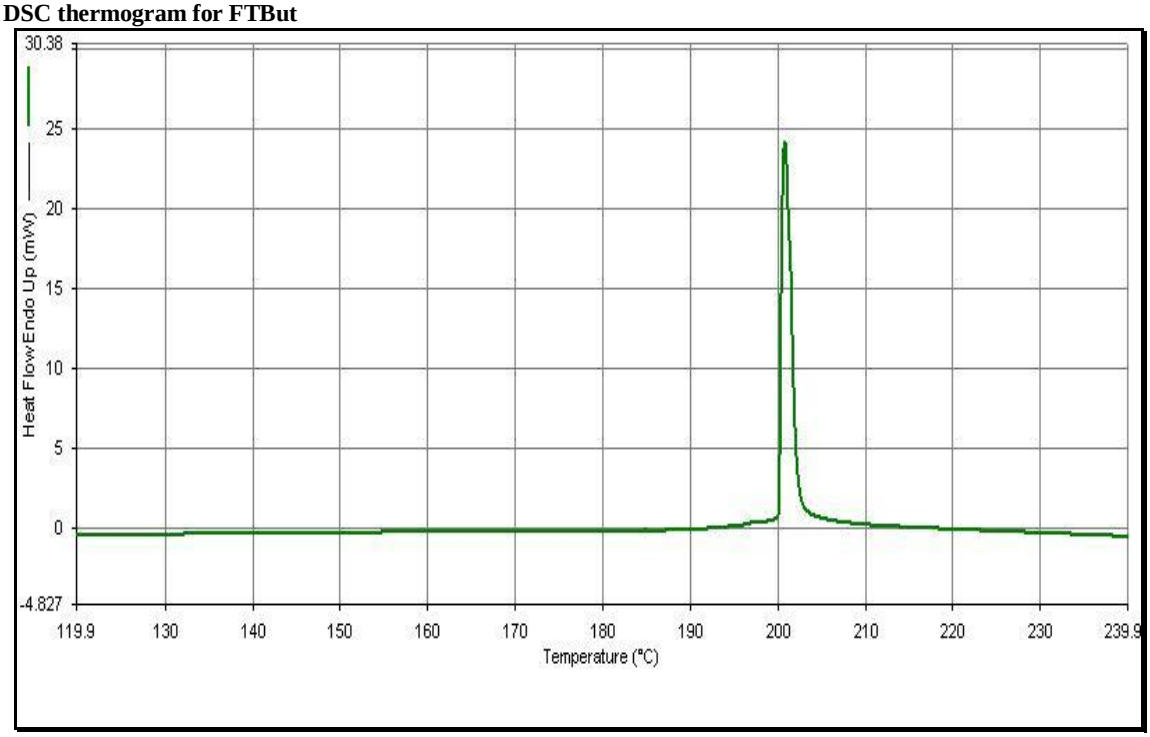

DSC thermogram for FAMP1

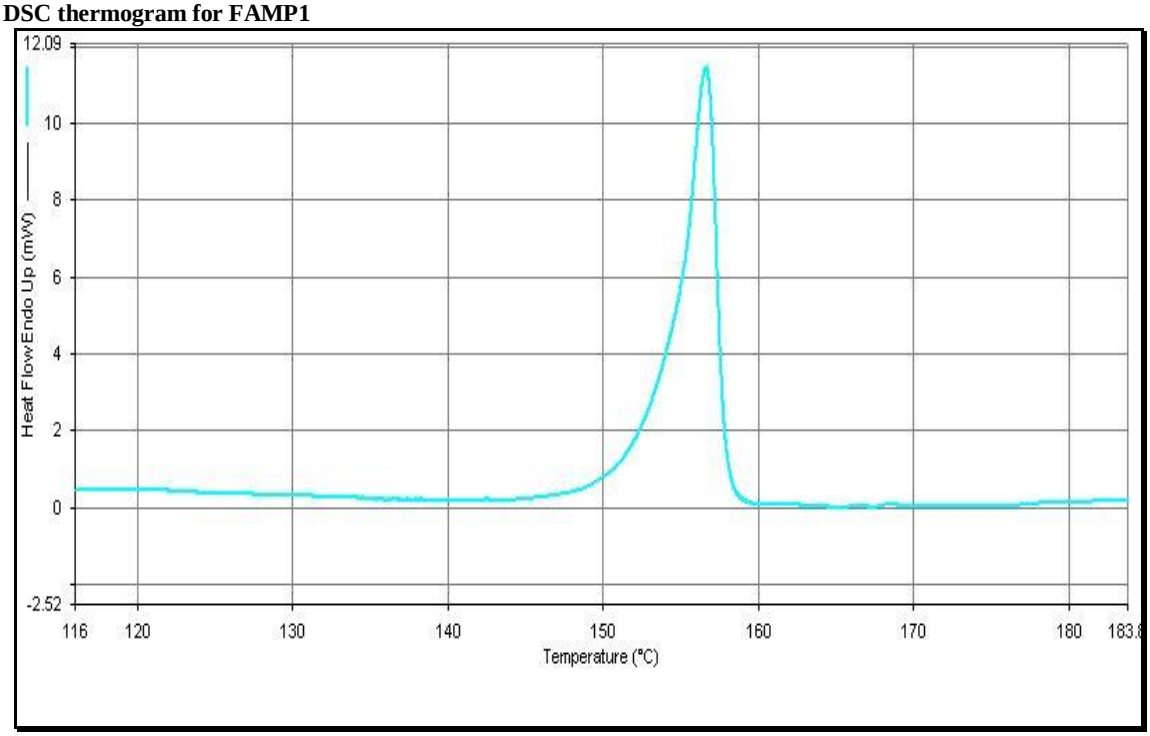

DSC thermogram for FAMP2

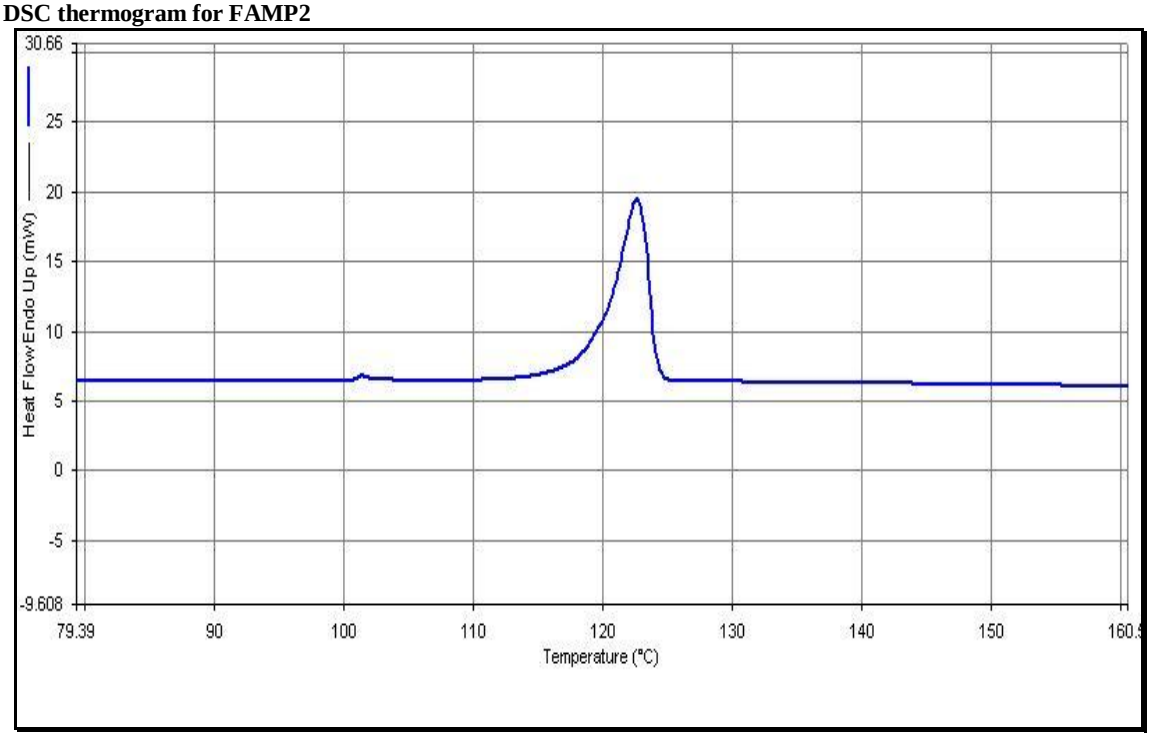

DSC thermogram for FDEA

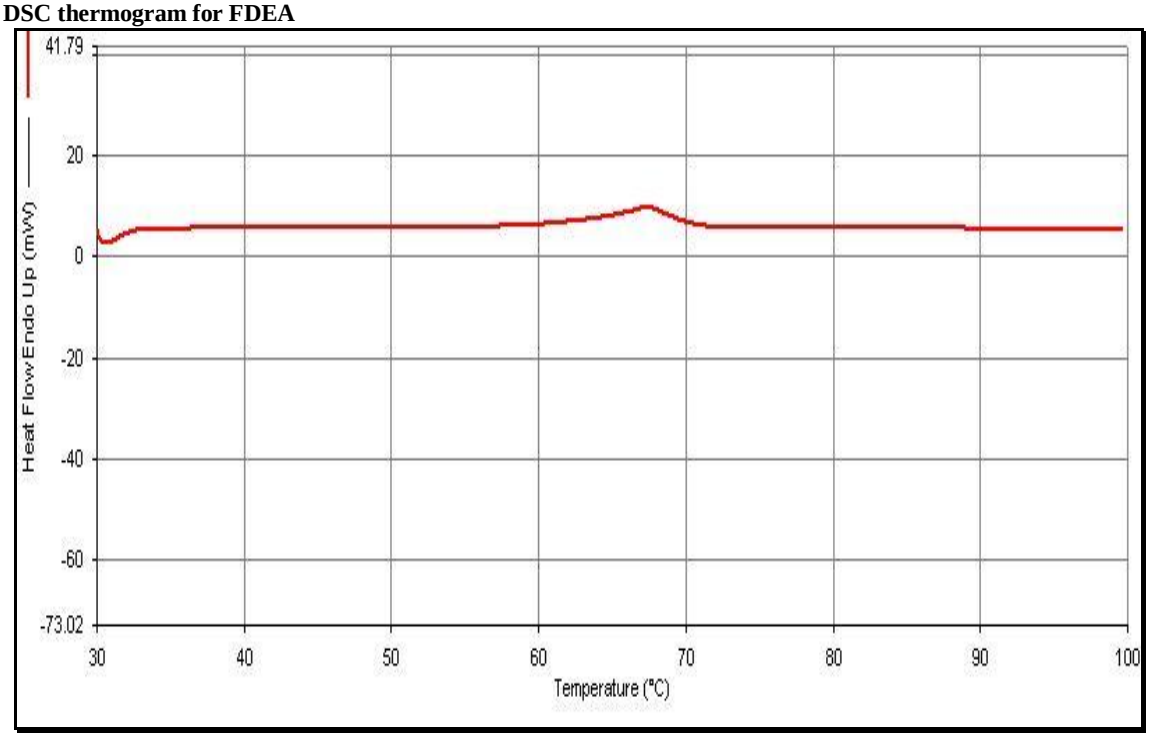

DSC thermogram for FTEA

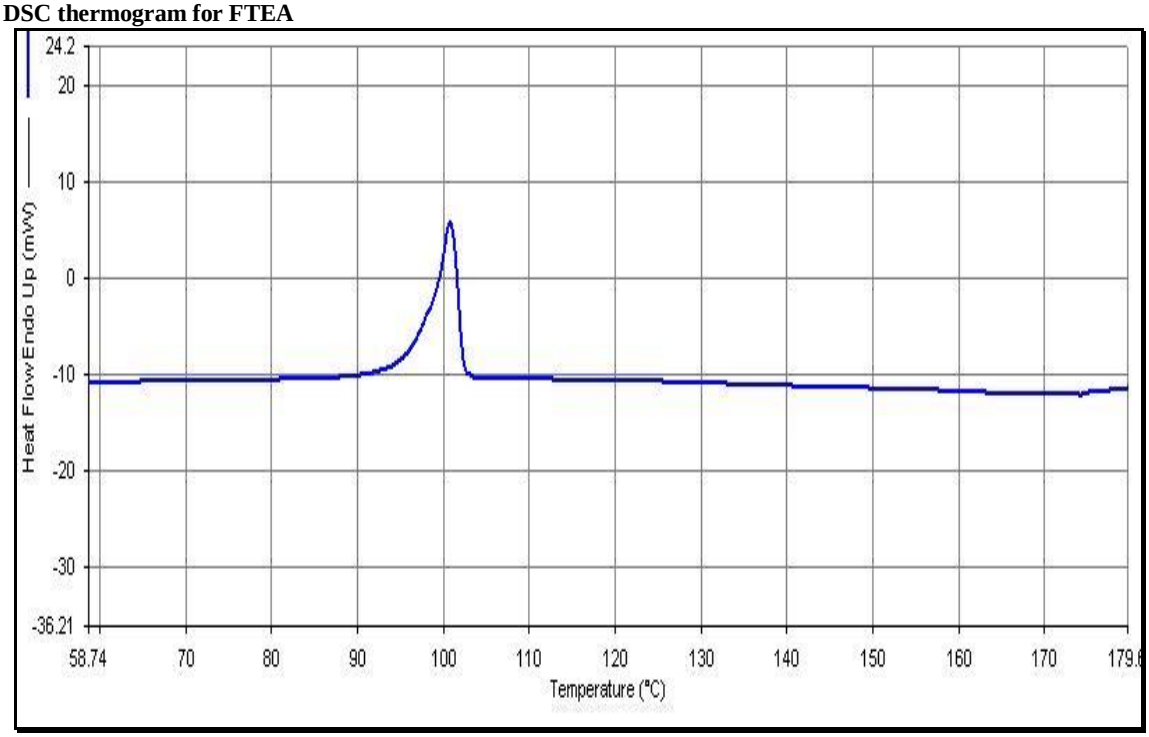

GEMFIBROZIL

DSC thermogram for GAdam

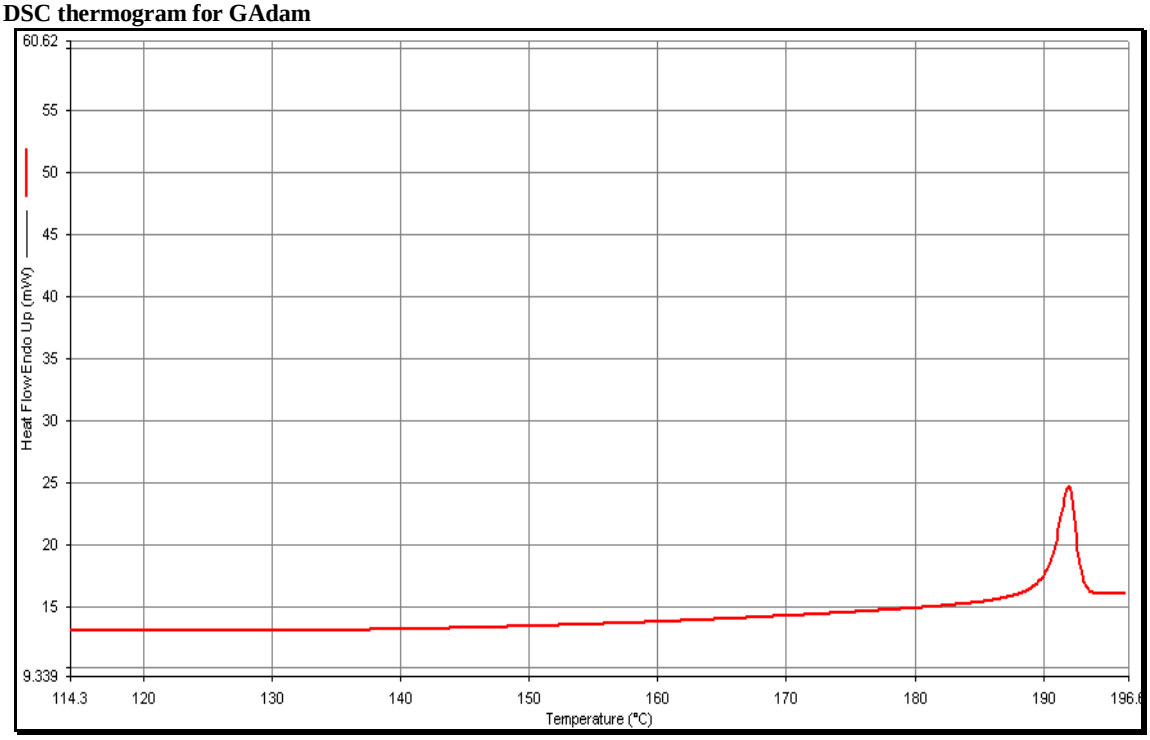

DSC themogram for GBenz

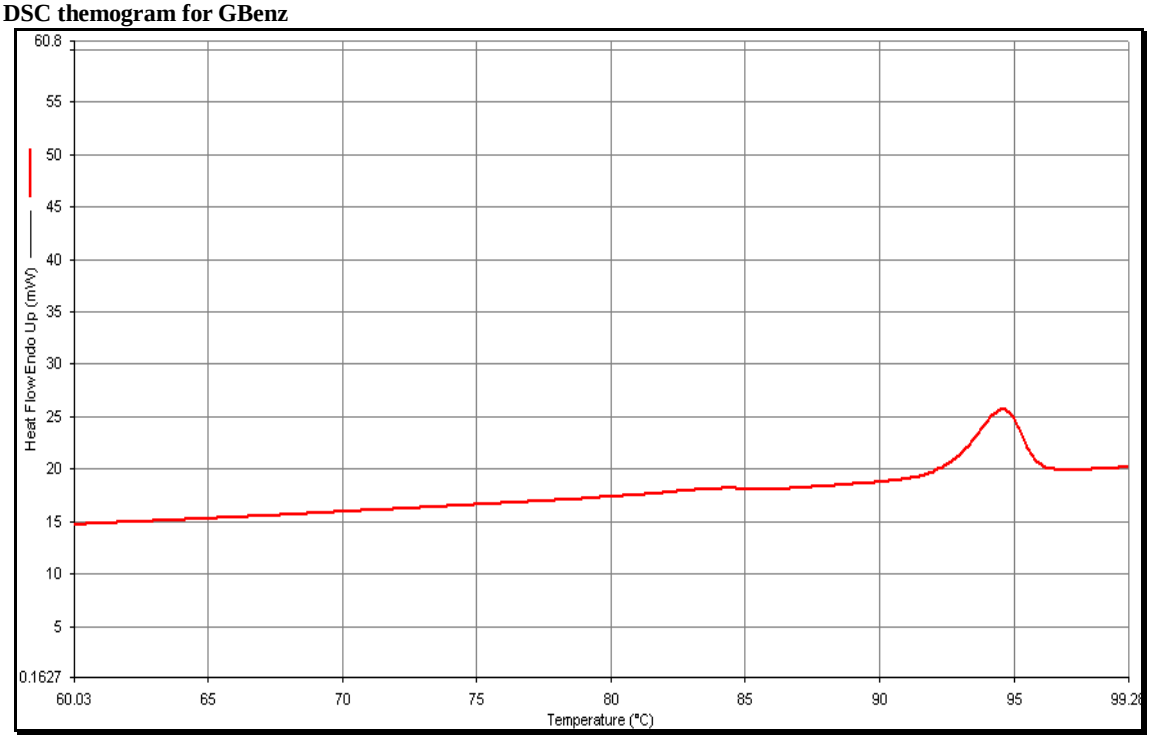

DSC thermogram for GCProp

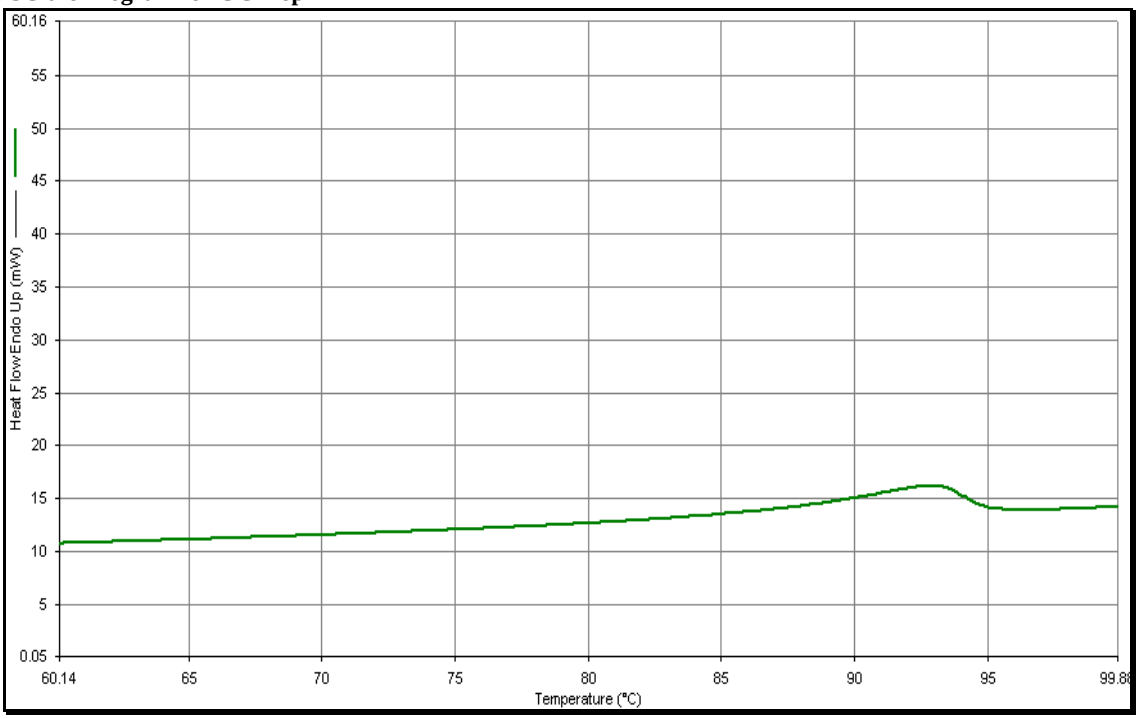

DSC thermogram for GCBut

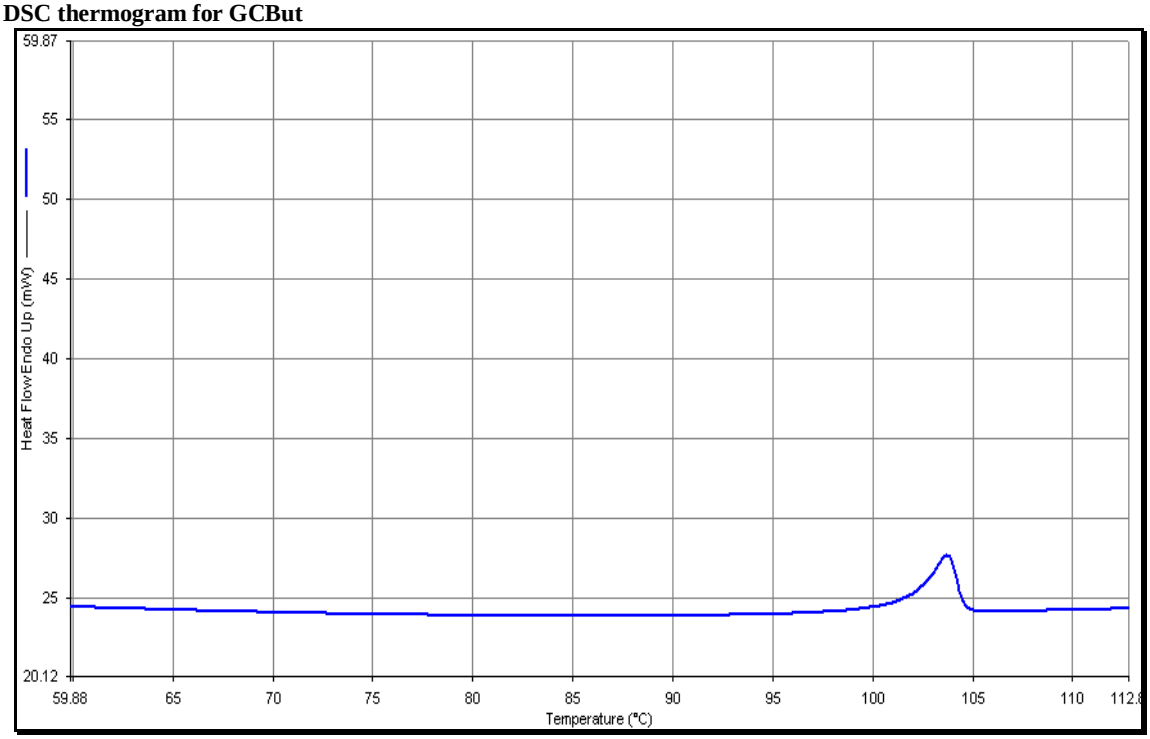

DSC thermogram for GCHex

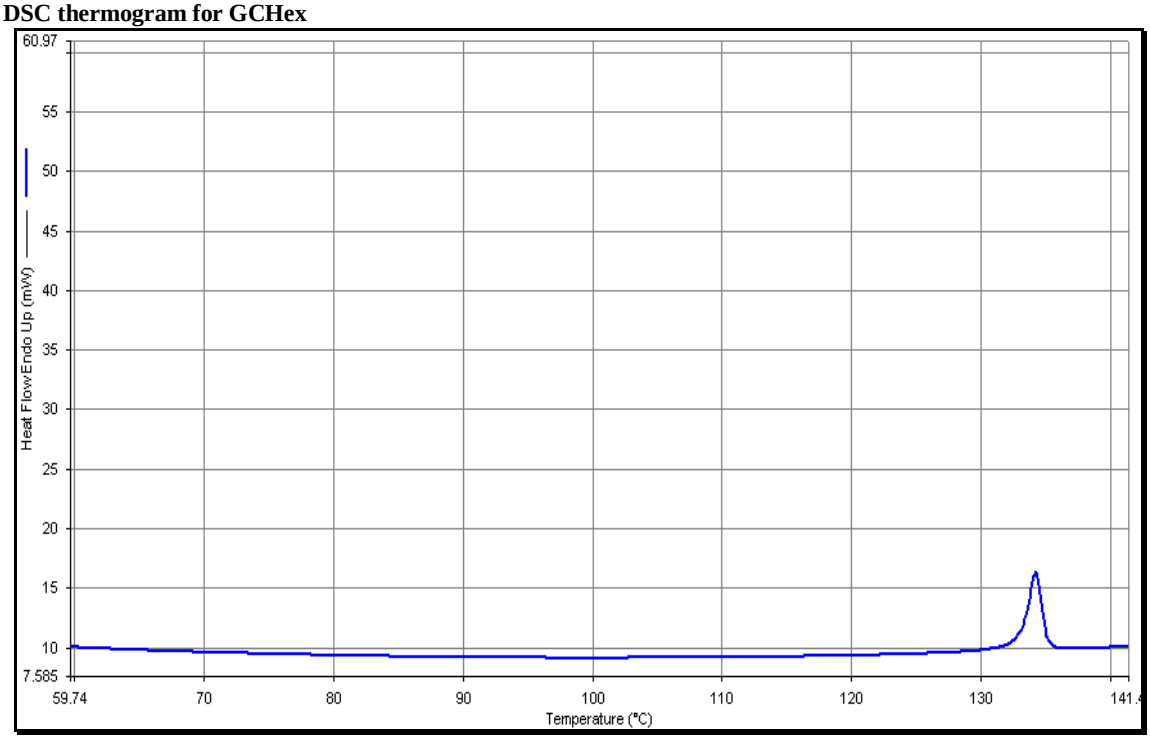

DSC thermogram for GTBut

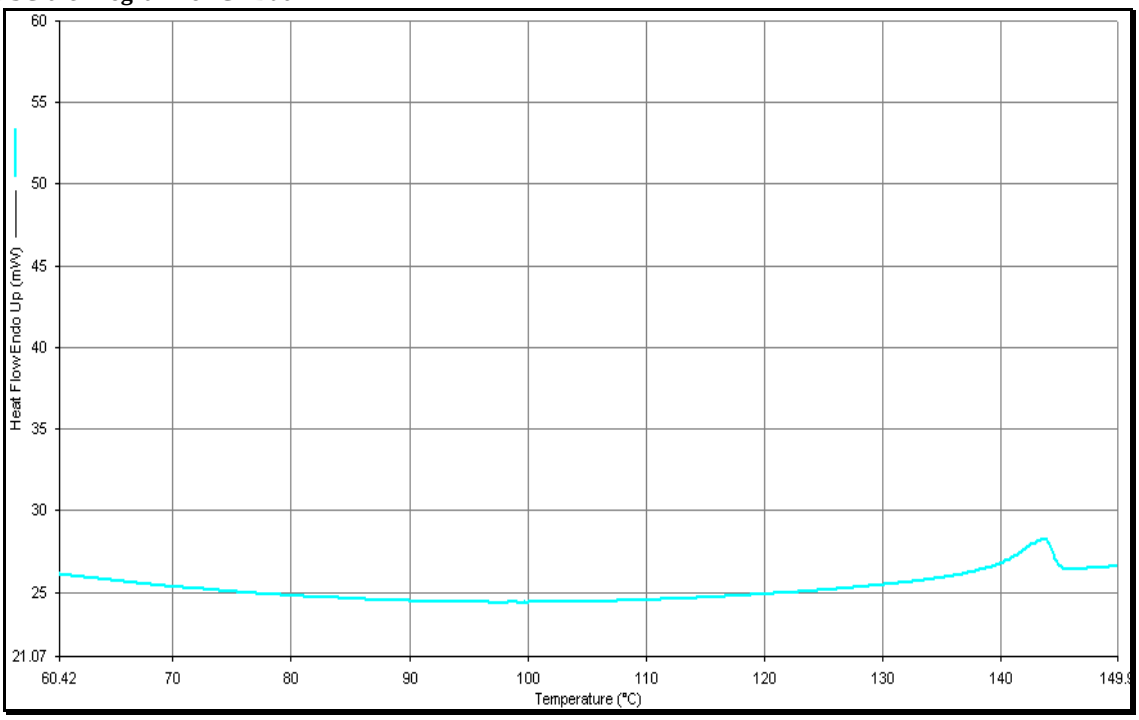

DSC thermogram for GAMP1

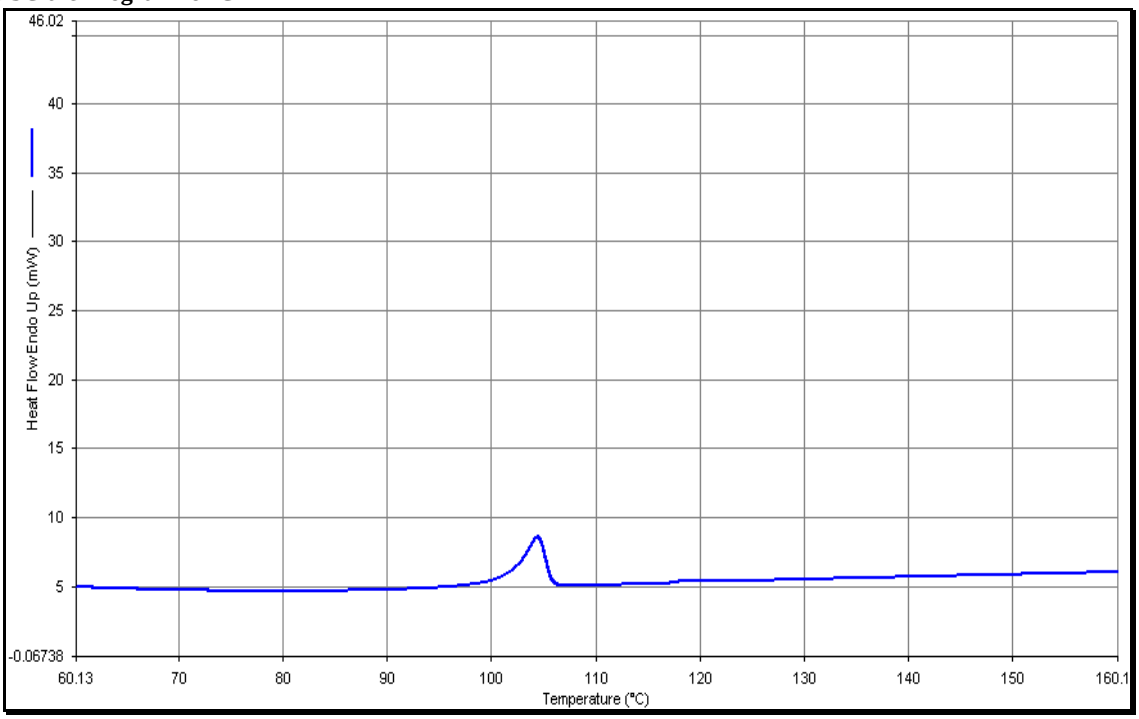

DSC thermogram for GAMP2

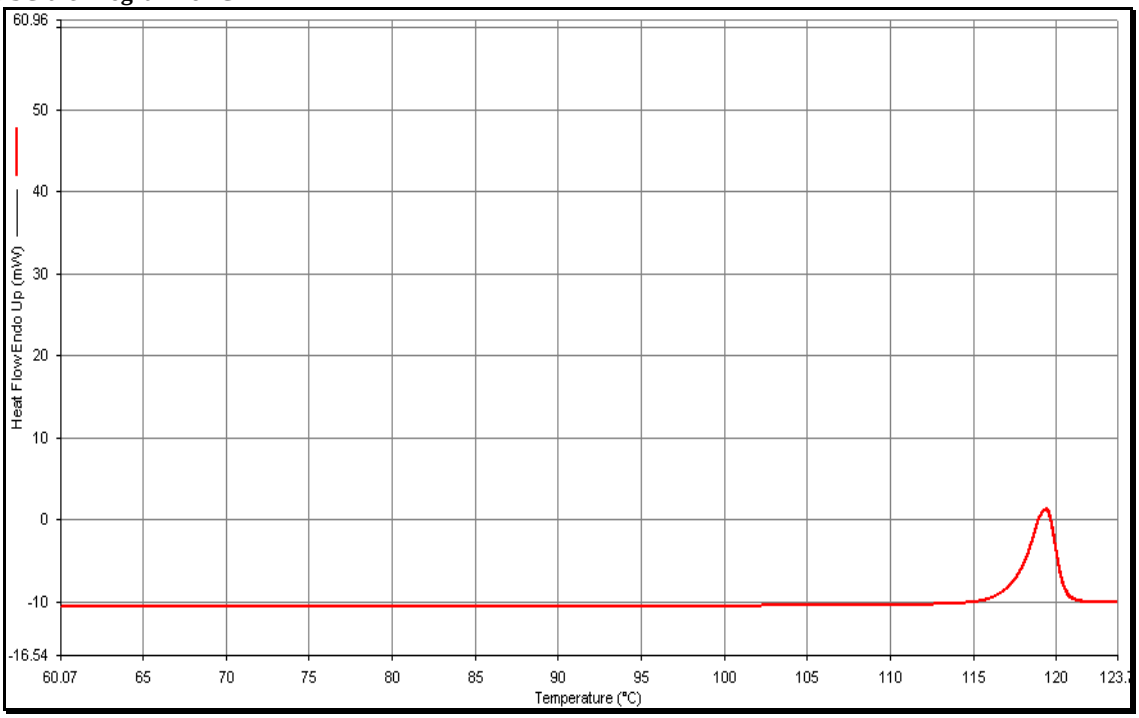

DSC thermogram for GTris

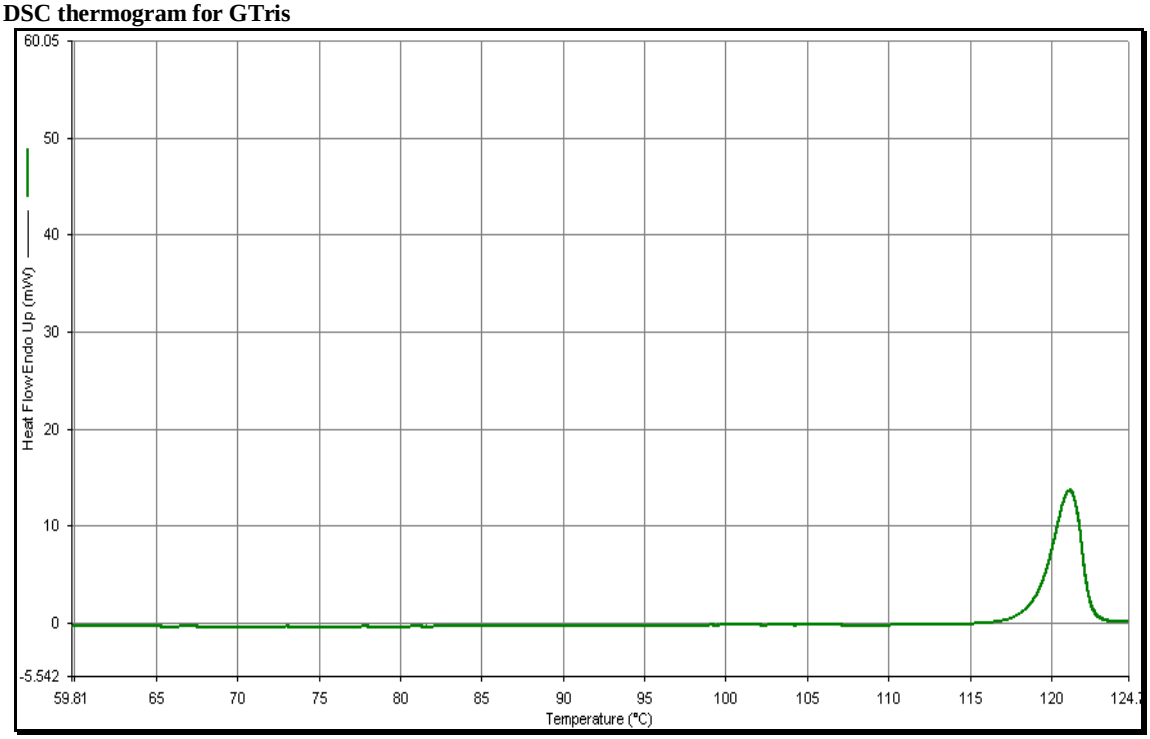

DICLOFENAC

DSC thermogram for DAdam

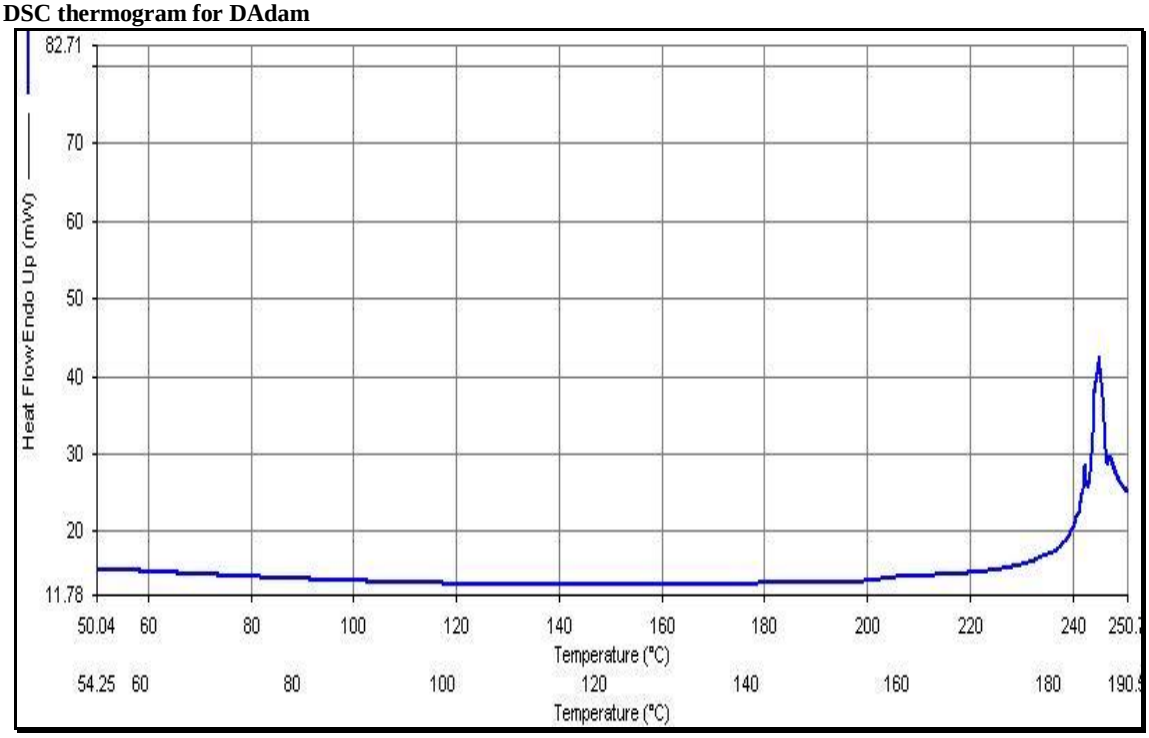

DSC thermogram for DBenz

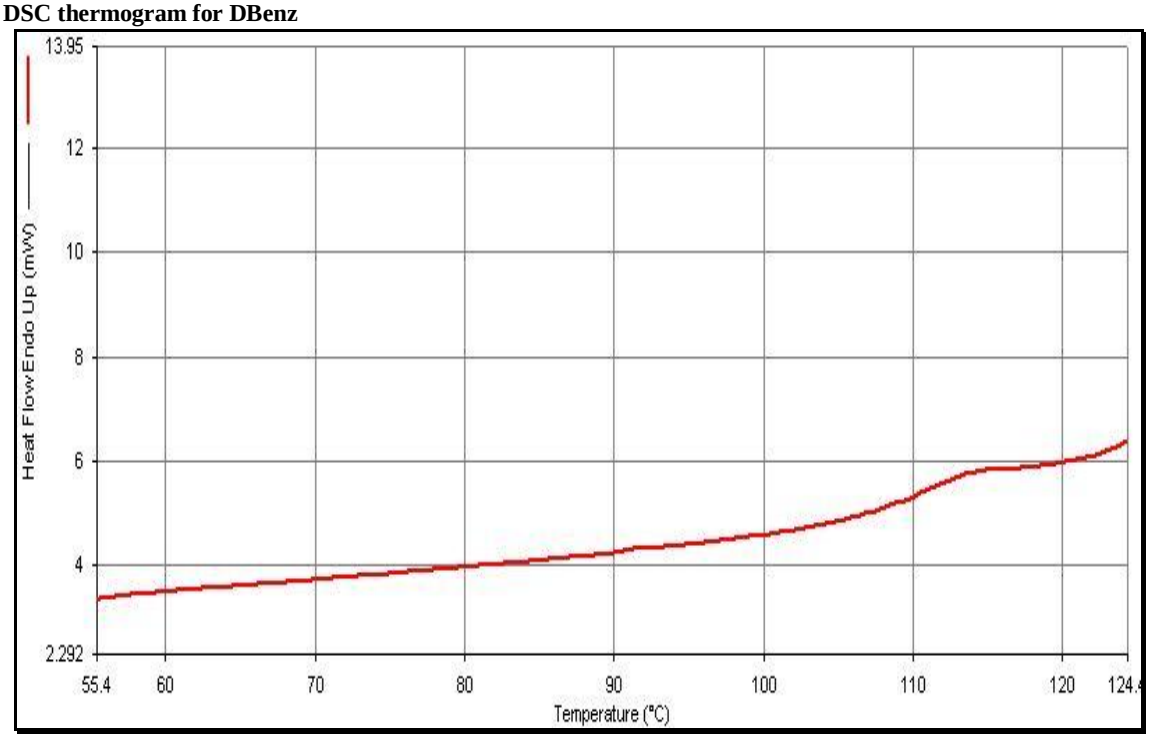

DSC thermogram for DTBut

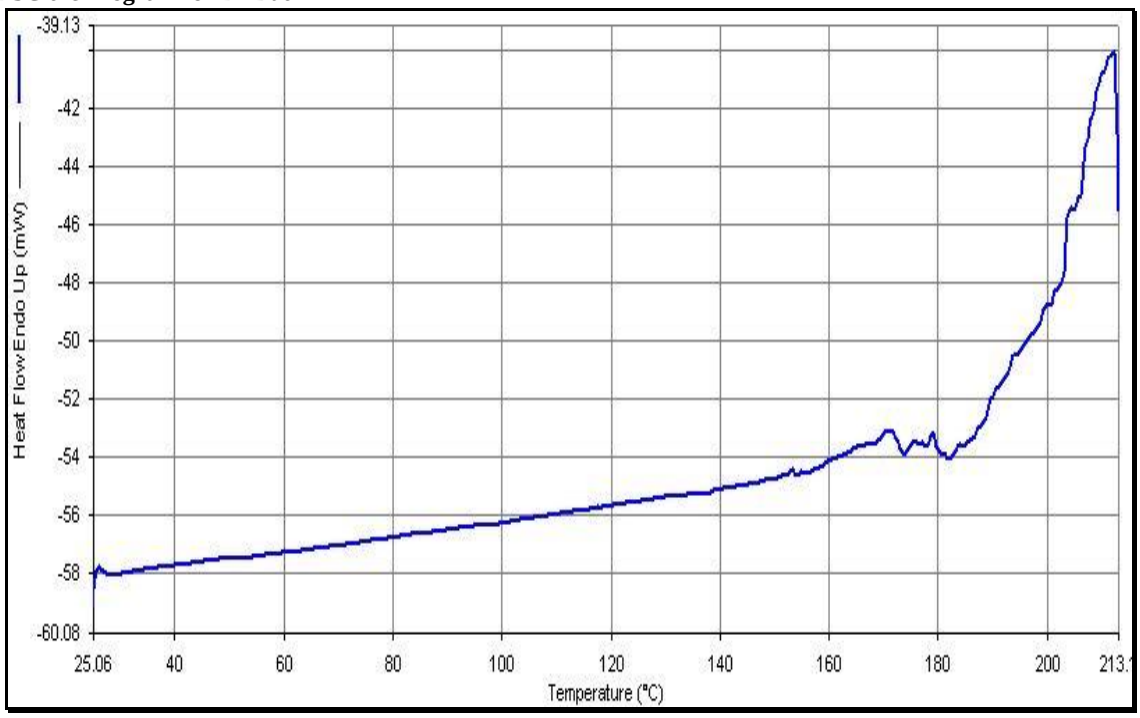

DSC thermogram for DAMP1

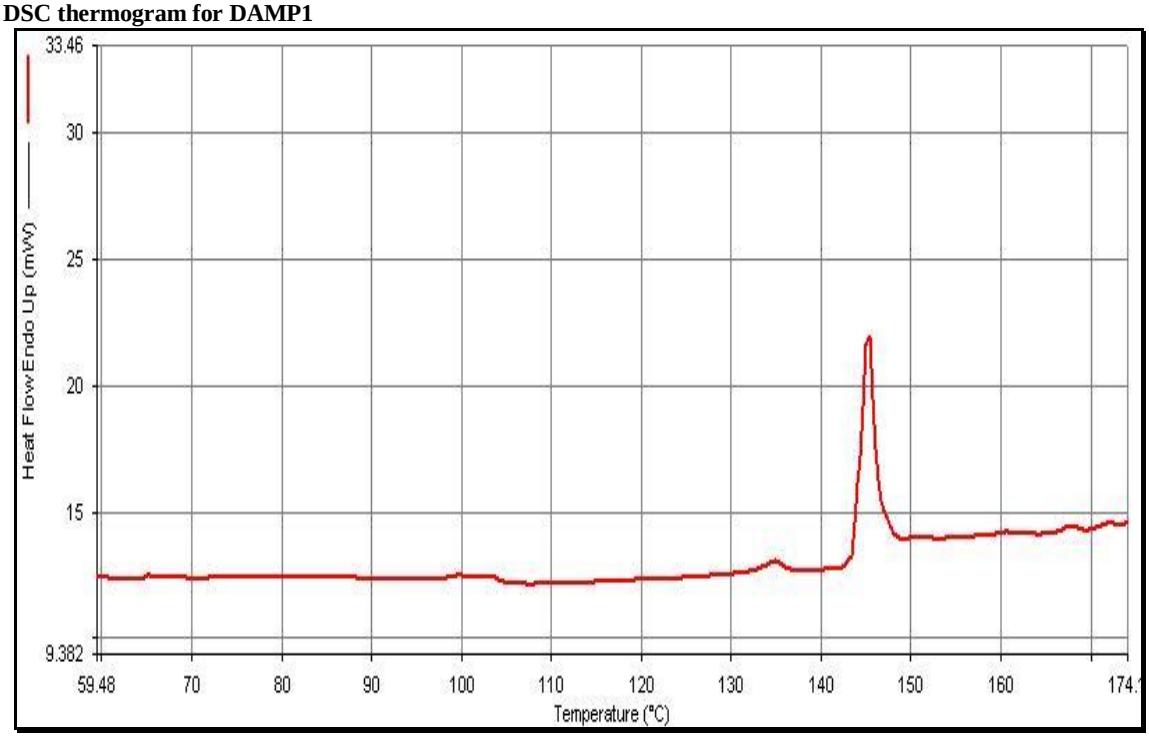

DSC thermogram for DMEA